

**INVESTIGATING THE PHYSIOLOGICAL ROLE
OF HYPOTHALAMIC GLUCOKINASE IN
APPETITE AND GLUCOSE HOMEOSTASIS**

SYED SUFYAN HUSSAIN

A THESIS SUBMITTED FOR THE DEGREE OF

DOCTOR OF PHILOSOPHY IN THE DEPARTMENT OF MEDICINE

IN IMPERIAL COLLEGE LONDON

2013

For Ilfana and Yusuf

Abstract

The brain relies on glucose as a source of energy. Mechanisms that promote the taste-independent intake of glucose have been proposed but not demonstrated. The arcuate nucleus (ARC) of the hypothalamus plays a critical role in regulating energy homeostasis. It acts as a metabolic sensing unit responding to diverse signals, including glucose, to regulate appetite. Glucokinase is a glucose-sensing enzyme expressed in the ARC. The work in this thesis aims to investigate the physiological role of ARC glucokinase in energy homeostasis.

Recombinant adeno-associated virus (rAAV) expressing the pancreatic form of rat glucokinase mRNA (rAAV-GKS) was stereotactically delivered to the ARC of male Wistar rats (iARC-GKS). This approach specifically increased glucokinase activity in the ARC as compared to control rats (iARC-GFP). Pharmacological and genetic increase in ARC glucokinase activity resulted in a significant increase in food intake. Longitudinal experiments demonstrated that this food intake resulted in a significant increase in body weight and adiposity on normal chow and high-energy diets. Further work demonstrated that ARC glucokinase specifically promotes the intake of glucose, but not of fructose, and that the orexigenic effect of ARC glucokinase is driven by specific increase in appetite for glucose.

Similar changes in glucose appetite and food intake were demonstrated to occur with alterations in ARC ATP-sensitive potassium (K_{ATP}) channel activation. Glucose-stimulated NPY release was increased with increased ARC glucokinase activity. This suggests that ARC glucokinase mediates its orexigenic glucose appetite promoting effects in part via altered K_{ATP} channel activation and NPY release, which is consistent with previous work.

This work identifies ARC glucokinase as a regulator of glucose appetite and glucose appetite as an important driver of food intake. ARC glucokinase may represent the brain mechanism regulating the taste-independent intake of glucose and may underlie the phenomena of 'sweet tooth' and 'carbohydrate craving'.

Declaration of Contributors

The research and work described in this thesis was performed by the author. All collaboration and assistance is declared below.

Chapter 3 and 4:

Glucokinase activity assays were performed with assistance of Dr Errol Richardson and Dr Gavin Bewick.

Preparation of the GKS-pTR-CGW-plasmid and Northern Blots were performed with assistance of Dr Errol Richardson and Dr James V Gardiner.

Recombinant adeno-associated viral particles were prepared by Dr James V Gardiner.

Stereotactic injections and feeding experiments on iARC-GKS and iARC-GFP rats were performed with assistance of Dr Errol Richardson.

Chapter 5:

AMPK activity assays were performed with assistance of Mr Huza Zhang and Prof David Carling.

Intra-arcuate cannulation experiments were performed with assistance of Mr Christopher Holton and Dr David Ma.

Hypothalamic explant experiments were performed under the guidance of Dr. Emily Thompson.

Chapter 3 and 5:

Radioimmunoassays were performed under supervision of Professor Mohammad Ghatel. All reagents and protocols were developed by Professor Mohammad Ghatel.

Acknowledgements

Firstly, I would like to thank my supervisors Dr James Gardiner and Prof Sir Stephen Bloom for their guidance, scientific mentorship and enduring support during my Ph.D. I am particularly grateful to them for giving me the opportunity and providing the encouragement to discover the wonders of science in their prestigious laboratory. I would especially like to thank Dr James Gardiner for teaching me how to do science and Prof Sir Stephen Bloom for his patience and inspiration.

I would like to thank Errol Richardson, David Ma and Chris Holton for their camaraderie and support with in vivo work.

I am also extremely grateful for the expert advice and help from my collaborator Prof David Carling.

I would like to thank my funders, The Wellcome Trust, for this opportunity and for funding my training during this Fellowship.

As with any Ph.D., there are a number of seniors and colleagues who provided help, support and encouragement. I would especially like to thank MG, WSD, GB, KM, MJP, NK, JKJ, NB, KEB, AM, MB, SA, WR, LT and other members of the Bloom lab Hypo group.

Finally, I would like to thank my close friends and family, especially Ifana, Yusuf, Mum and Dad for their invaluable support and encouragement.

Abbreviations in Thesis

| | |
|---------|--|
| 2DG | 2-Deoxyglucose |
| 3OMG | 3-O-methyl-N-acetylglucosamine |
| 5TG | 5-thio-d-glucose-6-phosphate |
| AAV | Adeno-associated virus |
| ACC | Acetyl-CoA carboxylase |
| ADP | Adenosine diphosphate |
| AgRP | Agouti related peptide |
| Amp | Ampicillin resistance gene |
| AMPK | Adenosine Monophosphate Activated Protein Kinase |
| ANOVA | Analysis of variance |
| ARC | Arcuate nucleus |
| Arcuate | Arcuate nucleus |
| AS | Antisense |
| ATP | Adenosine triphosphate |
| BAT | Brown adipose tissue |
| BLAST | Basic Local Alignment Search Tool |
| Bp | Base pairs |
| cAMP | Cyclic adeno monophosphate |
| CART | Cocaine-and amphetamine-related transcript |

| | |
|-------|--|
| CCK | Cholecystokinin |
| cDNA | Copy DNA |
| CLAMS | Comprehensive laboratory animals monitoring system |
| CNS | Central nervous system |
| CpdA | Compound A, Glucokinase activator |
| CPT-1 | Carnitine palmitoyltransferase 1 |
| Cre | Cre - recombinase |
| CSF | Cerebrospinal fluid |
| Dia | Diazoxide |
| DIO | Diet induced obesity |
| DKA | Diabetic ketoacidosis |
| DMEM | Dubecco's modified eagle medium |
| DMN | Dorso medial nucleus |
| DMSO | Dimethyl sulfoxide |
| DNA | Deoxyribonucleic acid |
| dNTP | Deoxynucleotide triphosphate |
| DTT | Dithiothreitol |
| EDTA | Ethylenediaminetetraacetic acid |
| eGFP | Enhanced green fluorescent protein |
| ELISA | Enzyme-linked immune-sorbent assay |
| FAS | Fatty acid synthase |

| | |
|--------|--|
| FBS | Foetal Bovine Serum |
| GDW | Glass distilled water |
| GE | Glucose-excited |
| GEE | General estimating equation |
| GFP | Green fluorescent protein |
| GI | Glucose-inhibited |
| GIP | Glucose-dependant insulintropic peptide |
| GIPr | Glucose-dependant insulintropic peptide receptor |
| GK | Glucokinase |
| GKPF | Glucokinase pair-fed |
| GKS | Glucokinase sense |
| Glib | Glibenclamide |
| GLP-1 | Glucagon-like peptide-1 |
| GLP-1r | Glucagon-like peptide 1 receptor |
| GOD | Glucose oxidase |
| G-P-6 | Glucose-6-phosphate |
| GTE | Glucose tris EDTA |
| HBS | HEPES-buffered saline |
| HEK | Human embryonic kidney |
| HEPG2 | Human hepatocellular carcinoma |
| HFD | High fat diet |

| | |
|------------------|--|
| HHS | Hyperosmolar hyperglycaemia syndrome |
| HX | Hexokinase |
| iARC | Intra-arcuate nucleus |
| iARC-GKS | rAAV-GKS intra-arcuate nucleus injected rats |
| iARC-GFP | rAAV-GPF intra-arcuate nucleus injected rats |
| i.p. | Intraperitoneal |
| ICV | Intracerebroventricular |
| IP | Intraperitoneal |
| ITRs | Inverted terminal repeats |
| ITT | Insulin tolerance test |
| kcal | Kilocalorie |
| Kir | Inwardly rectifying potassium channels |
| Kir6.2 | Major subunit of the ATP-sensitive K ⁺ channel, associated with sulfonylurea receptor |
| Kj | Kilojoule |
| KO | Knock out |
| K _{ATP} | ATP-sensitive potassium channels |
| LCFA-CoA | Long chain fatty acyl-CoAs |
| LDH | Lactate dehydrogenase |
| LH | Lateral hypothalamus |
| MCH | Melanin-concentrating hormone |

| | |
|----------|---|
| MCT-1 | Monocarboxylate transporter |
| mRNA | Messenger Ribonucleic acid |
| MSH | Melanocyte stimulating hormone |
| NADPH | Nicotinamide adenine dinucleotide phosphate |
| NCBI | National Centre for Biotechnology Information |
| NPY | Neuropeptide Y |
| PBS | Phosphate buffered saline |
| PCR | Polymerase chain reaction |
| PFK | Phosphofructokinase |
| POD | Peroxidase |
| POMC | Pro-opiomelanocortin |
| PYY | Peptide YY |
| PVN | Paraventricular nucleus |
| QPCR | Quantitative polymerase chain reaction |
| rAAV | Recombinant adeno associated virus |
| rAAV-GKS | rAAV glucokinase |
| RIA | Radioimmunoassay |
| RNA | Ribonucleic acid |
| RT | Reverse transcriptase |
| SAP | Shrimp alkaline phosphatase |
| SDS | Sodium dodecyl sulfate |

| | |
|--------|---|
| SEM | Standard error of the mean |
| SF-1 | Steroidogenic factor-1 |
| SGLT-1 | Sodium-dependant glucose transporter 1 |
| SSC | Saline sodium citrate |
| SUR | Sulphonylurea receptor |
| TAE | Tris-Acetate EDTA |
| TE | Tris EDTA |
| tRNA | transfer Ribonucleic acid |
| UCP-1 | Uncoupling protein 1 |
| UV | Ultraviolet |
| VMH | Ventromedial hypothalamic area |
| VMN | Ventromedial hypothalamic nucleus |
| WAT | White adipose tissue |
| WPRE | Woodchuck hepatitis virus promoter response element |

Table of Contents

| | | |
|----------|---|-----------|
| 1 | GENERAL INTRODUCTION..... | 17 |
| 1.1 | THE OBESITY PANDEMIC..... | 18 |
| 1.2 | ENERGY HOMEOSTASIS AND OBESITY..... | 18 |
| 1.3 | ROLE OF THE HYPOTHALAMUS IN ENERGY HOMEOSTASIS..... | 18 |
| 1.3.1 | <i>Lateral hypothalamus.....</i> | 19 |
| 1.3.2 | <i>Arcuate Nucleus.....</i> | 19 |
| 1.3.3 | <i>Ventromedial hypothalamic nucleus.....</i> | 21 |
| 1.4 | OTHER CENTRAL PATHWAYS CONTROLLING ENERGY HOMOEOSTASIS..... | 21 |
| 1.4.1 | <i>Role of the brainstem in energy homoeostasis.....</i> | 21 |
| 1.4.2 | <i>Role of the cortico-limbic system in energy homoeostasis.....</i> | 21 |
| 1.5 | GLUCOSE-SENSING BY THE HYPOTHALAMUS AND REGULATION OF ENERGY HOMEOSTASIS..... | 22 |
| 1.5.1 | <i>Hypothalamic glucose-sensing and food intake.....</i> | 22 |
| 1.5.2 | <i>Hypothalamic glucose-sensing and glucose homoeostasis.....</i> | 23 |
| 1.5.3 | <i>Glucose-Sensitive Neurons.....</i> | 23 |
| 1.5.4 | <i>Glucokinase and glucose-sensing.....</i> | 24 |
| 1.5.5 | <i>Mechanism of hypothalamic glucose-sensing.....</i> | 25 |
| 1.5.6 | <i>Hypothalamic distribution of glucose-sensing neurons.....</i> | 28 |
| 1.5.7 | <i>Glucokinase and neuronal glucose-sensing.....</i> | 29 |
| 1.5.8 | <i>Glucose-sensing neurons as metabolic sensors.....</i> | 30 |
| 1.6 | APPROACHES TO STUDY NEURAL CIRCUITS CONTROLLING ENERGY HOMOEOSTASIS IN RODENTS..... | 33 |
| 1.6.1 | <i>Direct administration of compounds.....</i> | 33 |
| 1.6.2 | <i>Genetic modification.....</i> | 33 |
| 1.7 | SUMMARY..... | 40 |
| 2 | MATERIALS AND METHODS..... | 41 |
| 2.1 | MOLECULAR AND IN-VITRO TECHNIQUES..... | 42 |
| 2.1.1 | <i>Production of GKS (glucokinase-sense) using RT and PCR.....</i> | 42 |
| 2.1.2 | <i>Cloning of GK DNA into pTR-CGW.....</i> | 46 |
| 2.2 | IN VIVO METHODS..... | 62 |
| 2.2.1 | <i>Animals.....</i> | 62 |
| 2.2.2 | <i>Intra-arcuate AAV microinjections.....</i> | 62 |
| 2.2.3 | <i>Intra-arcuate cannulations.....</i> | 63 |
| 2.2.4 | <i>Feeding studies.....</i> | 64 |
| 2.2.5 | <i>Intra-arcuate cannulation.....</i> | 64 |
| 2.2.6 | <i>Collection of tissue samples.....</i> | 65 |
| 2.3 | IN VITRO METHODS..... | 65 |
| 2.3.1 | <i>In situ hybridisation for glucokinase mRNA.....</i> | 65 |
| 2.3.2 | <i>Cresyl violet staining of ink injected rat brains.....</i> | 68 |
| 2.3.3 | <i>Glucokinase activity assays.....</i> | 69 |
| 2.3.4 | <i>Quantification of mRNA by qPCR.....</i> | 73 |
| 2.3.5 | <i>Northern Blot Analysis of mRNA.....</i> | 76 |

| | | |
|----------|--|------------|
| 2.3.6 | <i>Transfer of RNA to Nylon Filters</i> | 78 |
| 2.3.7 | <i>AMPK activity (SAMS peptide) assay</i> | 83 |
| 2.3.8 | <i>Hypothalamic explant static incubation system</i> | 84 |
| 2.3.9 | <i>Body composition analysis</i> | 85 |
| 2.3.10 | <i>Analysis of plasma metabolites and hormones</i> | 86 |
| 2.4 | STATISTICAL ANALYSIS | 93 |
| 3 | EFFECT OF INCREASED ARCUATE GLUCOKINASE ACTIVITY ON FOOD INTAKE AND BODY WEIGHT | 95 |
| 3.1 | INTRODUCTION | 96 |
| 3.1.1 | <i>Evidence for the glucostatic control of food intake</i> | 96 |
| 3.1.2 | <i>Glucokinase and food intake</i> | 97 |
| 3.1.3 | <i>Role of the ARC in modulating food intake in response to changes in glucose</i> | 98 |
| 3.2 | HYPOTHESIS AND AIMS | 100 |
| 3.2.1 | <i>Hypothesis</i> | 100 |
| 3.2.2 | <i>Aims and Objectives</i> | 100 |
| 3.3 | RESULTS | 101 |
| 3.3.1 | <i>Effect of nutritional state on glucokinase activity in hypothalamic nuclei</i> | 101 |
| 3.3.2 | <i>Effect of acutely increasing ARC glucokinase activity on food intake</i> | 103 |
| 3.3.3 | <i>Production of rAAV-GKS</i> | 105 |
| 3.3.4 | <i>Confirmation of altered glucokinase activity following transfection of GKS-pTR-CGW plasmid</i> | 110 |
| 3.3.5 | <i>rAAV production</i> | 111 |
| 3.3.6 | <i>Effect of chronically increased arcuate glucokinase activity on food intake and body weight on a standard chow diet</i> | 111 |
| 3.3.7 | <i>Effect of chronically increased arcuate glucokinase activity on food intake and body weight on a high-energy diet</i> | 123 |
| 3.3.8 | <i>Confirmation of increased glucokinase activity in the ARC</i> | 125 |
| 3.4 | DISCUSSION | 126 |
| 3.4.1 | <i>ARC glucokinase is involved in the regulation of food intake</i> | 126 |
| 3.4.2 | <i>ARC glucokinase exerts orexigenic role</i> | 126 |
| 3.4.3 | <i>Production of rAAV encoding glucokinase</i> | 128 |
| 3.4.4 | <i>Stereotactic injection of rAAV-GKS into the ARC increases glucokinase activity specifically in the ARC</i> | 128 |
| 3.4.5 | <i>Effect of glucokinase activity on energy homoeostasis on a normal chow diet</i> | 129 |
| 3.4.6 | <i>Effect of increasing ARC glucokinase activity on energy homoeostasis on a high energy diet</i> | 131 |
| 3.4.7 | <i>Conclusion</i> | 131 |
| 4 | EFFECT OF INCREASED ARCUATE GLUCOKINASE ACTIVITY ON SELECTION OF MACRONUTRIENTS | 132 |
| 4.1 | INTRODUCTION | 133 |
| 4.1.1 | <i>Neuronal mechanisms leading to nutrient selectivity and preference</i> | 134 |
| 4.2 | HYPOTHESIS AND AIMS | 139 |
| 4.2.1 | <i>Hypothesis</i> | 139 |
| 4.2.2 | <i>Aims and Objectives</i> | 139 |
| 4.3 | RESULTS | 140 |
| 4.3.1 | <i>Effect of increasing ARC glucokinase activity on glucose intake</i> | 140 |
| 4.3.2 | <i>Effect of increasing ARC glucokinase activity on preference of glucose over other foods</i> | 146 |
| 4.3.3 | <i>Effect of increasing ARC glucokinase activity on long-term food, glucose and total caloric intake with ad libitum access to 10% glucose and standard chow</i> | 158 |
| 4.3.4 | <i>Effect on glucose intake</i> | 159 |

| | | |
|----------|---|------------|
| 4.3.5 | <i>Effect of increasing ARC glucokinase activity on caloric intake with ad libitum access to 10% glucose and normal chow</i> | 160 |
| 4.3.6 | <i>Effect on bodyweight gain</i> | 161 |
| 4.4 | DISCUSSION | 162 |
| 4.4.1 | <i>ARC glucokinase selectively alters glucose intake but does not alter fructose intake</i> | 162 |
| 4.4.2 | <i>ARC glucokinase selectively alters glucose intake over other foods</i> | 162 |
| 4.4.3 | <i>Conclusion</i> | 164 |
| 5 | INVESTIGATING THE CELLULAR MECHANISMS BY WHICH ARCUATE GLUCOKINASE MAY MEDIATE ITS EFFECT ON APPETITE | 165 |
| 5.1 | INTRODUCTION | 166 |
| 5.1.1 | <i>Mechanisms by which ARC glucokinase may influence neuronal activity</i> | 166 |
| 5.1.2 | <i>Neurotransmitters likely to be involved in mediating the effects of ARC glucokinase in energy homeostasis</i> | 169 |
| 5.2 | HYPOTHESIS AND AIMS | 171 |
| 5.2.1 | <i>Hypothesis</i> | 171 |
| 5.2.2 | <i>Aims and Objectives</i> | 171 |
| 5.3 | RESULTS | 172 |
| 5.3.1 | <i>Effect of increasing arcuate glucokinase activity on enzyme expression in chow-fed animals</i> | 172 |
| 5.3.2 | <i>Effect of increasing arcuate glucokinase activity on hypothalamic AMPK activity</i> | 174 |
| 5.3.3 | <i>Effect of inhibiting K_{ATP} channels in the arcuate nucleus on food intake, glucose intake and glucose preference</i> | 175 |
| 5.3.4 | <i>Effect of activating ATP sensitive potassium channels in the arcuate nucleus on food intake, glucose intake and glucose preference</i> | 180 |
| 5.3.5 | <i>Effect of increasing arcuate glucokinase activity on hypothalamic neuropeptide expression in chow-fed animals</i> | 186 |
| 5.3.6 | <i>Effect of increased arcuate glucokinase activity on glucose-stimulated NPY-release from hypothalamic neurons</i> | 187 |
| 5.3.7 | <i>Effect of increased arcuate glucokinase activity on glucose-stimulated α-MSH release from hypothalamic neurons</i> | 188 |
| 5.4 | DISCUSSION | 189 |
| 5.4.1 | <i>Changes in hypothalamic energy-sensing enzymes with increased ARC glucokinase activity</i> | 189 |
| 5.4.2 | <i>K_{ATP} channels play a part in transducing the effects of ARC glucokinase</i> | 190 |
| 5.4.3 | <i>Changes in neuropeptide expression and NPY release with increased ARC glucokinase activity</i> | 190 |
| 5.4.4 | <i>Conclusion</i> | 192 |
| 6 | DISCUSSION | 193 |
| 6.1 | SUMMARY OF RESULTS AND MECHANISMS INVOLVED | 194 |
| 6.2 | IMPLICATIONS FOR CURRENT UNDERSTANDING OF ENERGY HOMOEOSTASIS | 197 |
| 6.3 | LIMITATIONS, UNRESOLVED QUESTIONS AND FUTURE WORK | 199 |
| 7 | REFERENCES | 203 |
| 8 | APPENDIX | 219 |
| 8.1 | APPENDIX I – SOLUTIONS | 219 |
| 8.2 | APPENDIX II – CORONAL SECTION OF RAT BRAIN | 224 |
| 8.3 | APPENDIX III – NUTRITIONAL INFORMATION FOR RM1 NORMAL CHOW DIET | 225 |
| 8.4 | APPENDIX IV – NUTRITIONAL INFORMATION FOR HIGH ENERGY DIET (RESEARCH DIETS INC, USA) | 226 |
| 8.5 | APPENDIX V – LIST OF SUPPLIERS | 227 |

Table of Figures

| | |
|---|------------|
| <i>Figure 1.1 Glucose excited neuron: Mechanism for glucose-sensing in the GE neurons.....</i> | <i>26</i> |
| <i>Figure 1.2 Glucose inhibited neuron: Potential mechanism for glucose-sensing in GI neurons.....</i> | <i>27</i> |
| <i>Figure 1.3 A possible integrated mechanism for neuronal metabolic sensing.....</i> | <i>32</i> |
| <i>Figure 2.1 Diagram of wild-type AAV-2 serotype genome.....</i> | <i>38</i> |
| <i>Figure 2.2 PCR primers used for amplification of GKS gene sequences.....</i> | <i>45</i> |
| <i>Figure 2.3 Two plasmid system for rAAV production.....</i> | <i>56</i> |
| <i>Figure 2.4 Diagram of rAAV plasmid pTRCGW with transgene insert.....</i> | <i>57</i> |
| <i>Figure 2.5 Diagram of helper-plasmid pDG structure.....</i> | <i>57</i> |
| <i>Figure 3.1 Effect of nutritional state on glucokinase activity in hypothalamic nuclei.....</i> | <i>102</i> |
| <i>Figure 3.2 Confirmation of cannula placement in rats cannulated into the ARC.....</i> | <i>103</i> |
| <i>Figure 3.3 Effect of increasing ARC glucokinase activity on food intake.....</i> | <i>104</i> |
| <i>Figure 3.4 Visualisation of GKS plasmid production using gel electrophoresis.....</i> | <i>106</i> |
| <i>Figure 3.5: BLAST analysis of GKS-pTR-CGW and pCMV4.GKB1 sequences.....</i> | <i>109</i> |
| <i>Figure 3.6 In vitro validation of GKS-pTR-CGW plasmid glucokinase activity.....</i> | <i>110</i> |
| <i>Figure 3.7 Confirmation of gene transfer by in situ hybridisation.....</i> | <i>111</i> |
| <i>Figure 3.8 Effect of iARC rAAV-GKS on food intake.....</i> | <i>112</i> |
| <i>Figure 3.9 Effect of iARC rAAV-GKS on 24hr food intake following 24hr fast.....</i> | <i>114</i> |
| <i>Figure 3.10 Effect of iARC rAAV-GKS on bodyweight gain.....</i> | <i>115</i> |
| <i>Figure 3.11 Effect of iARC rAAV-GKS on percentage body fat.....</i> | <i>117</i> |
| <i>Figure 3.12 Effect of iARC rAAV-GKS on percentage bodyweight protein.....</i> | <i>117</i> |
| <i>Figure 3.13 Effect of iARC rAAV-GKS on BAT weight.....</i> | <i>118</i> |
| <i>Figure 3.14 Effect iARC-GKS on glucose homeostasis.....</i> | <i>120</i> |
| <i>Figure 3.15 Effect of iARC GKS on hormones involved in appetite regulation.....</i> | <i>122</i> |
| <i>Figure 3.16 Effect of iARC rAAV-GKS on food intake.....</i> | <i>123</i> |
| <i>Figure 3.17 Effect of iARC rAAV-GKS on bodyweight gain with Western diet.....</i> | <i>124</i> |
| <i>Figure 3.18 Glucokinase activity in hypothalamic nuclei of iARC-GKS and iARC-GFP rats.....</i> | <i>125</i> |
| <i>Figure 4.1 Effect of increasing ARC glucokinase activity on glucose intake.....</i> | <i>142</i> |
| <i>Figure 4.2 Effect of increasing ARC glucokinase activity on twenty-four hour intake of 2% w/v sugar Solutions.....</i> | <i>144</i> |
| <i>Figure 4.3 Effect of increasing ARC glucokinase activity on twenty-four hour intake of 10% w/v sugar solutions.....</i> | <i>145</i> |
| <i>Figure 4.4 Effect of increasing ARC glucokinase activity on glucose and food intake with ad libitum access to 2% w/v glucose solution and normal chow.....</i> | <i>148</i> |

| | |
|--|------------|
| <i>Figure 4.5 Effect of chronically increasing ARC glucokinase activity on twenty-four hour glucose, food and caloric intake with ad libitum access to 2% w/v glucose solution and normal chow.....</i> | <i>150</i> |
| <i>Figure 4.6 Effect of chronically increasing ARC glucokinase activity on twenty-four hour glucose, food and caloric intake with ad libitum access to 10% w/v glucose solution and normal chow.....</i> | <i>152</i> |
| <i>Figure 4.7 Effect of chronically increasing ARC glucokinase activity on twenty-four hour glucose, food and caloric intake with ad libitum access to 20% w/v glucose solution and normal chow.....</i> | <i>154</i> |
| <i>Figure 4.8 Effect of increasing ARC glucokinase activity on twenty-four hour intake of food.....</i> | <i>155</i> |
| <i>Figure 4.9 Comparison of the effects of increasing ARC glucokinase activity on twenty-four hour caloric intake during studies with ad libitum access to chow and glucose solutions.....</i> | <i>157</i> |
| <i>Figure 4.10 Effect of increasing ARC glucokinase activity on food intake with long-term ad libitum access to 10% w/v glucose and standard chow.....</i> | <i>158</i> |
| <i>Figure 4.11 Effect of increasing ARC glucokinase activity on glucose intake with long-term ad libitum access to 10% w/v glucose and standard chow.....</i> | <i>159</i> |
| <i>Figure 4.12 Effect of increasing ARC glucokinase activity on caloric intake with long-term ad libitum access to 10% w/v glucose and standard chow.....</i> | <i>160</i> |
| <i>Figure 4.13 Effect of increasing ARC glucokinase activity on bodyweight gain with long-term ad libitum access to 10% w/v glucose and standard chow.....</i> | <i>161</i> |
| <i>Figure 5.1 Effect of increased arcuate glucokinase activity on energy-sensing enzymes.....</i> | <i>173</i> |
| <i>Figure 5.2 Effect of increased arcuate glucokinase activity on hypothalamic AMPK activity.....</i> | <i>174</i> |
| <i>Figure 5.3 Effect of inhibiting arcuate nucleus K_{ATP} channels on food intake.....</i> | <i>176</i> |
| <i>Figure 5.4 Effect of inhibiting arcuate nucleus K_{ATP} channels on glucose intake.....</i> | <i>177</i> |
| <i>Figure 5.5 Effect of inhibiting arcuate nucleus K_{ATP} channels on glucose appetite.....</i> | <i>179</i> |
| <i>Figure 5.6 Effect of activating arcuate nucleus K_{ATP} channels on food intake.....</i> | <i>181</i> |
| <i>Figure 5.7 Effect of activating arcuate nucleus K_{ATP} channels on glucose intake.....</i> | <i>182</i> |
| <i>Figure 5.8 Effect of activating arcuate nucleus K_{ATP} channels on glucose appetite.....</i> | <i>184</i> |
| <i>Figure 5.9 Effect of activating arcuate nucleus K_{ATP} channels on glucose appetite.....</i> | <i>185</i> |
| <i>Figure 5.10 Effect of increased arcuate glucokinase activity on energy-sensing enzymes.....</i> | <i>186</i> |
| <i>Figure 5.11 Effect of increased arcuate glucokinase activity on glucose-stimulated NPY-release from hypothalamic neurons.....</i> | <i>187</i> |
| <i>Figure 5.12 Effect of increased arcuate glucokinase activity on glucose-stimulated αMSH-release from hypothalamic neurons.....</i> | <i>188</i> |
| <i>Figure 6.1 Proposed mechanism for the effects of ARC glucokinase on energy homoeostasis.....</i> | <i>196</i> |
| <i>Figure Appendix 1: Coronal section of the rat brain.....</i> | <i>224</i> |
| <i>Figure Appendix 2: Nutritional information for RM1 normal chow diet.....</i> | <i>225</i> |
| <i>Figure Appendix 3: Nutritional information for high-energy diet.....</i> | <i>226</i> |

1 General Introduction

1.1 The obesity pandemic

Obesity is a pandemic with myriad medical complications that shorten lifespan and decrease quality of life in humans (Hussain and Bloom, 2011b, Levin et al., 2004). Obesity increases the risk of developing a number of medical conditions, including type 2 diabetes mellitus (T2DM), hypertension, dyslipidaemia, coronary heart disease, stroke, osteoarthritis and cancer (Bray, 2004). The last few decades has seen a steep rise in the worldwide prevalence of obesity. The WHO projects that by 2015 approximately 2.5 billion adults will be overweight and 700 million adults will be obese (WHO, 2006). This has enormous health implications but also impacts on societal disease burden and healthcare costs. Treatment options at present are limited (Hussain and Bloom, 2011a). Therefore, a better understanding of the mechanisms governing energy homeostasis is urgently needed in order to develop safe and effective treatment options for this growing problem.

1.2 Energy homeostasis and obesity

Energy homeostasis or energy balance involves coordinated responses that allow food intake, energy expenditure, and body adiposity to be homeostatically regulated. The aim of energy homeostasis is to achieve a balance between promoting hunger, satiety, efficient digestion and nutrient absorption and augmenting energy stores whilst food is available. This balance is dependant on a number of factors and involves integrating neural, nutrient and hormonal signals from various parts of the body involved in energy intake or expenditure. The primary cause for the current rise in obesity is an imbalance between energy intake, e.g. excessive calorie intake due to increased access to calorie dense foods, and decreased energy expenditure, e.g. sedentary lifestyle (James, 2008, Friedman, 2003).

1.3 Role of the hypothalamus in energy homeostasis

The hypothalamus is considered as the 'gate-keeper' in the control of energy homeostasis. Neural, nutrient and endocrine signals converge directly and indirectly on the hypothalamus. These signals emanate from various peripheral organs such as the gut, pancreas, liver and other parts of the CNS, such as the brainstem (Hussain and Bloom, 2012). The hypothalamus can integrate the signals and generate homeostatic responses

such as hunger and satiety. The hypothalamus also has a number of important anatomical and functional links between a number of important central and peripheral nervous system regions regulating energy homeostasis. Through these connections, the hypothalamus may be able to communicate with higher cortical centres influencing memory and reward and the brainstem which influences the sympathetic and parasympathetic nervous system that can regulate a number of other important homeostatic processes.

The hypothalamus is located at the base of the brain and in between the cerebral cortex and the midbrain. It can be subdivided into four regions in the anteroposterior axis each containing discrete neuronal populations or nuclei (Swanson, 1999). It is thought that several different nuclei are important in the homeostatic regulation of different processes.

1.3.1 Lateral hypothalamus

Historically, the lateral hypothalamus was thought of as the 'hunger centre'. This was based on lesioning experiments in animals where damage to the lateral hypothalamus produced anorexia (Anand and Brobeck, 1951). Whilst this view still largely holds true, it has been recently refined by our enhanced understanding of the role of individual nuclei within the hypothalamus and communication between them. In relation to energy homeostasis, there are two well established populations of neurons in the LH; those expressing orexin and another expressing melanin concentrating hormone (MCH) (de Lecea et al., 1998, Broberger et al., 1998). Activation of NPYergic neurons, which project from the ARC to the LH, causes the release of orexin A and B from orexin neurons (Horvath et al., 1999). Orexins are orexigenic neuropeptides which increase arousal and food searching behaviour (Sakurai et al., 1998). Evidence from mice with targeted deletion of either MCH or the MCH receptor, and intracerebroventricular injection of MCH suggest that MCH may play an opposing role to that of the orexins (Qu et al., 1996, Rossi et al., 1997).

1.3.2 Arcuate Nucleus

The arcuate nucleus (ARC) is one of the main hypothalamic nuclei regulating appetite (Konner et al., 2009). It is situated adjacent to the third ventricle and close to the median

eminence. A semi-permeable blood-brain barrier resulting from a highly fenestrated local capillary network is thought to allow peripheral signals, such as hormones and nutrients, to gain access to the central nervous system (Broadwell et al., 1983). Lesions of the ARC in mice result in hyperphagia and obesity (Olney, 1969). The ARC is responsive to a wide range of hormones and nutrients. The importance of ARC was highlighted when it was demonstrated as a potent site of leptin action (Cone et al., 2001).

Two well characterized groups of arcuate neurons have been shown to regulate food intake and energy homeostasis. These are the orexigenic neuropeptide Y (NPY)/ agouti-related peptide (AgRP) neurons and anorexigenic neurons containing pro-opiomelanocortin (POMC)/ cocaine- and amphetamine-regulated transcript (CART) neurons (Cone et al., 2001). These neuronal populations have been shown to contain the necessary cellular apparatus to sense nutrients and hormones. For example, these neuronal populations have been shown to contain a high density of insulin receptor, ghrelin receptor and leptin receptor. This allows ARC neuronal populations to be activated and inhibited by peripheral signals. NPY neurons are activated by ghrelin and inhibited by leptin. POMC neuronal populations are activated by leptin and insulin (Cone et al., 2001, Konner et al., 2009).

The ARC neuronal populations communicate with other hypothalamic nuclei implicated in the control of food intake, such as paraventricular nucleus (PVN), dorsomedial nucleus (DMN), lateral hypothalamus (LH), and ventromedial nucleus (VMN) (Kalra et al., 1999, Bouret et al., 2004). The POMC and NPY neuronal populations have efferent projections to other hypothalamic nuclei and other extra-hypothalamic regions of the brain implicated in energy homeostasis (Cone et al., 2001). NPY/AgRP neurons project to the LH and the PVN. POMC/CART neurons project to numerous hypothalamic and extra-hypothalamic regions (Cone et al., 2001). The presence of key neuronal populations that are capable of sensing and responding to peripheral signals and that have neuro-anatomical connections to other brain regions important in energy homeostasis allows the ARC to act as a critical regulator of energy homeostasis.

1.3.3 Ventromedial hypothalamic nucleus

Historically the VMN was considered to be the 'satiety centre'. Lesions of the medial hypothalamus led to hyperphagia (Mayer and Thomas, 1967). The VMN receives input from hypothalamic nuclei including the PVN, DMN and LH and returns projections to the LH and DMN. Unlike the ARC and LH, the neuropeptide expression of the VMN is less well characterised. Recent work suggests that brain-derived neurotrophic factor and steroidogenic factor-1 both play important roles in regulating energy homeostasis downstream of melanocortin-4 and leptin receptors, respectively (Xu et al., 2003, Dhillon et al., 2006).

1.4 Other central pathways controlling energy homeostasis

1.4.1 Role of the brainstem in energy homeostasis

The caudal brainstem also plays an important role in controlling energy homeostasis (Grill and Kaplan, 2002). The dorsal vagal complex in the caudal brainstem enables communication between the periphery and hypothalamus to control energy homeostasis. Neural, nutrient and hormonal signals from the periphery, especially the gastrointestinal tract, are sensed in the brainstem by mechanisms similar to those in the hypothalamus (Blevins and Baskin, 2010, Grill et al., 2002, Lebrun et al., 2006). These signals converge in the brainstem and are relayed to the hypothalamus (Schwartz, 2000, Price et al., 2008, ter Horst et al., 1984). The hypothalamus integrates these and other signals to generate an efferent signal which is transmitted via the brainstem to modulate appetite and gastrointestinal function (Blevins and Baskin, 2010, ter Horst et al., 1984, Grijalva and Novin, 1990). The vagus plays an important role in the transmission of afferent and efferent neural signals between gastrointestinal system and nucleus of the tractus solitarius in the dorsal vagal complex (Schwartz, 2000).

1.4.2 Role of the cortico-limbic system in energy homeostasis

Hedonism, reward and mnemonic representations of food experiences strongly affect the homeostatic control of food intake (Berthoud, 2006). These non-homeostatic factors are influenced by the environment and processed via the corticolimbic system. The

corticolimbic system consists of structures including prefrontal cortex, nucleus accumbens, ventral striatum, hippocampus and amygdala. The importance of communication between homeostatic and non-homeostatic centres in altering food intake is highlighted by histochemical and pharmacological studies demonstrating connections and influences from the corticolimbic system to the hypothalamic centres controlling appetite (Berthoud, 2006). Recent data suggests that non-homeostatic systems are modulated by homeostatic signals (Grill et al., 2007, De Silva et al., 2011). It has also been postulated that altered sensing of homeostatic signals in common obesity may alter the desire to consume calorie dense foods (Page et al., 2011a).

1.5 Glucose-sensing by the hypothalamus and regulation of energy homeostasis

1.5.1 Hypothalamic glucose-sensing and food intake

The brain uses glucose as its predominant energy substrate for its metabolic needs during normal physiology (Amiel, 1995). The idea of food intake regulation by the brain in response to changes in plasma glucose levels was first proposed by Jean Mayer more than 50 years ago as the 'glucostatic theory of feeding' (Mayer, 1952). Mayer hypothesized the presence of hypothalamic glucoreceptors that altered their electrical activity in response to changes in their rate of glucose utilisation, i.e. glucose-sensitive neurons. He proposed that feelings of hunger, when plasma glucose was reduced, and satiety, when plasma glucose was sufficient, were conveyed by these neurons (Mayer, 1953). In keeping with this hypothesis, it has been demonstrated that marked peripheral and central glucoprivation can stimulate feeding, as seen during hypoglycaemia (Miselis and Epstein, 1975, Biggers et al., 1989, Tsujii and Bray, 1990, Dunn-Meynell et al., 2009) In the same way, acute and chronic central glucose infusions reduce feeding in rodents (Kurata et al., 1986, Davis et al., 1981). The VMH was shown to have a central role in this, as chronic glucose infusions directly into the VMH reduced feeding by 27% (Panksepp and Rossi, 1981). Mayer's hypothesis was further strengthened by the identification of glucose-sensitive neurons in the hypothalamus (Oomura et al., 1964, Anand and Pillai, 1967). However, the precise role of central glucose-sensing in day to day food intake in normal physiology still remains to be addressed.

1.5.2 Hypothalamic glucose-sensing and glucose homeostasis

Glucose-sensing by the hypothalamus is also an essential component of the counterregulatory response (CRR) to hypoglycaemia. The role of the VMH in this response has been well characterised using in-vivo rodent models. Peripheral hypoglycaemia with central euglycaemia, maintained via bilateral carotid and vertebral glucose infusions, results in a markedly reduced CRR (Biggers et al., 1989). Furthermore, direct VMH glucose infusions abolish the CRR to hypoglycaemia and VMH infusion of 2-deoxyglucose (2DG), a glucose anti-metabolite, in the setting of peripheral euglycaemia initiates a CRR (Borg et al., 1995, Borg et al., 1997). Therefore, the VMH plays a key role in detecting glucose and mediating the CRR in response to glucoprivation. Other nuclei, such as DMH and PVN, have also been shown to modulate CRR (Evans et al., 2003, Evans et al., 2004).

More recently it has also been demonstrated that disruption of glucose-sensing mechanisms in neuronal pathways implicated in the melanocortin system alters glucose homeostasis possibly via changes to hepatic glucose output (Parton et al., 2007b, Kong et al., 2010, Rossi et al., 2011). Transgenic mice expressing mutant form of the ATP-sensitive K⁺ channel (K_{ATP}) subunit Kir6.2 under the transcriptional control of the POMC promoter demonstrate disrupted glucose-sensing in the POMC neurons, as well as impaired glucose homeostasis (Parton et al., 2007b). A similar approach in MCH neurons of the lateral hypothalamus impaired glucose homeostasis (Kong et al., 2010). Re-expression of melanocortin-4 receptors (MC4R) in cholinergic neurons of MC4R knockout mice improves glucose homeostasis (Rossi et al., 2011). Preliminary evidence also suggests a role for hypothalamic glucose-sensing in modulating insulin secretion, however further work is needed to confirm this (Osundiji et al., 2012).

1.5.3 Glucose-Sensitive Neurons

The identification of glucose-sensitive neurons in regions of the hypothalamus involved in the regulation of appetite and glucose points towards a physiological role for these neurons

in allowing the hypothalamus to detect changes in glucose and respond accordingly (Levin et al., 2004). Apart from the hypothalamus, glucose-sensitive neurons have also been found in the hindbrain, motor cortex, amygdala and septum (Ishihara et al., 2003, McCrimmon, 2008). In the amygdala, these neurons may also be involved in modulating the CRR to hypoglycaemia (Zhou et al., 2010) . In other parts of the CNS, the precise function of these neurons requires further investigation.

Hypothalamic glucose-sensing neurons are divided into two groups based on their electrophysiological response to glucose. Glucose-excited (GE) neurons increase their activity as glucose levels rise, and glucose-inhibited (GI) neurons increase their activity as glucose levels fall (Levin et al., 2004, Routh, 2002). As in β cells, glucokinase has a prominent role in the glucose-sensing mechanism and acts as a neuronal glucose-sensor (Levin et al., 2004).

1.5.4 Glucokinase and glucose-sensing

The first step in glycolysis involves phosphorylation of glucose to form glucose-6-phosphate. In majority of the cells in the body this first step is catalysed by hexokinase (also known as hexokinase I). Hexokinase is saturated by glucose at physiological levels and is inhibited by its own product, glucose-6-phosphate. However, in the pancreatic β -cells this is also catalysed by glucokinase (also known as hexokinase IV) (Ilyedjian et al., 1989). Glucokinase is a 50kDa hexokinase isoenzyme. It differs from other hexokinases because it has high K_m for glucose and is not inhibited by its product (glucose-6-phosphate). This allows the rate of glycolysis to be dependent on cellular glucose rather than enzymatic capacity (Matschinsky et al., 2006). Therefore by catalysing this first step in glycolysis, pancreatic glucokinase allows coupling of insulin secretion to changes in plasma glucose and acts as a 'glucose-sensor'.

A point worth mentioning in relation to the glucose-sensing role of glucokinase is that intracellular ATP is very well buffered even with fluctuations in utilisation of glucose (Levin et al., 2004). Glucokinase is unlikely to have a significant effect on cellular ATP in cells expressing this enzyme. This makes its role in mediating the effects of glucose via altered ATP

generation from altered glycolytic flux difficult to understand. In the islet cell, glucokinase has been shown to directly alter the activity of K_{ATP} channels and this is very well established. It has been suggested that subcellular localisation and mobility patterns of glucokinase may influence the location of ATP generation (Levin et al., 2004, Ashcroft, 1988). The close proximity of glucokinase to membrane bound K_{ATP} channels may result in local changes in ATP near the channel and alter their activity. Direct evidence for this is lacking, however specific localisation patterns have been seen with glucokinase in hepatocytes (Mukhtar et al., 1999). Therefore, glucokinase's effects on K_{ATP} channels are less likely to be influenced by hexokinase, which may control the cells overall glucose metabolism and ATP levels.

Glucokinase is expressed in, liver and pancreatic forms in the pancreas, liver and hypothalamus. Although the enzymatic activity of the liver and pancreatic isoforms is identical, they perform different functions in each tissue and are differentially regulated. In the liver, glucokinase allows rapid take up of glucose following feeding, and expression varies between the fed and fasted states (Massa et al., 2011). In the hypothalamus, the precise physiological role of glucokinase is unclear; however, as discussed earlier, it acts as a glucose-sensor in glucose-sensitive neurons.

1.5.5 Mechanism of hypothalamic glucose-sensing

The mechanisms used by GE neurons to detect a decrease in glucose are analogous to the glucose-sensing mechanism of the pancreatic β -cells. A rise in glucose results in increased ATP/ADP production via glycolysis and causes closure of ATP sensitive K^+ channels, leading to neuronal membrane depolarisation, action potential and neurotransmitter release (Levin et al., 2004). Glucokinase plays a key role in the glucose-sensing mechanism in these neurons (Levin et al., 2004) (figure 1.1). In keeping with this, 70% of GE neurons express glucokinase (Kang et al., 2006). POMC neuron-specific mutation in the K_{ATP} channel subunit Kir.2 impairs glucose-sensing in mouse POMC (Parton et al., 2007b). This suggests that glucose-sensing in anorexigenic POMC neurons occurs via a similar mechanism to β -cell. K_{ATP} channels are also present in NPY/AgRP expressing neurons of the ARC and their response to

glucose is blunted in Kir6.2 knockout mice (Van den Top et al., 2007, Park et al., 2011, Lynch et al., 2000).

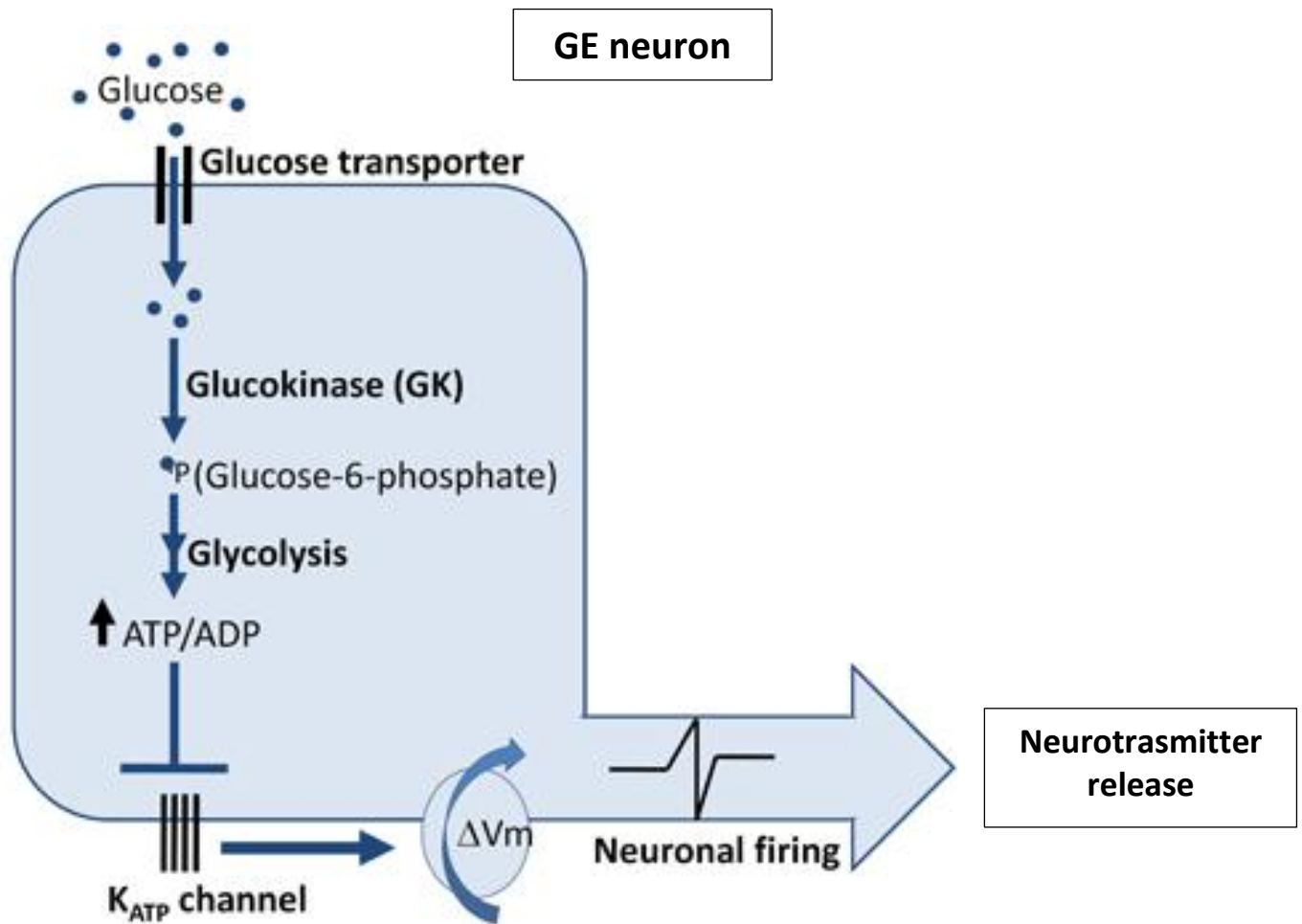


Figure 1.1 Glucose excited neuron: Mechanism for glucose-sensing in the GE neurons. Glucokinase allows glycolytic flux to be coupled with glucose entry. Therefore, increased glucose entry leads to increased ATP/ADP ratio. This results in closure of ATP sensitive K⁺ channel leading to subsequent membrane depolarisation and neurotransmitter release. Adapted from (Diggs-Andrews et al., 2009).

It is thought that GI neurons also utilise a mechanism involving glucokinase, as well as nitric oxide and adenosine 5'-monophosphate-activated protein kinase (AMPK) to depolarize in response to low glucose levels (Canabal et al., 2007, Fioramonti et al., 2010, Kang et al., 2006). In keeping with this, approximately 45% of GI neurons express glucokinase. (Kang et al., 2004). Furthermore, AMPK knockout in AgRP neurons, which are thought to be GI neurons, impairs glucose-sensing in these neurons (Claret et al., 2007). Activation of AMPK

may phosphorylate, and inhibit membrane chloride channels, leading to depolarisation (Mountjoy and Rutter, 2007) (figure 1.2).

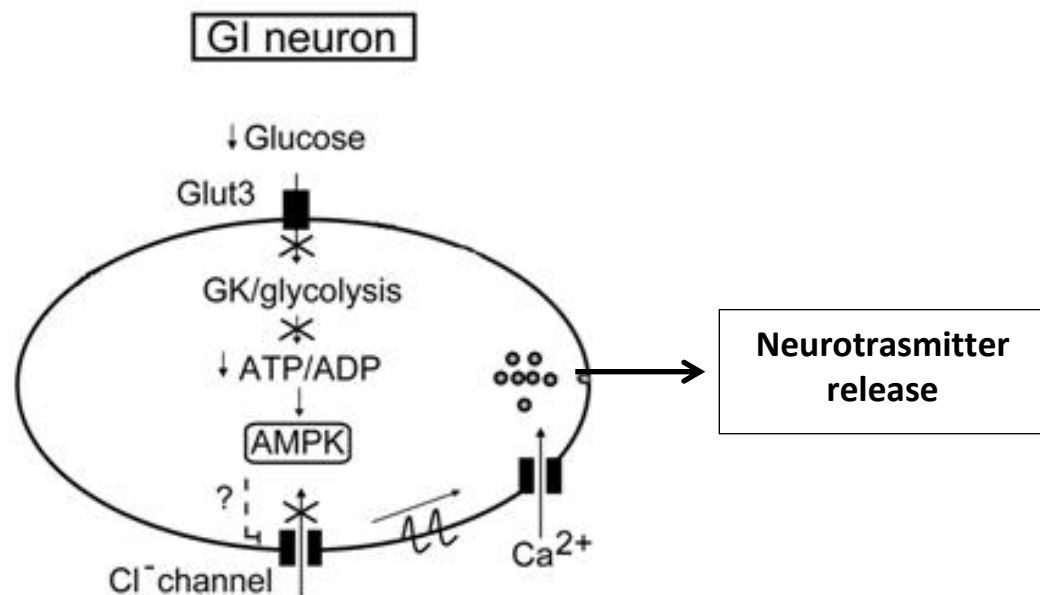


Figure 1.2 Glucose inhibited neuron: Potential mechanism for glucose-sensing in GI neurons. Glucokinase allows glycolytic flux to be coupled with glucose entry. In response to reduced glucose entry, reduced rate of glycolysis results in reduced cellular ATP and increased activation of AMPK. Increased AMPK activity inhibits membrane Cl⁻ channels leading to membrane depolarisation and neurotransmitter release. Adapted from (Mountjoy and Rutter, 2007).

GE neurones may also utilise AMPK to enable them to respond to glucose. In support of this, AMPK knockout in POMC neurons impairs glucose-sensing in POMC neurons (Claret et al., 2007). It is currently not clear as to how AMPK allows POMC neurons to sense glucose. It is possible that AMPK may regulate expression of GLUT family members or may affect K_{ATP} channel opening (Belgardt et al., 2009).

Taken together, above postulated mechanisms and current evidence suggest that glycolytic flux is influenced by glucokinase activity and glucose entry into neuronal cells. Both K_{ATP}

channels and AMPK activity may provide mechanisms which allow neuronal cells to alter their depolarisation in response to changes in glycolytic flux. Both mechanisms may operate in NPY and POMC neurons and these mechanisms are not exclusive to a particular cell type.

1.5.6 Hypothalamic distribution of glucose-sensing neurons

Hypothalamic glucose-sensing neurons are located in the PVN, LHA, VMN and ARC; the latter two nuclei are collectively referred to as the VMH (Lynch et al., 2000). Most of the evidence regarding the functional role and neurotransmitter identity of these glucose-sensing neurons relates to the VMH and LHA.

1.5.6.1 *The arcuate nucleus (ARC)*

The ARC contains a large number of glucose-sensing neurons, which overlap with both orexigenic NPY/AgRP and anorexigenic POMC/CART neurons suggesting a role in appetite (Mountjoy and Rutter, 2007). 94% of GI neurons isolated from the rat ARC have been shown to be immunoreactive for NPY (Muroya et al., 1999). The identity of the NPY neuron as a GI neuron has been consistently repeated by other investigators (Mountjoy and Rutter, 2007). Following electrophysiological studies of POMC neurons in mice, it was considered that POMC neurons are GE neurons (Ibrahim et al., 2003). Disruption of K_{ATP} channels in POMC neurons impairs glucose-induced excitation, supporting the identity of POMC neurons as GE neurons.(Parton et al., 2007b).

1.5.6.2 *The Ventromedial Nucleus*

As discussed earlier, the VMH, consisting of the VMN as well as the ARC, has been shown to have a very important role in the regulation of glucose homeostasis. Despite the extensive work on the physiological role of the VMN glucose-sensing neurons, their neuropeptide expression has not been well characterised (Burdakov et al., 2005b).

1.5.6.3 *The Lateral Hypothalamic Area (LH)*

In the LH, a majority of the orexin neurons have been shown to be inhibited by glucose (GI neurons) (Burdakov et al., 2005a, Burdakov et al., 2005b). It has been postulated that these glucose-sensing neurons may regulate alertness and arousal patterns in response to glucose in the LH. A majority of the MCH neurons in the lateral hypothalamus have been shown to be excited by glucose (GE neurons) (Burdakov et al., 2005b). Recent work highlights that glucose induced excitability in MCH neurons is mediated by K_{ATP} channels and is involved in regulating glucose homeostasis (Kong et al., 2010).

1.5.7 Glucokinase and neuronal glucose-sensing

The presence of the pancreatic form of glucokinase, the glucose sensor in pancreatic β -cells, in regions of the brain where glucose responsive neurons are present and functionally important supports an important role for glucokinase in the detection of glucose (Levin et al., 2004). Pharmacological activation of glucokinase increases GE neuronal activity and decreases GI neuronal activity to low glucose (Kang et al., 2006). Reduction of glucokinase mRNA by 90% in cultured VMH neurons abolishes glucose sensitivity in GE and GI neurons (Kang et al 2006). For this reason glucokinase is considered as the primary regulator of neuronal glucose-sensing (Levin et al., 2004).

Despite the strong evidence for its role as a glucose sensor, doubts over its ability to sense glucose in the brain have been raised. Blood glucose in the brain is lower than plasma glucose and may not exceed 5 mmol/L (Routh, 2002) (Roncero et al., 2000, Silver and Erecinska, 1994). Therefore, the inflection point of glucokinase, considered to be 3.5mmol/L, is likely to be higher than glucose in the brain (Matschinsky et al., 2006). If this prediction is correct, glucokinase may not be able to sense glucose in the brain, especially as GE neurons appear to be most sensitive to changes in glucose concentrations of <2mmol/l (Wang et al., 2006). However, changes in glucokinase lead to changes in glucose sensitivity in GE neurons (Kang et al., 2006). Reasons for this discrepancy between predictions and observed results are not clear. It is possible that glucose levels in regions where blood brain barrier is not complete, e.g. the ARC, may be high enough to permit glucose-sensing via glucokinase. Alternatively, the *in vitro* assessment of glucokinase's inflection point in

relation to glucose may not be applicable to *in vivo* settings, where other factors such as regulatory proteins alter glucokinase's activity (Postic et al., 2001, Matschinsky et al., 2006).

As mentioned earlier, glucokinase is not expressed in all GE and GI neurons and supports the presence of alternative mechanisms for neuronal glucose-sensing. Such mechanisms have been proposed, one of which involves an astrocyte-neuron lactate shuttle (Pellerin et al., 1998, Lam et al., 2005a). This mechanism involves lactate in the brain, which is released primarily from astrocytes, and is taken up by neurons via the monocarboxylate transporter (MCT1). Once transported across the cell membrane, lactate is converted to pyruvate by lactate dehydrogenase (LDH). Metabolism of pyruvate results in an increase in ATP/ADP ratio, closing ATP-sensitive K⁺ channels (Penicaud et al., 2006). Specific pharmacological inhibition of lactate dehydrogenase results in loss of central glucose-sensing following glucose infusion (Lam et al., 2008).

The mechanism of neuronal glucose-sensing is under considerable debate. The current evidence implicates glucokinase as one of the main glucose-sensors in the hypothalamus. However, it is likely that other neuronal mechanisms such as the lactate shuttle play an important role in altering neuronal excitability in response to changes in glucose. Despite evidence indicating that glucokinase has an important role in glucose-sensing and that glucose-sensing is likely to have important roles in appetite, the physiological role of hypothalamic glucokinase in appetite has not been conclusively demonstrated (Levin et al., 2011).

1.5.8 Glucose-sensing neurons as metabolic sensors

Although glucose is an important energy signal, other metabolic signals also play an important role in coordinating energy homeostasis. Glucose-sensitive neurons also respond to other hormonal and metabolic signals, such as insulin, leptin, lactate, ketone bodies, and long chain fatty acids (LCFA) (Levin, 2006). The observation that lipid administration to the basomedial hypothalamus results in decreased feeding and decreased glucose production by the liver suggests an important role for lipids in the control of appetite and glucose homeostasis (Lam et al., 2005c). The excitability and inhibition of ARC

neuronal populations to oleic acid, the most abundant fatty acid in human adipose tissue, is influenced by glucose (Kokatnur et al., 1979, Wang et al., 2006). This suggests an interaction between glucose and fatty acid metabolism regulates neuronal excitability in the ARC. Neurophysiological studies demonstrate that glucose regulates leptin's effects on neurons in the ARC (Ma et al., 2008b). Thus, glucose sensitive neurons may represent focal points where signals converge to alter appetite and allow various signals to act in concert to influence the initiation and termination of meals. The mechanisms by which signals from different metabolites are integrated to generate a net physiological output from neuronal populations regulating energy homeostasis are still under investigation. Current hypothesis suggests that key cellular processes relevant to energy homeostasis are altered by the cellular influx of a variety of metabolites and provide a unifying mechanism for neuronal cells to integrate a variety of signals (Jordan et al., 2010). One such pathway which may integrate alterations in cellular biochemistry resulting from LCFA, glucose, insulin, ghrelin and leptin is the malonyl-CoA/ LCFA-CoA/AMPK pathway (fig 1.3) (Lam et al., 2005c, Lam et al., 2009, Loftus et al., 2000, Andersson et al., 2004, Minokoshi et al., 2004). This may provide a common metabolic pathway to alter ATP production and lipid accumulation in neuronal cells, leading to altered neuronal depolarisation in response to different metabolites and nutrients. (Penicaud et al, 2006)

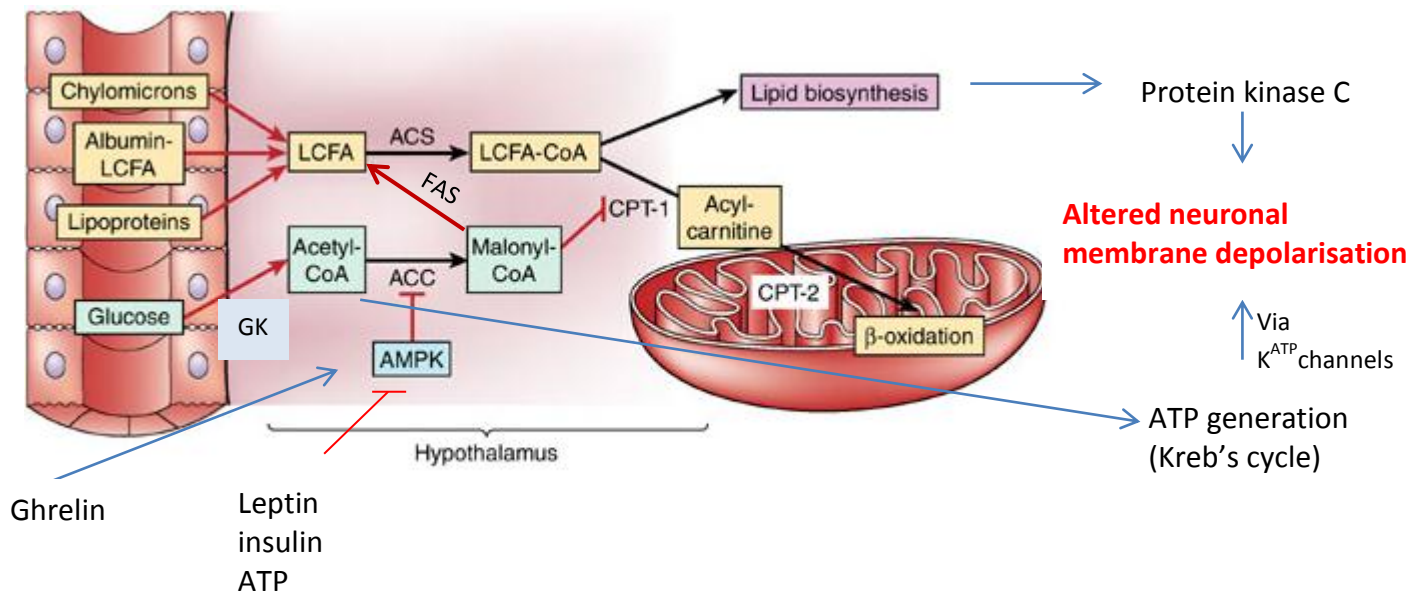


Figure 1.3 A possible integrated mechanism for neuronal metabolic sensing: In the presence of LCFA, LCFA-CoA is formed which can be used for β -oxidation by the mitochondria or intracellular lipid biosynthesis. Influx of glucose leads to inhibition of β -oxidation by malonyl-CoA, leading to increased intracellular lipid biosynthesis and accumulation of lipid in the cytoplasm. The termination of lipid in the cytoplasm activates Protein kinase C and causes membrane depolarisation. Influx of glucose also leads to ATP generation via glycolysis the Krebs cycle resulting in increased ATP synthesis and altered membrane depolarisation via K_{ATP} channels. The effect of ghrelin, leptin and insulin may converge on this pathway via their influences on AMPK activity. The net effect is altered neuronal membrane depolarisation in response to varied nutrients and metabolites leading to hunger or satiety. Adapted from (Lam et al, 2005)

1.6 Approaches to study neural circuits controlling energy homeostasis in rodents

1.6.1 Direct administration of compounds

Direct administration of compounds to specific neuroanatomical areas in the brain via cannulation has greatly enhanced our understanding of the neural control of energy homeostasis (Zarjevski et al., 1993, Davis et al., 1981). This approach allows precise delivery of neuropeptides, pharmacological agents and nutrients to regions of the brain involved in control of energy homeostasis, such as specific hypothalamic nuclei. However, there are certain technical and practical limitations of these techniques. Direct injection of compounds can only be used for short-term studies due to the short duration of action of most pharmacological agents. Furthermore, direct injections should only be repeated for a limited number of times as repeated injections result in inflammation and destruction of brain tissue at the injection site. Therefore, this approach is useful for the study of the acute effects of administered compounds but may not be feasible for chronic studies.

1.6.2 Genetic modification

The limitations of direct administration of compounds can be overcome by the use of genetic modification of rodents. The aim of this technique is to selectively alter the expression of genes, implicated in energy homeostasis, and compare the resulting phenotype with appropriate controls. Several different approaches are possible, each having their own advantages and disadvantages.

1.6.2.1 *Transgenic mice*

Since the description of a method to produce transgenic mice, genetically manipulated or 'knockout' mice have been widely used and have provided great insight into the field of energy homeostasis (Gordon et al., 1980). However, problems related to developmental compensation to genes knocked out, embryonic lethality of global genetic knockouts and widespread alterations of the gene being studied in all cell types of knockout animals have made it difficult to fully assess the role and impact of individual genes. For example,

AgRP/NPY knockout mice do not display any alterations in food intake and body weight, whereas mice with post-embryonic ablation of AgRP using an alternative approach were lean and hypophagic (Qian et al., 2002, Bewick et al., 2005). Another example includes glucokinase knockout mice. Homozygous glucokinase knockout mice die within the first week of birth owing to the lethal effects of global glucokinase knockout (Yang et al., 2007). Heterozygous glucokinase knockout mice are described as hyperphagic (Orban et al., 1992) but also have impaired glucose homeostasis as glucokinase expression is altered in the pancreas and liver, making it difficult to assess the involvement of neuronal glucokinase on appetite in this model. Therefore knockout mice have their limitations. These limitations have prompted the use tissue-specific targeting strategies for gene modification to study the neural control of appetite.

1.6.2.2 *Cre-lox mice*

By using tissue-specific promoters, gene expression can be altered in specific cell types. Cre-recombinase (Cre) is an enzyme that removes or inverts DNA that is found between lox-p sites (Hoess and Abremski, 1985). By crossing a mouse in which Cre expression is driven by a specific promoter with a mouse that has lox-P sites intersecting the gene of interest, the gene of interest is removed only in those cells where the specific promoter is expressed (Orban et al., 1992). This approach has been used successfully in a number of mouse models that have allowed production of cell type or tissue-specific genetic ablation. Unfortunately, specific promoters do not always exist for regions or cells of interest and this technique has its limitation in the settings. For example, the ARC does not have any specific promoters. This strategy would therefore not be particularly suitable for specifically targeting the ARC.

1.6.2.3 *Gene delivery vectors*

Gene transfer via vectors allows direct targeting of genes to a specific region of interest. The gene delivered can also be expressed specific promoter to allow more precise targeting. These strategies allow spatial and temporal control of gene expression, preventing problems related to global alterations in gene expression and developmental compensation. They also have the advantage of manipulating gene expression in larger animals such as rats, as well as mice. Furthermore, long breeding times typically incurred when using transgenic mice

can be avoided and large groups of animals can be studied at one particular time point. There are some limitations for the study of neural control of energy homeostasis. Precise delivery of the vector to specific hypothalamic nuclei requires accurate stereotaxic injections in adult rodents. This is currently possible using stereotaxic methods for smaller nuclei (e.g. ARC) in larger animals (e.g. adult rats) or larger regions (e.g. VMH) in smaller animals (e.g. mice). The consistent accuracy of small nuclei such as the ARC may be difficult to achieve in smaller animals such as mice. Adequate time must be allowed for maximal stable gene expression to be achieved. This varies on the type of vector used but can be up to four weeks.

An ideal vector should achieve efficient, long-term transduction and desired expression levels in the tissue or cell being studied. It also should be safe, simple to produce, non-toxic and non-immunogenic. Nonviral and viral vectors can be used to deliver genetic information, each having certain advantages and disadvantages as described in the section below.

Non-viral vectors

Non-viral transfection methods include naked vector DNA, liposomes, cationic polymers, electroporation of cells, etc. The efficiency of cell transfection with non-viral vectors is lower, more variable and short-term compared to viral vectors, however they have the potential to carry larger amounts of DNA (Gardlik et al., 2005). Non-viral vectors are generally used for *in vitro* gene transfer.

Viral vectors

Vectors utilise the properties of viruses to insert their genome into the host cell nucleus and produce transgene expression. A number of different viruses have been adapted for use as viral vectors. These include adenoviruses, retroviruses, lentiviruses, herpesviruses, and adeno-associated viruses. These viruses differ in their toxicity, immunogenicity, safety, complexity, abilities to produce sustained transgene expression for a desired length of time, target specific tissues and carry certain sizes of DNA.

Adenoviruses are double-stranded DNA viruses capable of carrying large transgenes. They achieve high levels of infectivity and infect a wide range of tissues. Immunity to previously exposed adenoviruses severely reduces the duration of transgene expression, making this a less favourable vector (Kaplan et al., 1997). Furthermore, due to its size manipulation of the genome is difficult. It is also not selective to neuronal cells and also co-infects glial cells. (Duale et al., 2005)

Retroviruses are single-stranded RNA viruses. They require conversion to double-stranded DNA in the host cell and integration of this double-stranded DNA into the host genome. This integration occurs randomly and introduces a possibility of insertional mutagenesis of host genes (Temin and Baltimore, 1972). Retroviruses are also only capable of transducing their genetic material into actively replicating cells (Miller et al., 1990). These problems limit the utility of retroviruses as a gene transfer vector.

Lentiviruses are a subfamily of retroviruses. They overcome the problems associated with retroviruses. They are used as vectors for gene transfers into a number of different tissues and especially as vectors for delivery of short-interfering RNA (Naldini et al., 1996, Miyoshi et al., 1997, Sachdeva et al., 2007). Their safety is a concern, especially in the laboratory setting, as these viruses can be pathogenic in humans. They also have a tendency to spread which is a problem for stereotaxic injections.

Herpesviruses are double-stranded DNA viruses. They display neuronal tropism and have the ability to carry large transgenes. Replication defective herpes viruses are an attractive choice as a vector. However, problems related to its size, immunogenicity, cytotoxicity limit their potential use.

Adeno-associated virus

Adeno-associated virus (AAV) is a small (20-25 nm), single stranded, non-enveloped, virus, which has been widely used as a gene transfer vehicle (Daly, 2004b). The single-stranded genome is approximately 4.7kb and can be packaged into as positive-sense (5'-3') or negative-sense (3'-5') (Berns and Adler, 1972). AAV viruses are dependoviruses and

therefore replication defective. They require the presence of a helper virus (adenovirus or herpes simplex virus) to replicate and complete their life cycle. When a cell is infected with AAV the viral genome is conveyed to the nucleus and converted to a double-stranded form; however the virus cannot synthesise capsid proteins or be packaged without a helper virus. AAV also possesses no lytic capability and relies on the helper virus to liberate newly formed viral particles making it safe to work with and modify (Atchison et al., 1965). AAV has not been linked to any disease or immunological response (Blacklow et al., 1968, Samulski et al., 1989). 12 human serotypes and more than 100 primate serotypes have been described. Each of these displays tropism for specific cell type (Palomeque et al., 2007). AAV-2 is one of the best studied serotypes. It displays neuronal tropism and maintains stable gene expression in neurones for over one year (Klein et al., 2002, Daly, 2004b). It also does not induce any immunological responses in transfected organs (Ponnazhagan et al., 1997). These properties of AAV-2 make it particularly useful for the study of energy homeostasis.

AAV genome consists of two open reading frames (ORF) that are flanked on either side by two 145 base pair palindromic sequences known as inverted terminal repeats (ITRs) (Srivastava et al., 1983). ITRs are necessary for viral DNA replication, packaging and integration into the host genome. The palindromic sequences form a hairpin structure, which contributes to self-priming or primer independent second strand DNA synthesis (Lusby et al., 1980, Bohenzky et al., 1988). The AAV genome contains Rep gene in its 5' ORF. This gene produces for proteins Rep 78, Rep 68, Rep 52, and Rep 40 (Kyostio et al., 1994). Rep 78 and 68 are large regulatory proteins transcribed via the p5 promoter. Rep 52 and 40 are smaller proteins transcribed via the p19 promoter and have roles in viral DNA packaging (Im and Muzyczka, 1990). The Rep proteins suppress AAV gene expression when the helper virus is not present (Trempe and Carter, 1988). The AAV genome also contains the Cap gene in its 3' ORF. This gene produces VP1, VP2, and VP3 viral capsid proteins which are transduced via the p40 promoter. These proteins form the icosahedral viral protein coat of the AAV with VP3, accounting for 85% of the protein mass (Rose et al., 1971, Jay et al., 1981).

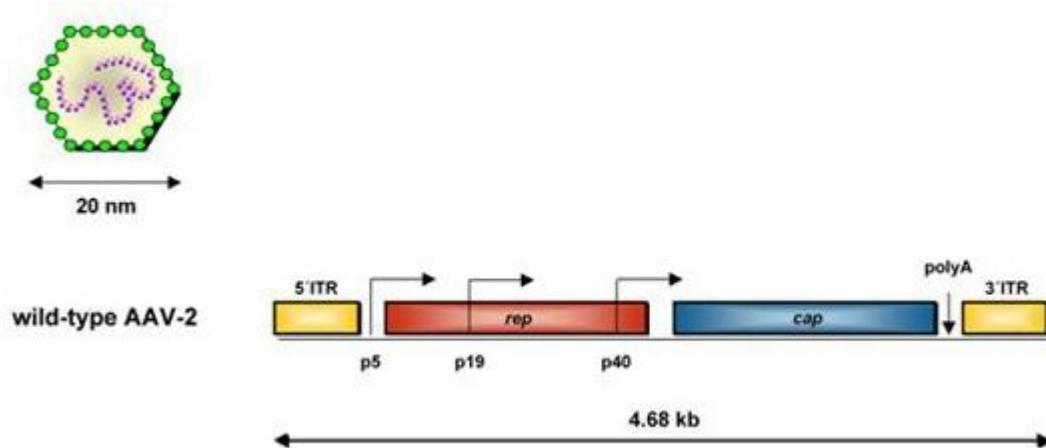


Figure 2.1 Diagram of wild-type AAV-2 serotype genome. ITRs flank the Rep and Cap genes and their promoters (p5, p19 and p40). Adapted from (Daya and Berns, 2008).

Recombinant AAV

Recombinant AAV (rAAV) differs from AAV in that the two genes necessary for producing structural and non-structural proteins (*cap* and *rep*) have been removed. The removal of these genes ensures that rAAV cannot form viral packages in the presence of a helper virus. During the production of rAAV, the *rep* and *cap* genes are provided in cis- along with necessary helper functions. Recombinant AAV contains the two inverted terminal repeats (ITRs) necessary for the production and function of the virus. The ITRs frame the expression cassette, which can be modified to include genes and promoters of choice, with the packaging capacity of approximately 4.5kb. After infecting the host cell, single-stranded viral genome of rAAV is converted to double-stranded DNA. This is considered as the rate-limiting step in allowing transgene expression (Afione et al., 1999, Ferrari et al., 1996). Hence, the steady-state for gene expression can take up to three weeks to achieve. The rAAV genome can integrate randomly into the host genome or may be present episomally in the host cell nucleus (Duan et al., 1998). rAAV does not produce any viral proteins, and, since ITRs are not translated (Samulski et al., 1989). It is therefore less immunogenic, which allows sustained transgene expression. Like AAV serotype-2, rAAV serotype-2 also displays strong neuronal tropism and lack tropism for glial cells, which is useful for studying the

neural control of energy homeostasis (Summerford and Samulski, 1998, Bartlett et al., 1998).

There are some limitations to rAAV. Although it is neurotropic, rAAV is relatively non-specific in which neurons it infects. Within a hypothalamic nucleus there may be different neuron types with different functions co-localised in one area. For example, in the ARC there are NPY and POMC neurons. rAAV would infect all neurons indiscriminately (Daly, 2004a). rAAV is also fairly difficult to produce. However, rAAV technology allows high level and stable transgene expression to be induced in animals. This, combined with neuronal tropism, nonpathogenic nature, lack of cytotoxicity and ease of manipulation make it a suitable vector for manipulating gene expression in neuronal cells. In this regard it has been successfully used to increase and decrease specific gene expression within the hypothalamus (Tiesjema et al., 2009, Gardiner et al., 2005). Therefore, this technology is particularly well-suited for studying the effects of altering glucokinase expression in specific hypothalamic nuclei on energy homeostasis.

1.7 Summary

The hypothalamus plays an integral role in the integration of a variety of neural, nutrient and hormonal signals to coordinate energy homeostasis. Recent work has identified the arcuate nucleus as having a pivotal role in this regard. Glucose is the primary energy source in mammals and essential to neuronal metabolism. Therefore it is not surprising that hypothalamic nuclei, which play a critical role in regulating energy homeostasis, also respond to changes in glucose. The exact mechanism by which this occurs and is integrated with sensing of other signals is currently under investigation. However, current evidence supports that glucokinase has a prominent role in glucose-sensing glucokinase is expressed in hypothalamic nuclei, such as the ARC, which have important roles in controlling energy homeostasis. The physiological role of ARC glucokinase and glucose-sensing in regulating appetite has not been investigated. Modulating glucokinase activity in the ARC may help elucidate this. The use of stereotaxically delivered pharmacological agents and rAAV in rodents provides a suitable approach to investigate this and forms the basis of this thesis.

2 Materials and Methods

All reagents were supplied by Sigma, Poole, Dorset, UK, unless otherwise stated.

2.1 Molecular and In-Vitro Techniques

2.1.1 Production of GKS (glucokinase-sense) using RT and PCR

2.1.1.1 *Tri reagent method for hypothalamic RNA extraction*

Materials

Tri-reagent (Helena Biosciences, Tyne and Wear, UK)

Absolute ethanol

Isopropanol

1-Bromo-chloro-propane

Glass distilled water (GDW)

Methods

Total RNA was extracted from tissues using Tri-reagent according to the manufacturer's protocol. Up to 100 mg hypothalamic tissue was ground under liquid nitrogen with a mortar and pestle before being homogenised in 1 ml Tri-reagent. The homogenised product was transferred to 1.5 ml eppendorf tubes and incubated at room temperature for 5 minutes. One hundred microlitres of bromo-chloro-propane was added to the homogenised product, vigorously mixed for 15 seconds, and incubated at room temperature for a further 5 minutes. RNA was separated by centrifugation at 4°C for 15 minutes at 12,000xg (centrifuge 5417 C/R, Eppendorf, Hamburg, Germany) with the brake off. The upper aqueous phase was transferred to a 1.5 ml eppendorf tube, precipitated using 500µl of room temperature isopropanol for 10 minutes at room temperature, and subjected to centrifugation for 10 minutes at 12,000xg and 4°C. The supernatant was discarded and the resulting pellet washed with one volume (1 ml) of 75 % (v/v) ethanol in GDW and subjected to centrifugation for a further 10 minutes at 12,000xg and 4°C. The pellet was then air dried, and dissolved in 400µl of autoclaved GDW. RNA concentration was determined spectrophotometrically. RNA was diluted 1:100 in GDW and 1 ml transferred into a quartz cuvette. Absorbance was read at 260 and 280 nm on a UV 1101 spectrophotometer (WPA, Cambridgeshire, UK). The concentration was calculated using the following formula: concentration (µg/ml) = (A₂₆₀ x dilution factor) x 40. Following quantification, RNA samples were ethanol precipitated using 0.1 volumes of sodium acetate (pH 5.2) and 2.5 volumes of

ice cold absolute ethanol. Samples were incubated at -20°C for a minimum of 1 hour and the RNA recovered by centrifugation for 20 minutes at 12,000xg and room temperature (F45-12-11 microfuge, Eppendorf, Hamburg, Germany). The supernatant was discarded and the pellet air dried under vacuum for 5 minutes. RNA was dissolved in the appropriate volume of GDW to give a 5 mg/ml solution.

2.1.1.2 Formaldehyde gel to confirm RNA integrity

Materials

Agarose, type II-A medium EEO

Formaldehyde

20x MOPS, pH 7.0 (appendix I)

0.4 M 3-(N-Morpholin) propanesulphonic acid (MOPS)

0.1 M sodium acetate

70 % (v/v) Formamide (appendix I)

3.5 % (v/v) Formaldehyde

1.5x MOPS

Gel loading buffer (appendix I)

0.02 M EDTA

0.04 % formaldehyde

10 mg/ml Ethidium bromide 70

DENAT

25 % (v/v) glycerol

0.1% orange G

25 mM EDTA

100x TE, pH 7.5 (appendix I)

1 M Tris base

0.1 M EDTA

2 M Sodium acetate, pH 5.2

GDW

Methods

RNA integrity was confirmed using a formaldehyde gel. A 1 % agarose denaturing gel was made in 7.5 % (v/v) formaldehyde and 1x MOPS buffer. 1µl RNA was added to 12µl of DENAT. Samples were incubated at 65°C for 5 minutes. 3µl of gel loading buffer was added thereafter. The samples were loaded onto the gel and electrophoresed in 1x MOPS and 7.5% formaldehyde (v/v) at 15 V/cm for 10 cm. The gel was stained for 30 minutes in 1x TE containing 0.01 mg/ml ethidium bromide on a shaking platform. The gel was destained in 1x TE overnight. The presence of 18 S and 28S ribosomal bands visualised under UV light (300 nm) confirmed RNA integrity.

2.1.1.3 Reverse transcription

Materials

Rat hypothalamic RNA (5mg/ml)

10mM dNTPs (GE Healthcare, Buckinghamshire, UK)

Oligo dT₍₁₂₋₁₈₎ 200ng/µl (GE Healthcare)

5x Reverse transcriptase buffer (Promega, Madison, WI)

Avian myoblastoma virus reverse transcriptase (RT) 10U/µl (Promega)

Methods

One milligram per millilitre RNA, 1x reverse transcriptase buffer, 1mM dNTPs and 10mg/ml oligo dT were made up to a final volume of 20 µl. This reaction mixture was heated to 65°C for 5 minutes and then cooled to room temperature for 30 minutes. 10U RT was then added and the reaction was incubated at 42°C for 1 hour. This reaction was then used in the polymerase chain reaction (PCR) as detailed below.

2.1.1.4 PCR

Materials

10x Taq buffer

10mM dNTPs (GE Healthcare)

Taq DNA polymerase (5U/µl)

For GKS: pCMV4.GKB1 encoding full length glucokinase (gift from M.Magnuson, Vanderbilt University)

20µM oligonucleotide primers (Oswel DNA service, Southampton, UK):

| Primer | Sequence |
|-------------|--|
| GKS forward | 5''-ACGTACCGGTATTCACATCTGGTACCTGGG-3'' |
| GKS reverse | 5''-AGCTCGTACGTATTAGGACAAGGCTGGTGG-3'' |

Figure 2.2 PCR primers used for amplification of GKS gene sequences

Methods

One microlitre pCMV4.GKB1 was added to 1x taq buffer, 0.2mM dNTPs, 200nM oligonucleotide primers (nucleotides 787-2247, figure 2.2). The reaction was heated to 95°C for 5 minutes. 5U taq DNA polymerase was then added. The reaction was then cycled as follows: 95°C for thirty seconds, 55°C for thirty seconds and 72°C for thirty seconds.

After completion of the reaction, 10µl of the PCR products were visualised by gel electrophoresis on a 1% TAE/agarose gel.

2.1.1.5 Visualisation of PCR products

Materials

Agarose, type II-A medium EEO

0.05M EDTA pH 8.0

Ethidium Bromide (10mg/ml) (VWR International Ltd, Poole, UK)

2M Tris-Acetate pH 8.5

50x TAE: (appendix I)

DNA marker (BRL 1Kb plus ladder, Invitrogen , Paisley, UK)

Gel loading buffer (appendix I)

Methods

Agarose was dissolved in 1x TAE using a microwave oven to prepare a 1% (w/v) agarose gel. Ethidium bromide was added to the agarose gel to a final concentration of 0.5µg/ml after the gel was cooled to 45°C. The gel was placed into an electrophoresis tank containing 0.5 TAE with 0.5µg/ml ethidium bromide after the gel was set. 3 µL of gel loading buffer was added to 10µl PCR product and to a mixture of 1µl of DNA marker and 9µl GDW. The samples were loaded onto the gel and electrophoresed at 10V/cm. DNA was visualised by illumination with UV light (300nm).

2.1.2 Cloning of GK DNA into pTR-CGW

Restriction endonucleases are enzymes isolated from bacteria that recognise and cleave specific target sites within double-stranded DNA. These cut fragments can be ligated using a viral enzyme that catalyses the formation of phosphodiester bonds between a free 5'' phosphate and a free 3'' hydroxyl group (Sambrook et al., 1989).

2.1.2.1 Restriction endonuclease digestion of PCR products and pTR-CGW

Materials

PCR products

pTR-CGW (rAAV plasmid) (gift from Dr. Verhaggen, Amsterdam)

Restriction endonucleases: BamHI, BsrGI, BsiWI, AgeI (New England Biolabs, Hitchin, Hertfordshire, UK)

10x Restriction buffer (as supplied) (appendix I)

10x Bovine serum albumin (BSA) (New England Biolabs)

Shrimp alkali phosphatase (SAP) 4U/µl (GE Healthcare)

Phenol/Chloroform pH8 (VWR)

5M Sodium acetate, pH 5.2 (appendix I)

Autoclaved glass distilled water (GDW)

Methods

The PCR products and pTR-CGW were diluted in GDW separately. Restriction buffer and BSA were added to give a final concentration of 1x. Forty units of AgeI and BsiWI were added. The total volume of enzyme added was kept less than 10% of the final volume. The reaction was incubated at 37° C for at least one hour. 8U SAP was added 30 minutes before the end of the incubation for the digestion of pTR-CGW. SAP removes 5'' phosphate groups preventing self-ligation of the plasmid. The reactions were extracted and phase separated with an equal volume of phenol/chloroform by centrifugation at 13,000xg for 3 minutes. The DNA was ethanol precipitated with 0.1 volumes sodium acetate pH5.2 and 2.5 volumes absolute ethanol at -20°C for at least one hour. The DNA was recovered by centrifugation at 13,000xg for 7 minutes (F45-12-11 microfuge, Eppendorf, Hamburg, Germany).

2.1.2.2 Electroelution of DNA fragments

In order to purify the DNA and remove contaminating fragments, DNA from the restriction dissection was size fractionated by electrophoresis on an agarose gel and the bands of interest were electroeluted.

Materials

50x TAE

Gel loading buffer (appendix I)

DNA marker (Invitrogen)

Dialysis tubing (VWR)

Methods

The DNA product from restriction digestion was dissolved in 20 µL GDW. 6 µL loading buffer was added. 1 µL DNA marker was dissolved in 9µl GDW and 3µl loading buffer. Samples were electrophoresed after loading onto a 1% agarose gel (prepared as described in section 2.1.1.5) at 10V/cm. DNA was visualised under UV light at 300 nm. The band of interest was cut from the gel using a scalpel. The band was put into dialysis tubing sealed at one end using a clip. 400 µL of 0.5x TAE was added to the dialysis tubing containing the cut band. The

air was excluded from the end of keeping by pressing firmly after which the open end was sealed using a clip. TAE was removed from the tubing after this. DNA was extracted by phenol/chloroform extraction and ethanol precipitation (as described in section 2.1.2.1) and quantified visually by running 1µl dissolved in GDW on a 1% agarose gel, as described earlier.

2.1.2.3 Ligation of PCR product into pTR-CGW

Materials

T4 DNA ligase, 6U/µl (New England Biolabs)

10x Ligase buffer (New England Biolabs)

PCR products*

pTR-CGW*

*products of restriction digestion purified as above

Methods

GK were inserted into pTR-CGW plasmid using DNA ligation. 20 ng of digested plasmid DNA was dissolved in GDW. Digested PCR product was added in x4 molar excess. 1 µL ligase buffer and 6U T4 DNA ligase added to result in a final volume of 10µl. The reaction was incubated overnight at 16°C. This product was then used to transform bacteria.

2.1.2.4 Preparation of GKS-pTR-CGW-plasmid

Transformation of competent JC811 bacteria by electroporation

The plasmid is induced into the bacterial cell by a process known as electroporation. This involves passing a voltage across the bacteria to open its membrane pores transiently, thus allowing the plasmid to enter into the bacterial cell. This transformed product can then be incubated. The pTR-GCW plasmid contains an ampicillin resistance gene. Ampicillin antibiotics can be incorporated into an agar plate used to grow the bacteria. This allows the selection of bacteria carrying the plasmid of interest.

Materials

Ligation reaction

LB (appendix I)

LB(amp) plates

JC811 bacteria (ATCC, Middlesex, UK)

Glycerol (VWR)

Methods

All salts must be removed from the reaction mixture prior to transforming the bacteria as otherwise this could lead to arcing during electroporation. The reaction was ethanol precipitated for at least one hour (as described earlier) after adding 1 μ L of glycogen, which acts as a carrier. DNA was recovered as described earlier using centrifugation for 7 minutes at 13000xg. The DNA was dissolved in 10 μ l of GDW.

An aliquot of frozen JC811 bacteria was thawed on ice. 10ng of plasmid (5 μ l ligation reaction) was added. The mixture transferred to an electrocuvette with an intra-electrode distance of 1mm. A 1.4 kilovolts voltage was passed across the cuvette to electroporate the bacteria. 200 μ l of warmed LB was then added and the reaction incubated at 37°C for an hour. Agar plates (with 100 μ g/ml ampicillin) were warmed and 150 μ l of the transformed bacteria added to the plate. The bacteria were spread over the surface of the agar plate. The agar plate was then inverted and incubated at 37°C overnight.

Small scale preparation of plasmid

Initially plasmids were isolated on a small scale culture (Sambrook et al., 1989). This allowed several clones to be analysed simultaneously. In order to isolate the plasmid from bacteria, the cell wall of the bacteria is disrupted using alkaline SDS. Contaminants such as bacterial debris, proteins, genomic DNA and RNA are precipitated using potassium acetate and treated with RNaseA. This removes most of the contaminants.

Materials

LB(amp)

GTE (appendix I)

0.2M sodium hydroxide 1% SDS (v/v) (appendix I)

5M potassium acetate (appendix I)

5M sodium acetate (appendix I)

Phenol/Chloroform

Propan-2-ol (VWR)

Methods

Two millilitres of LB (supplemented with 0.05 mg/ml ampicillin, LB(amp)) was inoculated with a single bacterial colony. This was incubated overnight at 37°C with vigorous shaking. 1.5ml of this mixture was removed into a clean tube and centrifuged for 3 minutes at 13,000xg. The remaining mixture was stored at 4°C to enable it to be used later. The supernatant was removed and the bacterial pellet was resuspended in 100µl GTE. 200 µl alkaline SDS was added to the bacteria and the mixture left for 5 minutes on ice. 150µl 5M KAc was then added and the mixture was left on ice for a further 5 minutes. The mixture was then centrifuged at 13,000xg for 5 minutes and 350µl supernatant was removed into a fresh tube. Phenol chloroform extraction was carried out as described previously. DNA was precipitated by the addition of 0.6 volume propan-2-ol and incubation at room temperature for 10 minutes. This was centrifuged again at 13,000xg for 7 minutes to pellet the DNA. DNA was recovered by removing the supernatant and dissolved in 100µl GDW. The DNA was ethanol precipitated with 0.1 volumes sodium acetate pH5.2 and 2.5 volumes absolute ethanol and was incubated at -20°C for at least one hour. Restriction endonuclease digestion was carried out (as described earlier) in order to identify which clones contained an insert of the correct size. Purified DNA was dissolved in 10µl GDW; AgeI and BsiWI was used to digest the GKS plasmid. Both plasmids were also digested by XmaI to confirm the presence of ITRs. The products were visualised by gel electrophoresis. Clones containing the correct insert and ITRs were selected for large scale preparation.

Large scale preparation of plasmid

Materials

LB(amp)

GTE

50,000 U/mg Lysozyme

0.2M sodium hydroxide/1% (w/v) SDS

5M potassium acetate (KAc)

Propan-2-ol

100x TE (appendix I)

DNase free RNase A 10mg/ml in GDW (GE Healthcare)

Phenol/Chloroform (VWR)

Methods

A small quantity of bacteria containing pTR-CGW with the correct size insert was inoculated into 500ml LB(amp) and incubated at 37°C overnight with vigorous shaking. The bacteria were recovered by centrifugation for 8 minutes at 3000xg (4000rpm in HS-4 rotor in RC-5B superspeed centrifuge, Du Pont, Bristol, UK) and at 4°C. The pellet was resuspended in 25ml GTE supplemented with 2mg/ml lysozyme and the sample was then incubated at room temperature for 5 minutes. Fifty millilitres of SDS/NaOH were added, the sample mixed by inversion and incubated on ice for 5 minutes. 38ml 5M KAc was then added. The sample mixed by inversion and incubated on ice for 10 minutes. Bacterial debris was removed by centrifugation for 15 minutes at 9000xg (7000rpm in HS-4 rotor in RC-5B superspeed centrifuge, Du Pont) at 4°C. The supernatant was transferred to a clean tube and 0.6 volumes propan-2-ol added. The sample was incubated on ice for 15 minutes and the DNA recovered by centrifugation for 15 minutes at 9000xg at 4°C. The pellet was dissolved in 10ml GDW to which 100µl 100x TE was added. RNase A was added at a concentration of 0.1mg/ml and the reaction incubated at 37°C for 30 minutes. The reaction was extracted with an equal volume of phenol/chloroform and the phases separated by centrifugation for 20 minutes at 10000xg and 4°C. The DNA was recovered by addition of 0.1 volumes 2M sodium acetate pH 5.2 and one volume propan-2-ol and incubation at -20°C for at least one hour. The DNA was then purified by caesium chloride gradient as detailed below.

Caesium chloride gradient purification

A caesium chloride gradient was used to purify the large-scale plasmid preparation. This purification method depends on the decrease in density of nucleic acids when bound to ethidium bromide, which binds by intercalation into DNA and causes its helix to unwind. In closed circular DNA such as plasmids, due to increased supercoiling, binding of ethidium bromide is limited and the plasmid has a higher buoyant density than linear or cut plasmids. This difference in buoyant density allows separation of the plasmid on a caesium chloride density gradient.

Materials

TES:

50mM Tris-HCL, pH 8.0 (appendix I)

50mM sodium chloride

5 mM EDTA

Caesium chloride (Boehringer, Berkshire, UK)

10mg/ml ethidium bromide

Caesium chloride-saturated propan-2-ol (appendix I)

Methods

DNA obtained from large scale plasmid purification was recovered by centrifugation for 20 minutes at 24,000xg (12,000rpm in HBS rotor in RC5B superspeed centrifuge, Du Pont) and 4°C. The DNA was then dissolved in 8.25ml TES. 8.4 grams of caesium chloride was dissolved in the DNA solution and 150µl of ethidium bromide was added and the solution mixed. The sample was divided into two polyallomer tubes (Ultracrimp, Du Pont), balanced, and overlaid with mineral oil. The tubes were sealed and centrifuged for 16 hours at 20°C and 216,518xg (60,000rpm in a T-8100 rotor in a Sorvall 100SE centrifuge, Fisher Scientific, Loughborough, UK). After centrifugation, DNA bands were visualised by UV illumination and the band containing the closed pTR-CGW DNA removed using a 20-gauge needle and a 2ml syringe. Ethidium bromide was removed from the plasmid by repeated extraction with an equal volume of caesium chloride saturated propan-2-ol, until both phases were colourless.

The DNA was precipitated by addition of two volumes of GDW and six volumes of room temperature absolute ethanol. DNA was recovered by centrifugation at 24,000xg and 20°C for 15minutes. The DNA pellet was dissolved in 0.4ml GDW, ethanol precipitated and recovered by centrifugation for 7 minutes at 13,000xg. The DNA was then dissolved in 1ml GDW. pTR-CGW was then quantified spectrophotometrically, 10µl DNA was diluted 1:100 and placed into a quartz cuvette. Absorbance was read at 260 and 280nm UV 1101 spectrophotometer (WPA, Cambridgeshire, UK). The reading at 280nm gives an indication of the purity of the sample as phenol absorbs more strongly at 280nm than DNA. The concentration of the DNA was calculated using the following formula:

$$\text{Concentration } (\mu\text{g/ml}) = (A_{260} \times \text{dilution factor}) \times 50$$

Samples were subjected to endonuclease digestion. GKS-pTR-CGW was digested AgeI and BsiWI. Both plasmids were digested by XmaI to confirm the presence of ITRs.

Insert sequences were confirmed by DNA sequencing (Genomics Core Laboratory, Imperial College London, UK). Briefly, 200 ng of each respective plasmid was diluted and mixed with 3.2 pmole of either the forward or reverse primer used in the PCR reaction in section 2.1.1.4. Samples were cycle sequenced using BigDye v3.1 (Applied Biosystems Ltd, Warrington, UK). Sequencing results were analysed for homology to known rat glucokinase gene sequences using the Basic Local Alignment Search Tool (BLAST) on the National Centre for Biotechnology Information (NCBI) internet site.

2.1.2.5 Cell Culture

Maintenance of cells

Materials

All cell-culture materials were purchased from Invitrogen unless stated otherwise

Human embryonic kidney cells (HEK293T. ATCC)

Human hepatocellular carcinoma (HEPG2. ATCC)

Dulbeccos modified eagle medium (DMEM)

Foetal Bovine Serum, heat inactivated (FBS)
2.5% Trypsin in hanks balanced salt solution
Versene: (appendix I)
0.14M sodium chloride
2.7mM potassium chloride
8mM di-sodium hydrogen orthophosphate
3mM EDTA
1.5mM potassium di-hydrogen orthophosphate
0.1%(v/v) phenol red

Methods

Human embryonic kidney cells (HEK 293T) and human hepatocellular carcinoma cells (HEPG2) were cultured in DMEM containing 4.5mg/ml glucose and 1mM sodium pyruvate supplemented with 10% (v/v) FBS at 37C in a 5% carbon dioxide atmosphere. Medium was changed every three days and the cells sub-cultured when 70-80% confluent using 0.25% trypsin in versene. The medium was aspirated and the cells incubated at 37C with fresh versene/trypsin until they detached from the flask. The trypsin was inactivated by the addition of 10ml of fresh medium and the cells recovered by centrifugation for 5 minutes at 100xg. The cells were resuspended in fresh medium and transferred to a new flask at a 1:10 dilution.

Transfection of cells with GKS pTR-CGW plasmids

Exogenous naked DNA can be absorbed by untreated mammalian cells, however the rate of absorption is slow and the efficiency can be poor. Therefore, large quantities of exogenous naked DNA need to be used. Calcium phosphate co-precipitation can improve the transfection efficiency. HEK293T cells, which do not express glucokinase, were transfected with GKS plasmid. pTR-CGW was transfected as a control.

Materials

2x HEPES-buffered saline (HBS) (appendix I)
280mM sodium chloride

10mM potassium chloride
1.5mM di-sodium hydrogen orthophosphate
12mM dextrose
50mM HEPES, pH7.05
2M calcium chloride (appendix I)
0.1xTE:
1mM Tris-HCl, pH 8.0
0.1mM EDTA, pH 8.0
DNA in 0.1 x TE:
40µg/ml plasmid DNA
DMEM

Methods

Twenty-four hours before transfection, cells at approximately 60% confluence were sub-cultured and plated at a density of 1×10^4 cells/cm in 90mm Petri dishes. The following day media was replaced with fresh media. A co-precipitate was formed by mixing 300µl 10xHBS with 28µg plasmid DNA in 2.5ml of GDW and then slowly adding 180µl 2M calcium chloride, while gently mixing using air expelled from a pipette aid. The solution was incubated at room temperature for 5 minutes to allow formation of the precipitate. The precipitate was added to the cells and they were incubated at 37°C in 5% carbon dioxide for 18 hours. The medium containing the precipitate was replaced with fresh media, cells were incubated for 48 hours after which time cells were lysed in glucokinase extraction buffer and enzymatic assay was performed for glucokinase activity as described in section 2.3.2.

2.1.2.6 Production of recombinant adeno-associated virus (rAAV) particles

rAAV can be produced using several different methods. The method employed and detailed below is based on the 'two-plasmid system' that does not require the use of an adenovirus (Grimm et al., 1998) (figure 2.3). This system uses a packaging plasmid containing the transgene of interest and a helper plasmid containing Rep, Cap as well as other adenovirus genes required to propagate the virus. In this study pTRCGW and pDG were used as packaging and helper plasmids respectively (figure 2.4 and 2.5).

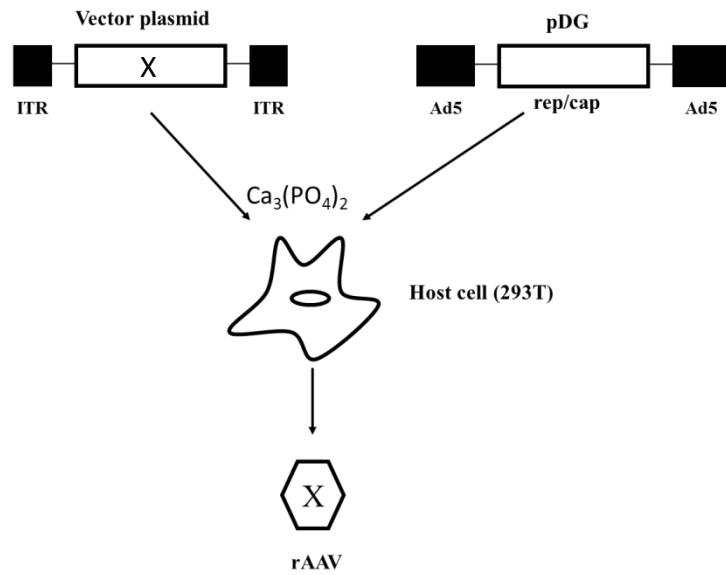


Figure 2.3 Two plasmid system for rAAV production (Grimm et al., 1998). Cells are transfected with the vector plasmid and a pDG hybrid helper plasmid. X, transgene; ITR, inverted terminal repeats; Ad5, adenovirus helper genes.

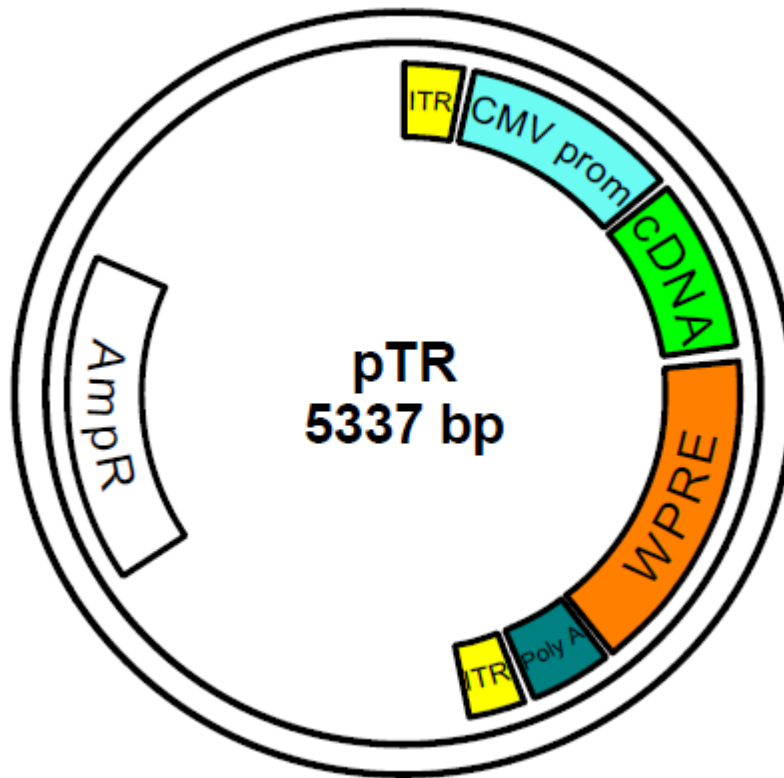


Figure 2.4 Diagram of rAAV plasmid pTRCGW with transgene insert. ITRs flank the expression cassette which contains the cDNA insert and CMV promoter. Outside of the expression cassette the gene for ampicillin resistance is included to aid selection of rAAV positive bacterial colonies.

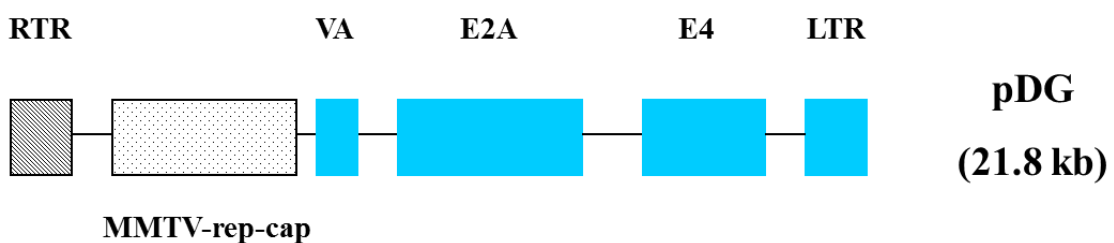


Figure 2.5 Diagram of helper-plasmid pDG structure. AAV and adenovirus genes required for amplification and packaging of rAAV are contained within this plasmid. Right terminal repeat (RTR) and MMTV-Rep-Cap includes a promoter region encoding Rep and Cap proteins. Expression is driven by mouse mammary tumour virus (MMTV). Long terminal repeat (LTR), VA, E2A and E4 are adenovirus helper genes required for replication.

Production of rAAV

Adeno-associated virus was produced by Dr. J. Gardiner (Division for Diabetes, Endocrinology and Metabolism) using the two plasmid system. Briefly, host cells (HEK293) are co-transfected with the rAAV plasmid pTR-CGW and a helper plasmid pDG using calcium phosphate. There is no homology between the two plasmids so they cannot recombine and form wild-type virus. This results in the production of rAAV particles. To release the particles cells are lysed by freeze thawing and the rAAV produced is purified.

HEK293 cells were maintained in DMEM containing 4500 μ g/ml glucose and 1mM sodium pyruvate supplemented with 10% (v/v) FBS.

Calcium phosphate transfection

Materials

HEK293 cells

Plasmids

pTR-CGW (containing transgene)

pDG

10x HEBS buffer:

1.36M NaCl

0.05M KCl

0.007M Na₂HPO₄·2H₂O

0.2M HEPES

0.125M glucose

2M CaCl₂

Methods

Cells were plated into a 10 chamber cell factory (L x W x H (mm): 335 x 205 x 190, culture area: 6320cm²). Cells were incubated in 2000ml DMEM with 10% FBS. After 24 hours, when

cells were 50% confluent, the culture medium was replaced (250ml culture medium was retained for transfection) and transfection performed 2 hours later.

Transfection mix was prepared for the cell factory, consisting of 560µg pTRCGW, 1.68mg pDG, 7.2ml 2M CaCl₂ and 52ml GDW. Immediately before transfection 12ml 10x HEBS buffer in 48ml GDW was added and mixed gently. After standing at room temperature for 1 minute the mixture was added slowly to 250ml DMEM supplemented with 10% FBS and added to the cell factory.

Recovery and purification of rAAV

Materials

0.01M PBS

DNaseI

Sepharoes column (GE Healthcare)

Iodixanol (Life Sciences Technology, Eggenstein, Germany)

0.3x PBS/0.1M NaCl

0.3x PBS/2mM EDTA

2M MgCl₂

Benzonase (Novagen, Nottingham, UK)

Lysis buffer (appendix I)

Methods

Forty-eight hours after transfection, cell medium was removed and cells were washed using 500ml PBS and then harvested using 1 L PBS/2mM EDTA. Cells were then recovered by centrifugation at 5000xg for 10 minutes, washed in 150ml PBS and recovered by centrifugation at 5000xg for 10 minutes. Cells were then resuspended in 60ml lysis buffer and aliquoted into four falcon tubes. Cells were subjected to three cycles of 10 minutes in dry ice/ethanol followed by 10 minutes in a 37°C waterbath. Seven point three microlitres of 2M MgCl₂ and 1.2µl Benzonase were then added to each falcon tube and incubated at 37°C for 30 minutes. The reactions were then centrifuged at 2000xg for 10 minutes to pellet cell debris. The supernatant was removed and loaded into four 50ml polyallomer tubes

(Beckman Coulter (U.K.), Buckinghamshire, UK) under layered with 100ml iodixanol gradient. The tubes were then topped up with lysis buffer, heat sealed and subjected to centrifugation at 69,000xg for 1 hour at 18°C (in a Type 70 Ti rotor in a Sorvall 100SE centrifuge, Fisher Scientific). The top of each tube was punctured with an 18G needle and rAAV collected by puncturing the bottom of the tube and collecting 5ml of iodixanol gradient from the 60/40% interface. The fractions from the four tubes were pooled, added to 20ml PBS and loaded onto a Sepharose column which had been pre-washed with 25ml 0.1M NaCl/0.3x PBS and 50ml 0.3x PBS. The column was then washed with 50ml 0.3x PBS and the virus was eluted using 15ml 350mM NaCl/0.3xPBS. The elutant was transferred to an Apollo Concentrator containing 10ml PBS and subjected to centrifugation at 4000xg for 5 minutes. The flow through was discarded and 5ml PBS was added below the filter and 19.5ml PBS above. The tube was then subjected to centrifugation at 4000xg for 5 minutes and the 0.5ml remaining in the filter (which contained the rAAV) was aliquoted into eppendorf tubes. The viral titre was quantified by dot blot analysis.

2.1.2.7 Determination of Total Viral Titre by Dot Blot Analysis

The level of transgene expression is affected by the rAAV titre so total viral particle number was determined by dot blot analysis. Dot blot analysis is based on similar principles to Southern and Northern blots; a specific probe can be used to quantify a specific DNA or RNA species in a sample. Rather than being separated by size and transferred to a membrane, the sample being analysed is placed directly onto a membrane. The DNA or RNA species present in the sample can be detected and quantified using radiolabelled probes.

Materials

rAAV viral preparation

Solution A (appendix I)

Solution B (appendix I)

1mg/ml proteinase K

Phenol/chloroform

3M sodium acetate (appendix I)

Ethanol (VWR International Ltd, Poole, UK)

Glycogen

Denaturing solution: 1.5M NaCl 0.5M NaOH

Neutralising solution: 1M Tris/HCl pH7.4 1.5M NaCl

pTRCGW

Hybridisation buffer (appendix I)

Amasino wash buffer (appendix I)

Universal wash buffer (appendix I)

Methods

Forty-five microlitres of solution A was added to 5µl rAAV virus stock and incubated for 30 minutes at 37°C. Two hundred microlitres of solution B was added and the sample was incubated at 55°C for 1 hour. DNA was extracted by adding an equal volume of phenol/chloroform. Ethanol precipitation of the DNA was performed by adding 1/10 volume 3M sodium acetate pH 5.2, 40µg glycogen and 2.5 volumes ice cold ethanol. After 1 hour at -20°C the solution was centrifuged at 8000g at 4°C, the supernatant removed, the pellet washed in 75% cold ethanol and air-dried. The pellet was dissolved in 10µl GDW and 1µl applied to a nylon membrane (Hybond-N). A series of dilutions of pTRCGW (50 to 0.1ng) were also applied to the membrane to act as a standard curve. The membrane washed for 5 minutes in denaturing solution, then washed twice for 5 minutes in neutralising solution. The membrane was then baked at 80°C for 2 hours.

A cDNA fragment of WPRE was used as a probe for rAAV transgenes. The probe was radio labelled with ³²P dCTP as described in section 2.4.6.4. Half of the labelled probe was boiled and added to 10ml hybridisation buffer. Hybridisation was carried out overnight at 60°C. The following day the membrane was washed as described in section 2.3.5.2. The membrane was then placed on a phosphorimager screen overnight. Radiolabelled areas were visualised and quantified by image densitometry using ImageQuant software (Molecular Dynamics). Quantification was performed by comparing viral DNA to known amounts of pTR-CGW in the standard curve.

2.2 *In vivo* methods

2.2.1 Animals

Male Wistar rats (specific pathogen free, Charles River UK Ltd, Margate, Kent, UK) were maintained under a controlled environment (temperature 21-23°C, 12 hour light-dark cycle, lights on at 07:00) with *ad libitum* access to food (RM1 diet, Special Diet Services UK Ltd, Witham, Essex, UK), except where stated, and water. All animal procedures were approved under the British Home Office Animals (Scientific Procedures) Act 1986 (Project licence no. 70/6377). Prior to all experiments animals were acclimatised to the Imperial College animal unit for 7 days. Animals were randomised to treatment and control groups of approximately equal mean and standard error of mean bodyweight.

2.2.2 Intra-arcuate AAV microinjections

Rats were anaesthetised with 2L/minute oxygen and 4% inhaled isoflurane (Abbott Laboratories Ltd, Queenborough, Kent, UK). Animals were placed in the induction chamber until they lost the pedal reflex. Once anaesthetised, animals were administered intra-peritoneal prophylactic antibiotics (amoxicillin (37.5mg/kg) and flucloxacillin (37.5mg/kg)) to prevent post-operative infection. Rats were immobilised on a stereotaxic frame (David Kopf Instruments, California, USA). The incisor bar was set at 3.0mm below the interaural plane. The surgical area was shaved, and cleaned with 10% w/v povidine-iodine solution (Betadine). A small (<2cm) rostro-caudal incision was made in the scalp. Animals were injected bilaterally into the ARC using coordinates -3.4mm caudal, +/-0.5mm lateral to the bregma, and 10.5mm below the skull, determined from the rat brain atlas of Paxinos and Watson and previous studies in similar strain and weight rats (Paxinos and Watson, 2009, Patterson et al., 2009). A stereotaxically mounted drill was used to make a 0.65mm burr hole in the skull. Each animal was injected via a 33 gauge steel injector (Plastics-One, Roanoke, Virginia, USA) inserted into and projecting 1mm below, the tip of a guide cannula. Animals received either 1µl rAAV-GKS at a titre of 2.96×10^{12} genome particles/ml or 1µl rAAV-eGFP at a titre of 5.04×10^{12} genome particles/ml injected bilaterally into the ARC. The pressure was removed from the injector and the cannula/injector unit was maintained *in situ* for 5 minutes before being slowly extracted to minimise backflow. The incision was

sutured with two mattress sutures with 6.0 proline thread. Animals were administered subcutaneous buprenorphine (45mg/kg, Schering-Plough Corp, Welwyn Garden City, Hertfordshire, UK) for post-operative analgesia and rehydrated with 0.9% sodium chloride (3ml/rat). The animal was removed from the frame and placed in a heated box for recovery. Once the rat had regained the righting reflex it was housed individually and monitored for a recovery period of 7 days. The animals were given *ad libitum* access to food (unless otherwise stated) and food intake and body weight were measured at least 3 times per week following the 7 day post-operative recovery period.

2.2.3 Intra-arcuate cannulations

Rats were anaesthetised with 2L/minute oxygen and 4% inhaled isoflurane (Abbott Laboratories Ltd, Queenborough, Kent, UK). Animals were placed in the induction chamber until they lost the pedal reflex. Once anaesthetised, animals were administered intra-peritoneal prophylactic antibiotics (amoxicillin (37.5mg/kg) and flucloxacillin (37.5mg/kg)) to prevent post-operative infection. Rats were immobilised on a stereotaxic frame (David Kopf Instruments, California, USA). The incisor bar was set at 3.0mm below the interaural plane. The surgical area was shaved, and cleaned with 10% w/v povidine-iodine solution (Betadine). A small (<2cm) rostro-caudal incision was made in the scalp. Animals were cannulated with a permanent 22-gauge stainless steel cannula (Plastics One Inc., Roanoke, Virginia, USA) projecting 9.5 mm below the skull unilaterally into the ARC using coordinates - 3.4mm caudal, +0.5mm lateral to the bregma, and 9.5mm below the skull, determined from the rat brain atlas of Paxinos and Watson (Paxinos and Watson, 2009). A stereotaxically mounted drill, was used to make a 0.65mm burr hole in the skull. Dental cement (Associated Dental Products Ltd, Swindon, Wiltshire, UK) was used to hold the cannula in position and seal the wound; this was anchored by three stainless steel screws inserted into the skull. Animals were administered subcutaneous buprenorphine (45mg/kg, Schering-Plough Corp, Welwyn Garden City, Hertfordshire, UK) for post-operative analgesia and rehydrated with 0.9% sodium chloride (3ml/rat). A plastic-topped wire cap (Plastics One Inc.) was inserted into the cannula to prevent blockage. Animals were administered subcutaneous buprenorphine (45mg/kg, Schering-Plough Corp, Welwyn Garden City, Hertfordshire, UK) for

post-operative analgesia and rehydrated with 0.9% sodium chloride (3ml/rat). The animal was removed from the frame and placed in a heated box for recovery. Once the rat had regained the righting reflex it was housed individually and monitored for a recovery period of 7 days. The animals were given *ad libitum* access to food (unless otherwise stated) and food intake and body weight were measured at least 3 times per week following the 7 day post-operative recovery period. Each animal was injected via a 33 gauge steel injector (Plastics-One, Roanoke, Virginia, USA) inserted into and projecting 1mm below, the tip of the permanent guide cannula. After the 7 day recovery period, animals were handled daily and acclimatised to the injection procedure by two sham injections of 1µL normal saline.

2.2.4 Feeding studies

Studies with a high-energy diet involved using a diet containing 32% kcal from fat and 25% kcal from sugars (Research Diets, Inc.; D12266B) (Appendix III). Acute twenty-four hour normal chow and sugar intake feeding studies with AAV injected animals commenced at lights out (1900 hours). Fasts for studies involving twenty-four hour fasts commenced at 0900 hours. Fasts for studies involving fourteen hour fasts commenced at lights out (1900 hours). Caloric content was calculated as 3.523kcal/g for RM1 diet and 4kcal/g for glucose.

2.2.5 Intra-arcuate cannulation

Rats received intra-arcuate injections between 0930 and 1030h with either drug or vehicle control on 2 separate days, 72 hours apart, as part of a cross-over study. Rats were subjected to a fourteen hour overnight fast for studies with diazoxide only. All compounds were administered in a 1-µl volume over a period of 1 min via a stainless steel injector (Plastics One) projecting 1 mm beyond the tip of the cannula. Drug dosages per rat were 0.5 nmol Cpd A (2-Amino-5-(4-methyl-4H-(1,2,4)-triazole-3-yl-sulfanyl)-N-(4-methyl-thiazole-2-yl)benzamide, Merck) in 1% DMSO; 2 nmol glibenclamide (Sigma) and 1nmol diazoxide (Sigma), both in 1% DMSO and 5mM NaOH. The dosages chosen were based on experiments reported previously (Levin et al., 2008a, Zhang et al., 2004, Chan et al., 2007). 24 hour feeding studies were undertaken with measurements of food and glucose intake at 0, 0.5, 1,

2, 4, 8 and 24 hours after injection. Cannula placement was confirmed using ink injection and cresyl violet staining at the end of the studies. Each animal was injected unilaterally via a stainless steel injector (Plastics One) inserted into the guide cannula after decapitation with 10% dilution of India ink in water. Following injection, brains were rapidly dissected. Brains were fixed in a 4% formaldehyde solution (Appendix I) at 4°C overnight, and then dehydrated in a 30% sucrose solution at room temperature for five days. Brains were frozen and sliced to 30µm thickness using a Shandon microtome. Cresyl violet was carried out as described in section 1.3.2. Only animals that had cannula positioned correctly for the arcuate nucleus were used in subsequent analysis of feeding studies.

2.2.6 Collection of tissue samples

Fasting plasma was collected by tail vein sampling following a fourteen hour fast in EDTA-chelated microtubes (Starstedt microvette) containing 3µl aprotinin, and was immediately placed on ice before centrifugation at 4°C to obtain plasma. Rats were killed by decapitation in the early light phase. Brains are rapidly removed and lateral sections cut away using a razor blade to isolate hypothalami, which were frozen in liquid nitrogen before storage at -80° C. Blood was collected in heparinised or EDTA-chelated tubes containing 100µl aprotinin, and was immediately placed on ice before centrifugation at 4°C to obtain plasma. An aliquot of plasma was separated and 1µl 1 M HCl was added for every 20µl of plasma. All plasma samples were stored at -80°C immediately until assay. Interscapular BAT was dissected, weighed, frozen in liquid nitrogen and stored at -80°C until RNA extraction. The contents of rat gastrointestinal tracts were removed before storing carcasses at -20°C until body content analysis.

2.3 *In vitro* methods

2.3.1 *In situ* hybridisation for glucokinase mRNA

In situ hybridisation is a method for the detection and quantification of mRNA whilst maintaining the structural integrity of the tissue. It relies on the hybridisation of a

complementary probe, usually radiolabelled RNA, to the target mRNA in tissue mounted on poly-lysine slides.

Following rAAV-GKS injections transgene expression was confirmed in brains taken from three animals using a ³⁵S labelled riboprobe specific for glucokinase. The ³⁵S glucokinase riboprobe was labelled as described below using pBluescript-GK as a template. The pBluescript-GK plasmid was created by endonuclease digestions of pBluescript and full length glucokinase cDNA using BamHI and PstI (as described in 2.1.2.1). Following endonuclease digestion pBluescript and GK were ligated and the plasmid was amplified and purified (as described in section 2.1.2.4.2 and 2.1.2.4.3).

Production of radiolabelled RNA probe for in situ hybridisation

Materials

Linearised template (pBluescript-GK (200ng/μl) linearised by digestion with BamHI for antisense probe)

100M DTT

RNase inhibitor, 30U/μl

10x nucleotide mix: 10mM of each ATP, UTP, GTP;

T7 RNA polymerase, 20U/μl (Promega)

10x RNAPolymerase buffer (Promega)

DNase I, 7.5 U/μl (GE Healthcare)

10x DNase buffer

5M Ammonium acetate (appendix I)

[³⁵S]CTPαS, 30TBq/mmol, 1.5GBq/ml (GE Healthcare)

Methods

Radioactively labelled RNA was produced using an in vitro transcription reaction. Two hundred nanograms of template were added to a reaction buffer containing 10mM DTT, 1x nucleotide mix, 1x polymerase buffer, 30U RNase inhibitor and 3.75MBq [³⁵S]CTPαS in a total volume of 9μl. To this 20U of T7 RNA polymerase was added and the reaction incubated for at least 2 hours at 37°C. After incubation, 6μl GDW, 1μl DNase I and 3μl DNase

buffer was added. This was followed by a 15-minute incubation at 37°C. Ammonium acetate was added to a final concentration of 2M and 2.5volumes ice cold absolute ethanol was added and the mixture left at -20°C for at least an hour for the RNA to precipitate. RNA was recovered by centrifugation at 8,000xg for 7 minutes and the pellet was dissolved in 100µl GDW. To measure the activity of the radiolabelled probe, 1µl was counted on a microbeta counter (Wallace, Waltham, MA).

2.3.1.1 *In situ hybridisation*

Materials

4% (v/v) formaldehyde in 0.1M phosphate buffered solution (PBS)

100% acetic anhydride (VWR)

0.1M triethanolamine pH 8.0

20x SSC (appendix I)

70% ethanol in distilled water

Chloroform (VWR)

Hybridisation buffer (appendix I)

50% (v/v) Formamide

600mM sodium chloride

80mM Tris-HCl, pH 7.5

4mM EDTA

100mM DTT

0.1 mg/ml yeast tRNA

2% (w/v) Dextran sulphate, mw ~500,000

1x RNase buffer

10mM Tris pH 8

1mM EDTA

0.5M sodium chloride

Methods

Twelve micrometre brain sections were cut on a cryostat at -25°C (Bright instrument Company, Huntingdon, Cambridgeshire, UK). The sections were mounted onto poly-lysine

coated slides and stored at -20°C until hybridisation. In situ hybridisation was carried out on every third slide. The sections were fixed in 4% (v/v) formaldehyde in 0.1M PBS for 20 minutes. Slides were washed twice in 0.1MPBS, for 5 minutes. Sections were then incubated in 0.1M TEA for 2 minutes and acetylated in 0.25% (v/v) acetic acid anhydride in 0.1M TEA for 10 minutes. Sections were washed twice in 0.01M PBS for 2 minutes and then dehydrated by immersion in 70% ethanol for 3 minutes. Finally, slides were delipidated in chloroform for 5 minutes and allowed to air dry. All steps were performed at room temperature unless otherwise stated.

Hybridisation buffer was supplemented with the ³⁵S labelled probe (1 x 10⁶ Bq) and 80µl added to each slide. A coverslip was placed over each slide and the slides were hybridised at 60°C overnight. Next, the slides were washed in 4x SSC with gentle agitation to remove coverslips and then washed four times in 4x SSC for 5 minutes. Slides were then RNase treated by incubation for 30 minutes at 37°C in 1x RNase buffer containing 100µg/ml RNase A. This was followed by two 5 minute washes in 10mM DTT/2x SSC at room temperature. Slides were washed in 10mM DTT/1x SSC followed by 10mM DTT/0.5x SSC for 10 minutes each. Slides were then washed in 10mM DTT/0.1x SSC at 60°C for 30 minutes. Finally, slides were rinsed in 10mM DTT/0.1x SSC and dehydrated in 70% ethanol for 3 minutes before being allowed to air dry. After washing and dehydration, the slides were exposed to Bio-Max film (Kodak, Hemel Hempstead, Herts, UK) at room temperature. After three days exposure the film was developed and transgene expression determined by observation of specific hybridisation.

2.3.2 Cresyl violet staining of ink injected rat brains

Materials

Acetic acid (VWR)

Ethanol (VWR)

Cresyl violet stain (Mix 2g cresyl violet, 300ml GDW, 30ml 1M NaAc and 170ml acetic acid, and pH to 3.7-3.9. Filter before use.)

Xylene (VWR)

DPX (Thermo Fisher Scientific, Epsom, Surrey, UK)

Method

Once mounted onto slides, brain sections containing India ink were allowed to dry for at least four hours. Slides were fixed in a solution of 5% acetic acid in 100% ethanol, and then stained in cresyl violet for 15 minutes. Slides were washed twice in GDW, dehydrated in 70% ethanol and delipidated in xylene overnight. The following morning, slides were mounted with DPX and coverslips. Animals with ink more than 0.2mm outside the ARC when viewed under the microscope (Nikon, Eclipse 50i) were removed from subsequent analysis.

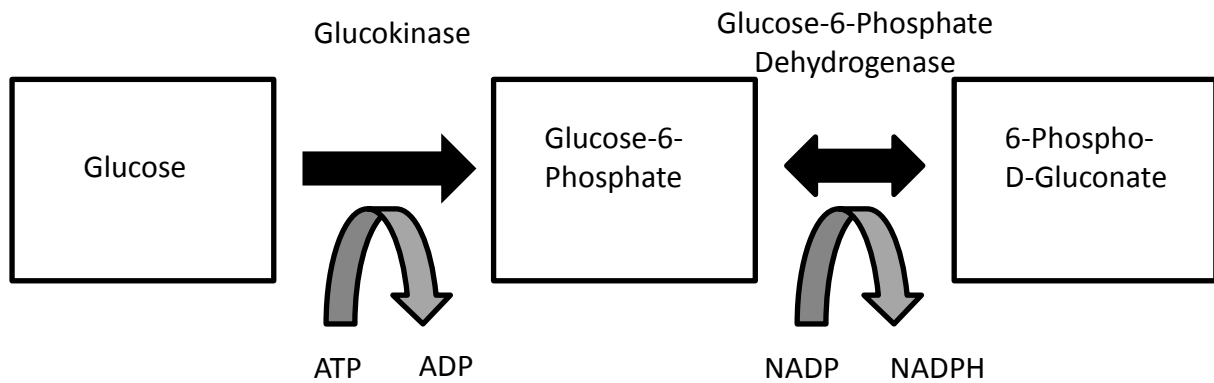
2.3.3 Glucokinase activity assays

2.3.3.1 Isolation of hypothalamic nuclei by micro-punch

Rats were killed by decapitation, and brains removed. Hypothalamic nuclei were isolated using a micro-punch technique (Palkovits, 1983). Brains were then placed on filter paper with the ventral surface facing upwards so that the hypothalamus was visible, and sections lateral to the hypothalamus on either side were cut away using a razorblade. The remaining block of brain was then frozen using isopentane cooled on dry ice. Frozen brains were mounted upon a freezing sled microtome (Shandon Southern Products Ltd). Sagittal sections of 1.2mm containing the ARC, VMH and PVN were then cut and mounted on slides. Slides were kept on dry ice to re-freeze sections and nuclei were identified and removed using a 22 gauge neuropunch (Fine Science Tools).

2.3.3.2 Glucokinase activity assay

Glucokinase activity can be determined spectrophotometrically using an NADP⁺-coupled assay with glucose-6-phosphate dehydrogenase (Goward et al., 1986). Glucokinase catalyses the phosphorylation of glucose to form glucose -6-phosphate (G-6-P) in the presence of ATP. G-6-P is converted to 6-phospho-D-gluconate by glucose-6-phosphate dehydrogenase. The generation of NADPH is proportional to glucokinase activity and can be quantified by measuring the change in absorbance at 340 nm using a spectrophotometer. The principles of this assay are summarised below.



Glucokinase and hexokinase both phosphorylate glucose. However, glucokinase has a low affinity and high K_m for glucose compared to hexokinase. Therefore, at low concentrations of glucose, hexokinase activity is near maximal whereas that of glucokinase is low and vice versa for high concentrations of glucose. Hence, to differentiate glucokinase from hexokinase the assay can be performed in a reaction containing either 100mM or 0.5mM glucose as a substrate. Glucokinase activity for each sample can be calculated as:

$$A(100\text{mM glucose}) - A(0.5\text{mM glucose}) = \text{Glucokinase activity}$$

Alternatively, to differentiate glucokinase from hexokinase addition of 5-thio-d-glucose-6-phosphate (5TG) (at a final concentration of 45 μM) and 3-O-methyl-N-acetylglucosamine (3OMG) (at a final concentration of 0.5mM) can be used. 5TG inhibits hexokinase activity without effecting glucokinase, while 3OMG inhibits N-acetylglucosamine kinase, which phosphorylates glucose at high glucose concentrations (Miwa et al., 1994, Fenner et al., 2011). This method is preferred as it increases the accuracy of the assay and avoids the assay being carried out with 0.01M D-glucose as the substrate as well. Hence, this method was used to determine glucose is activity as detailed below.

Materials

Glucose-6-Phosphate Dehydrogenase

Glucokinase extraction buffer (appendix I)

Glucokinase from *Bacillus stearothermophilus* (0.25 $\mu\text{g/ml}$)

100mM adenosine trisphosphate
2M D-glucose
100mM Gly-Gly, pH8
12.5mM NADP
1M MgCl₂
2U glucose-6-phosphate dehydrogenase (type IX, from Baker's yeast)
3-O-methyl-N-acetylglucosamine
5-thio-d-glucose-6-phosphate
100mM Gly-Gly, pH8 (appendix I)
1M MgCl₂ (appendix I)

Methods

Tissue samples or cells were homogenised in 200µl glucokinase extraction buffer using a handheld homogeniser. The homogenate was centrifuged for 40 minutes at 13000xg at 4°C. The supernatant was then removed. In order to calculate glucokinase activity in samples a standard curve for glucokinase activity was used containing: 0.025µg glucokinase, 0.02µg, 0.0175µg, 0.015µg, 0.01µg, 0.0075µg, 0.005µg and 0.001µg of glucokinase.

Assay reactions were set up in a total volume of 1ml, containing: 500µl 100mM Gly-Gly, 7.5µl 1M MgCl₂, 50µl 100mM ATP, 60µl 12.5mM NADP, 0.002µg glucose-6-phosphate dehydrogenase, and 50µl of either 2M or 10mM glucose. 3-O-methyl-N-acetylglucosamine and 5-thio-d-glucose-6-phosphate are added to the reaction mixture prior to the addition of the glucokinase standard or cell/hypothalamic homogenate. The reaction was initiated by the addition of either glucokinase standard or hypothalamus homogenate.

The reaction was incubated at 37°C for 1 hour. Assays were performed in triplicate. Absorbance at 340nm was measured for each sample using a UV 1101 spectrophotometer (WPA, UK).

NADPH production was calculated using the millimolar extinction coefficient 6.27 (ξmM) at 340nm using the following equation

A340nm/6.27 ξ mM= mM concentration of NADPH

Glucokinase activity was expressed as units (of glucokinase from *Bacillus stearothermophilus*) per milligram protein. Sample protein concentration was determined by BCA protein assay (Pierce) as detailed below.

2.3.3.3 Protein assay on punch biopsy samples

Due to the variability in the amount of hypothalamic tissue collected by punch biopsy, the protein content of the punch biopsy homogenate must be calculated in order to standardise the results of the glucokinase activity assay.

Homogenate protein content was measured using a well-established modified Lowry protein assay. This method involves reaction of proteins with cupric sulphate and tartrate in an alkaline solution to form tetradentate copper-protein complexes. These copper-protein complexes produce a peak in absorbance at 750nm and can be measured spectrophotometrically to quantify the amount of protein in a sample.

Materials

Lowry protein assay kit (Pierce, Rockford, IL, USA)

Bovine serum albumin (BSA) stock solution

2X Folin-Ciocalteu reagent

Methods

BSA stock solution was diluted in GDW to make up nine standard solutions of 1, 5, 25, 125, 250, 500, 750, 1,000, and 1,500 μ g/ml. One times Folin-Ciocalteu reagent was prepared by diluting the supplied 2X reagent 1:1 with ultra-pure water. All other reagents were supplied ready to use.

Fifty microlitres of BSA standard and 50 μ l of sample were added to microfuge tubes. One millilitre of modified Lowry reagent was then added to each tube at 15 second intervals,

mixed, and incubated for 10 minutes. One hundred microlitres of the prepared 1X Folin-Ciocalteu reagent was then added and the solution was vortexed. The tubes were covered and incubated at room temperature for 30 minutes. The A750 of the samples was then measured in a spectrophotometer. Absorbance values of the blank readings were subtracted from the absorbance readings of all samples and a standard curve plotted. The protein concentration of each of the unknown samples was determined by comparison to the standard.

2.3.4 Quantification of mRNA by qPCR

Quantitative PCR (qPCR) was used to analyse the expression of a range of mRNA sequences in dissected hypothalami using TaqMan® gene expression assays. Total RNA was extracted from tissue samples. From this RNA, mRNA was amplified by reverse transcription and used for qPCR analysis. All materials for qPCR were supplied by Applied Biosystems, Warrington, UK, unless otherwise stated.

2.3.4.1 RNA Extraction for qPCR

Materials

Tri-reagent (Helena Biosciences, Sunderland, Tyne and Wear, UK)

Purelink RNA Mini kit

Chloroform (VWR International Ltd, Poole, UK)

Purelink DNase

Methods

RNA was extracted from hypothalami using the Tri-reagent method according to the manufacturer's protocol. Hypothalamic tissue was homogenised in 1ml Tri-reagent before subsequent transfer to a 1.5ml eppendorf and incubation at room temperature for five minutes. Sample RNA needed to be devoid of any genomic DNA contamination in order to accurately analyse mRNA levels by TaqMan® probe assay. This was achieved by treating the RNA samples with DNase solution. Following nucleoprotein dissolution with Tri-reagent, nucleic acids were extracted by adding 200µl of chloroform per 1ml of Tri-reagent used.

RNA samples were processed for DNA removal using the Purelink RNA mini kit according to the manufacturer's protocol.

The RNA was then dissolved and stored in RNase-free water before its yield was determined spectrophotometrically according to the following equation:

$$\text{RNA } (\mu\text{g}) = \text{dilution factor} \times 40 \times \text{OD}_{260} \times \text{sample volume (ml)}$$

2.3.4.2 Reverse Transcription of Hypothalamic mRNA

Messenger RNA was converted into its complementary cDNA sequence by reverse transcription in order to allow its amplification by PCR. The High Capacity cDNA Reverse Transcription Kit uses the random primer scheme for initiating cDNA synthesis.

Materials

High Capacity cDNA Reverse Transcription Kit

96 Well Assay Plate

Methods

500ng of each RNA sample was added in triplicate to reaction wells containing 1X RT buffer, 4mM dNTP mix, 1X RT random primers, and Multiscribe reverse transcriptase. The plate was then foil-sealed before its incubation in a thermal cycler programmed to the following conditions: 25°C for 10 minutes, 37°C for 120 minutes, 85°C for 5 minutes. Following cycle completion, cDNA templates were stored at -20°C.

Endogenous control cDNA templates were prepared by adding 50ng of each RNA sample before following the above procedure.

2.3.4.3 qPCR Assays from Hypothalamic cDNA

Each qPCR TaqMan® assay allows accurate quantification of gene expression by incorporating a reporter-tagged probe, which is complementary to part of the targeted cDNA sequence, into the amplification process. Probes were designed to cross exon-exon junctions to ensure amplification was limited to mRNA only. During PCR, the minor-groove binding probe anneals specifically to a complementary sequence between the forward and

reverse primer sites. When the probe is intact, the proximity of the reporter dye to the quencher dye results in suppression of the reporter fluorescence, primarily by Förster-type energy transfer. The DNA polymerase cleaves only probes that are hybridized to the target. Cleavage separates the reporter dye from the quencher dye to allow fluorescence of the reporter.

Materials

Sample cDNA template (25µg/ml)
Endogenous control cDNA template (2.5µg/ml)
TaqMan® Gene Expression Assay
TaqMan® Gene Expression Master Mix
384 Well Assay Plate

Methods

The following constituents were mixed in each well for each qPCR reaction: 1µl of cDNA template (25ng), 10µl master mix, and GDW to give a 20µl reaction volume. For total RNA quantification, a gene expression assay targeting the 18S ribosomal subunit and 2µl of cDNA template (5ng) were used. Each reaction was mixed before the plate was sealed.

The sealed plate was loaded onto a 7900HT Fast Real-Time PCR System (Applied Biosystems, Warrington, UK) thermal cycler, on the $\Delta\Delta C_t$ programme, under the following conditions: Held at 50°C for 2 minutes before 95°C for 10 minutes. Thermal cycling then proceeded where 15 seconds incubation at 95°C followed by 1 minute incubation at 60°C was repeated for 40 cycles. The amplification data for the target gene was normalised to the expression of the 18S endogenous control and expressed relative to an internal calibrator (control group sample), using the $2^{-\Delta\Delta CT}$ method (Livak and Schmittgen, 2001).

2.3.4.4 Validation of qPCR Assays

Each qPCR assay was validated for use in a particular tissue prior to analysis, to assess suitability of 18S as an endogenous control target. This involved generating standard curves from hypothalamic RNA (at concentrations covering 3 logs) using both the 18S assay and target assay.

Materials

High Capacity cDNA Reverse Transcription Kit

96 Well Assay Plate

TaqMan® Gene Expression Assay

TaqMan® Gene Expression Master Mix

384 Well Assay Plate

Methods

Standard curves of RNA mouse were prepared in triplicate for reverse transcription in the following manner:

| Assay | Standards (ng/μl) | | | | | | |
|---------------|-------------------|----|----|----|----|-----|-----|
| 18S | 50 | 25 | 10 | 5 | 1 | 0.5 | 0.1 |
| Target | 100 | 75 | 50 | 25 | 10 | - | - |

2.3.5 Northern Blot Analysis of mRNA

Northern blotting was used to analyse the size and quantity of UCP-1 RNA in BAT. The RNA is size fractionated on a denaturing agarose gel by electrophoresis, transferred by capillary action to a nylon filter and covalently linked to it by baking. The RNA is denatured to remove secondary structure ensuring the rate of migration of the RNA is proportional to its total length.

2.3.5.1 Total RNA Extraction

Materials

Tri-reagent (Helena Biosciences, Sunderland, Tyne and Wear, UK)

Bromo-Chloro-Propane (Sigma-Aldrich, Poole, UK) 77

Isopropanol (VWR International Ltd, Poole, UK)

Ethanol (VWR International Ltd, Poole, UK)

GDW

Methods

Total RNA was extracted from brown adipose tissue ground under liquid nitrogen with a pestle and mortar using the Tri-reagent method according to the manufacturer's protocol, as described in Section 2.3.4.1. One hundred microlitres of bromo-chloro-propane were then added, mixed vigorously for 15 seconds, and then incubated for a further five minutes at room temperature. The emulsion was then centrifuged at 4°C, for 15 minutes, at 12000g, with the brake off. The upper aqueous phase was transferred to a clean eppendorf, precipitated with a half volume (300µl) room temperature isopropanol for five minutes at room temperature, and then centrifuged at 12000g for ten minutes at 4°C. This resulted in a pellet which was washed with 1 volume (1ml) 75% ethanol in GDW, centrifuged at 12000g for a further 10 minutes at 4°C, the pellet was then air dried, and dissolved in 400µl autoclaved GDW. RNA concentration was determined spectrophotometrically as described in Section 2.3.4.2.

Following quantification on the spectrophotometer the RNA samples were ethanol precipitated with 0.1 volumes sodium acetate pH 5.2 and 2.5 volumes ice cold absolute ethanol. The samples were precipitated at -20°C for a minimum of one hour and centrifuged at 12000g for 20 minutes, the supernatant was discarded and the pellet vacuum dried for five minutes. The pellets were re-suspended in the appropriate volume of GDW to give a 5mg/ml solution.

2.3.5.2 Integrity Analysis of the Total RNA

Materials

Agarose, type II-A medium EEO 78
Formaldehyde (VWR International Ltd, Poole, UK)
20x MOPS pH 7.0 (appendix 1)
Ethidium bromide (VWR International Ltd, Poole, UK)
DENAT (appendix I)
Gel loading buffer (appendix I)
100x TE pH 7.5 (appendix 1)
2M Sodium acetate pH 5.2
GDW

Methods

The RNA secondary structure was denatured before confirming the integrity of the samples using a formaldehyde gel. One microlitre of this solution was added to 12µl DENAT. The samples were denatured at 65°C for five minutes and 3µl gel loading buffer added. The samples were loaded onto the gel and run in 1x MOPS buffer with 7.5 % formaldehyde (v/v) at 10 V/cm. The gel was stained in 1x TE with 0.1 mg/ml ethidium bromide on a shaking platform for thirty minutes and de-stained overnight in 1x TE to allow visualisation of the 18S and 28S ribosomal bands under UV light. The presence of intact ribosomal bands indicated the RNA was not degraded.

2.3.6 Transfer of RNA to Nylon Filters

Materials

Formaldehyde (VWR International Ltd, Poole, UK)
20x MOPS pH 7.0 (appendix 1)
Hybond-N (GE Healthcare, Little Chalfont, Buckinghamshire, UK)

Methods

An agarose gel was made by dissolving 1g agarose in GDW, 20x MOPS was added to a final concentration of 1x and formaldehyde added to 3% (v/v). Once set, the gel was transferred to an electrophoresis tank containing 1x MOPS, and 3% formaldehyde (v/v). Before loading, 50µg of total RNA was denatured by addition of 10µl denaturing buffer and incubation at 60°C for 5 minutes. After denaturation, 3µl loading buffer was added and the samples loaded onto the gel. The gel was electrophoresed at a constant voltage of 10V/cm. After electrophoresis, the RNA in the gel was transferred to Hybond-N by capillary action.

2.3.6.1 *Random Primer Labelling of DNA Fragments*

Materials

DNA fragment

5x ABC Buffer (appendix I)

12.5mM magnesium chloride

125mM Tris-HCl, pH8.0

23µM 2-mercaptoethanol

50µM dATP (GE Healthcare, Little Chalfont, Buckinghamshire, UK)

20x SSC (appendix I)

Filter paper

Saran wrap

Inverted gel

Hybond-N (GE Healthcare, Little Chalfont, Buckinghamshire, UK)

Paper towels

Glass plate

Weight (approx. 200g)

50µM dGTP (GE Healthcare, Little Chalfont, Buckinghamshire, UK)

50µM dTTP (GE Healthcare, Little Chalfont, Buckinghamshire, UK)

1M N-2-hydroxyethylpiperazine-N^{''}-2-ethanesulphonic acid (HEPES) (Sigma Aldrich, Poole, UK)

34µg/ml random deoxynucleotide hexamers (GE Healthcare, Little Chalfont, Buckinghamshire, UK)

10mg/ml BSA, fraction V (Sigma Aldrich, Poole, UK)

[α -³²P]-dCTP: 10Ci/ml, 3000Ci/mmol (GE Healthcare, Little Chalfont, Buckinghamshire, UK)

DNA polymerase I, Klenow fragment 9U/ μ l (GE Healthcare, Little Chalfont, Buckinghamshire, UK)

Sephadex G50 (appendix I)

1x TE (appendix I)

Methods

20ng DNA in a total volume of 15 μ l GDW was boiled for five minutes. After boiling, the solution was made up to a total volume of 25 μ l containing 1x ABC buffer, 5mg/ml BSA, 10 μ Ci dCTP and 1U Klenow. The reaction was incubated at 37°C for one hour and incorporation calculated. Incorporation of radionucleotide into the oligonucleotide was measured using a mini Sephadex G50 column. The column was prepared by plugging a glass Pasteur pipette with glass wool and adding Sephadex G50. The labelling reaction volume was made up to 200 μ l with 1x TE and this was loaded onto the column. The column was eluted with 1x TE and 200 μ l fractions collected. The fractions were counted and the percentage incorporation calculated. The hottest two fractions were pooled and half added to the hybridisation mix.

2.3.6.2 Hybridisation of Northern Filters

Materials

Hybridisation/pre-hybridisation buffer (appendix I)

Amasino wash (appendix I)

Universal wash buffer (appendix I)

Methods

The baked nylon filter was pre-hybridised in a clean plastic bag with 20ml of pre-hybridisation buffer at a 60°C for at least two hours. Before hybridisation of the nylon filter, the radio-labelled probe was denatured for five minutes in a boiling water bath. The pre-hybridisation mix was then removed and replaced with 20ml fresh hybridisation buffer and 200 μ l probe was added to this and sealed. The sealed filter was then left to hybridise with the radio-labelled probe overnight at 60°C. The following day, the filter was washed to

remove any non-specifically bound probe. The filter was washed three times in 50ml Amasino wash buffer for 20 minutes each time at 60°C. The filter was washed a further three times in Universal wash; each wash lasted for 20 minutes at 60°C. Finally the filter was exposed to a phosphor screen for two days and quantified using the ImageQuant computer package (GE Healthcare, Little Chalfont, UK).

2.3.6.3 Filter Stripping

Following hybridisation with a radiolabelled probe, northern filters can be stripped of radioactivity and re-used with minimal loss of RNA. Most northern filters can be stripped and re-probed five or six times depending on the abundance of the transcript of interest.

Materials

100 x TE (appendix I)

20% SDS

Methods

The filter was stripped in 100-200 ml of 1xTE/0.5% SDS for 30 minutes in an 80°C water bath. The filter was then exposed overnight to a phosphorimager plate to ensure that all radioactive probe had been removed.

2.3.6.4 Oligo dT Correction

To correct for variation in gel loading and RNA transfer when performing northern analysis, total mRNA on filters was quantified by oligo dT probing. The radiolabelled oligo dT probe hybridises with the poly A tail of mRNA species.

Materials

20ng Oligo dT template

5x Reaction buffer:

500mM cacodylate, pH6.8

5mM cobalt (II) chloride

0.5mM dithiothreitol (DTT)

0.5mg/ml Bovine serum albumin (BSA)

Terminal deoxytransferase, 20U/ μ l (Promega, Madison, WI, USA)
[α -32P]-dATP: 10ci/ml (GE Healthcare, Little Chalfont, Buckinghamshire, UK)
20x SSPE: (appendix 1)
3.6M sodium chloride
120mM di-sodium hydrogen orthophosphate
20mM EDTA
Sephadex G50 (appendix 1)
1x TE (appendix 1)

Methods

Twenty nanograms of oligonucleotide were added to 1x reaction buffer that contained 70 μ Ci of dATP and 20U of terminal transferase, in a final volume of 20 μ l. The reaction was incubated for one hour at 37°C. Incorporation of nucleotide into the oligonucleotide was measured using a mini Sephadex G50 column. The column was prepared by plugging a glass Pasteur pipette, with glass wool, and adding Sephadex G50. The labelling reaction volume was made up to 200 μ l with TE and this was loaded onto the column. The column was eluted with 1x TE and 200 μ l fractions collected. The fractions were counted and the percentage incorporation calculated. The hottest two fractions were pooled and one tenth added to the hybridisation mix. Filters were prehybridised in 20ml of prehybridisation buffer (5x SSPE, 0.2% (w/w) milk powder, 0.2% (v/v) nonidet) for a minimum of two hours at room temperature in a polythene bag on a shaking platform. Hybridisation solution was made by adding one tenth of the labelled probe to 10ml of the prehybridisation buffer. The prehybridisation solution was removed and replaced with the hybridisation solution. Hybridisation was carried out overnight at room temperature. Non-specifically bound probe was removed by increasingly stringent washes. All wash steps were performed at room temperature. The first washes were carried out in; 5x SSPE; 0.2% SDS. The hybridisation solution was removed and replaced with 20ml of washing buffer and washed for five minutes at room temperature. This was repeated and then followed by two washes for thirty minutes each in 2x SSPE/0.2% SDS. Following this, the filter was exposed to a phosphoimager screen and radiolabelled bands quantified by image densitometry using ImageQuant software (Molecular Dynamics, Sunnyvale, CA, U.S.A.)

2.3.7 AMPK activity (SAMS peptide) assay

AMPK assay was carried out according to a published protocol in collaboration with Mr. Huza Zhang under the supervision of Professor David Carling (Davies et al., 1989). This assay relies on the precipitation of AMPK using an antibody generated against the β subunit of AMPK on hypothalamic protein extract. In order to preserve the activity of AMPK, hypothalamic protein extract must be treated with appropriate phosphorylation inhibitors at the time of protein extraction. AMPK activity was assessed by incorporation of radiolabelled [32 P] γ -ATP into the SAMS peptide, HMRSAMSGLHLVKR+R+, a synthetic peptide based on the 13-residue sequence around the unique AMPK phosphorylation site of rat acetyl-CoA carboxylase (ser79, **S**) (Davies et al., 1989). The site for cyclic-AMP-dependant protein kinase phosphorylation (ser77) is replaced by an alanine (**A**) to allow specific phosphorylation by AMPK and two C-terminal arginine residues (positively charged) to facilitate binding to phosphocellulose P-81 paper.

Materials

HEPES

Sodium fluoride

Sodium pyrophosphate (NaPP)

Sucrose

EDTA

Dithiothreitol

Benzamidine

Trypsin inhibitor (Roche applied science, Indianapolis, USA)

Phenylmethylsulfonyl fluoride

Anti- AMPK (β subunit) antibody (generated and provided by Prof David Carling)

SAMS peptide (HMRSAMSGLVLKRR) (Tocris bioscience, Bristol, UK)

AMP

Triton

32 P-ATP (Perkin Elmer, Massachusetts, USA)

p81 cellulose phosphate paper (Whatman)

Methods

Frozen tissues (~100 mg) were homogenized in 0.2 ml of ice-cold 50 mM HEPES, pH 7.4, 50 mM sodium fluoride (NaF), 5 mM sodium pyrophosphate (NaPP), 250 mM sucrose, 1 mM EDTA, 1 mM dithiothreitol, 1 mM benzamidine, 1 mM trypsin inhibitor, 0.1% (w/v) phenylmethylsulfonyl fluoride using an UltraTurax homogenizer (3 × 30-s bursts). Insoluble material was removed by centrifugation and the resulting supernatant used for immunoprecipitation of AMPK. AMPK was immunoprecipitated using the pan- β subunit antibody against AMPK from 100 μ g of cell lysate in the presence of Protein A (Sigma). The resin was washed twice with lysis buffer. The assay was conducted in duplicate. 5 μ l resin sample was incubated at 37°C whilst shaking for 30 minutes with 200 μ M AMP, 200 μ M SAMS peptide (HMRSAMSGLVKRR), 10mM Hepes, 0.2 % Triton, and 200 μ M 32 P-ATP in a total volume of 25 μ L. The reaction was terminated by spotting aliquots (20 μ l) onto P-81 paper and unincorporated [32 P] γ -ATP removed by washing with 1% (v/v) phosphoric acid until blank samples reached background levels as assessed with a Geiger counter. Following drying of the sample papers, phosphate incorporation was determined via liquid scintillation counting for 30 seconds. Specific activity was calculated by subtraction of the background level (lacking SAMS peptide) from the averaged duplicates. AMPK activity was expressed as fold activity as compared to controls.

2.3.8 Hypothalamic explant static incubation system

The static incubation system used was a modification of the method previously described and has been used previously in to measure glucose-stimulated neurotransmitter release from hypothalamic (Beak et al., 1998, Parton et al., 2007b). 20 male Wistar rats (10 iARC-GKS rats and 10 iARC-GFP rats) were killed by decapitation 28 days after intranuclear AAV injection and whole brains were removed immediately. The brain was mounted with ventral surface uppermost and placed in a vibrating microtome (Microfield Scientific Ltd., Dartmouth, UK). A 1.7-mm slice was taken from the basal hypothalamus and incubated in individual tubes containing 1 ml of artificial cerebrospinal fluid (aCSF) (20 mM NaHCO₃, 126 mM NaCl, 0.09 mM Na₂HPO₄, 6 mM KCl, 1.4 mM CaCl₂, 0.09 mM MgSO₄, 5 mM glucose, 0.18 mg/ml ascorbic acid, and 100 μ g/ml aprotinin), equilibrated with 95% O₂ and 5% CO₂. The tubes were placed on a shaking platform in a water bath maintained at 37 C. After an

initial 2 hour equilibration period, the hypothalamic explants were incubated for three 45 min periods in 600 µl aCSF containing 3, 8 (baseline) and 15 mM glucose in randomised order. Finally, the viability of the tissue was verified by 45-minute incubation in aCSF containing 56 mM KCl. At the end of each incubation period, supernatants were removed and tested for NPY release by radioimmunoassay as mentioned in section 1.3.10.5.3. Only hypothalami that showed a 100% secretion over baseline in response to 56 mM KCl were used in the analysis.

2.3.9 Body composition analysis

Body composition was analysed to establish the ratio of fat mass to lean body mass. Rat carcasses were dissolved (saponified) in a strong organic solvent before glycerol and protein concentrations were measured using standard assay procedures.

2.3.9.1 Saponification of Carcass

Materials

3M KOH 65% ethanol (v/v) (Appendix I)

Ethanol (VWR International Ltd, Poole, UK)

Methods

Animals were weighed and placed in separate 1L plastic containers. Carcasses were dissolved using 3M KOH in 65% ethanol in equal volume to carcass weight (1ml/g). Vessels were then incubated at 70°C for one hour to initiate liquefaction. Following this, the containers were placed in an oven at 70°C for 5 days. The resultant liquid was made up to 1.7L with absolute ethanol and stored at room temperature until required.

2.3.9.2 Glycerol Assay

In order to determine total fat content in rats, a glycerol assay was used. Whole carcass glycerol concentrations were determined using reagents and methods from Randox laboratories Ltd, Crumlin, Co. Antrim.

Materials

1M Glycerol (VWR International Ltd, Poole, UK)

Glycerol Assay Kit (Randox Laboratories Ltd, Crumlin, Co. Antrim)

Buffer R (appendix 1)

Reagent R (appendix 1)

Methods

In order to determine the total fat content per rat a glycerol assay was used. All buffers were supplied ready to use and one vial of reagent R was reconstituted with 15 ml of buffer R. One molar glycerol stock solution was diluted in GDW to provide standard glycerol concentrations of 5mM, 2mM, 1mM, 0.5mM, 0.2mM, 0.1mM, and 0.05mM. Ten microlitres of dissolved carcass sample was diluted 1:100 with GDW in separate microtubes ready for use in the assay. To begin the assay 1 ml reagent R was added to a new set of tubes. To this 30µl of sample, standard, or buffer R (for blank value) was added and left to incubate at room temperature for 10 minutes. Each tube was then read using a spectrophotometer at an absorbance of 520 nm. The carcass fat content was calculated from the glycerol reading by assuming a molecular weight of 885 per triglyceride molecule (Bergmeyer and Gawehn, 1974).

2.3.9.3 Lowry Protein Assay

The Lowry protein assay was performed on 10 µL of dissolved carcass sample diluted in 1 mL GDW as described in section 2.3.2.3.

2.3.10 Analysis of plasma metabolites and hormones

2.3.10.1 Glucose assay

Materials

Glucose assay kit (Randox Laboratories Ltd. UK)

Methods

Plasma glucose concentrations were determined using reagents and methods from Randox Laboratories Ltd. This assay involves two linked reactions which are shown below. In the

first reaction glucose is oxidised by glucose oxidase (GOD) to give gluconic acid and hydrogen peroxide. In the second reaction hydrogen peroxide reacts with 4-aminophenazone and phenol under catalysis of peroxidase (POD). The products of the second reaction are water and quinoneimine.

GOD

Glucose + O₂ + H₂O → gluconic acid + H₂O₂

POD

2 H₂O₂ + 4-aminophenazone + phenol → quinoneimine + 4 H₂O

All buffers were supplied ready to use and the GOD-PAP reagent was reconstituted using one vial R1b buffer. Plasma samples were thawed on wet ice and diluted 1:5 in GDW. Standard glucose concentrations were produced using standard glucose solution and methods provided by Randox. On a 96 well plate 5µl of sample or standard was mixed with 280µl of reconstituted GOD-PAP reagent and incubated for 10 minutes at 37°C. The A₅₀₀ of the samples was then measured in a spectrophotometer. Absorbance values of the blank readings were subtracted from the absorbance readings of all samples and standards, and a standard curve plotted. The glucose concentration of each of the unknown samples was determined by comparison to the standard curve.

2.3.10.2 Plasma insulin ELISA

Material

Rat ultra-sensitive insulin ELISA kit (Crystal Chem, Illinois, USA)

Methods

Plasma insulin concentrations were determined using reagents and methods as described in the manufacturer's protocol. 10X wash buffer was diluted 1:10 in GDW. Five microlitres of sample, premixed rat insulin standard or quality control were added to wells containing 95 µL sampled diluent. Plates were sealed and incubated at 4°C for 2 hours on a plate shaker at 400rpm. Following incubation, solution was decanted from wells as previously described and wells washed five times with 300µl wash buffer. Next, 100 µL anti-insulin enzyme

conjugate (conjugated with streptavidin-horseradish peroxidase) was added to each well and was incubated for 30 min at room temperature on a plate shaker at 400 rpm. Following incubation, solution was decanted from wells as previously described and wells washed seven times with 300µl wash buffer. One hundred microlitres of enzyme substrate reagent was added, containing 3,3',5,5'-tetramethylbenzidine, and was incubated for 40 min at room temperature on plate shaker at 400 rpm and covered to prevent exposure to light. 100 µL of enzyme reaction stop solution were added to each well. The A450 and A630 of the samples was then measured in a spectrophotometer. Absorbance values of A450 were subtracted by absorbance values at A630. These values of all samples and standards were subtracted from the values of the blank readings, and a standard curve plotted. The insulin concentration of each of the unknown samples was determined by comparison to the standard curve.

2.3.10.3 Plasma leptin ELISA

Material

Rat leptin ELISA kit (Crystal Chem, Illinois, USA)

Methods

Plasma leptin concentrations were determined using reagents and methods as described in the manufacturer's protocol. 10X wash buffer was diluted 1:10 in GDW. Five microlitres of sample, premixed standard or quality control were added to wells containing 45 µL sampled diluent. 50 µL of guinea pig anti-mouse leptin serum were added to each well. Plates were sealed and incubated at 4°C for 16-20 hours (overnight). Following incubation, solution was decanted from wells as previously described and wells washed five times with 300µl wash buffer. Next, 100 µL anti-pig IgG enzyme conjugate was added to each well and was incubated for three hours at 4° C. Following incubation, solution was decanted from wells as previously described and wells washed seven times with 300µl wash buffer. Next, 100µl of enzyme substrate, containing 3,3',5,5'-tetramethylbenzidine, and was incubated for 30 min at room temperature on plate shaker at 400 rpm and covered to prevent exposure to light. 100 µL of enzyme reaction stop solution were added to each well. The A450 and A620 of the samples was then measured in a spectrophotometer. Absorbance values of A450 were

subtracted by absorbance values at A620. These values of all samples and standards were subtracted from the values of the blank readings, and a standard curve plotted. The insulin concentration of each of the unknown samples was determined by comparison to the standard curve. A high and low quality control (provided by the manufacturer) was used to validate the assay.

2.3.10.4 Plasma active glucagon-like peptide-1 ELISA

Material

Rat Glucagon-like Peptide-1 (Active) ELISA kit (Millipore, Missouri, USA)

Methods

Plasma active glucagon-like peptide-1 (GLP-1) concentrations were determined using reagents and methods as described in the manufacturer's protocol. Biologically active forms of GLP-1 are inactivated by peptidases and enzyme such as dipeptidyl peptidase IV. This kit allows non-radioactive quantification of biologically active forms of GLP-1 i.e. GLP-1 (7-36 amide) and GLP-1 (7-37) in plasma. It is highly specific for the immunologic measurement of active GLP-1 and will not detect other forms of inactive GLP-1 (e.g., 1-36 amide, 1-37, 9-36 amide, or 9-37), providing a more reliable measure of biologically important GLP-1 levels. This assay is based, capture of active GLP-1 from sample by a monoclonal antibody, immobilized in the wells of a microwell plate, that binds specifically to the N-terminal region of active GLP-1 molecule, washing to remove unbound materials, binding of an anti GLP-1-alkaline phosphatase detection conjugate to the immobilized GLP-1, washing off unbound conjugate, and quantification of bound detection conjugate by adding methyl umbelliferyl phosphate which in the presence of alkaline phosphatase forms the fluorescent product umbelliferone. Since the amount of fluorescence generated is directly proportional to the concentration of active GLP-1 in the unknown sample, the amount of GLP-1 can be derived by reference to the standard curve of known concentrations of active GLP-1.

10X wash buffer was diluted 1:10 in GDW. 300 µL wash buffer was added to each well and the plate was incubated at room temperature for 5 min. The residual buffer was removed by gently tapping on absorbent towels. 100 µL of assay buffer was added to each well

thereafter. 100 µL of sample or standard or quality control were added to wells. Plates were sealed and incubated at 4°C for 16-20 hours (overnight). Following incubation, solution was decanted from wells as previously described and wells washed five times with 300µl wash buffer. Next, 200 µL detection conjugate was added to each well and was incubated for two hours at room temperature. Following incubation, solution was decanted from wells as previously described and wells washed three times with 300µl wash buffer. Next, 200µl of substrate and was incubated for 20 min at room temperature or plate shaker at 400 rpm and covered to prevent exposure to light. 50 µL of enzyme reaction stop solution were added to each well. Fluorescence at 355 nm/460 nm was read on a fluorescence microplate reader (Gemini™ XPS Fluorescence Microplate Reader). A high and low quality control (provided by the manufacturer) was used to validate the assay.

2.3.10.5 Radioimmunoassays

Radioimmunoassay (RIA) was used to determine the concentrations of plasma hormones. The principle of RIA is based on the competitive nature of the binding of radiolabelled ligand and cold ligand for limited antibody binding sites.

Plasma gut hormones peptide tyrosine tyrosine (PYY) and ghrelin were calculated using in-house RIA methods. Human PYY, αMSH and neuropeptide Y (NPY) were iodinated using the iodogen or Bolter and Hunter method by Professor Mohammed Ghatei and purified by HPLC (Wood et al., 1981, Adrian et al., 1985). All assays were performed using 0.06M phosphate buffer (Appendix I). Standard curves for each assay were prepared using synthetic peptide.

PYY radioimmunoassay

Materials

Phosphate Buffer (appendix I)

¹²⁵I labelled PYY

Rabbit anti-PYY (1:50,000 dilution)

Sheep anti-rabbit antibody (Pharmacia & Upjohn, Sweden)

PYY standard peptide (Bachem, UK)

Methods

PYY-like IR was measured using a specific and sensitive RIA (Adrian et al., 1985). The assay measured the hormone fragment, PYY3-36, and the full length hormone, PYY1-36, both of which are biologically active. The antiserum (Y21) was produced in rabbits against synthetic porcine PYY coupled to BSA by glutaraldehyde and used at a final dilution of 1:50,000. This antibody cross-reacts fully with the biologically active circulating forms of PYY, but not with PP or other known gastrointestinal hormones. The ¹²⁵I-PYY was prepared by the iodogen method and purified by high pressure liquid chromatography. The assay was performed in duplicate in a total volume of 0.7 ml of 0.06 M phosphate buffer PH 7.2 containing 0.3% BSA. The assay was incubated for three days at 4°C before separation of the free from antibody bound label by sheep anti-rabbit antibody. These free and bound fractions were counted for 180 seconds in a gamma scintillation counter and sample concentrations were calculated using a data reduction program (NE1600, NE Technology, UK). Sample concentrations were calculated using a data reduction program (NE1600, NE Technology, UK). The detection limit of the assay was 2.5 pmol/l, with an intra-assay coefficient of variation of 5.8 %. All samples were assayed in one assay to avoid inter-assay variation.

Ghrelin radioimmunoassay

Materials

Phosphate Buffer (appendix I)

¹²⁵I labelled ghrelin (Bolton & Hunter reagent, Amersham International UK)

Rabbit anti-ghrelin (1:70,000 dilution) (G0 antibody, Bachem UK)

Rabbit anti-ghrelin (1:50,000 dilution) (SC10368, Santa Cruz)

Sheep anti-rabbit antibody (Pharmacia & Upjohn, Sweden)

Ghrelin standard peptide (Bachem, UK)

Methods

Ghrelin-like IR was measured using a specific and sensitive RIA (Patterson et al., 2005). The G0 antiserum was produced in rabbits against synthetic human ghrelin (Bachem, UK) coupled to BSA by glutaraldehyde and used at a final dilution of 1:70,000. This antibody cross-reacts fully with the biologically active circulating forms of ghrelin (acylated ghrelin),

but not with other known gastrointestinal hormones or des-acylated ghrelin. The SC10368 antiserum was produced in rabbits against synthetic human ghrelin (Santa Cruz, USA) and used at a final dilution of 1:50,000. This antibody cross-reacts fully with all circulating forms of ghrelin, but not with other known gastrointestinal hormones. The ¹²⁵I-ghrelin was prepared by the iodogen method and purified by high pressure liquid chromatography using a linear gradient from 10 to 40% acetonitrile (AcN), 0.05% Tri-fluoroacetic acid (TFA) over 90 mins. The assay was performed in duplicate in a total volume of 0.7 ml of 0.06 M phosphate buffer PH 7.2 containing 0.3% BSA on acidified plasma samples. The assay was incubated for three days at 4°C before separation of the free from antibody bound label by sheep anti-rabbit antibody. These free and bound fractions were counted for 180 seconds in a gamma scintillation counter and sample concentrations were calculated using a data reduction program (NE1600, NE Technology, UK). Sample concentrations were calculated using a data reduction program (NE1600, NE Technology, UK). The assay detected changes of 15 pmol/l of plasma ghrelin with 95% confidence limit. The intra and inter-assay coefficients of variation were 6.2% and 9.5% respectively. All samples were assayed in one assay to avoid inter-assay variation.

NPY radioimmunoassay

Materials

Phosphate Buffer (appendix I)

¹²⁵I labelled NPY

Rabbit anti-NPY (1:50,000 dilution)

Sheep anti-rabbit antibody (Pharmacia & Upjohn, Sweden)

NPY standard peptide (Bachem, UK)

Methods

NPY-like IR was measured using a specific and sensitive RIA (Allen et al., 1984). The antiserum (YN7) was produced in rabbits against synthetic porcine NPY coupled to BSA by glutaraldehyde and used at a final dilution of 1:50,000. This antibody cross-reacts fully with NPY, but not with other peptides, including PYY. The ¹²⁵I-NPY was prepared by the iodogen method and purified by high pressure liquid chromatography. The assay was performed in

duplicate in a total volume of 0.35 ml of 0.06 M phosphate buffer PH 7.2 containing 0.3% BSA. The assay was incubated for three days at 4°C before separation of the free from antibody bound label by sheep anti-rabbit antibody. These free and bound fractions were counted for 180 seconds in a gamma scintillation counter and sample concentrations were calculated using a data reduction program (NE1600, NE Technology, UK). Sample concentrations were calculated using a data reduction program (NE1600, NE Technology, UK). The sensitivity of the assay was 1000 pmol/ml. The intra- and inter-assay variation was 7% and 8% respectively. All samples were assayed in one assay to avoid inter-assay variation.

α MSH radioimmunoassay

Materials

Phosphate Buffer (appendix I)

¹²⁵I labelled α -MSH

Rabbit anti- α -MSH (1:120,000 dilution) (Chemicon International Inc., USA)

Sheep anti-rabbit antibody (Pharmacia & Upjohn, Sweden)

α -MSH standard peptide (Bachem, UK)

Methods

α -MSH -like IR was measured using a specific and sensitive RIA (Kim et al., 2000). The anti-serum cross-reacts fully with α -MSH, but not with other POMC products. The assay was performed in duplicate with 0.06 M phosphate buffer PH 7.2 containing 0.3% BSA. The assay was incubated for three days at 4°C before separation of the free from antibody bound label by sheep anti-rabbit antibody. These free and bound fractions were counted for 180 seconds in a gamma scintillation counter and sample concentrations were calculated using a data reduction program (NE1600, NE Technology, UK). Sample concentrations were calculated using a data reduction program (NE1600, NE Technology, UK). All samples were assayed in one assay to avoid inter-assay variation.

2.4 Statistical analysis

Results are shown as mean and s.e.m unless indicated. Generalized estimating equation (GEE) was used to compare cumulative data between control and treatment groups. GEE is

used to analyse longitudinal data (for example food intake, bodyweight, glucose intake or caloric intake during chronic studies). Data from multiple groups for glucokinase activity assays and hypothalamic explant studies were analysed using one-way statistical analysis of variance (ANOVA) followed by *post-hoc* Holm-Sidak test. A paired Student's *t*-test was used to compare absolute food and glucose intake data from cross-over studies. An unpaired Student's *t*-test was used to compare all other data. Significance was set at $P < 0.05$ for all analysis. Data analysis was performed using Graphpad Prism 5 software except for GEE, which was performed using Stata 9 software (Stata, Stata Corp LP, USA).

3 Effect of increased arcuate glucokinase activity on food intake and body weight

3.1 Introduction

The brain responds to circulating nutrient signals, such as glucose, and regulates energy balance accordingly (Schwartz et al., 2000). Recent evidence suggests a strong interaction between peripheral and central nutrient sensing neurons in the regulation of energy homeostasis (Jordan et al., 2010). Glucose-sensing neurons play a significant role in allowing the brain to detect glucose. Hypothalamic glucose-sensing neurons are anatomically and functionally capable of playing an important integrative role in energy balance and glucose homeostasis. Glucokinase acts as part of the glucose sensing mechanism in these neurons (Dunn-Meynell et al., 2002b, Levin et al., 2004, Kang et al., 2006). It is now well accepted that the brain not only responds to these signals and adjusts food intake, but also changes peripheral functions such as glucose homeostasis (Levin, 2006, Lam et al., 2009). However, the precise role that glucose-sensing and alterations in glucose-sensing machinery play on influencing day-to-day food intake remained unaddressed.

3.1.1 Evidence for the glucostatic control of food intake

In 1953, Jean Mayer first proposed the “glucostatic theory”, which suggested that changes in blood glucose were sensed by “glucoreceptors” in the hypothalamus leading to alterations in hunger and satiety (Mayer, 1953). The discovery of glucose-sensing neurons provided support for this theory (Oomura et al., 1964). Since then, a number of approaches have been attempted to confirm the existence of the glucostatic control of food intake (Levin et al., 2004). Alteration of glucose levels in the general circulation of rodents and primates and portal circulation of rodents leads to changes in feeding behaviour (Smith and Epstein, 1969, Tordoff et al., 1989). Furthermore in rodents and humans, spontaneous feeding is preceded by a fall in plasma glucose levels (Campfield et al., 1985, Melanson et al., 1999, Dunn-Meynell et al., 2002a). ICV infusion of glucose in rodents dose dependently decreases subsequent food intake (Kurata et al., 1986). Repeated infusion of glucose into the VMH decreases food intake and body weight gain (Panksepp and Rossi, 1981). ICV and VMH infusion of a glucose antimetabolite, 2-deoxyglucose, increases food intake (Tsuji and Bray, 1990, Lenin Kamatchi et al., 1986). Glucoprivation has been shown to increase mRNA levels of orexigenic NPY in the ARC (Sergeyev et al., 2000, Akabayashi et al., 1993). Attenuation of glucoprivic feeding has been demonstrated in NPY KO and rats treated with

NPY-antiserum in the hypothalamus (Sindelar et al., 2004, He et al., 1998). Glucose results in a dose-dependent increase in anorexigenic POMC release from the hypothalamus in hypothalamic explants of lean mice (Parton et al., 2007a). In obese mice, this increase is disrupted suggesting alterations in glucose-sensing with altered anorexigenic POMC release in obesity. The effect of leptin on POMC release has also been shown to be modulated by glucose levels in neurons from the ARC (Ma et al., 2008a). Glut 2 null mice with pancreatic re-expression of glut 2 demonstrate hyperphagia and altered leptin sensitivity in NPY and POMC neurons suggesting that altered brain glucose-sensing may alter food intake (Bady et al., 2006, Mounien et al., 2010).

Although the above observations support a role for glucose-sensing in the hypothalamus, particularly the VMH, and the regulation of food intake; other observations do not support this. Intravenous or intragastric glucose infusion did not alter food intake and appetite compared with intravenous or intragastric saline treatment in normal humans in a crossover study (Bernstein and Grossman, 1956). Unlike the infusion of 2-deoxyglucose, the infusion of glucose epimers such as D- mannose, D-galactose and D-allose in rodents does not need to altered food intake. Although the disruption of K_{ATP} channels in POMC neurons of mice altered glucose-sensing in hypothalamic neurons, it did not alter food intake and body weight in these mice (Parton et al., 2007a). It has also been argued that supraphysiological levels of glucose have been used in most central nervous system infusion studies. Brain glucose levels are much lower than systemic glucose levels with a narrow range of variation (de Vries et al., 2005).

Therefore approaches so far have not conclusively demonstrated the existence of glucostatic control of food intake, with some observations being in contrast to others. The exact role of glucostatic regulation in modulating food intake via the hypothalamus in normal physiology, as opposed to experimentally induced glucoprivation, is not clear.

3.1.2 Glucokinase and food intake

Diet-induced obese (DIO) and DIO-prone rats have increased ARC glucokinase mRNA expression, suggesting that ARC glucokinase may play a role in energy homeostasis and

that this system is altered in obesity (Dunn-Meynell et al., 2002b). Assessing the precise role of hypothalamic glucokinase on food intake has been difficult since global alterations of glucokinase disrupt glucose homeostasis (Yang et al., 2007). Pharmacological studies suggest that hypothalamic glucokinase played a role in modulating food intake. ICV infusions of glucosamine, a non-selective inhibitor of glucokinase, at 15nmol/min in rats increases glucoprivic feeding (Osundiji et al., 2010). ICV infusions of glucosamine at a much larger dose of 150 nmol/min during the mid-light cycle in overnight fed rats increase food intake and is associated with increased c-fos, a marker of neuronal activation, in NPY neurons of the ARC and orexin neurons of the LH (Zhou et al., 2011). Glucosamine also inhibits hexokinase (Bertoni, 1981). Therefore, its infusion at high doses into the ICV is likely to cause marked non-specific effects leading to altered appetite. Using alloxan and short-interfering RNA mediated knockdown of glucokinase with an adenoviral vector, Levin and colleagues were unable to demonstrate a role for VMH glucokinase in feeding over twenty-four hours and fourteen days, respectively (Dunn-Meynell et al., 2009). Alloxan is a toxic glucose analogue that generates reactive oxygen species and is likely to have detrimental effects in neurons (Salkovic-Petrisic and Lackovic, 2003). Adenoviral vectors generate immune responses which lead to inflammation and compromise the efficacy of gene transfer (Kaplan et al., 1997). Therefore, none of these short studies have satisfactorily addressed the role of glucokinase on appetite.

3.1.3 Role of the ARC in modulating food intake in response to changes in glucose

The ARC is positioned at the base of the hypothalamus and possesses a highly fenestrated blood brain barrier. Circulating factors such as glucose, fatty acids, leptin and ghrelin can access neurons situated in the ARC (Cone et al., 2001). The supply of glucose is likely to be greater in the ARC, and possibly the VMN than in the deeper regions of the brain (Mountjoy and Rutter, 2007). Furthermore, the ARC contains the orexigenic NPY/ AgRP neurons and the anorexic POMC/CART neurons, some of which are believed to be glucose sensitive and express glucokinase. Therefore, ARC glucose-sensing neurons are well placed to act as primary central “metabolic sensors” that respond to glucose, as well as other metabolic signals such as insulin, leptin, lactate and fatty acids. Their location and co-localisation with NPY/ AgRP and POMC/CART neurons may allow them to act as “metabolic effectors” by influencing the desire to feed. Taken together, the above data suggests that ARC nucleus is

likely to play an important role in altering food intake in response to changes in glucose via glucose-sensing. Altering the components involved in glucose-sensing specifically in these nuclei may lead to alterations in food intake and provide insight into the role of glucose-sensing in energy homeostasis.

Glucose-sensing in the hypothalamus has been implicated in the regulation of food intake. Glucokinase has a prominent role in glucose-sensing and is expressed in hypothalamic nuclei, such as the ARC, which have important roles in controlling energy homeostasis. However, the role of glucokinase and glucose-sensing on the physiological regulation of food intake has not been conclusively demonstrated. This chapter attempts to address this by altering glucokinase expression in the ARC using two different approaches. The first involves pharmacological activation of glucokinase by direct administration of glucokinase activator compound A (CpdA) into the ARC. CpdA is an allosteric activator of glucokinase (Kamata et al., 2004, Iino et al., 2009). It has previously been used *in vitro* and *in vivo* to alter glucokinase activity (Kang et al., 2006, Levin et al., 2008a). The second involves chronically increasing glucokinase mRNA expression in the ARC by developing and delivering rAAV-2 encoding the pancreatic form of glucokinase to the ARC.

3.2 Hypothesis and Aims

3.2.1 Hypothesis

Selectively altering glucokinase activity in the ARC of the hypothalamus, using stereotactic injections of pharmacological glucokinase activators and rAAV encoding glucokinase mRNA, will alter food intake and bodyweight regulation in male Wistar rats.

3.2.2 Aims and Objectives

To investigate this, I will:

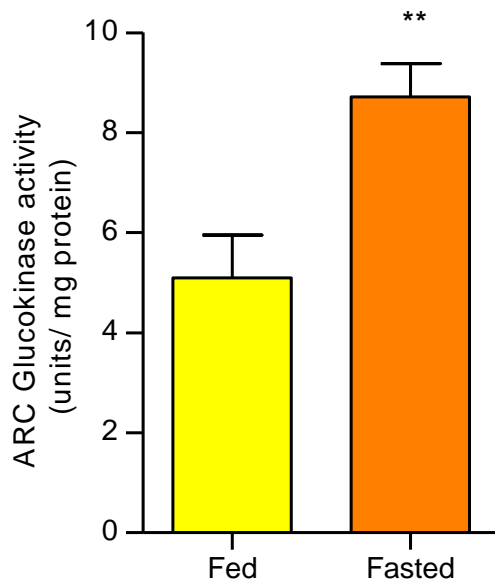
1. Determine whether glucokinase activity is altered by nutritional state by measuring glucokinase activity in hypothalamic nuclei of fed and fasted male Wistar rats.
2. Investigate the effect of increased glucokinase activity on short-term food intake by delivering the pharmacological glucokinase activator, compound A, into the ARC.
3. Produce rAAV encoding rat pancreatic glucokinase (rAAV-GKS) and confirm ability of this construct to alter glucokinase activity *in vitro*.
4. Stereotactically inject rAAV-GKS into the ARC and confirm increased glucokinase mRNA expression and activity in the ARC.
5. Investigate the effect of chronically increased arcuate glucokinase activity on food intake and bodyweight using a standard chow diet and a high-energy, obesogenic diet.

3.3 Results

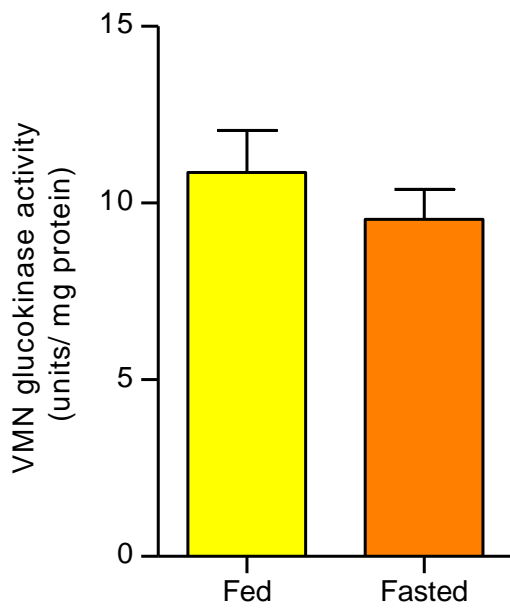
3.3.1 Effect of nutritional state on glucokinase activity in hypothalamic nuclei

Glucokinase activity in the ARC was significantly increased following a twenty-four hour fast compared to fed controls (fold change, 1.71 ± 0.13 ; mean \pm s.e.m, $n=8$, $p < 0.01$) (figure 3.1a). There was no difference in the glucokinase activity between fed and fasted state in either the VMN (fold change 0.88 ± 0.08 ; mean \pm s.e.m, $n=10$) or PVN (fold change 0.94 ± 0.07 ; mean \pm s.e.m, $n=8-9$) (figure 3.1b and c).

a)



b)



c)

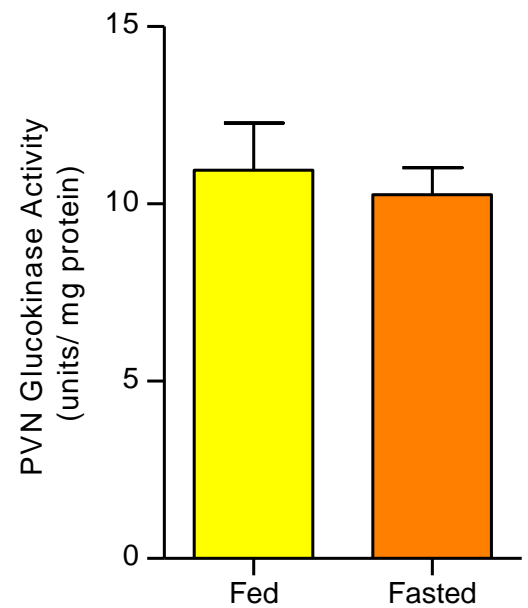


Figure 3.1 Effect of nutritional state on glucokinase activity in hypothalamic nuclei.

Glucokinase activity in fed and twenty-four hour fasted rats in the ARC, VMN and PVN. Data are expressed as mean \pm SEM for all groups, $n = 8-11$. Statistical significance was analysed by student's t test: **= $p < 0.01$

3.3.2 Effect of acutely increasing ARC glucokinase activity on food intake

ARC glucokinase activation was increased acutely using the glucokinase activator CpdA, injected via cannulas stereotactically implanted into the ARC. Acute arcuate glucokinase activation increased food intake during the first hour after injection, as compared to vehicle injected controls (control, 0.38 ± 0.13 g; CpdA, 1.07 ± 0.27 g; $n=10$, $p < 0.05$) (figure 3.3). Although there was an increase in food intake at later time points, including 24 hours, this was not significant (control, 24.0 ± 1.80 g; CpdA, 26.3 ± 1.52 g; $n=10$) (figure 3.3). Cannula placement in an area corresponding to the ARC and VMN boundary using cresyl violet staining (figure 3.2 for representative image). Animals that did not have correct placement of cannula were removed from subsequent analysis of feeding studies.

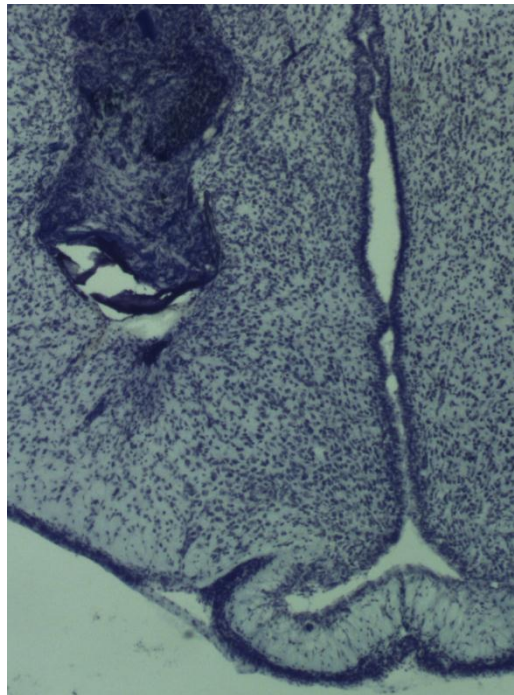


Figure 3.2 Confirmation of cannula placement in rats cannulated into the ARC. Cresyl violet staining of brain section representing the ARC of the hypothalamus and demonstrating correct placement of cannula in the ARC and VMN boundary. Dark blue staining corresponds to Indian ink and indicates the point of cannula insertion with surrounding gliosis. Injections were delivered 1 mm below this to the area corresponding to the ARC.

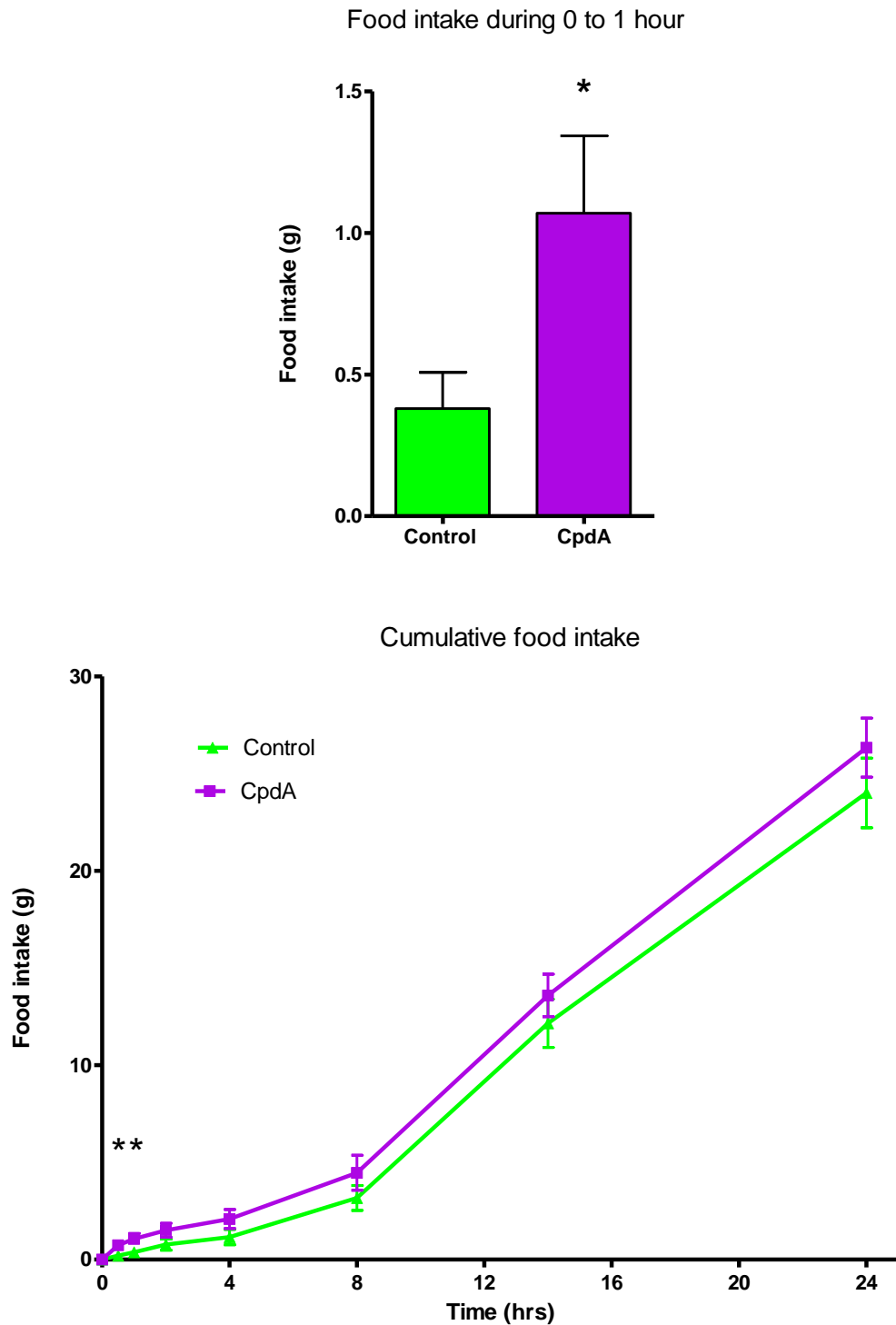


Figure 3.3 Effect of increasing ARC glucokinase activity on food intake. (a) Food intake one hour after ARC glucokinase activation using stereotactic injection of 0.5 nmol CpdA as compared to the vehicle injected controls during a crossover study. (b) Twenty-four-hour food intake after ARC glucokinase activation using stereotactic injection of 0.5 nmol CpdA as compared to the vehicle injected controls during a crossover study. Data are expressed as mean +/- SEM for all groups, n= 10. Statistical significance was analysed by student's t test: *=p<0.05.

3.3.3 Production of rAAV-GKS

3.3.3.1 PCR products

GKS

Following PCR, 10ul of GKS PCR product was visualised by gel electrophoresis. Comparison of the PCR product with a 1kb DNA ladder (Invitrogen) confirmed the presence of a band of between 1400-1500bp. The expected product size of this reaction was 1460bp. The presence of this band suggests that the reaction was successful.

Restriction endonuclease digestion of small scale plasmid preparation

DNA from small scale plasmid preparation was subjected to restriction endonuclease analysis to identify which clones contained the correct plasmid insert and retained their ITR's. GKS plasmid was digested by AgeI and BsiWI which should yield two bands; the cut plasmid of 4912bp and the GKS insert of 1460bp). The plasmids were also digested by XmaI to check for presence of ITR's. All products were visualised by gel electrophoresis. GKS samples with the correct sized bands and strong ITR's were selected and used for large-scale plasmid preparation.

3.3.3.2 Restriction endonuclease digestion of large scale plasmid preparation

GKS

Restriction endonuclease digestion of purified DNA from large scale GKS plasmid preparation using Age1 and BsiW1 produced a band of ~1450bp. Digestion with Xma1 showed strong ITR's (figure 3.4). Taken together this indicates that the plasmid contains the correct insert and the ITR's to allow integration of the viral DNA to the host genome.

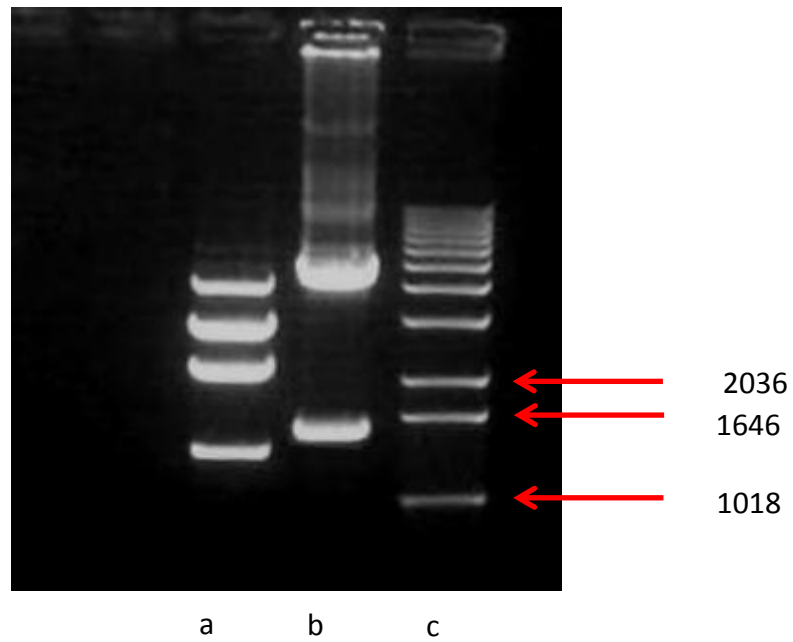


Figure 3.4 Visualisation of GKS plasmid production using gel electrophoresis: (a) Digestion with XmaI revealed bands consistent with ITR. (b) Purified GKS plasmid DNA was digested by AgeI and BsiwI to produce the expected ~1450 BP band indicating the correct insert. (c) Size of band compared to Invitrogen one kb ladder.

DNA sequencing

GKS

Sequencing results produced by the Imperial College Genomics Core laboratory were analysed using the nucleotide BLAST tool on the NCBI internet site. BLAST analysis of the GKS-pTR-CGW sequencing data revealed that the plasmid contained a full length copy of glucokinase gene with 100% homology to pCMV4.GKB1 plasmid gifted from Vanderbilt University (figure 3.5).

```
Query 1 CTGGGCTGGTGGCTGCGCAGATGCTGGATGACAGAGCCAGGATGGAGGCCACCAAGAAGG 60
|
Sbjct 1 CTGGGCTGGTGGCTGCGCAGATGCTGGATGACAGAGCCAGGATGGAGGCCACCAAGAAGG 60

Query 61 AAAAGGTCGAGCAGATCCTGGCAGAGTTCAGCTGCAGGAGGAAGACCTGAAGAAGGTGA 120
|
Sbjct 61 AAAAGGTCGAGCAGATCCTGGCAGAGTTCAGCTGCAGGAGGAAGACCTGAAGAAGGTGA 120

Query 121 TGAGCCGGATGCAGAAGGAGATGGACCGTGGCCTGAGGCTGGAGACCCACGAGGAGGCCA 180
|
Sbjct 121 TGAGCCGGATGCAGAAGGAGATGGACCGTGGCCTGAGGCTGGAGACCCACGAGGAGGCCA 180

Query 181 GTGTAAAGATGTTACCCACCTACGTGCGTTCACCCCAGAAGGCTCAGAAGTCGGAGACT 240
|
Sbjct 181 GTGTAAAGATGTTACCCACCTACGTGCGTTCACCCCAGAAGGCTCAGAAGTCGGAGACT 240

Query 241 TTCTTCCTTAGACCTGGGAGGAACCAACTTCAGRGTGATGCTGGTCAAAGTGGGAGAGG 300
|
Sbjct 241 TTCTTCCTTAGACCTGGGAGGAACCAACTTCAGRGTGATGCTGGTCAAAGTGGGAGAGG 300

Query 301 GGGAGGCAGGGCAGTGGAGCGTGAAGACAAAACACCAGATGTACTCCATCCCCGAGGACG 360
|
Sbjct 301 GGGAGGCAGGGCAGTGGAGCGTGAAGACAAAACACCAGATGTACTCCATCCCCGAGGACG 360

Query 361 CCATGACGGGCACTGCCGAGATGCTCTTTGACTACATCTCTGAATGCATCTCTGACTTCC 420
|
Sbjct 361 CCATGACGGGCACTGCCGAGATGCTCTTTGACTACATCTCTGAATGCATCTCTGACTTCC 420

Query 421 TTGACAAGCATCAGATGAAGCACAAGAACTGCCCTGGGCTTACCTTCTCCTTCCCTG 480
|
Sbjct 421 TTGACAAGCATCAGATGAAGCACAAGAACTGCCCTGGGCTTACCTTCTCCTTCCCTG 480

Query 481 TGAGGCACGAAGACCTAGACAAGGGCATCCTCCTCAATTGGACCAAGGGCTTCAAGGCCT 540
|
Sbjct 481 TGAGGCACGAAGACCTAGACAAGGGCATCCTCCTCAATTGGACCAAGGGCTTCAAGGCCT 540

Query 541 CTGGAGCAGAAGGGAACAACATCGTAGGACTTCTCCGAGATGCTATCAAGAGGAGAGGGG 600
|
Sbjct 541 CTGGAGCAGAAGGGAACAACATCGTAGGACTTCTCCGAGATGCTATCAAGAGGAGAGGGG 600
```



```

Query 1381 GCGGTGGCCTGCAAGAAGGCTTGCATGCTGGCCCAGTGAAATCCAGGTCATATGGACCGG 1440
          ||||||||||||||||||||||||||||||||||||||||||||||||||||||||||
Sbjct 1381 GCGGTGGCCTGCAAGAAGGCTTGCATGCTGGCCCAGTGAAATCCAGGTCATATGGACCGG 1440

Query 1441 GACCTCTAG 1449
          ||||||||
Sbjct 1441 GACCTCTAG 1449

```

Figure 3.5: BLAST analysis of GKS-pTR-CGW and pCMV4.GKB1 sequences. 100% homology demonstrated and the sequence in GKS-pTR-CGW contained start and stop codons (highlighted in red).

3.3.4 Confirmation of altered glucokinase activity following transfection of GKS-pTR-CGW plasmid

3.3.4.1 GKS

Transfection of HEK293T cells with GKS-pTR-CGW plasmid resulted in significantly increased glucokinase activity as compared to GFP-pTRCGW controls (controls 0.11 +/- 0.048 vs. GKS 0.34 +/-0.02 arbitrary units, n=4, P<0.05) (figure 3.6).

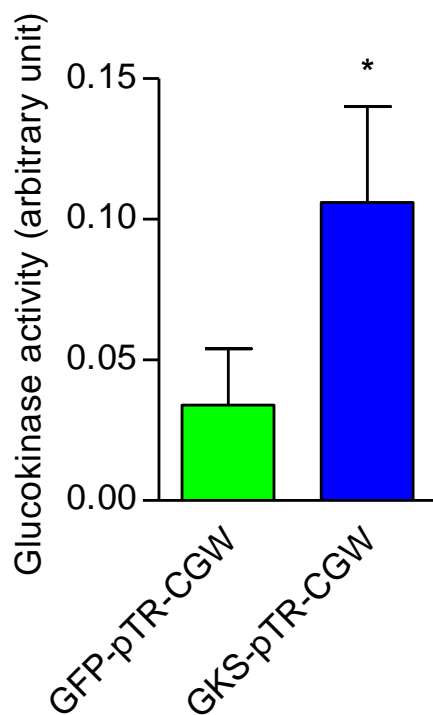


Figure 3.6 *In vitro* validation of GKS-pTR-CGW plasmid. Glucokinase activity in HEK293 cell lysates after transfection with either GFP-pTR-CGW plasmid or GKS-pTR-CGW plasmid. Data are expressed as mean +/- SEM for all groups, n= 4. Statistical significance was analysed by student's t test: *=p<0.05.

3.3.5 rAAV production

Recombinant AAV encoding GK (rAAV-GKS), or enhanced green fluorescent protein (rAAV-eGFP) was produced, isolated and purified as described in chapter 2. The titre for rAAV-eGFP was 5.04×10^{12} genome particles/ml and the titre for rAAV-GKS was 2.96×10^{12} genome particles/ml.

3.3.6 Effect of chronically increased arcuate glucokinase activity on food intake and body weight on a standard chow diet

rAAV-GKS was stereotactically injected into the arcuate nucleus of male Wistar rats (iARC-GKS). rAAV-GFP was stereotactically injected into the arcuate nucleus of control male Wistar rats (iARC-GFP).

3.3.6.1 Confirmation of gene transfer by *in situ* hybridisation

In situ hybridisation was used to demonstrate glucokinase mRNA expression in iARC-GKS and iARC-GFP rats four weeks after stereotactic injection. Increased glucokinase mRNA expression was localised to the ARC in iARC-GKS rats (figure 3.7).

a)



b)

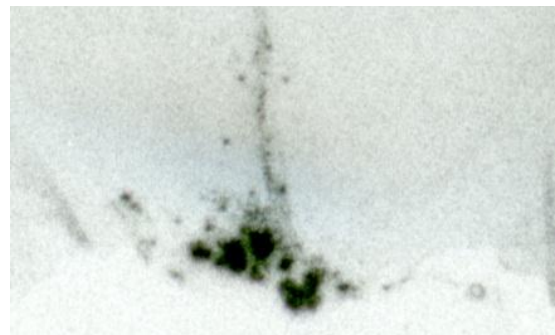


Figure 3.7 Confirmation of gene transfer by *in situ* hybridisation: Glucokinase mRNA expression in coronal sections of brains from male Wistar rats a) endogenous expression in the ARC 4 weeks post injection with rAAV-GFP b) increased expression in the ARC 4 weeks after injection with rAAV-GKS

3.3.6.2 Effect on food intake

Thirty-three days after recovery from rAAV injections, there was a significant increase in cumulative food intake (iARC-GFP, $1094.3 \pm 22.39\text{g}$ vs. iARC-GKS, $1194.1 \pm 24.92\text{g}$, $n=12-15$, $p<0.01$) in iARC-GKS rats, as compared to controls, on a standard chow diet (figure 3.8).

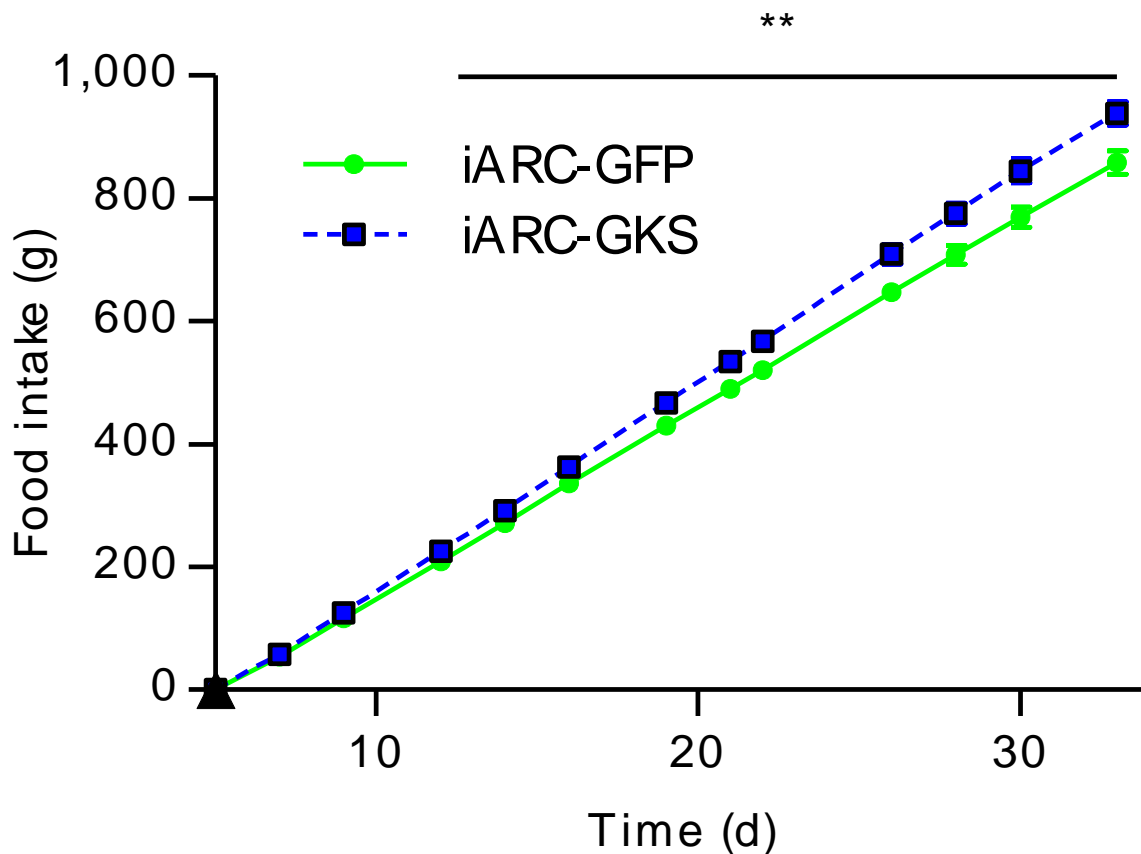


Figure 3.8 Effect of iARC rAAV-GKS on food intake: Food intake following bilateral injection of 1ul rAAV-eGFP (green line, $n=12$) or 1ul rAAV-GKS (blue line, $n=15$) in male Wistar rats fed on normal chow. Data are expressed as mean \pm SEM for both groups. Statistical significance was analysed by GEE: *= $p<0.05$, **= $p<0.01$.

3.3.6.3 Effect of iARC rAAV-GKS on 24hr standard chow food intake and bodyweight following 24hr fast

Food intake was not different between the groups until 8-24hr period following re-feeding when the iARC-GKS group ate significantly more compared to the iARC-GFP control group (iARC-GFP 9.6+/-0.82g vs. iARC-GKS 12.5+/- 0.64g, n=10-14, P=<0.05) (figure 3.9). Cumulative 24hr food intake was similar between the 2 groups (iARC-GFP 35.5+/- 0.59g vs. iARC-GKS 36.7+/- 0.75g, n=10-14, P=>0.05) (figure 3.9).

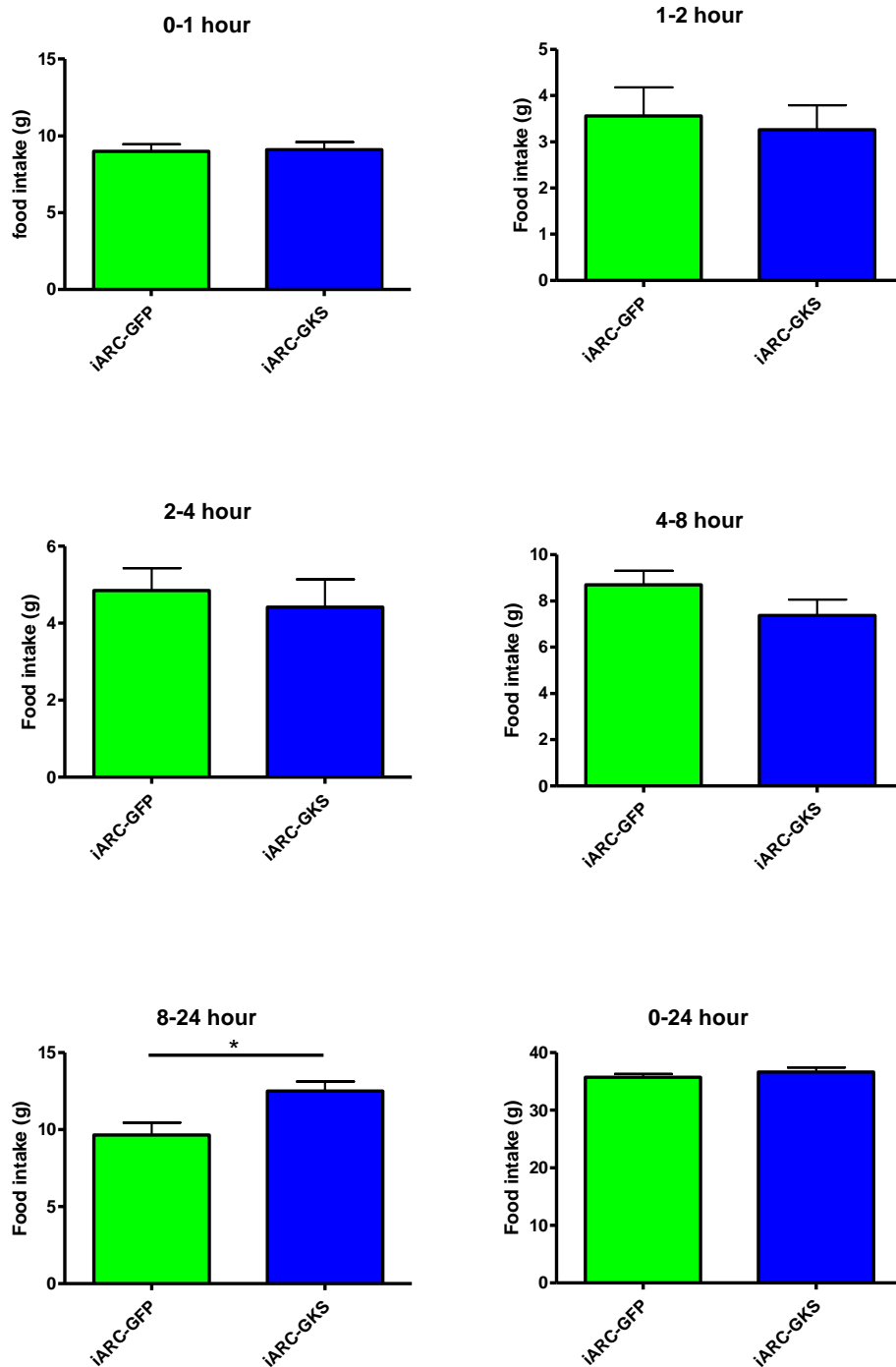


Figure 3.9 Effect of iARC rAAV-GKS on 24hr food intake following 24hr fast: 24hr food intake of male Wistar rats injected with 1ul rAAV-eGFP (green bars) and 1ul rAAV-GKS (blue bars). Both groups were fasted for 24hr and allowed ad libitum access to standard chow for a 24hr period at the start of the dark phase. Data are expressed as mean +/- SEM for all groups, n=10-14. Statistical significance was analysed by student's t test: *=p<0.05.

3.3.6.4 Effect on body weight and body weight gain

Thirty-three days after recovery from rAAV injections, there was a significant increase in body weight gain (iARC-GFP, $151.67 \pm 8.86\text{g}$ vs. iARC-GKS, $175.33 \pm 4.87\text{g}$, $n=12-15$, $p < 0.01$) in iARC-GKS rats, as compared to controls, on a standard chow diet (figure 3.10) (initial body weight: iARC-GFP, $270.08 \pm 3.04\text{g}$; iARC-GKS $273.60 \pm 2.75\text{g}$).

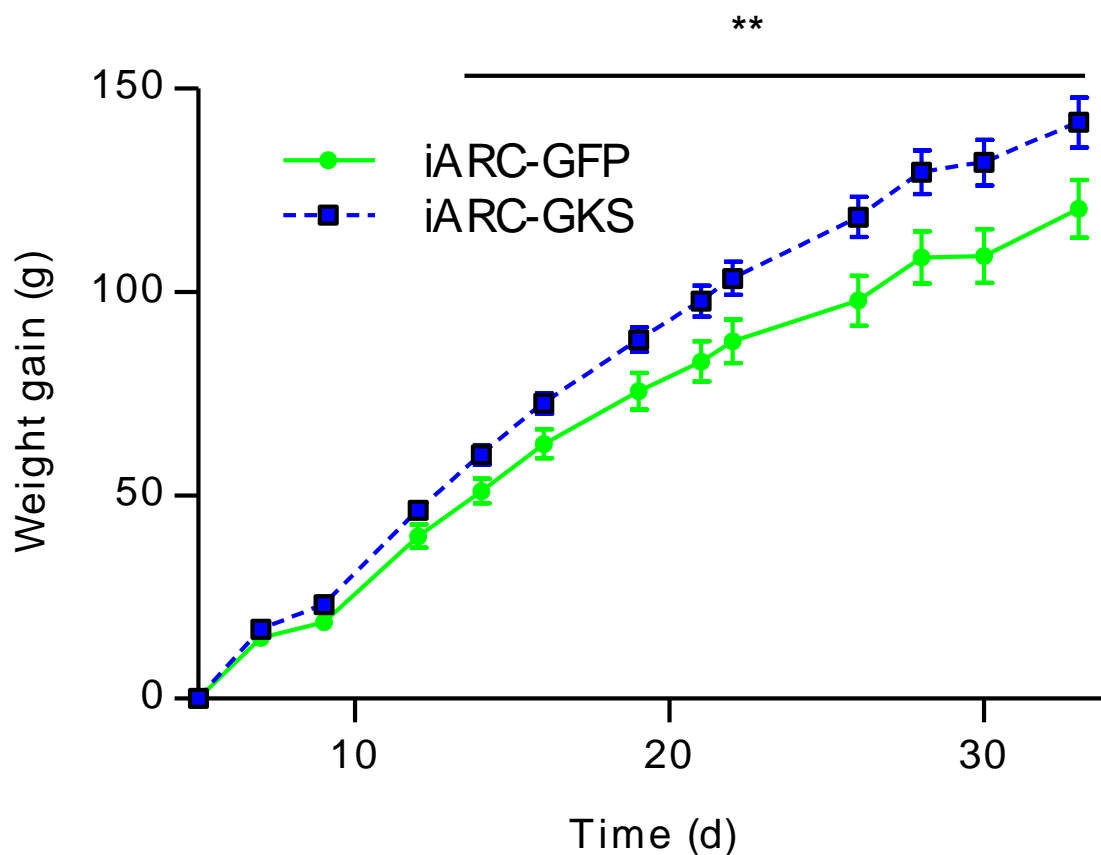


Figure 3.10 Effect of iARC rAAV-GKS on bodyweight gain: Weight gain following bilateral injection of 1ul rAAV-eGFP (green line, $n=12$) or 1ul rAAV-GKS (blue line, $n=15$) Male Wistar rats were fed normal chow. Data are expressed as mean \pm SEM for groups. Statistical significance was analysed by GEE: $*=p < 0.05$, $**=p < 0.01$.

3.3.6.5 *Effect on body composition*

Percentage body fat

Thirty-three days after recovery from rAAV injections, there was a significant increase in percentage body fat (iARC-GFP, 22.12 ± 1.73 ; iARC-GKS 28.0 ± 1.62 , $n=12-15$, $p < 0.05$) in iARC-GKS rats, as compared to controls, on a standard chow diet (figure 3.11).

Lean body mass

There was no difference in percentage lean body mass (iARC-GFP, 16.99 ± 0.37 ; iARC-GKS 16.7 ± 0.49 , $n=12-15$, $p < 0.05$) (figure 3.12).

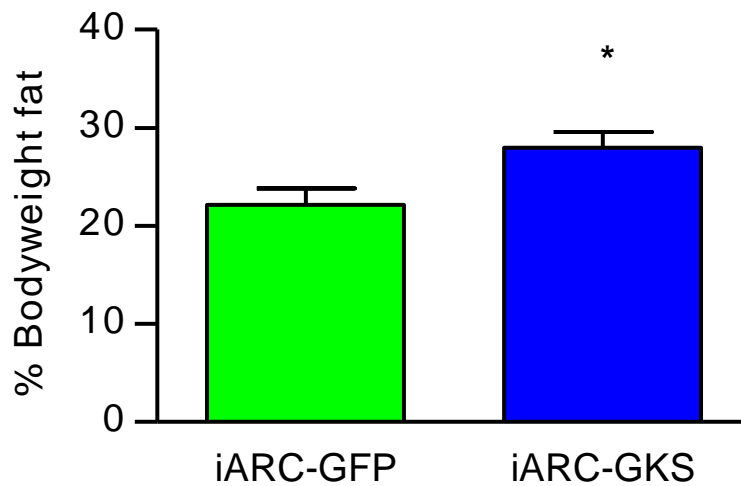


Figure 3.11 Effect of iARC rAAV-GKS on percentage body fat: Percentage body fat measured using body composition analysis thirty-three days after intra-arcuate injection with rAAV-GKS (n=15) or rAAV-GFP (n=12) in rats. Data are expressed as mean +/- SEM for all groups. Statistical significance was analysed by student's t test: *=p<0.05.

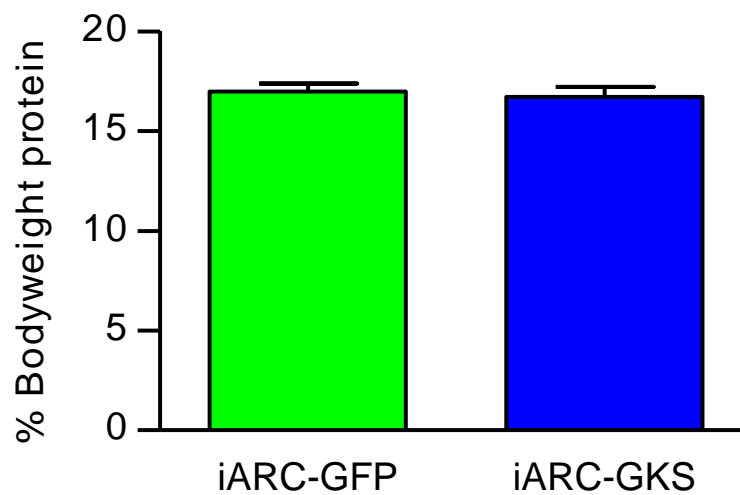


Figure 3.12 Effect of iARC rAAV-GKS on percentage bodyweight protein: Percentage bodyweight protein measured using body composition analysis thirty-three days after intra-arcuate injection with rAAV-GKS (n=15) or rAAV-GFP (n=12) in rats. Data are expressed as mean +/- SEM for all groups.

BAT and BAT UCP-1 expression

BAT weight (iARC-GFP, 1.14 ± 0.05 g/kg; iARC-GKS 1.22 ± 0.07 g/kg, $n=10-13$) was similar in both groups (figure 3.13a). BAT UCP1 mRNA expression was similar in both groups. (iARC-GFP, 4.67 ± 0.4 arbitrary units vs iARC-GKS 4.87 ± 0.9 arbitrary units, $n=6-11$) (figure 3.13b).

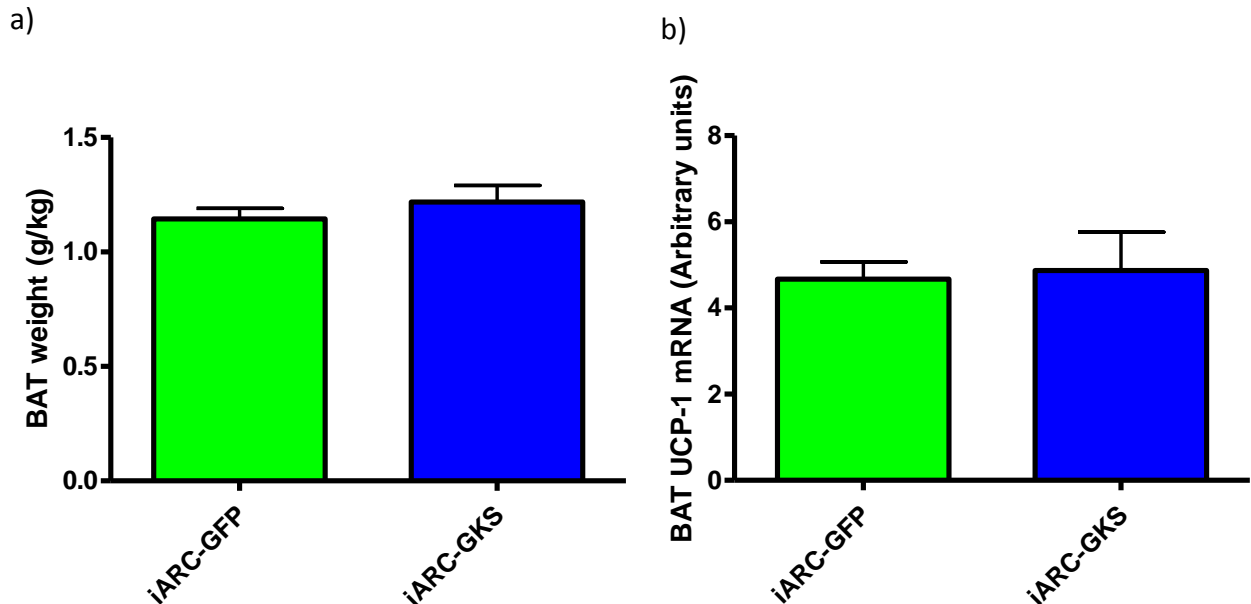


Figure 3.13 Effect of iARC rAAV-GKS on BAT: a) BAT weight corrected to bodyweight thirty-three days after intra-arcuate injection with rAAV-GKS ($n=15$) or rAAV-GFP ($n=12$) in rats. (b) BAT UCP1 mRNA expression from overnight fed intra-arcuate injected rAAV-GKS ($n=11$) or rAAV-GFP ($n=6$) rats. Data are expressed as mean \pm SEM for all groups. Statistical significance was analyzed by student's *t* test: $*=P<0.05$.

3.3.6.6 *Effect on glucose and plasma hormones in standard chow diet fed animals*

Glucose

Fasting glucose (iARC-GFP, 3.88 ± 0.09 mmol/L; iARC-GKS 3.92 ± 0.17 mmol/L, n=9-11) and fed glucose (iARC-GFP, 5.39 ± 0.13 mmol/L; iARC-GKS 5.50 ± 0.13 mmol/L, n=9-11) was similar in both groups (figure 3.14a and b).

Insulin

Fasting insulin (iARC-GFP, 1.12 ± 0.22 ng/ml; iARC-GKS 1.19 ± 0.11 ng/ml, n=9-11) and fed insulin (iARC-GFP, 1.77 ± 0.10 ng/ml; iARC-GKS 2.15 ± 0.19 ng/ml, n=9-11) was similar in both groups (figure 3.14c and d).

Active GLP-1

Fasting active GLP-1 (iARC-GFP, 9.47 ± 1.89 pmol/L; iARC-GKS 7.00 ± 0.92 pmol/L, n=9-10) and fed active GLP-1 (iARC-GFP, 16.11 ± 2.79 pmol/L; iARC-GKS 15.5 ± 1.89 pmol/L, n=9-10) was similar in both groups (figure 3.14e and f).

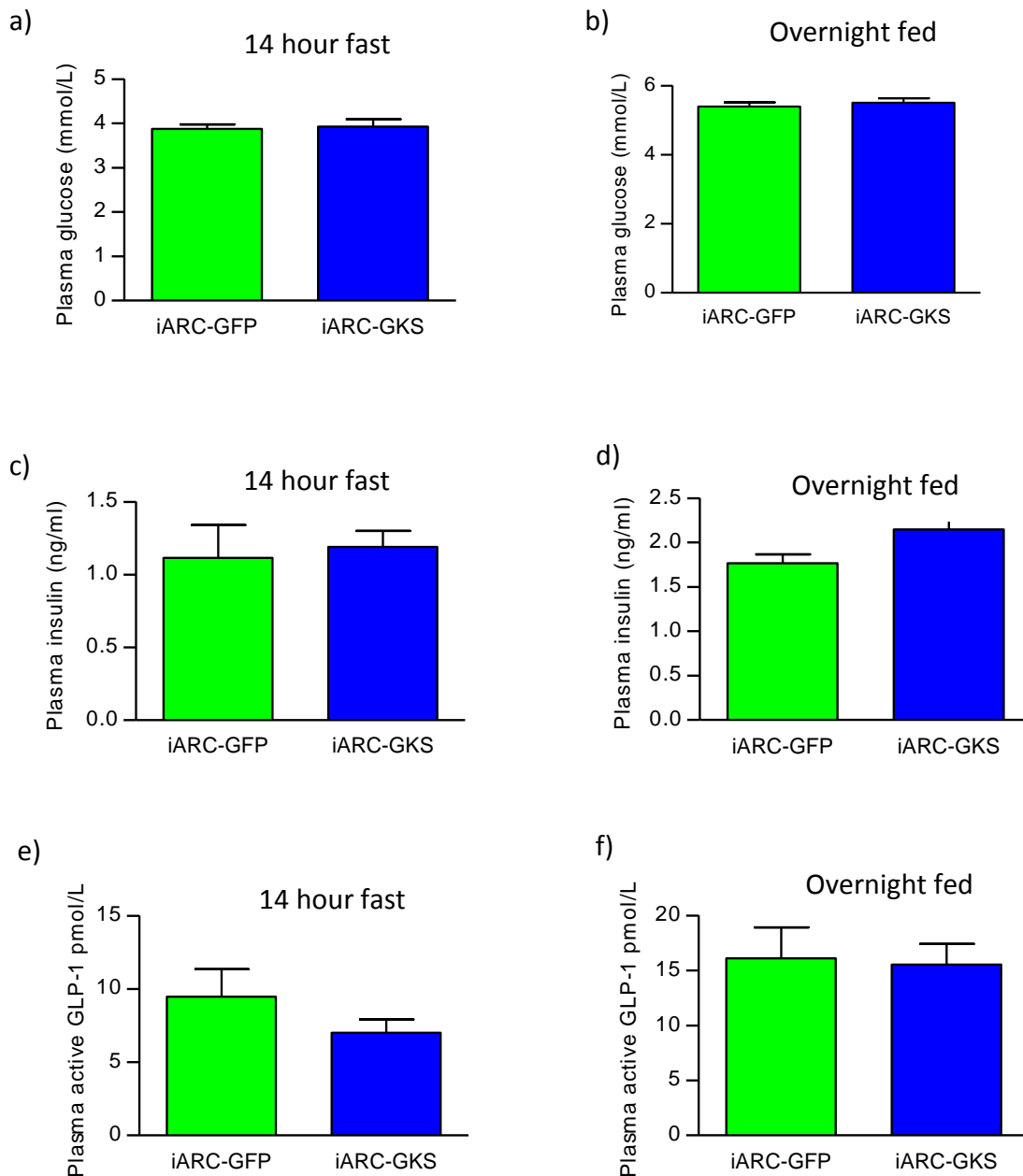


Figure 3.14 Effect iARC-GKS on glucose homeostasis: (a) Fasting glucose levels, (b) fed glucose levels, (c) fasting insulin levels, (d) fed insulin levels, (e) fasting active GLP-1 levels and (f) fed active GLP-1 levels in iARC-GKS rats as compared to controls. Data are expressed as mean +/- SEM for all groups, n= 9-11. Statistical significance was analysed by student's t test: *=p<0.05.

Leptin

Fasting leptin was non-significantly elevated in iARC-GKS rats versus controls (iARC-GFP, 6.55 ± 0.87 ng/ml; iARC-GKS 7.35 ± 0.72 ng/ml, $n=10-13$) (figure 3.15a). Fed leptin was significantly elevated in iARC-GKS rats versus controls (iARC-GFP, 9.94 ± 1.36 ng/ml; iARC-GKS 15.2 ± 2.05 ng/ml, $n=10-13$) (figure 3.15b).

Ghrelin

Fasting total ghrelin was similar in both groups (iARC-GFP, 664.4 ± 46.9 fmol/ml; iARC-GKS 565.8 ± 36.4 fmol/ml, $n=10-11$) (figure 3.15c). However, fed acyl-ghrelin was significantly reduced in iARC-GKS rats versus controls (iARC-GFP, 106.4 ± 15.5 fmol/ml; iARC-GKS 66.4 ± 8.6 fmol/ml, $n=11-12$) (figure 3.15d).

PYY

Fasting and fed PYY were similar in both groups (Fasting: iARC-GFP, 32.3 ± 3.0 fmol/ml; iARC-GKS 32.5 ± 3.9 fmol/ml, $n=10$) (figure 3.15e). (Fed: iARC-GFP, 53.4 ± 2.95 fmol/ml; iARC-GKS 60.8 ± 4.97 fmol/L, $n=9-11$) (figure 3.15f).

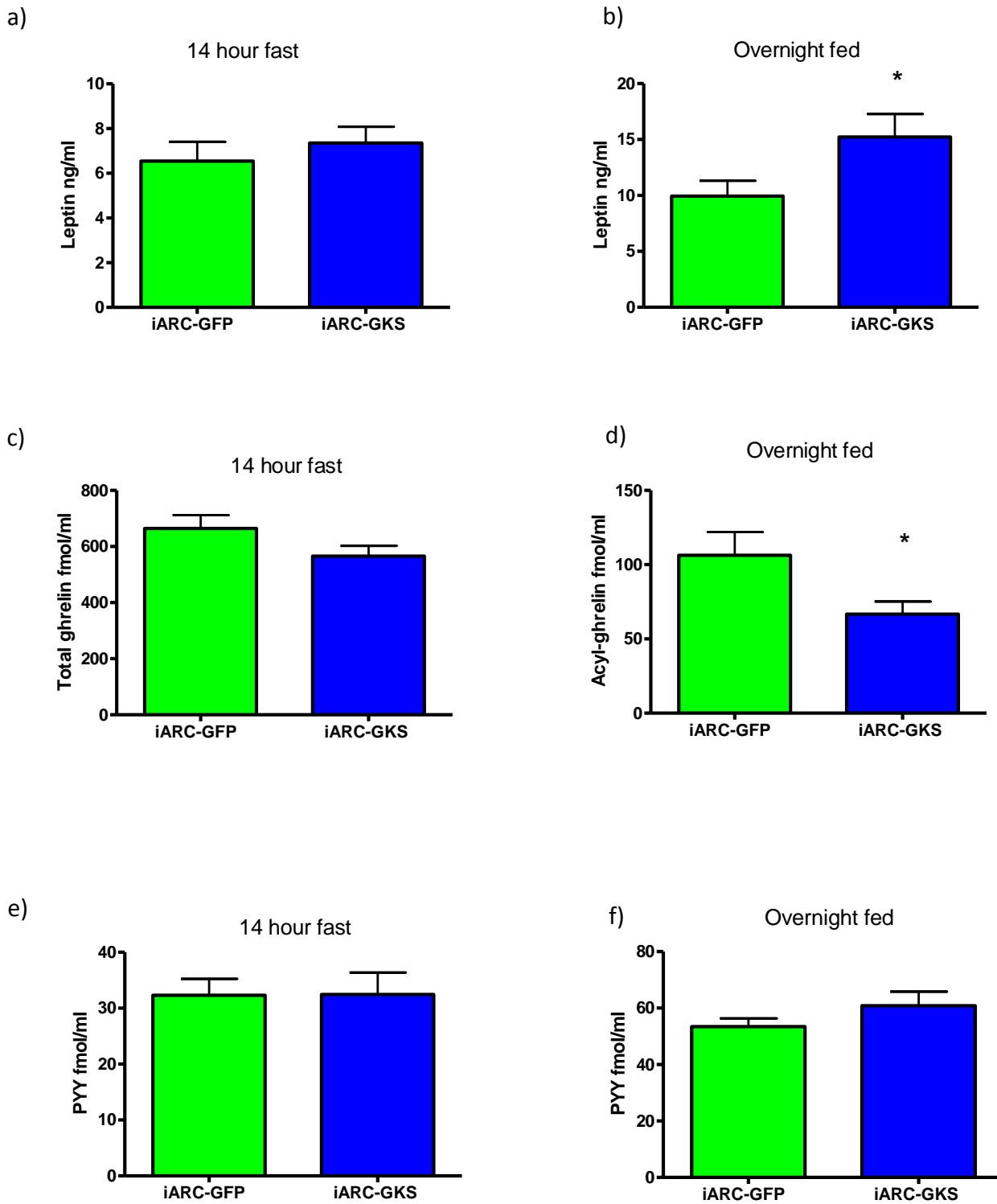


Figure 3.15 Effect of iARC GKS on hormones involved in appetite regulation: (a) Fasting leptin, (b) fed leptin, (c) fasting ghrelin, (d) fed acyl-ghrelin, (e) fasting PYY and (f) fed PYY in iARC-GKS rats as compared to controls. Data are expressed as mean +/- SEM for all groups, n= 9-13. Statistical significance was analysed by student's t test: *=p<0.05.

3.3.7 Effect of chronically increased arcuate glucokinase activity on food intake and body weight on a high-energy diet

3.3.7.1 Effect on food intake

Thirty-three days after being placed on a high-energy diet, there was a significant increase in cumulative food intake (iARC-GFP, 803.49 ±14.64g vs. iARC-GKS, 886.91±25.84g, n=10, p<0.01) in iARC-GKS rats, as compared to controls (figure 3.16).

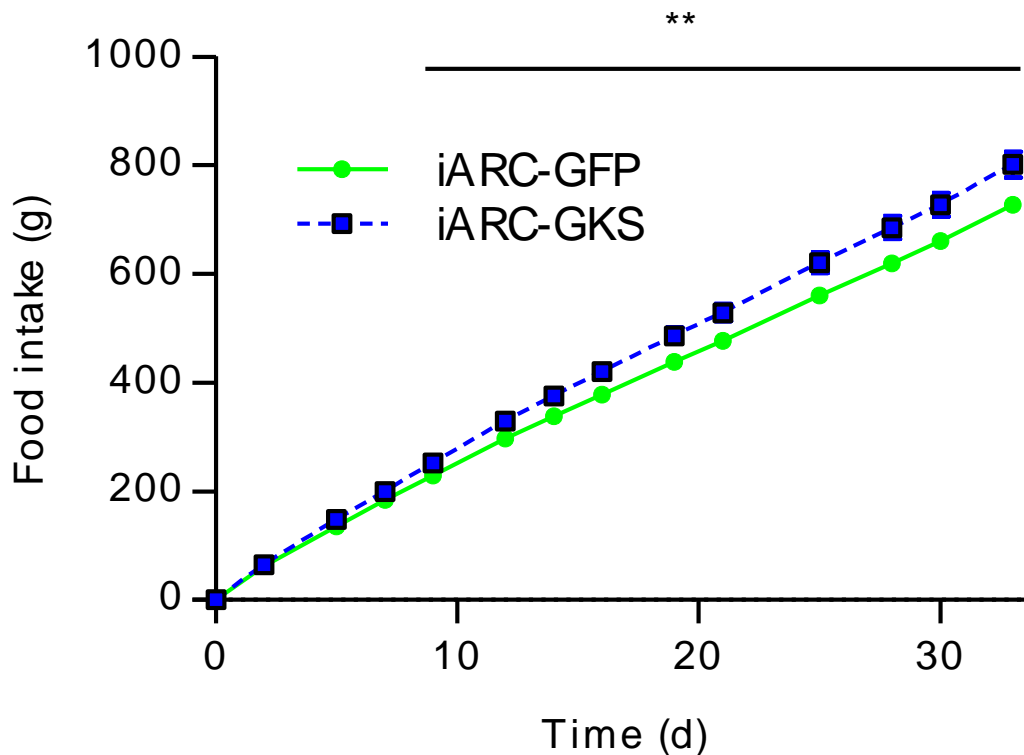


Figure 3.16 Effect of iARC rAAV-GKS on food intake: Food intake following bilateral injection of 1 μ l rAAV-eGFP (green line, n=10) or 1 μ l rAAV-GKS (blue line, n=10) in male Wistar rats fed on high-energy diet. Data are expressed as mean \pm SEM for both groups. Statistical significance was analysed by GEE: **= p <0.01.

3.3.7.2 Effect on body weight and body weight gain

Thirty-three days after being placed on a high-energy diet, there was a significant increase in body weight gain (iARC-GFP, $81.80 \pm 5.46\text{g}$ vs. iARC-GKS $102.73 \pm 7.17\text{g}$, $n=10$, $p<0.05$) in iARC-GKS rats, as compared to controls, on a standard chow diet (figure 3.17) (initial body weight: iARC-GFP, $441.30 \pm 9.73\text{g}$; iARC-GKS $447.09 \pm 9.14\text{g}$).

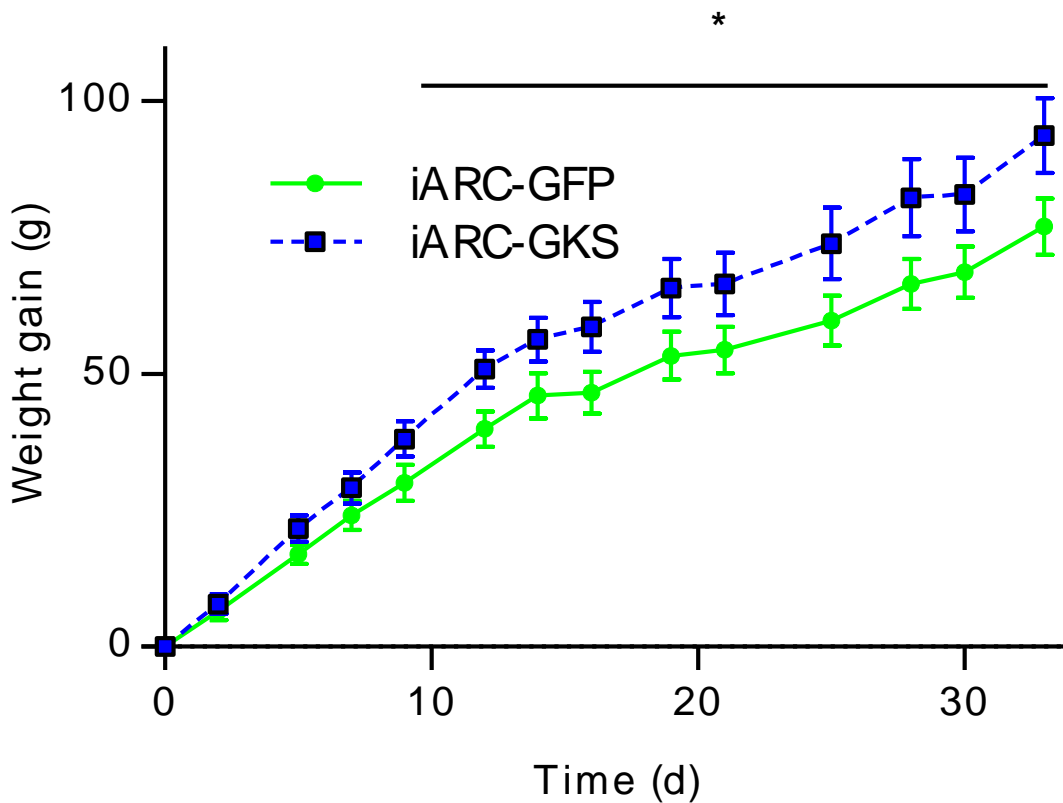


Figure 3.17 Effect of iARC rAAV-GKS on bodyweight gain with high-energy diet: Weight gain following bilateral injection of 1ul rAAV-eGFP (green line, $n=10$) or 1ul rAAV-GKS (blue line, $n=10$) in male Wistar rats fed on a high-energy diet. Data are expressed as mean \pm SEM for both groups. Statistical significance was analysed by GEE: $*=p<0.05$.

3.3.8 Confirmation of increased glucokinase activity in the ARC

Glucokinase activity was measured in hypothalamic nuclei of iARC-GKS and iARC-GFP rats. Glucokinase activity in the ARC was significantly increased in iARC-GKS rats compared to controls (fold change, 2.03 ± 0.30 ; mean \pm s.e.m, n=10-11, $p < 0.001$) (figure 3.18). Glucokinase activity was not altered in the VMN (fold change, 0.98 ± 0.17 ; mean \pm s.e.m, n=10-11) or PVN (fold change, 0.87 ± 0.08 ; mean \pm s.e.m, n=7-10) (figure 3.18).

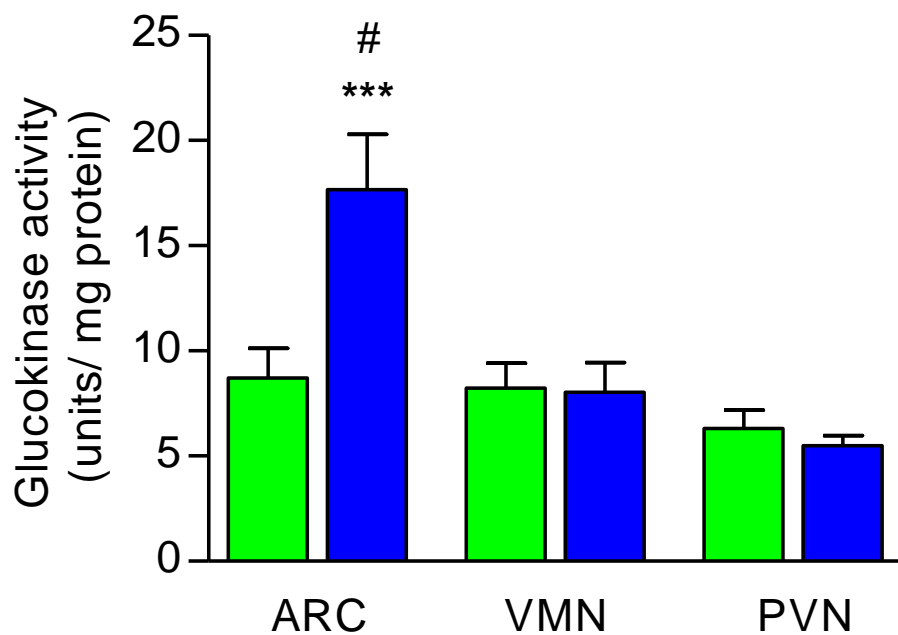


Figure 3.18 Glucokinase activity in hypothalamic nuclei of iARC-GKS and iARC-GFP rats: Glucokinase activity in homogenate supernatants from ARC, VMN and PVN micro-punches in iARC-GFP and iARC-GKS rats. Data are expressed as mean \pm SEM for all groups, n= 8-11. Statistical significance was analysed using one-way statistical analysis of variance followed by post-hoc Holm-Sidak test. *** $p < 0.001$ versus corresponding control values. # $p < 0.0001$ versus all other groups.

3.4 Discussion

3.4.1 ARC glucokinase is involved in the regulation of food intake

Glucokinase activity in the ARC is significantly increased by fasting and decreased by feeding, suggesting that the glucokinase in this nucleus may have a role in regulating energy homeostasis. This is in keeping with previous work demonstrating that glucokinase mRNA is increased with fasting (Kang et al., 2008). Insulin-induced hypoglycaemia, associated with increased drive to its feeding, also results in increased glucokinase mRNA expression and activity in the VMH (Dunn-Meynell et al., 2002b, Kang et al., 2008, Tkacs et al., 2000). This result supports that ARC glucokinase plays a physiological role in the regulation of or response to food intake. To investigate this further and determine the physiological role of ARC glucokinase on energy homeostasis, glucokinase activity was altered in the ARC.

3.4.2 ARC glucokinase exerts orexigenic role

To investigate the effect of glucokinase on food intake, glucokinase activity was increased pharmacologically using a selective glucokinase activator (Kamata et al., 2004, Kang et al., 2006). The glucokinase activator, CpdA, was stereotactically injected into the ARC to achieve this. Stereotactic delivery of CpdA has been used in previous studies to investigate the role of VMH glucokinase on counterregulatory responses to hypoglycaemia (Levin et al., 2008b). The dose used was shown to increase glucokinase activity. A similar dose and approach was used in this study. Acute arcuate glucokinase activation significantly increased food intake during the first hour after injection. Although there is no data on the pharmacokinetics of CpdA injected stereotactically in the brain, pharmacokinetic studies in rats revealed a half-life of 1.3 hours for an analog of CpdA (Iino et al., 2009). It is possible that long duration effects of stereotactically injected CpdA are limited due to this, as well as habituation of neuronal responses. Food intake was not significant at later time points; however the difference in food intake between the two groups at one hour was preserved up to 24 hours post injection, suggesting that there is no compensatory decrease in food intake at subsequent time points in the CpdA treated animals.

Although these results are consistent with increased glucokinase activity during fasting, they are not entirely consistent with previous short-term studies on glucose and glucokinase alterations in the brain. Glucose infusion into the VMH, which includes the ARC, reduces food intake acutely (Kurata *et al.*, 1986). ICV infusion of 2DG, an anti-metabolite of glucose, into the 3rd cerebral ventricle results in increased food intake (Tsujii and Bray, 1990). Glucose and 2-DG are likely to have non-specific effects on non-glucose sensing neurons due to osmotic effects and effects on energy production. They are also likely to change glucose to non-physiological levels which may severely affect activation and inhibition of a wide range of neurons. Glut 2 null mice with pancreatic re-expression of glut 2 demonstrate reduced food intake (Bady *et al.*, 2006). However, Glut 2 is expressed widely in the brain, liver, kidney and intestine. Therefore, replacing glut 2 only in the pancreas is likely to lead to non-specific effects in other organs which may produce the phenotype described and make these results difficult to interpret. However, if the above studies are correct, it could therefore be hypothesized that increasing glucokinase expression in the ARC should increase glucose-sensing and this would result in a reduction of food intake.

VMH knockdown of glucokinase activity using alloxan and short-hairpin RNA, delivered via an adenoviral vector, did not change appetite regulation at twenty-four hours and fourteen days, respectively (Dunn-Meynell *et al.*, 2009). As discussed earlier, this study also has severe limitations. Alloxan is a betacytotoxic glucose analogue that alters antioxidant defences in the brain and can lead to changes in neural gene expression and behaviour when injected into the brain in very small doses (Salkovic-Petrisic and Lackovic, 2003). Furthermore, adenoviral gene transfer generates immunogenic responses leading to inflammation and limits gene expression, as discussed previously in Chapter 1 (Kaplan *et al.*, 1997). Another study demonstrated that injection of high-dose glucosamine, a non-specific glucokinase inhibitor, into the third cerebral ventricle (icv) of rats stimulates food intake (Zhou *et al.*, 2011). This study also has considerable limitations. Glucosamine inhibits hexokinase and therefore would have a widespread effect on glycolysis in neurons (Bertoni, 1981). ICV injection can spread throughout the brain; hence ICV injection of agents causing widespread disturbances in neuronal function may have led to non-specific CNS effects on food intake.

In order to test this further and confirm the above observations, we produced a rat model of chronically increased ARC glucokinase activity using rAAV-2 and studied the effects on food intake and body weight in this model. This vector is non-immunogenic and allows chronic, sustained gene expression in neural populations (Gardiner et al., 2005, Ponnazhagan et al., 1997, Daly, 2004a).

3.4.3 Production of rAAV encoding glucokinase

In order to produce rAAV particles capable of altering glucokinase activity, the efficacy of the GKS-pTR-CGW (encoding pancreatic glucokinase mRNA) plasmid to alter glucokinase activity was tested *in vitro*. To do this, glucokinase activity was determined spectrophotometrically using an NADP⁺-coupled assay with glucose-6-phosphate dehydrogenase (Goward et al., 1986). This glucokinase assay uses 5-thio-D- glucose, a structural analogue of glucose, that inhibits other hexokinases, especially hexokinase I, but does not affect glucokinase 3-O-methyl-N-acetylglucosamine was incorporated in all assays to inhibit N-acetylglucosamine kinase which phosphorylates glucose at high glucose concentrations (Fenner et al., 2011, Miwa et al., 1994).

HEK293T cells, a commonly used cell line for transfecting plasmids and producing rAAV, were used to investigate the efficacy of GKS-pTR-CGW. The cells were transiently transfected with the plasmid and pTR-CGW control and lysed after 48 hours after which glucokinase activity was assessed. The results demonstrated a threefold increase in glucokinase activity as compared to controls confirming the efficacy of GKS-pTR-CGW plasmid *in vitro*.

After the plasmid efficacy in altering *in vitro* glucokinase activity was confirmed, AAV viral particles were produced using the plasmid. The titre of the plasmid was confirmed and found to be within acceptable levels for *in vivo* use and compared well with levels used in previous studies utilising AAV injected stereotactically into hypothalamic nuclei (Gardiner et al., 2005).

3.4.4 Stereotactic injection of rAAV-GKS into the ARC increases glucokinase activity specifically in the ARC

In situ hybridisation confirmed increased glucokinase mRNA expression specifically in the ARC of iARC-GKS rats, which are injected with rAAV-GKS, as compared to iARC-GFP rats. The main purpose of stereotactically injecting rAAV-GKS in rats is to selectively increase ARC glucokinase activity. Although the efficacy of the construct to increase glucokinase activity has been tested *in vitro* and increased glucokinase mRNA expression has been confirmed in the ARC using in situ hybridisation, ex vivo confirmation of increased glucokinase activity in the ARC is required.

In order to achieve this, micro-punches of hypothalamic nuclei were taken from iARC-GKS and iARC-GFP rats. Glucokinase activity was assessed using the glucokinase activity assay. The results confirm significant increase in glucokinase activity specifically in the ARC nucleus, with no increase in neighbouring VMN and PVN nuclei. The increase in ARC glucokinase activity is of similar magnitude to that produced by a twenty-four hour fast. This result confirmed the validity of the rat model of increased ARC glucokinase activity.

3.4.5 Effect of glucokinase activity on energy homeostasis on a normal chow diet

In the feeding study with standard chow diet, injection of rAAV-GKS into the ARC resulted in a significant increase in cumulative food intake accompanied by significantly increased bodyweight. The divergence of food intake between the two groups began early (approximately 9 days post injection of AAV) and continued until the end of the study (33 days post injection). The increase in bodyweight gain in the iARC-GKS group also began early but plateaued by day 22, after which, the iARC-GKS group remained 6 % heavier than the controls. Percentage bodyweight fat and fed leptin was increased in the iARC-GKS group in keeping with the difference in bodyweight and food intake. Disassociation between stored fat and leptin release during fasting may account for the non-significantly elevated fasting leptin levels despite significant differences in body fat between the two groups (Benoit et al., 2004).

The results of the 24hr fasted food intake study reveal an altered feeding pattern in the iARC-GKS group. The iARC-GKS group ate significantly more chow in the 8-24hr period than the controls. This corresponds to the latter half of the dark phase and light phase, when food intake is usually reduced in rats. Increasing ARC glucokinase activity may augment food intake during times when food intake is usually low, for example after a recent meal or

during the light phase. This effect is not noted when food intake is usually high, for example in the early part of the dark phase and after a prolonged fast. It is possible that the cumulative effect of this slight increase in food intake in the iARC-GKS group, at times when food intake is usually reduced in controls, may account for the significantly increased cumulative food intake in the initial feeding study. This may also explain the increased bodyweight and percentage body fat in iARC-GKS animals, as compared to controls.

Although formal investigations of energy expenditure have not been undertaken, the data suggests that bodyweight differences are due to altered food intake in iARC-GKS animals, rather than energy expenditure. In keeping with this BAT weight and BAT UCP-1 mRNA expression is similar in both groups. However, further studies involving pair-feeding of iARC-GKS animals with controls and CLAMS (Comprehensive Laboratory Animal Monitoring System) are needed to formally investigate the contribution of energy expenditure.

Glucose and insulin in both fasted and fed states were similar in both groups suggesting that glucose homeostasis may not be significantly altered in iARC-GKS rats as compared to controls despite significantly increased weight gain. Active GLP-1 levels are also similar in both groups and therefore alterations in GLP-1 are unlikely to be causing changes in satiety and glucose handling in iARC-GKS. Similar total ghrelin levels in the fasted state and reduced acyl-ghrelin levels in the fed state in iARC-GKS rats suggest that ghrelin is unlikely to be mediating the increased food intake noted in our studies and is in keeping with iARC-GKS rats having a more obese phenotype, since ghrelin levels are reduced in obesity (Rosicka et al., 2003). Further work with glucose tolerance tests and insulin tolerance tests are needed to investigate glucose homeostasis.

Taken together, this chronic feeding study on a standard chow diet suggests that increased ARC glucokinase activity alters feeding behaviour resulting in increased food intake. This increased energy intake results in increased bodyweight in the iARC-GKS rats. Although the role of energy expenditure has not been comprehensively evaluated, it is likely that the increase in food intake in these animals is causing an increase in weight gain rather than alterations in energy expenditure.

3.4.6 Effect of increasing ARC glucokinase activity on energy homoeostasis on a high energy diet

We studied the effect of increasing ARC glucokinase activity on a high-sugar and high fat diet. In this study iARC-GKS rats also consumed more high energy diet and gained more weight as compared to controls. This further confirms our previous findings and also demonstrates that the obesogenic effects of increased ARC glucokinase activity extends to a calorie dense diet used in rodents to replicate the effects of modern obesogenic diets implicated in the development of human obesity (Levin et al., 1983, Lauterio et al., 1994).

3.4.7 Conclusion

The findings from glucokinase activity assays fed and fasted animals, pharmacological studies using a glucokinase activator injected into the ARC and a validated rat model of increased ARC glucokinase activity suggest that ARC glucokinase exerts an orexigenic effect on energy homoeostasis. These findings are in contrast to previous suggestions but consistent with the observation that hypothalamic glucokinase mRNA expression is increased following insulin-induced hypoglycaemia and ARC glucokinase mRNA expression is increased in DIO-prone and DIO rats (Dunn-Meynell et al., 2002b). The mechanism by which ARC glucokinase promotes the intake of food requires further investigation.

4 Effect of increased arcuate glucokinase activity on selection of macronutrients

4.1 Introduction

Over the last few decades significant progress has been made in our understanding of the neural mechanisms controlling food intake. Neuronal populations in the hypothalamus, brainstem, and reward centres have been shown to play a prominent role in this. Despite considerable advances in our understanding, less is known about the neurobiology controlling food preference and selectivity of nutrients. Unbalanced and unhealthy diets, with increased consumption of sugars and fats, are one of the major factors promoting the development of obesity (Berthoud et al., 2012, Wurtman, 1985). Our current understanding of food selectivity suggests that neuronal nutrient-sensing may allow sensing of a particular nutrient. In response to changes in levels of the nutrient, altered sensing may lead to altered responses within hypothalamic or brainstem feeding circuits and altered consumption of that nutrient either via direct homeostatic effects or interaction with reward centres (Berthoud et al., 2012, Berthoud and Morrison, 2008, Levin et al., 2011, Kelley and Berridge, 2002, Berridge, 1996). This may change the drive to consume particular foods. In support of this, data from vertebrate and invertebrate studies suggests that appetite consumption regulates intake around a fixed macronutrient ratio (Simpson and Raubenheimer, 1997, Emmans, 1991, Raubenheimer and Simpson, 1997, Sorensen et al., 2008, Abraham et al., 1975, United States. Department of Health et al., 1972). This has led to the development of a 'Geometric framework' governing food intake, where the ratios of macronutrients are kept constant (Cheng et al., 2008, Simpson and Raubenheimer, 1997, Simpson and Raubenheimer, 2005). Following this theory, the decrease in one macronutrient prioritises intake of the deficient macronutrient over other macronutrients independent of caloric intake. In keeping with this, alterations in the drive to consume selective nutrients occurs in response to changes in physiological states, such as fasting associated glucoprivation which leads to increased consumption of glucose and calorie rich foods (Thompson and Campbell, 1977, Goldstone et al., 2009). Therefore, altered preference to consume foods may arise from taste, temperature, texture and appearance independent mechanisms that are based on promoting the intake of a nutrient that is required by the body for metabolic processes. In relation to the development of obesity, nutrient sensing and reward mechanisms have been shown to be altered in obese states, where increased calorie-dense food consumption is noted (Parton et al., 2007a, Page et al.,

2011a). It has been postulated that altered nutrient-sensing may alter the reward value of foods in obesity (Domingos et al., 2011).

The results described in chapter 3 demonstrate that increasing glucokinase activity in the arcuate nucleus results in increased consumption of food and adiposity. In this chapter, I describe the neuronal mechanisms by which food selectivity and preference may operate and test the hypothesis that arcuate glucokinase may alter macronutrient selection.

4.1.1 Neuronal mechanisms leading to nutrient selectivity and preference

Studying altered selectivity and preference for complex foods has been challenging due to alterations in food texture and taste that are caused by providing different foods. The presence of other components in complex foods is also likely to influence overall intake and selectivity. Furthermore, metabolic responses and post-ingestive influences following intake of foods, e.g. insulin and gut hormone release, complicate the scenario further. The study of energy homeostasis and sodium appetite has given useful clues with regards to the likely mechanism for nutrient selection. Mice demonstrate molecular changes in hypothalamic orexin neurons as a consequence of sodium depletion (Liedtke et al., 2011). Prevention of these changes selectively reduces sodium appetite (Liedtke et al., 2011). In another study, the mesolimbic dopamine, implicated in reward, has been shown to mediate sodium appetite (Lucas et al., 1999). Hypothalamic orexin neurons project to reward centres, raising the possibility of a two-step neural processing for sodium appetite involving detection at the level of hypothalamic orexin neurons in response to sodium depletion which then acts on reward pathways to influence motivation to consume sodium from food (Liedtke et al., 2011).

It is likely that this two-step neural processing model occurs for homeostatic-like regulation of nutrients (Berthoud et al., 2012). The first step involved in regulating nutrient selectivity and preference involves nutrient sensing by neural circuits involved in mediating appetite, such as the hypothalamus and brainstem. The second step involves increasing hunger and motivation to consume the required nutrient. This signal may be generated in the hypothalamus as well but is likely to involve cortical limbic structures implicated in reward processing leading to increased motivation to consume the desired nutrient. Evidence supporting this model is outlined below.

4.1.1.1 *Reward mechanisms influencing food selectivity*

The modulation of reward value of sugars by the meso-limbic dopaminergic system has been demonstrated in a number of studies (Lenoir et al., 2007, Hajnal et al., 2004, Sclafani et al., 2011, Ren et al., 2010, Domingos et al., 2011). Two recent studies demonstrate that sugar preference is linked with dopamine release in reward centres. In the first study taste receptor knockout mice (Trpm -/-), which lacked the cellular mechanisms for sweet taste transduction, display preference for glucose as compared to iso-caloric L-serine (Ren et al., 2010). Dopaminergic responses in the nucleus accumbens and dorsal striatum increased following intragastric glucose infusion. In another study, optogenetic stimulation of VTA dopaminergic neurons increased the reward value of nutrients (Domingos et al., 2011). Food restriction and central leptin treatment modulated this reward value, suggesting that leptin may change the reward value of a nutrient via a central mechanism and in keeping with the observation that leptin deficient humans have altered drive and motivation to consume calorie dense foods (Farooqi et al., 2007). These recent studies build on work from previous studies looking at dopaminergic neuronal activity and pharmacological manipulation of the dopaminergic system (Lenoir et al., 2007, Hajnal et al., 2004, Sclafani et al., 2011). The neurotransmitter serotonin, also implicated in reward pathways, has been shown to reduce the consumption of a high carbohydrate diet (Wurtman and Wurtman, 1979). Amphetamines, which modulate dopamine, serotonin and norepinephrine neurotransmitters in the brain, lead to reduced sucrose and fat consumption (Kanarek et al., 1996). Amphetamine derivatives have been used in the treatment of obesity, however due to their side effects, their clinical use has been very limited (Hussain and Bloom, 2011a).

It is thought the pathways similar to drug addiction may also operate in mediating the reward mechanisms of palatable foods (Lutter and Nestler, 2009). The neurotransmitters mentioned above provide some evidence for this. In keeping with this link, the anti-obesity drug rimonabant is also used in the management of smoking and cocaine seeking. The side-effects in relation to psychiatric problems and suicide, presumably via altering reward pathways, led to withdrawal of this drug from European and US drug markets (Hussain and Bloom, 2012).

Learned responses to previous experiences can promote consumption of foods, with high reward value, or lead to avoidance of foods, which lead to unpleasant responses. The amygdala is thought to control mnemonic representations of food in relation to reward and preference. Pharmacological treatment of opiate receptor blockers naloxone into the amygdala leads to reduced intake of preferred foods (Glass et al., 2000).

4.1.1.2 Homeostatic mechanisms influencing food selectivity

Less is known about the homeostatic mechanisms in the hypothalamus and brainstem that influence food selectivity, as most of the work to date relates to energy balance. It is likely that homeostatic mechanisms operate indirectly via reward pathways to influence the food selectivity (Berridge, 1996). Manipulation of hypothalamic neurotransmitters has provided some insight into the role of the hypothalamus in food preference.

For example, the role of hypothalamic NPY in food preference has been studied using ICV injections of NPY. These studies reveal that NPY treatment leads to a similar pattern of food preference seen during food deprivation with increased high-sucrose carbohydrate diet preference over fat and increased high-fat diet preference over corn starch diet (Levine et al., 2003, Cleary et al., 1996, Welch et al., 1994).

Opioid receptor blockade in the PVN is more effective in reducing fat consumption as compared to carbohydrate consumption (Marks-Kaufman and Kanarek, 1981, Marks-Kaufman and Kanarek, 1990). Again, variations in this occurred with changes in the carbohydrate source with opioid receptor blockade with naloxone being more effective in decreasing high sucrose diet intake as compared to cornstarch or polycose diet (Weldon et al., 1996).

These results suggest that the carbohydrate source of food seems to have a more profound impact than the neurotransmitter used. However, these studies have a number of limitations due to use of injection techniques that are not limited to defined anatomical area, pharmacological agents that are likely to have non-specific effects, variations in feeding protocols and compositions of diet. This has made it difficult to relate studies to each other and to normal physiology. With precise molecular techniques that can be delivered or expressed specifically in defined neuronal and neuroanatomical populations, it

is likely that we will be able to understand more about the direct role of these hypothalamic neurotransmitters in food selectivity. Furthermore, as discussed later, these refined strategies may also allow us to uncover the role of hypothalamic nutrient sensing in food selection.

4.1.1.3 Interplay between homeostatic and reward pathways linking nutrient-sensing with desire and motivation to consume foods

The hypothalamus, as well as the brainstem, is able to respond to nutrients and hormones, secreted in response to ingestion of certain macronutrients. It is likely that nutrient and hormone sensing information are processed by the hypothalamus and brainstem. This information influences reward centres. This may alter the reward value of nutrients via hedonic pathways. Current evidence, mainly from histochemical and pharmacological studies, links LH orexin and MCH neurons with reward seeking, hedonic pleasure and cognition centres of the brain (Berthoud, 2011, Berthoud, 2006, DeFalco et al., 2001, Borgland et al., 2006, Boutrel et al., 2005, Harris et al., 2005). Several studies provide evidence that gut hormones and leptin, considered as peripheral homeostatic signals, influence reward pathways. It is not clear if these hormones are acting directly on reward centres or are working indirectly via acting on homeostatic pathways such, as the arcuate, where majority of their action has been previously demonstrated (Grill et al., 2007, De Silva et al., 2011). Strategies to investigate this further, especially in relation to other hypothalamic nuclei, are currently underway. Evidence so far fits with a two-step neural pathway with sensing and processing of metabolites via homeostatic centres that influence hedonic pathways and motivation to consume a particular nutrient.

4.1.1.4 Hypothalamic Glucose-sensing and food selectivity

The presence of metabolite sensing pathways in the hypothalamus raises the possibility that the brain can detect the presence or absence of specific nutrients and respond by altering food preference accordingly via a two-step neural pathway described above. This has not yet been satisfactorily demonstrated. In relation to glucose-sensing, it is widely accepted that animals and humans can adjust glucose intake according to their physiological state (Thompson and Campbell, 1977). The presence of glucose-sensing pathways in the hypothalamus provides a likely mechanism to enable food selectivity and glucose

preference in certain states (Berthoud et al., 2012). Unfortunately, although counter-regulatory responses to hypoglycaemia and total food intake have been studied in relation to altered hypothalamic glucose-sensing, food selectivity remains unexplored. Our model of increased arcuate glucokinase activity provides an opportunity to study this.

4.2 Hypothesis and Aims

4.2.1 Hypothesis

Selectively altering glucokinase activity in the ARC of the hypothalamus, using stereotactic injections of rAAV encoding glucokinase mRNA and glucokinase activators, alters consumption of glucose.

4.2.2 Aims and Objectives

To investigate this, I will study the effect of increased ARC glucokinase activity on glucose intake and glucose preference over other foods.

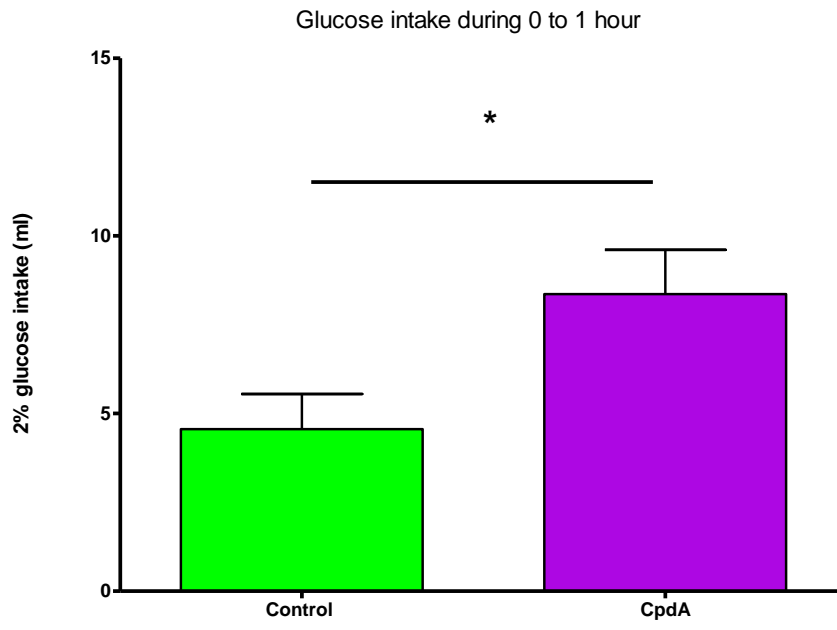
4.3 Results

4.3.1 Effect of increasing ARC glucokinase activity on glucose intake

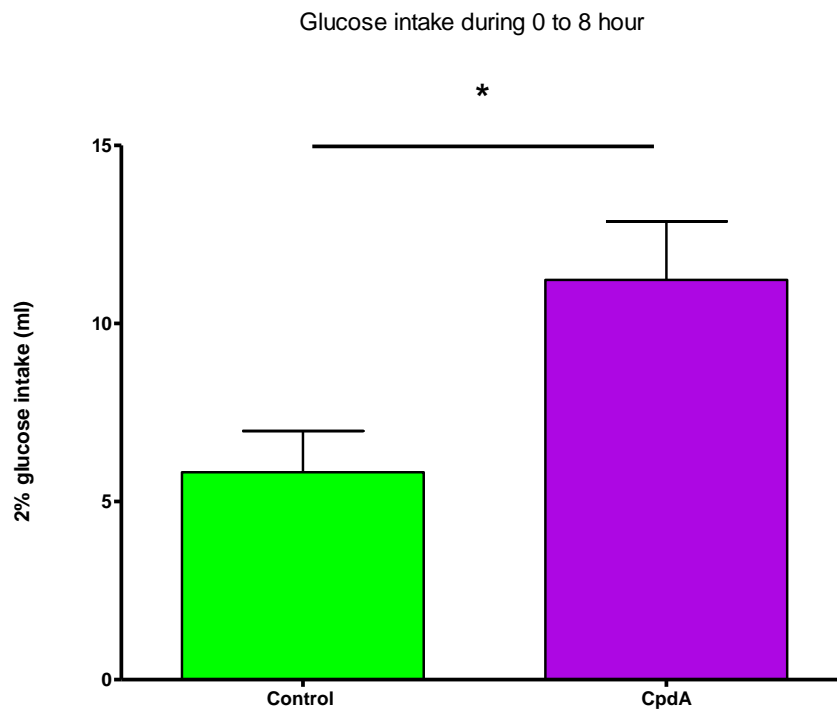
4.3.1.1 *Effect of pharmacologically increasing ARC glucokinase activity on glucose intake*

Acute arcuate glucokinase activation increased glucose intake during the first hour after injection, as compared to vehicle injected controls (control, 4.56 ± 0.99 ml; CpdA, 8.36 ± 1.25 ml; $n=8$, $p < 0.05$) (figure 4.1a). This effect was significant for up to eight hours (control, 5.83 ± 1.16 ml; CpdA, 11.23 ± 1.64 ml; $n=8$, $p < 0.05$) (figure 4.1b). Although there was an increase in glucose intake at later time points, including 24 hours, this was not significant (control, 62.8 ± 9.34 ml; CpdA, 73.8 ± 8.66 ml; $n=8$) (figure 4.1c).

a)



b)



c)

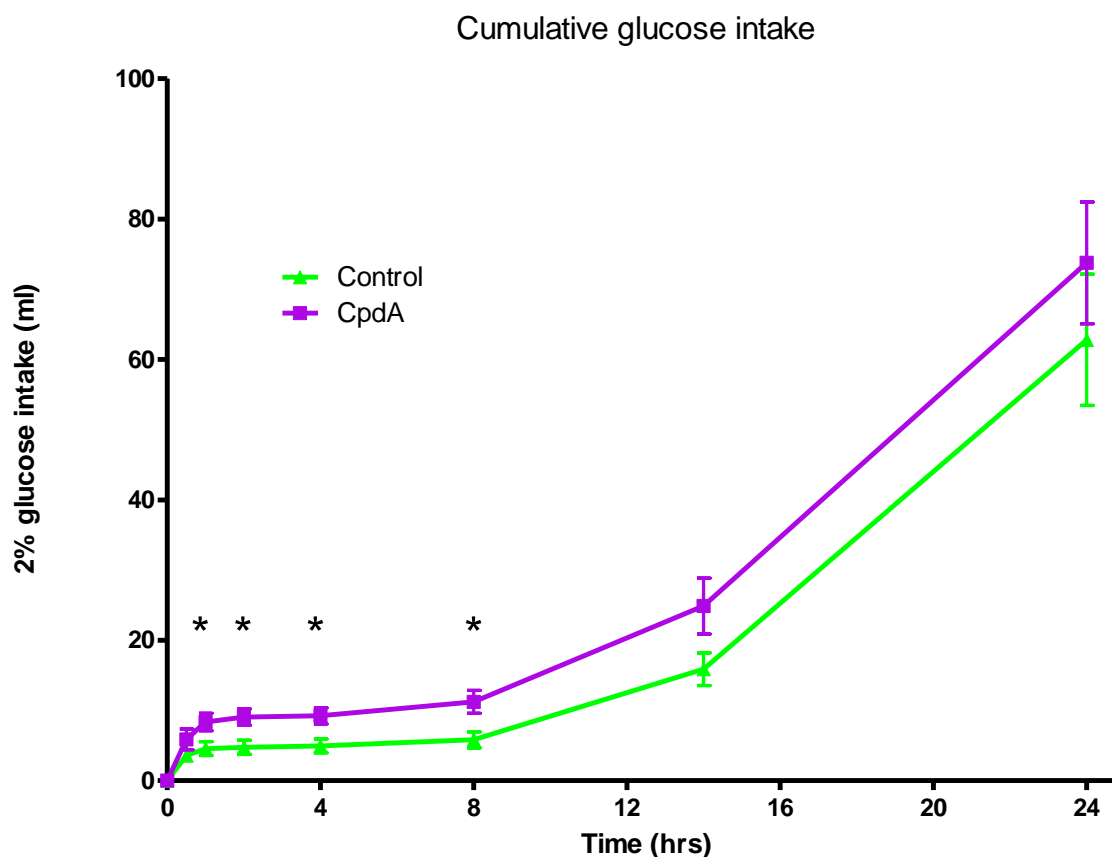


Figure 4.1 Effect of increasing ARC glucokinase activity on glucose intake. 2% w/v glucose solution intake (a) one hour and (b) eight hours after ARC glucokinase activation using stereotactic injection of 0.5 nmol CpdA as compared to the vehicle injected controls during a crossover study. (c) Twenty-four hour 2% w/v glucose intake after ARC glucokinase activation using stereotactic injection of 0.5 nmol CpdA as compared to the vehicle injected controls during a crossover study. Data are expressed as mean \pm SEM for all groups, $n=7$. Statistical significance was analysed by student's t test: $*=p<0.05$.

4.3.1.2 Effect of chronic ARC glucokinase activation on glucose and fructose intake

Effect on intake of 2% glucose and 2% fructose solutions

Cumulative glucose intake was significantly different between the groups at two, four, eight and twenty-four hours (at twenty-four hours: iARC-GFP 56.2 \pm 8.8ml vs. iARC-GKS 81.2 \pm 11.2ml, n=8, p<0.05) (figure 4.2). Cumulative fructose intake was similar between the 2 groups at all time points (at twenty-four hours: iARC-GFP 61.3 \pm 7.2ml vs. iARC-GKS 61.5 \pm 12.2 ml, n=8) (figure 4.2)

Effect on intake of 10% glucose and 10% fructose solutions

Cumulative glucose intake was significantly different between the groups at two, four, eight and twenty-four hours (at twenty-four hours: iARC-GFP 135 \pm 4.6ml vs. iARC-GKS 154.1 \pm 5.3ml, n=8, p<0.05) (figure 4.3). Cumulative fructose intake was similar between the 2 groups at all time points (at twenty-four hours: iARC-GFP 86.5 \pm 7.4ml vs. iARC-GKS 87.9 \pm 6.7 ml, n=8) (figure 4.3)

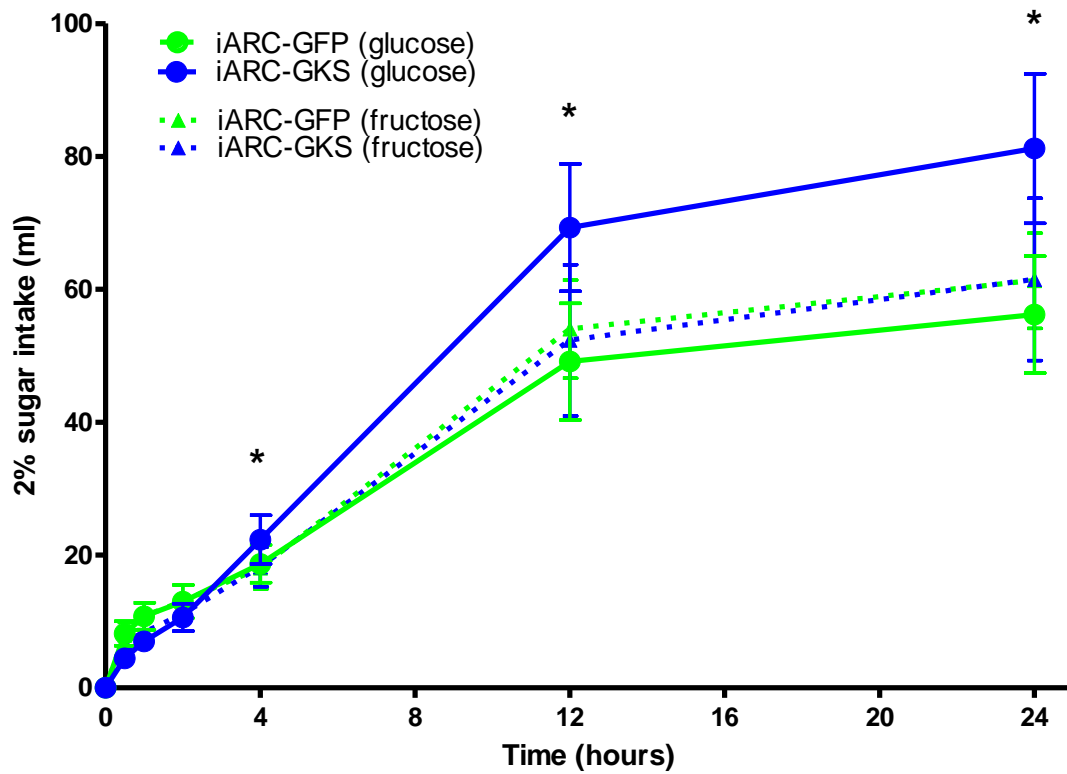


Figure 4.2 Effect of increasing ARC glucokinase activity on twenty-four hour intake of 2% w/v sugar solutions: Cumulative twenty-four hour 2% w/v glucose intake (solid line) and 2% w/v fructose intake (dotted line) following bilateral injection of 1ul rAAV-eGFP (green line, n=8) or 1ul rAAV-GKS (blue line, n=8) in male Wistar rats fed on normal chow. Data are expressed as mean +/- SEM for all groups, n=8. Statistical significance was analysed by student's t test: *=p<0.05.

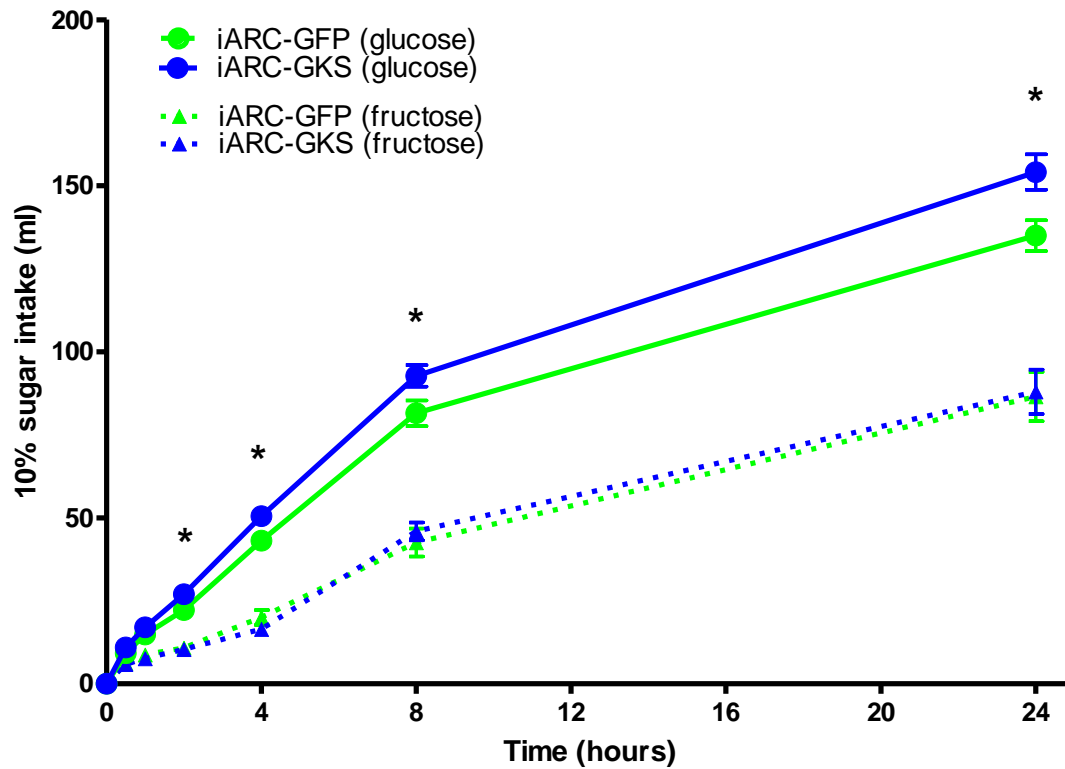
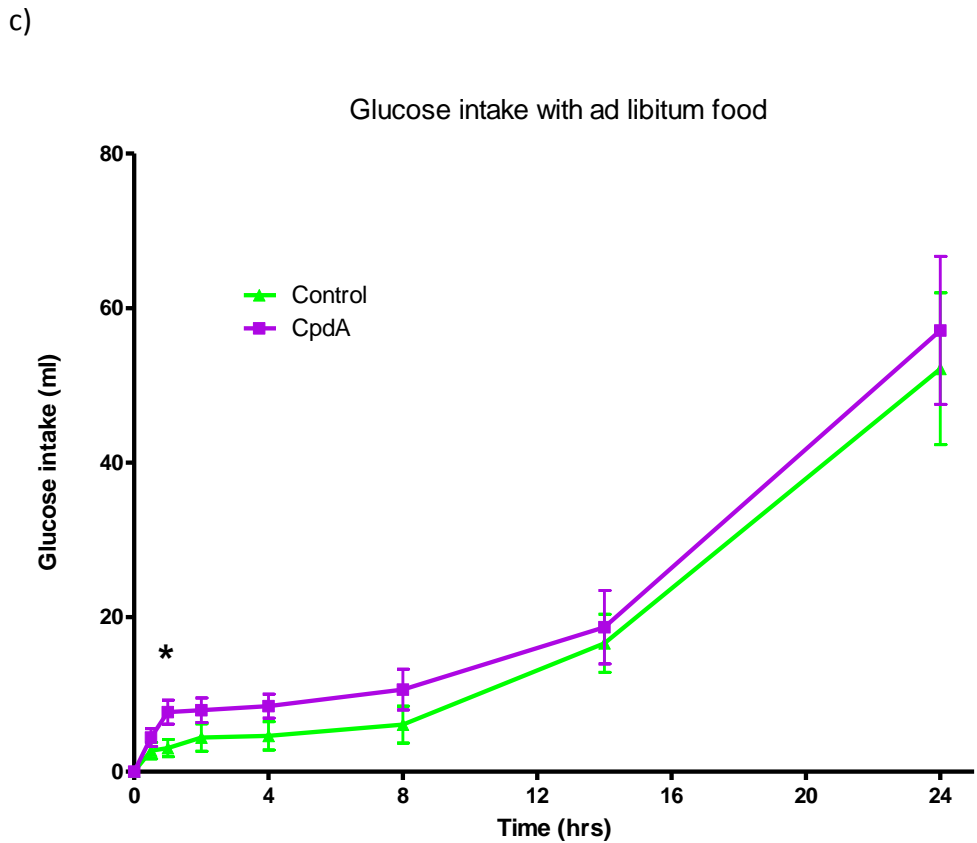
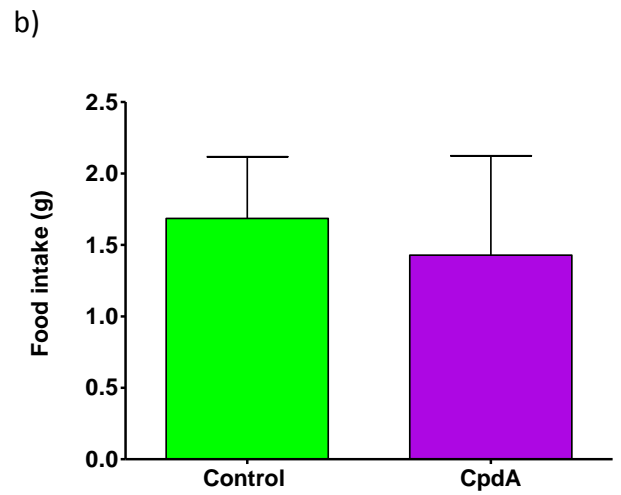
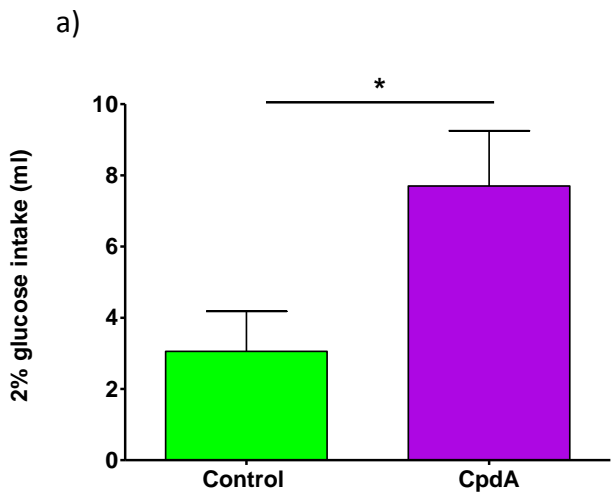


Figure 4.3 Effect of increasing ARC glucokinase activity on twenty-four hour intake of 10% w/v sugar solutions: Cumulative twenty-four hour 10% w/v glucose intake (solid line) and 10% w/v fructose intake (dotted line) following bilateral injection of 1ul rAAV-eGFP (green line, n=8) or 1ul rAAV-GKS (blue line, n=8) in male Wistar rats fed on normal chow. Data are expressed as mean +/- SEM for all groups, n=8. Statistical significance was analysed by student's t test: *=p<0.05.

4.3.2 Effect of increasing ARC glucokinase activity on preference of glucose over other foods

Acute arcuate glucokinase activation increased glucose intake during the first hour after injection, as compared to vehicle injected controls when 2% w/v glucose was given with normal chow (control, 3.06 ± 1.13 ml; CpdA, 4.11 ± 1.55 ml; $n=7$, $p < 0.05$) (figure 4.4a). There was no difference in food intake at this time point (control, 1.69 ± 0.43 g; CpdA, 1.43 ± 0.70 g; $n=7$, $p < 0.05$) (figure 4.4b). Although there was an increase in glucose intake at later time points, including twenty-four hours, this was not significant (at twenty-four hours: control, 52.1 ± 9.82 ml; CpdA, 57.11 ± 9.57 ml; $n=7$) (figure 4.4c). There was no significant difference in food intake at any of the time points during the twenty-four hours study (control, 27.23 ± 1.00 g; CpdA, 26.3 ± 2.15 g; $n=7$, $p < 0.05$) (figure 4.4d).



d)

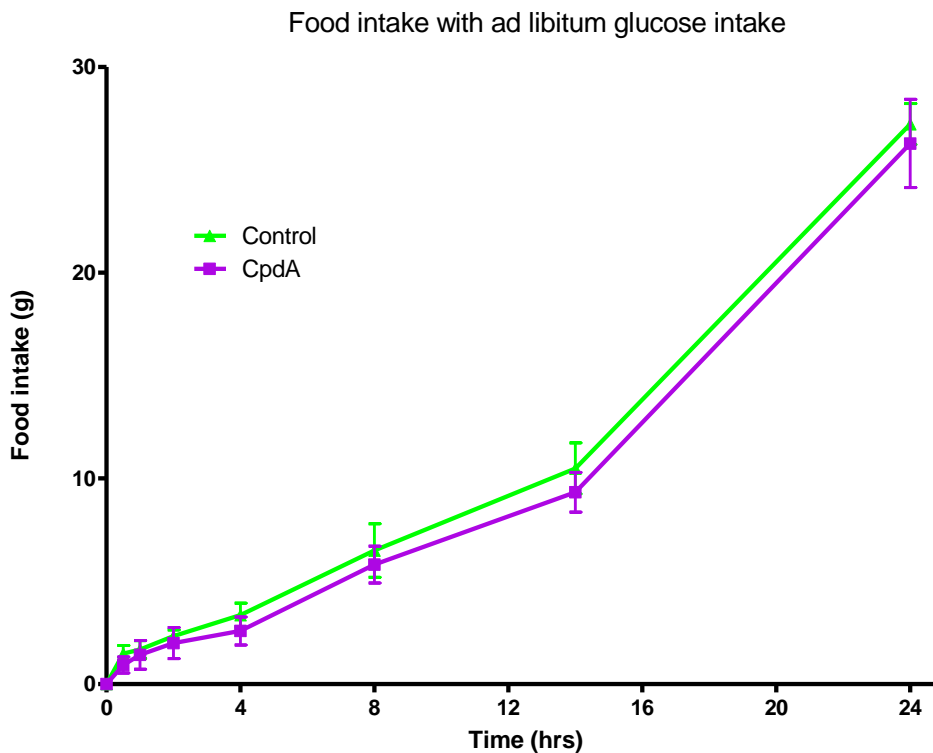


Figure 4.4 Effect of increasing ARC glucokinase activity on glucose and food intake with ad libitum access to 2% w/v glucose solution and normal chow. (a) 2% w/v glucose solution intake and (b) normal chow intake one hour after ARC glucokinase activation using stereotactic injection of 0.5 nmol CpdA as compared to the vehicle injected controls during a crossover study. (c) Twenty-four hour 2% w/v glucose intake and (d) after ARC glucokinase activation using stereotactic injection of 0.5 nmol CpdA as compared to the vehicle injected controls during a crossover study. Data are expressed as mean \pm SEM for all groups, $n=7$. Statistical significance was analysed by student's t test: $*=p<0.05$.

4.3.2.1 Effect of increasing ARC glucokinase activity on 24 hour intake of food, glucose and total caloric intake with ad libitum access to 2% w/v glucose and normal chow

24 hour food intake was similar in both groups at all time points with ad libitum access to a 2% glucose solution with normal chow (figure 4.5a), however cumulative 2% glucose intake was significantly increased in the iARC-GKS group, as compared to the iARC-GFP group, between 2 to 24 hours (at 24 hours: iARC-GFP 86.3 +/- 12.1 ml vs. iARC-GKS 145.4 +/- 11.6, n=7, P<0.05) (figure 4.5b). Total caloric intake, from normal chow and glucose, was similar in both groups at all time points (figure 4.5c).

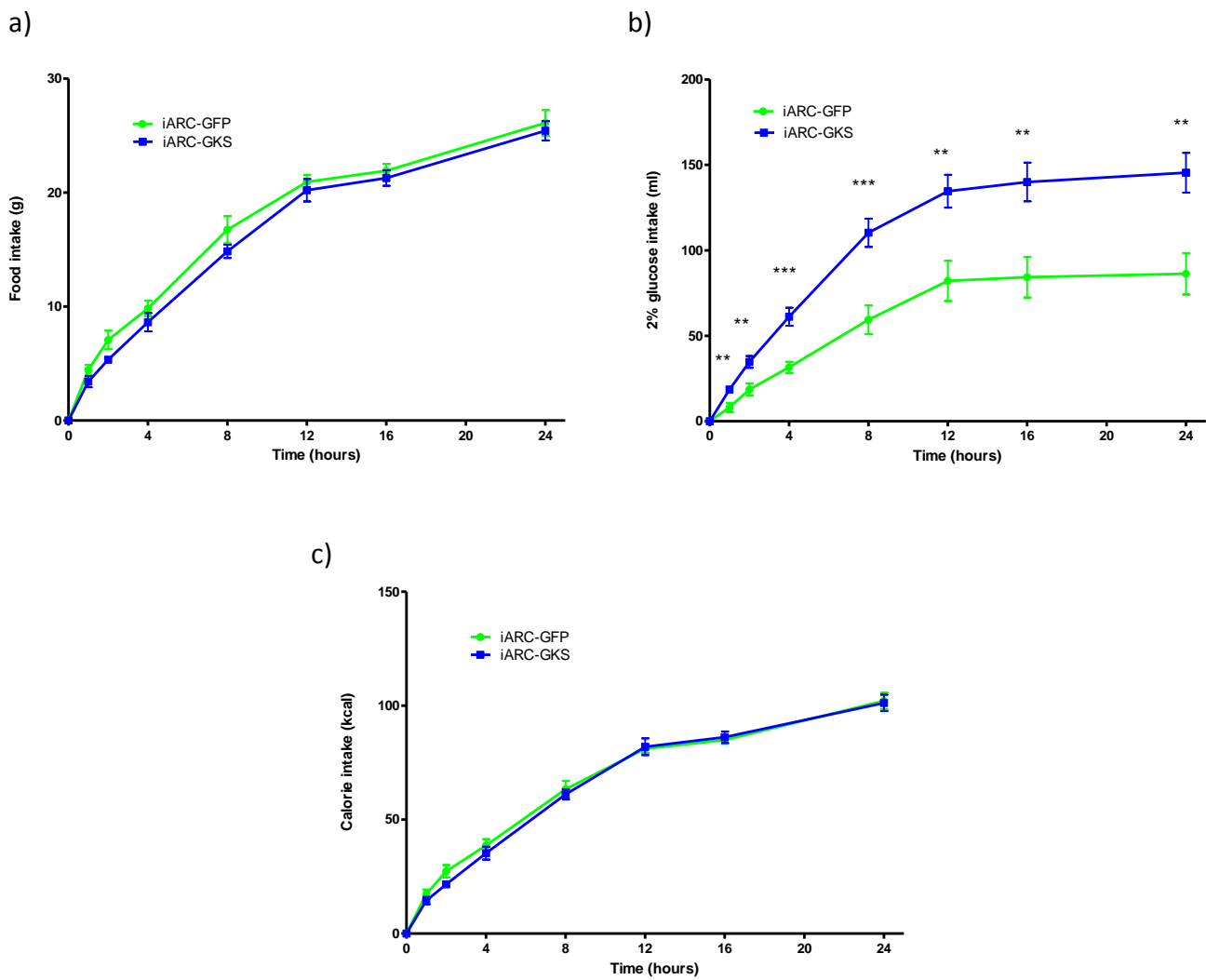


Figure 4.5 Effect of chronically increasing ARC glucokinase activity on twenty-four hour glucose, food and caloric intake with ad libitum access to 2% w/v glucose solution and normal chow. Cumulative twenty-four hour a) food intake, b) 2% w/v glucose intake and c) total caloric intake following bilateral injection of 1ul rAAV-eGFP (green line, n=7) or 1ul rAAV-GKS (blue line, n=7) in male Wistar rats fed on normal chow. Data are expressed as mean +/- SEM for all groups, n=7. Statistical significance was analysed by student's t test: *=p<0.05, **=p<0.01, ***=p<0.001

4.3.2.2 Effect of increasing ARC glucokinase activity on 24 hour intake of food, glucose and total caloric intake with ad libitum access to 10% w/v glucose and normal chow

24 hour food intake was similar in both groups at all time points with ad libitum access to a 10% glucose solution and normal chow (figure 4.6a), however cumulative 10% glucose intake was significantly increased in the iARC-GKS group, as compared to the iARC-GFP group, at 8 and 24 hours (at 24 hours: iARC-GFP 88.0 +/- 6.4 ml vs. iARC-GKS 107.6 +/- 4.4, n=8, p<0.05) (figure 4.6b). Total caloric intake, from normal chow and glucose, was similar in both groups at all time points (figure 4.6c).

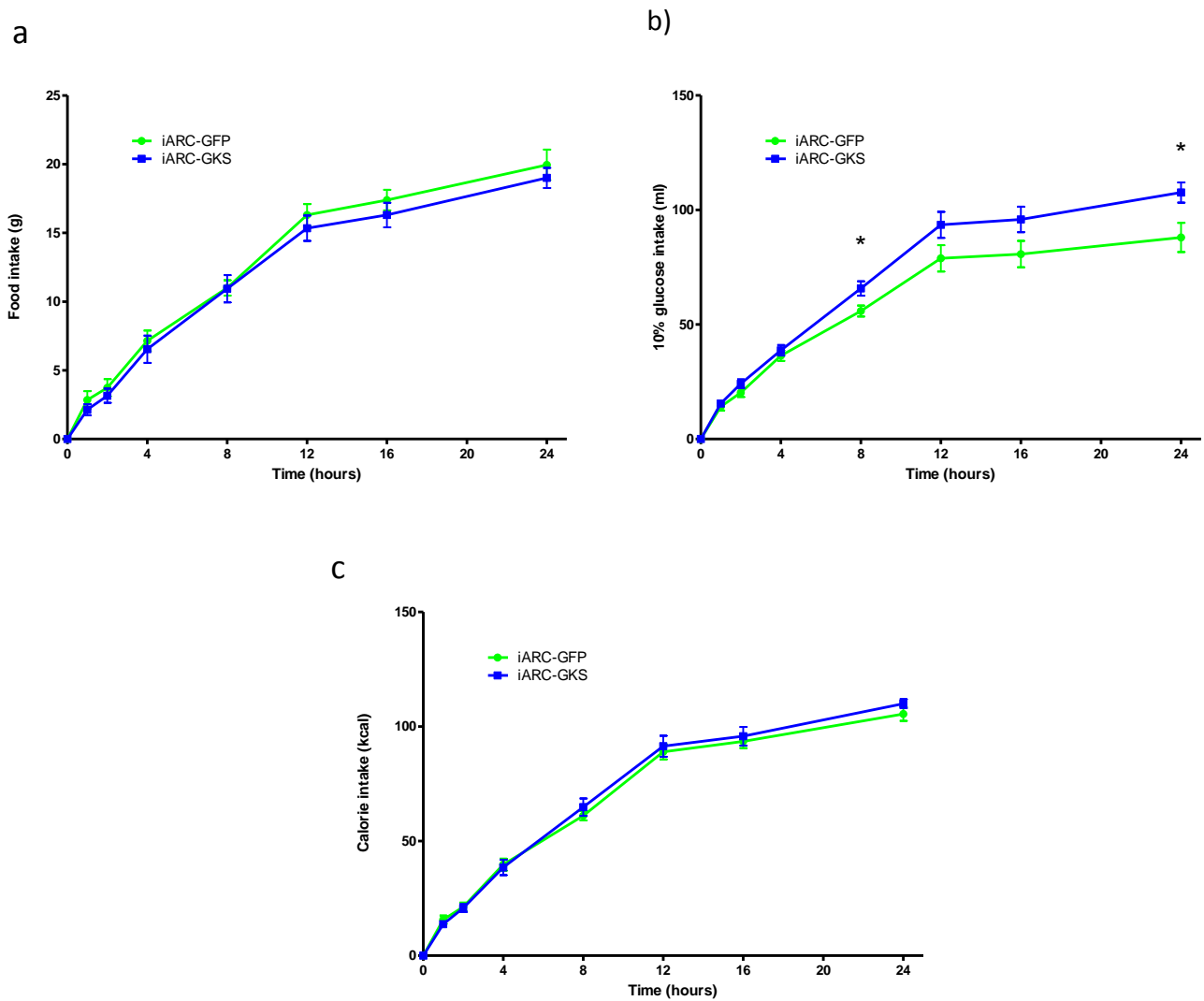


Figure 4.6 Effect of chronically increasing ARC glucokinase activity on twenty-four hour glucose, food and caloric intake with ad libitum access to 10% w/v glucose solution and normal chow. Cumulative twenty-four hour a) food intake, b) 10% w/v glucose intake and c) total caloric intake following bilateral injection of 1ul rAAV-eGFP (green line, n=8) or 1ul rAAV-GKS (blue line, n=8) in male Wistar rats fed on normal chow. Data are expressed as mean +/- SEM for all groups, n=8. Statistical significance was analysed by student's t test: *=p<0.05, **=p<0.01, ***=p<0.001

4.3.2.3 Effect of increasing ARC glucokinase activity on 24 hour intake of food, glucose and total caloric intake with ad libitum access to 20% glucose and normal chow

24 hour food intake was similar in both groups at all time points with ad libitum access to a 20% glucose solution and normal chow (figure 4.7a), however cumulative 20% glucose intake was significantly increased in the iARC-GKS group, as compared to the iARC-GFP group, at 18 and 24 hours (at 24 hours: iARC-GFP 75.3 +/- 3.8 ml vs. iARC-GKS 88.5 +/- 3.6, n=8, p<0.05) (figure 4.7b). Total caloric intake, from normal chow and glucose, was similar in both groups at all time points (figure 4.7c).

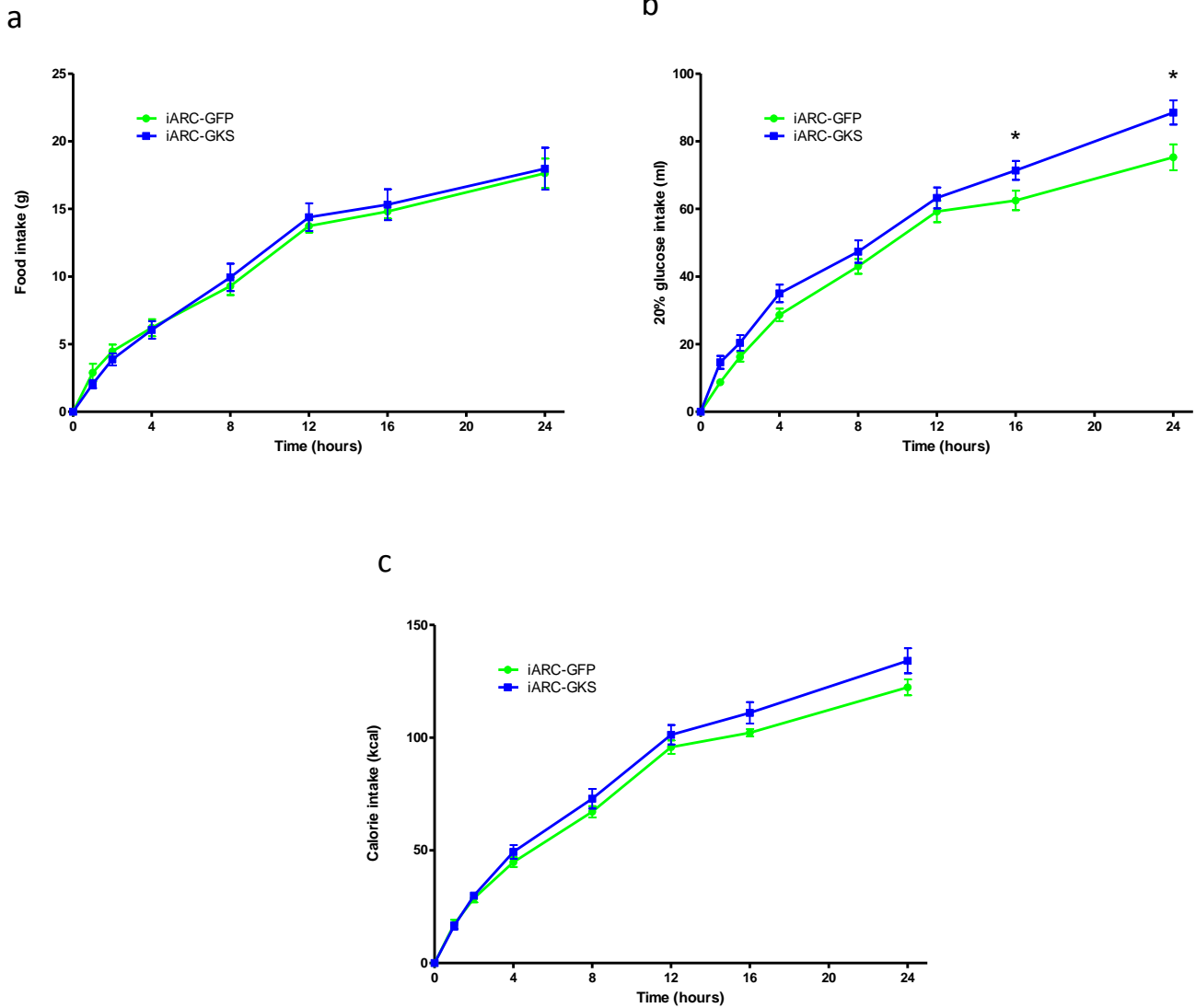


Figure 4.7 Effect of chronically increasing ARC glucokinase activity on twenty-four hour glucose, food and caloric intake with *ad libitum* access to 20% w/v glucose solution and normal chow. Cumulative twenty-four hour a) food intake, b) 20% w/v glucose intake and c) total caloric intake following bilateral injection of 1ul rAAV-eGFP (green line, n=8) or 1ul rAAV-GKS (blue line, n=8) in male Wistar rats fed on normal chow. Data are expressed as mean +/- SEM for all groups, n=8. Statistical significance was analysed by student's t test: *=p<0.05, **=p<0.01, ***=p<0.001

4.3.2.4 Effect of increasing ARC glucokinase activity on twenty-four hour normal chow food intake in iARC-GKS and iARC-GFP cohort previously given sugar solutions

Cumulative food intake was different between the groups at 8, 12, 16 and 24 hours, when the iARC-GKS group ate significantly more compared to the iARC-GFP control group (iARC-GFP 25.9 +/- 1.01g vs. iARC-GKS 29.5 +/- 1.27g, n=8) (figure 4.8).

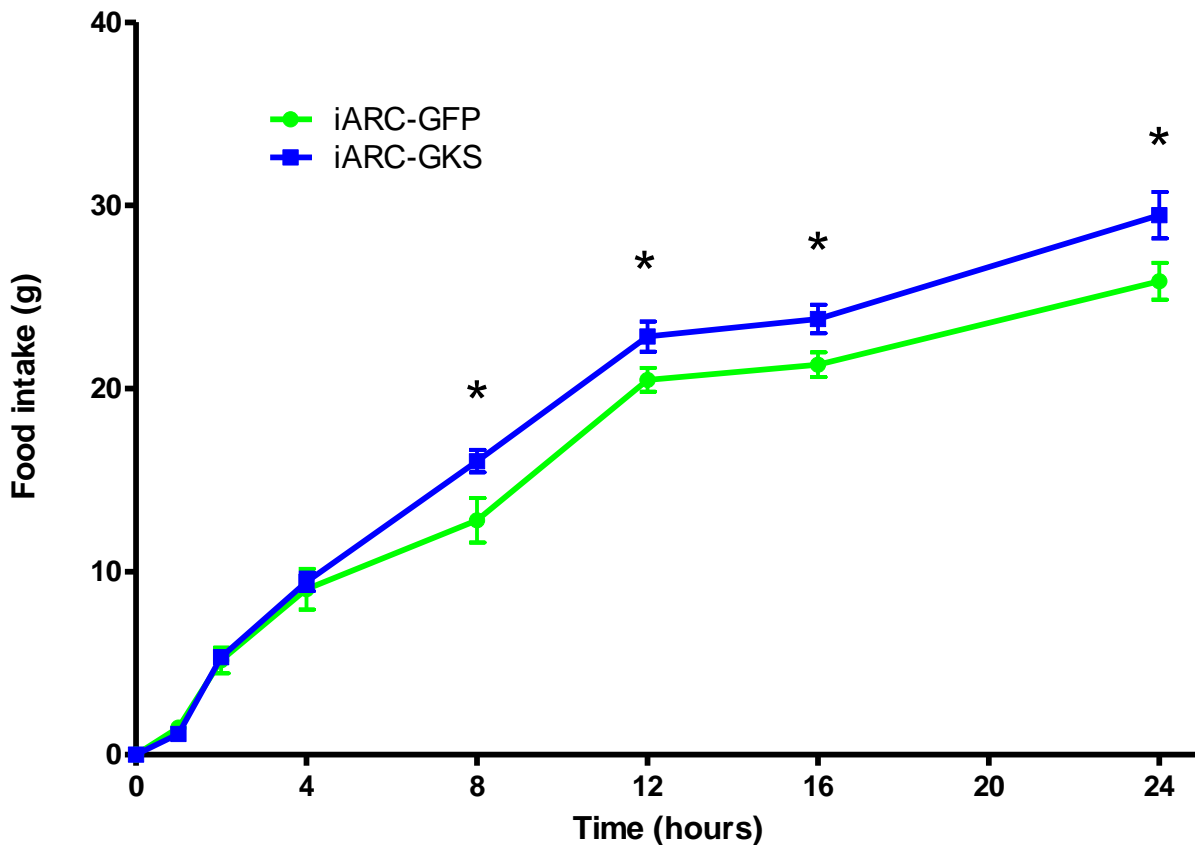


Figure 4.8 Effect of increasing ARC glucokinase activity on twenty-four hour intake of food. Cumulative twenty-four hour food intake following bilateral injection of 1ul rAAV-eGFP (green line, n=8) or 1ul rAAV-GKS (blue line, n=8) in male Wistar rats fed on normal chow. Data are expressed as mean +/- SEM for all groups, n=8. Statistical significance was analysed by student's t test: *=p<0.05.

4.3.2.5 Comparison of twenty-four hour caloric intake from chow, glucose and total caloric intake in studies with iARC-GKS and iARC-GFP rats

Twenty-four hour caloric intake from chow during studies with ad libitum access to normal chow supplemented with no glucose, 2% glucose, 10% glucose or 20% glucose in iARC-GKS and iARC-GFP rats is shown in figure 4.9a. Percentage calories from glucose over twenty-four hours in studies with ad libitum access to normal chow and 2% glucose, 10% glucose or 20% glucose in iARC-GKS and iARC-GFP rats is shown in figure 4.9b. Twenty-four hour total caloric intake during these studies is shown in the figure 4.9c.

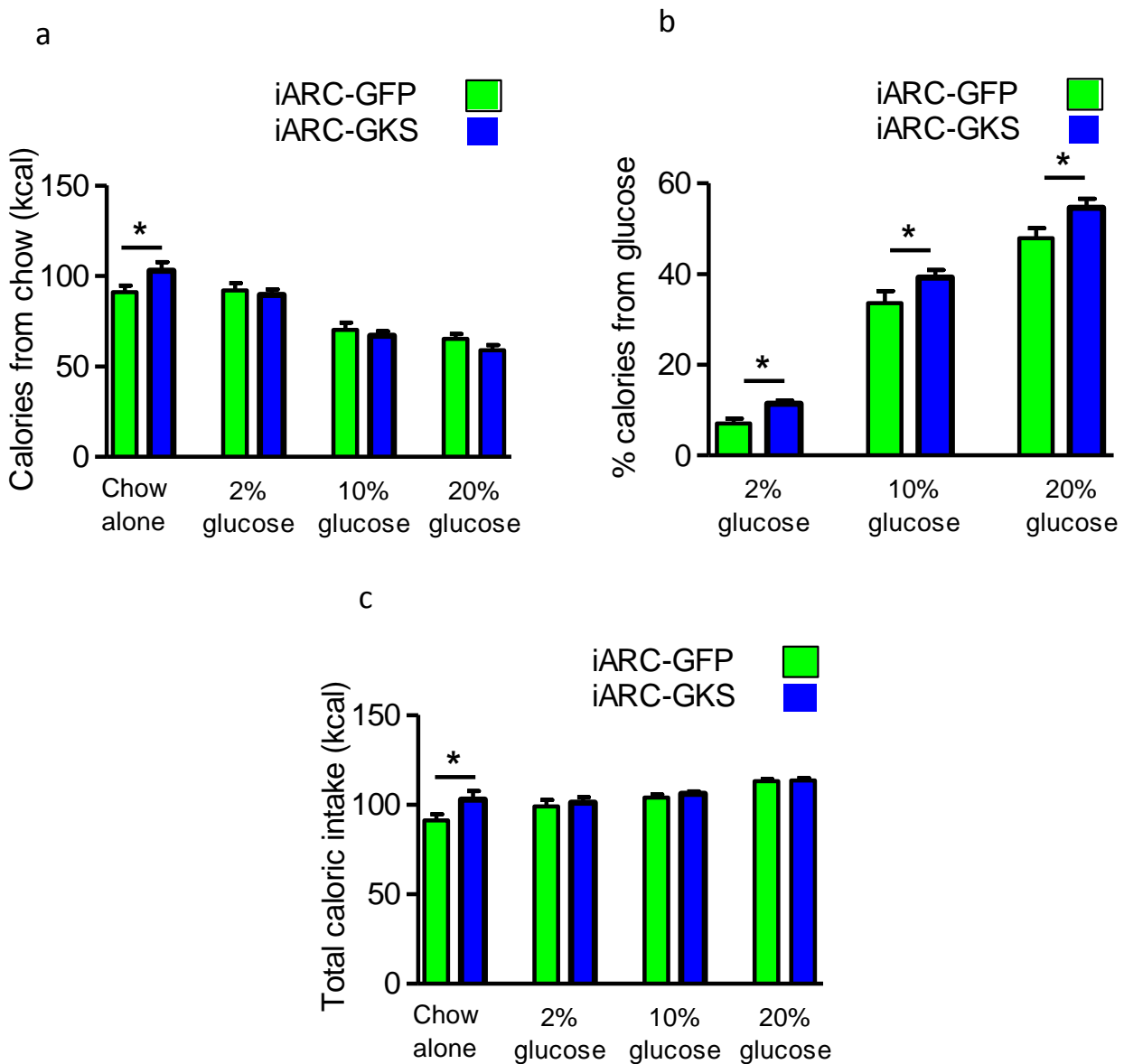


Figure 4.9 Comparison of the effects of increasing ARC glucokinase activity on twenty-four hour caloric intake during studies with ad libitum access to chow and glucose solutions. Twenty-four hour (a) caloric intake from chow, (b) percentage calories from glucose and (c) total caloric intake during studies during studies with ad libitum access to normal chow and glucose of varying concentrations following bilateral injection of 1ul rAAV-eGFP (green line, n=7-8) or 1ul rAAV-GKS (blue line, n=7-8) in male Wistar rats. Data are expressed as mean +/- SEM for all groups, n=7-8. Statistical significance was analysed by student's t test on absolute caloric intake values: * $p < 0.05$.

4.3.3 Effect of increasing ARC glucokinase activity on long-term food, glucose and total caloric intake with ad libitum access to 10% glucose and standard chow

4.3.3.1 Effect on food intake

At day 31 after injection, when the experiment was terminated, there was no significant difference between the food intake of the iARC-GFP group (699.4 +/- 19.4, n=8) and the iARC-GKS group (682.1 +/- 22.8g, n=8) (figure 4.10).

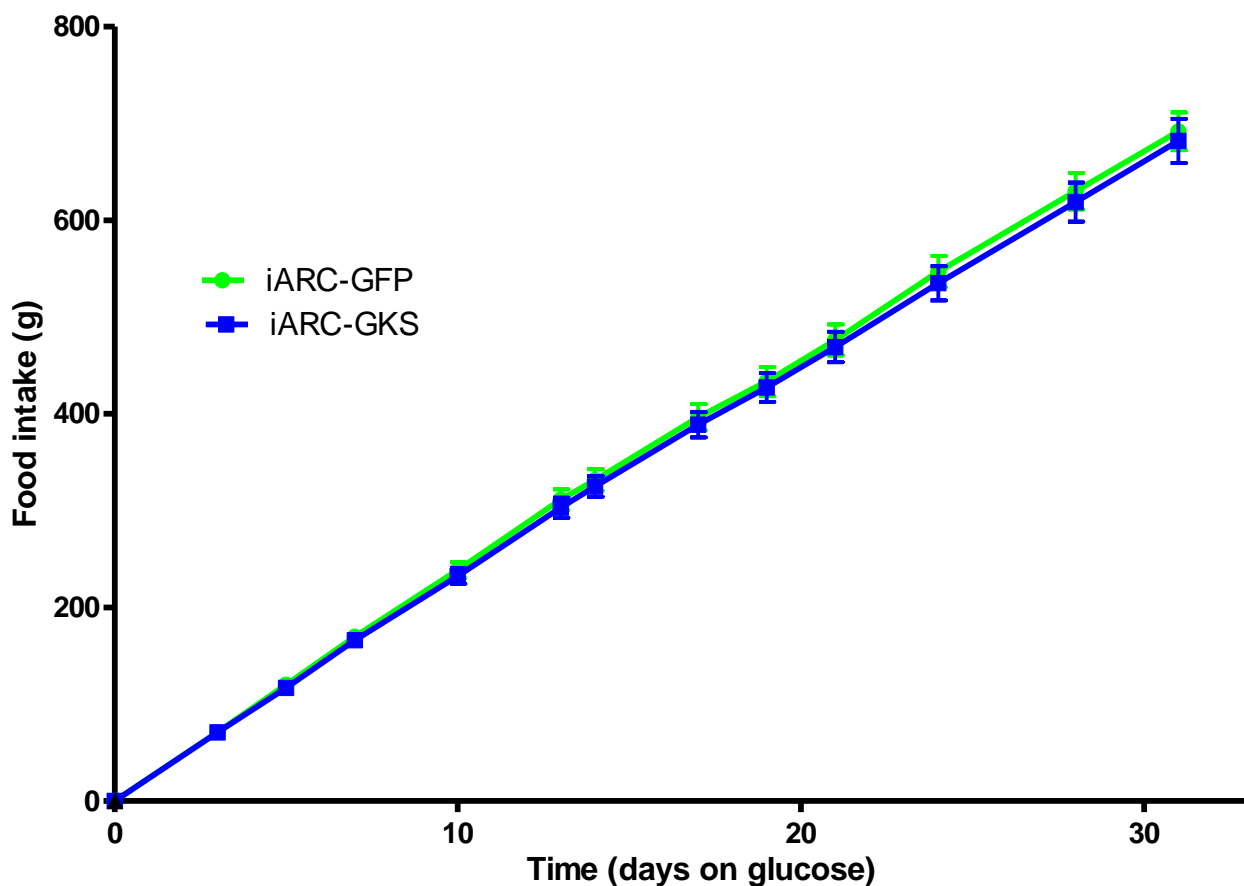


Figure 4.10 Effect of increasing ARC glucokinase activity on food intake with long-term ad libitum access to 10% w/v glucose and standard chow. Food intake with ad libitum access to 10% glucose following bilateral injection of 1ul rAAV-eGFP (green line, n=8) or 1ul rAAV-GKS (blue line, n=8) in male Wistar rats fed on normal chow over thirty-one days. Data are expressed as mean +/- SEM for both groups. Statistical significance was analysed by GEE.

4.3.4 Effect on glucose intake

At the termination of the experiment (day 31), the glucose intake was significantly increased in the iARC-GKS group, as compared to the iARC-GFP group (iARC-GFP 2812.9 +/- 91.9ml vs. iARC-GKS 3337.1 +/- 131.4ml, n=8, P=<0.05) (figure 4.11).

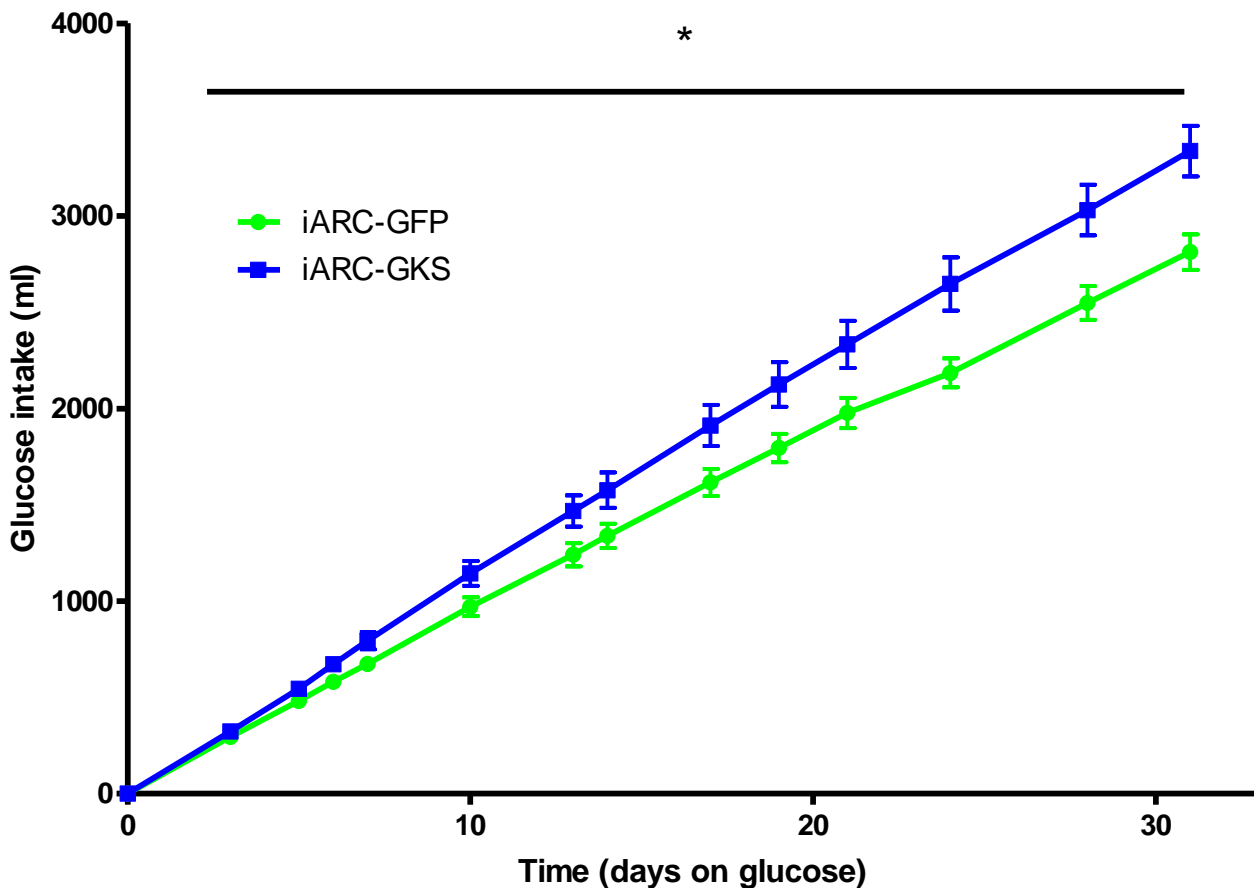


Figure 4.11 Effect of increasing ARC glucokinase activity on glucose intake with long-term *ad libitum* access to 10% w/v glucose and standard chow. 10% w/v glucose intake with *ad libitum* access to 10% w/v glucose and standard chow following bilateral injection of 1ul rAAV-eGFP (green line, n=8) or 1ul rAAV-GKS (blue line, n=8) in male Wistar rats fed on normal chow over thirty-one days. Data are expressed as mean +/- SEM for both groups. Statistical significance was analysed by GEE. *=p<0.05

4.3.5 Effect of increasing ARC glucokinase activity on caloric intake with ad libitum access to 10% glucose and normal chow

At the termination of the experiment (day 31), there was no significant difference between the caloric intake of the iARC-GFP group (3456.9 +/- 78.5kcal, n=8) and the iARC- GKS group (3615.32 +/- 100.4kcal, n=8) (figure 4.12).

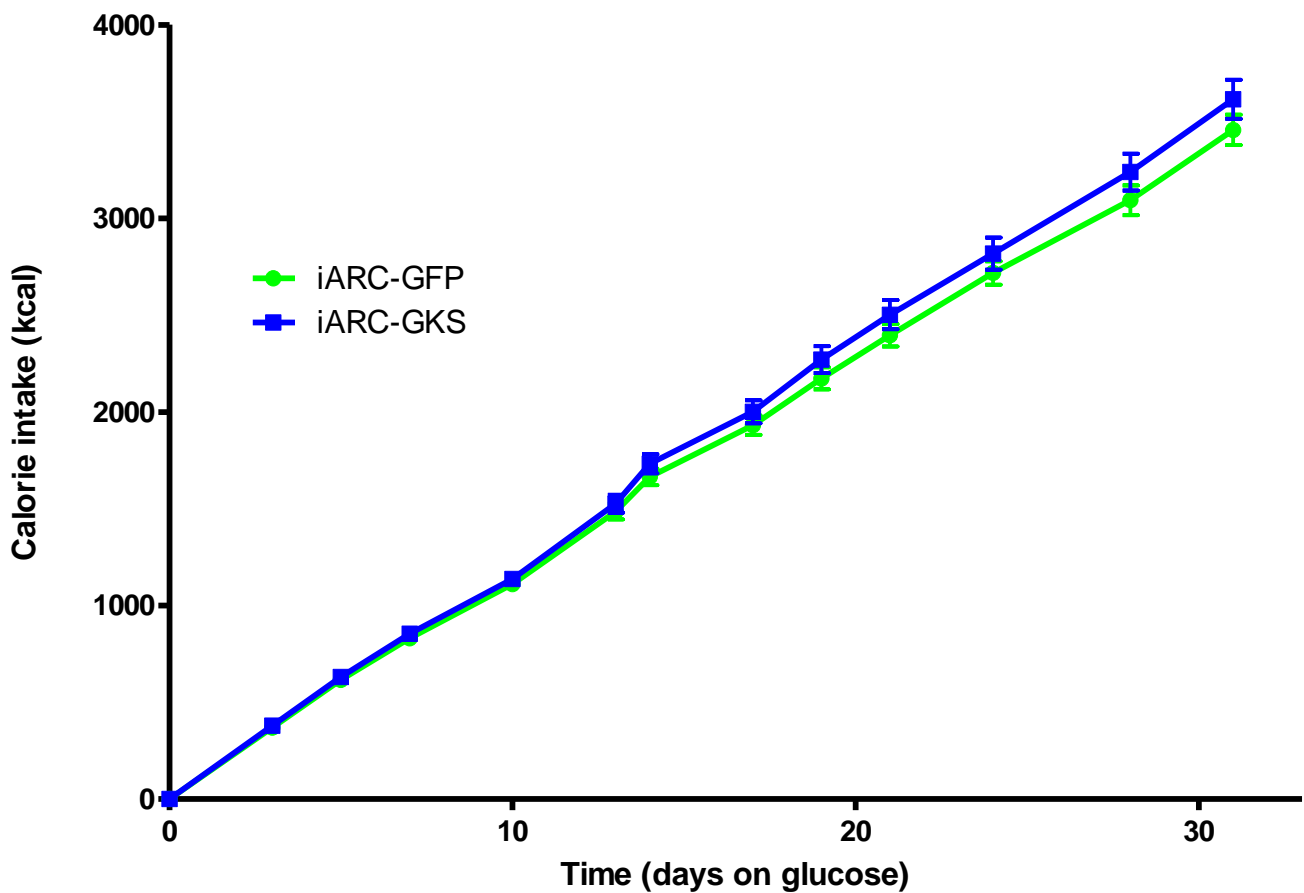


Figure 4.12 Effect of increasing ARC glucokinase activity on caloric intake with long-term ad libitum access to 10% w/v glucose and standard chow. Caloric intake with ad libitum access to 10% w/v glucose and standard chow following bilateral injection of 1ul rAAV-eGFP (green line, n=8) or 1ul rAAV-GKS (blue line, n=8) in male Wistar rats fed on normal chow over thirty-one days. Data are expressed as mean +/- SEM for both groups. Statistical significance was analysed by GEE.

4.3.6 Effect on bodyweight gain

At the termination of the experiment (day 31), there was no significant difference between the bodyweight gain of the iARC-GFP group (61.0 +/- 4.2g, n=8) and the iARC-GKS group (71.8 +/- 4.5g, n=8) (figure 4.13) (initial body weight: iARC-GFP, 428.63±11.58g; iARC-GKS 449.25±5.60g).

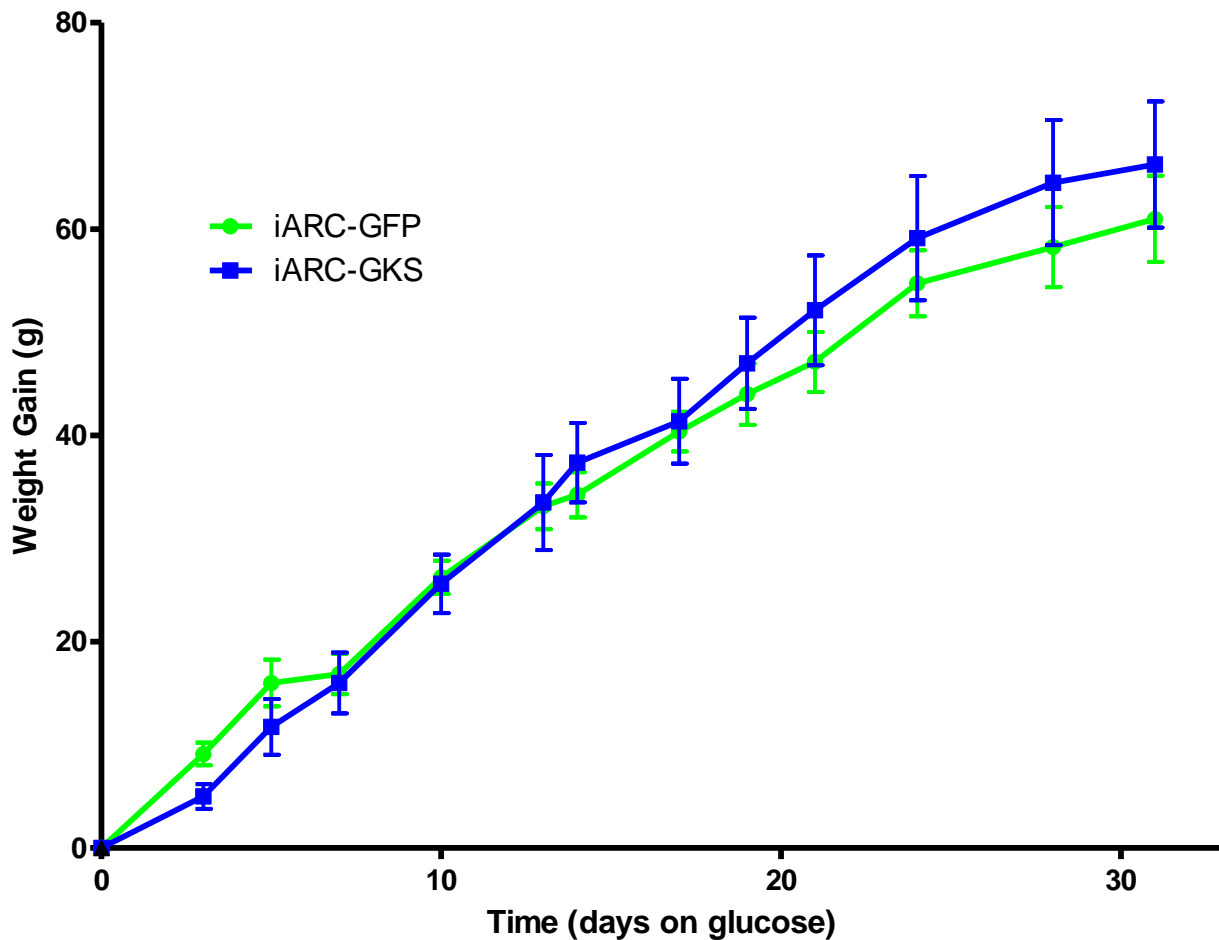


Figure 4.13 Effect of increasing ARC glucokinase activity on bodyweight gain with long-term ad libitum access to 10% w/v glucose and standard chow. Bodyweight gain with ad libitum access to 10% w/v glucose and standard chow following bilateral injection of 1ul rAAV-eGFP (green line, n=8) or 1ul rAAV-GKS (blue line, n=8) in male Wistar rats fed on normal chow over thirty-one days. Data are expressed as mean +/- SEM for both groups. Statistical significance was analysed by GEE.

4.4 Discussion

4.4.1 ARC glucokinase selectively alters glucose intake but does not alter fructose intake

Increasing arcuate glucokinase should enhance glucose flux and metabolism and may alter appetite via arcuate glucose-sensing neurons. This effect via glucokinase may be more pronounced in response to glucose consumption as compared to other non-glucose based hexose sugars. Fructose, a sweeter sugar than glucose, is not expected to be directly sensed via the glucokinase pathway and is unlikely to affect appetite via glucokinase since it is not metabolised by glucokinase and does not cross the blood-brain barrier (Printz et al., 1993, Oldendorf, 1971). Consistent with the above, we found that pharmacological increase in ARC glucokinase activity increased short-term glucose intake. To investigate the effect of glucose intake on increased ARC glucokinase activity further, we studied 24 hour glucose intake and 24 hour fructose intake in iARC-GKS animals using both 2% w/v and 10% w/v solutions. 2% and 10% w/v glucose intake was significantly increased in the iARC-GKS group versus the controls. Fructose intake was similar for both 2% and 10% w/v fructose between the two groups. These results supported the hypothesis that increased ARC glucokinase activity selectively alters glucose intake.

4.4.2 ARC glucokinase selectively alters glucose intake over other foods

We further tested our hypothesis and examined the effect of increasing ARC glucokinase activity on promoting the intake of glucose over other foods. Ad libitum access to glucose solutions of varying concentrations in addition to standard chow in animals with both pharmacologically and genetically increased ARC glucokinase activity resulted in significantly increase glucose intake compared to controls. Intake of standard chow and total caloric intake was similar in these studies, unlike studies with single mixed diet described in chapter 3. Twenty-four hour intake of standard chow alone in this cohort of iARC-GKS rats was increased as compared to controls, consistent with results from chapter 3. Thus, the addition of a glucose solution to standard chow diet resulted in an increased consumption of the glucose solution in animals with increased ARC glucokinase activity and normalisation of standard chow intake and calorie intake as compared to controls. We hypothesised that increased ARC glucokinase activity resulted in a selective increase in glucose appetite over

other foods. When this appetite is satisfied it results in normalisation of food intake and caloric intake.

To investigate this further iARC-GKS and iARC-GFP rats were given *libitum* access to a 10% glucose solution and normal chow for a period of 31 days. As was observed in the 24hr studies, there was a significant increase in the glucose intake in the GKS group, as compared to the controls. Standard chow intake, total calorie intake and bodyweight gain were similar between the groups in the study. This is in keeping with our above hypothesis. When glucose is provided separately its intake is selectively increased and that of chow and calories remained similar. Increased ARC glucokinase activity selectively increases glucose appetite. When this appetite is satisfied with a pure glucose diet, intake of chow and total calories is similar to controls.

The likely mechanism for this effect could be an interaction between homeostatic hypothalamic and reward centres. As discussed in the introduction, our current understanding is that hypothalamic centres 'sense' alterations in metabolites. This information is processed and leads to alterations in reward processing and increased 'incentive salience' to glucose consumption, promoting approach towards and consumption of glucose by enhancing reward (Berridge et al., 2009, Berthoud et al., 2012). ARC glucokinase may alter glucose-sensing leading to increase glucose consumption by altering the 'hedonic set-point' for glucose consumption (Egecioglu et al., 2011). In the absence of glucose, this is met by increased mixed diet consumption to achieve similar reward.

This effect could also be an independent homeostatic system by which glucose intake is regulated, such as those noted in invertebrates (Dus et al., 2011). Therefore, ARC glucokinase may alter the 'homeostatic set point' for glucose consumption. One potential flaw for this mechanism is that most homeostatic mechanisms tend to be negative feedback mechanisms. Reward mechanisms tend to have a positive feedback affect and enhance the consumption of a substance that is causing reward (Berthoud and Morrison, 2008). Therefore, it seems more likely that an interaction with reward pathways is mediating the effect of ARC glucokinase on increased glucose consumption via enhanced glucose-sensing, rather than a direct homeostatic effect on glucose appetite.

Another possibility is that suppression of food intake with glucose is enhanced in animals with increased ARC glucokinase activity. Manipulation of glucose levels alters feeding behaviour (Kanarek et al., 1996). This may explain the increased reduction in chow intake with normalisation of total caloric intake and bodyweight. However this does not explain the increased glucose intake and preference over chow and fructose in iARC-GKS animals.

4.4.3 Conclusion

In summary the results in this chapter show that glucose intake and glucose preference over other foods is specifically increased with increased ARC glucokinase activity. Possible mechanisms for this are via interaction with reward pathways, such as those in previous studies, or via a separate homeostatic system analogous to that recently described in invertebrates (Domingos et al., 2011, Ren et al., 2010, Dus et al., 2011). Nevertheless, this work demonstrates that alterations in hypothalamic metabolic pathways alter glucose intake. It is possible that increased drive for glucose may have led to increase food intake on single diets in Chapter 3. When this appetite for glucose is satisfied, food intake, caloric intake and body weight is similar to that of controls.

**5 Investigating the cellular mechanisms by which
arcuate glucokinase may mediate its effect on
appetite**

5.1 Introduction

Results from chapter 3 demonstrate that rats with increased ARC glucokinase activity have increased food intake and adiposity on a normal chow and high-energy diet. In chapter 4, increased ARC glucokinase activity in rats was shown to selectively increase glucose intake. The following chapter attempts to identify the cellular mechanisms involved in mediating these effects. Current evidence and techniques to investigate how glucokinase may alter neuronal depolarisation and ARC neuropeptide release are discussed.

5.1.1 Mechanisms by which ARC glucokinase may influence neuronal activity

5.1.1.1 *Energy-sensing enzymes involved in nutrient-sensing and alterations in hypothalamic neuronal activity*

As illustrated in figure 1.3 and discussed in chapter 1, energy-sensing enzymes have been implicated in nutrient-sensing, and provide an integrated model for the neuronal sensing of different metabolites, including glucose. Using this model, changes in the activity of enzymes leads to the formation of altered cellular metabolism intermediates. This can alter the flux of cellular metabolic reactions due to increased generation of precursor metabolites or alter enzyme activity. The net result of these changes in cellular biochemistry is to alter neuronal depolarisation. For example, increased generation of ATP via increased glucose entry and glycolytic flux (e.g. via glucokinase or hexokinase) results in a reduction of AMPK activity (Routh, 2010, Mountjoy and Rutter, 2007). Reduced AMPK activity has a number of effects including reduced inhibition of ACC (acetyl-CoA carboxylase) leading to changes in neuronal depolarization and energy homeostasis (Carling, 2004). Current thinking is that increased glucokinase activity would lead to a reduction of AMPK activity (Mountjoy and Rutter, 2007, Routh, 2010). This has not been conclusively demonstrated. If this is correct, a reduction in AMPK activity in the ARC should lead to reduced food intake, which is in contrast to our results in previous chapters (Andersson et al., 2004). The net effect of glucokinase on cellular biochemistry and neuronal activity is likely to be complex given the multiple interactions of metabolic pathways with each other (figure 1.3). Investigating alterations in expression and activity of energy-sensing enzymes, especially AMPK, which has a prominent role in energy sensing, is likely to provide important insights into the cellular biochemistry and mechanism of altered appetite in our model. Quantitative PCR can

be used to determine alterations in hypothalamic enzyme expression and provide a useful method to investigate this. Alterations in hypothalamic enzyme activity require more precise and sensitive biochemical enzyme activity assays. Enzyme activity assay for hypothalamic AMPK have been used previously to investigate changes in energy homeostasis in collaboration with Professor David Carling (Andersson et al., 2004). This assay can provide a suitable method to investigate the hypothalamic enzyme activity of AMPK in our model of altered ARC glucokinase activity.

5.1.1.2 Involvement of hypothalamic ATP-sensitive potassium channel in mediating the effect of glucokinase on neuronal activity and energy homeostasis

Glucose-induced excitation of glucose-sensitive hypothalamic neurons is linked to changes in activity of the ATP-sensitive potassium channels (K_{ATP}) (Ashford et al., 1990a). Glucokinase acts as a glucose sensor in hypothalamic neurons (Dunn-Meynell et al., 2002b, Kang et al., 2006). Presence of the K_{ATP} channel with glucokinase has been demonstrated in ARC neurons (Lynch et al., 2000, Van den Top et al., 2007). Therefore, glucokinase activity may be coupled with alterations in K_{ATP} channels with increased glucokinase activity resulting in closure of K_{ATP} channels in glucose-sensitive neurons (Mountjoy and Rutter, 2007). It is possible that K_{ATP} channels may mediate the effect of ARC glucokinase on food intake and glucose appetite. In keeping with this, alterations in K_{ATP} channels can lead to altered NPY expression, but not POMC expression, in response to glucose, suggesting that these channels play a prominent role in coupling effects of glucose to alterations in orexigenic NPY release (Park et al., 2011). Neurophysiological techniques, such as patch clamping, have been extensively used to determine alterations in neuronal activity with K_{ATP} channel inhibitors and activators (Ashford et al., 1990a, Ashford et al., 1990b, Spanswick et al., 1997). Given practical limitations and lack of a suitable neuronal tag in our model, neurophysiological techniques cannot be used. The use of pharmacological agents to activate and inhibit K_{ATP} channels in the hypothalamus of rats provides a strategy to investigate this (Zhang et al., 2004, Chan et al., 2007). Although this may not provide direct neurophysiological evidence, similar phenotypes produced by K_{ATP} channel inhibition to that of increased ARC glucokinase activity would support their combined involvement on energy homeostasis. Feeding study protocols similar to those used in chapter 2 and 3 can be adopted in iARC cannulated rats to investigate this.

Modulation of ARC K_{ATP} channel activity using stereotactically delivered pharmacological agents

The K_{ATP} channel consists of an octameric complex of four pore forming inwardly rectifying potassium channels (Kir) subunit and four regulatory sulphonylurea receptor (SUR) subunits (Dabrowski et al., 2002, Akrouh et al., 2009).

The Kir subunit acts as the channel pore. In most tissues, including the pancreas and brain, the pore consists of the Kir6.2 subunit (Dabrowski et al., 2002). In smooth muscles Kir6.1 is mainly expressed.

Kir subunits associate with different types of SUR. The SUR is an ATP binding cassette protein, which uses energy from ATP hydrolysis to mediate functions. It acts as an ion channel regulator and regulates the pore forming Kir subunits. The mechanism of this regulation is not fully understood. It endows channel with sensitivity to drugs, including sulphonylureas and magnesium nucleotides. Two main sub-types of SUR have been characterised (Hambrock et al., 2002). SUR1 is expressed in pancreatic beta cells and neurones. SUR2 is expressed in muscle, with SUR2A in skeletal muscle and SUR2B in smooth muscle.

The SUR subunits confer sensitivity to sulphonylureas, which inhibits and close K_{ATP} channels. Most sulphonylureas, used as hypoglycaemic's in the treatment of diabetes, show a high affinity to SUR1 and a low affinity to SUR2 (Nagashima et al., 2004). There are two binding sites for sulphonylurea drugs on SUR1, one a tolbutamide-binding site and the other a benzamide-binding site (Nagashima et al., 2004). Glibenclamide binds to both sites and this may contribute to its increased half-life (Nagashima et al., 2004). At low doses glibenclamide is highly-specific to Kir6.2/SUR1 K_{ATP} channels, the K_{ATP} channel expressed in neuronal tissue. Stereotactic delivery of glibenclamide has been previously used to deliver this agent to specific brain regions using low doses (Zhang et al., 2004, Chan et al., 2007). Therefore, given its previous stereotactic use with dosing protocols already established, specificity to Kir6.2/SUR1 and long duration of action, glibenclamide is the agent of choice to stereotactically inhibit K_{ATP} channels in the ARC.

Potassium channel openers also interact with the SUR to modulate K_{ATP} channel activity resulting in opening of the channel. A number of different potassium channel openers with different sensitivities and specificities have been described. Diazoxide, is the best described activator of Kir6.2/SUR1 channels, which are expressed in neuronal tissue (Dabrowski et al., 2002). It also has stimulatory effects on Kir6.2/SUR2b expressed in smooth muscle and weak stimulatory effects on Kir6.2/SUR2a expressed in skeletal muscle. More selective analogues of diazoxide are being developed however none have been used to alter neuronal activation, since they have mainly been tested in islet cells (Hansen, 2006). Diazoxide has been stereotactically delivered at low doses (Chan et al., 2007). Given its previous stereotactic use with established dosing protocols and the lack of a specific neuronal Kir6.2/SUR1 potassium channel opener, diazoxide is the agent of choice as the potassium channel opener.

5.1.2 Neurotransmitters likely to be involved in mediating the effects of ARC glucokinase in energy homeostasis

As mentioned in chapter 1.3.2, ARC neuropeptides NPY, AgRP, POMC and CART play a key role in energy homeostasis (Konner et al., 2009, Cone et al., 2001). Therefore, ARC glucokinase activity may lead to changes in ARC neuropeptide expression and release, resulting in changes to energy homeostasis. Increased NPY expression has been shown to occur in response to glucose in Kir6.2 KO mice, where K_{ATP} channels and therefore glucose-sensing was disrupted (Park et al., 2011, Ashford et al., 1990a). Alterations in glucose-sensing have been shown to change neurotransmitter release from glucose-sensing neurons (Routh, 2010). Therefore, investigating hypothalamic neurotransmitter expression, neurotransmitter release or neurophysiological activity of specific neurons may provide insights into the mechanisms of altered energy homeostasis in our rat model.

Quantitative PCR is a well-established method that can be used on hypothalamic samples to investigate neuropeptide expression. Depolarisation or neurotransmitter release in response to glucose can be assessed using ex-vivo techniques such as patch-clamp or hypothalamic explant incubations. Neurophysiological techniques such as patch-clamp have been used extensively to determine alterations in depolarisation of neuronal populations in response to glucose (Ashford et al., 1990a, Routh, 2010). As mentioned earlier,

neurophysiological approaches are not technically or practically feasible at present. Parton, et al used an alternative technique which relied on incubating freshly dissected hypothalamic slices in variable concentrations of glucose dissolved in artificial CSF (Parton et al., 2007b). This allowed neurotransmitter release in response to glucose to be assessed by collecting the artificial CSF after a designated incubation period and performing an assay for the neurotransmitter. This technique has been used previously in this lab (Abbott et al., 2003). Given this, and the availability of a suitable in-house radioimmunoassay to detect NPY, this technique can be modified to investigate changes in hypothalamic NPY and α MSH release in response to glucose.

As discussed above, several possible approaches can be taken to investigate the cellular mechanisms of glucokinase's effects in ARC neurons. In the remaining chapter I will present results from studies conducted to investigate this.

5.2 Hypothesis and Aims

5.2.1 Hypothesis

Altered ARC energy-sensing enzyme activity and K_{ATP} channel activation may account for differences in appetite regulation of rats with increased ARC glucokinase activity. Altered ARC K_{ATP} channel activation leads to similar effects on food intake and glucose appetite as that seen in rats with increased ARC glucokinase activity, supporting their involvement in mediating the effects of ARC glucokinase on energy homeostasis. These effects lead to altered ARC neuropeptide release.

5.2.2 Aims and Objectives

To investigate this, I will:

6. Investigate the mechanisms by which ARC glucokinase may alter neuronal activity.
 - a. Determine whether hypothalamic energy-sensing enzyme expression (AMPK, ACC, FAS) is altered by increased ARC glucokinase activity using quantitative PCR.
 - b. Reconfirm that glucokinase expression is altered in the hypothalamus of iARC-GKS rats, using quantitative PCR.
 - c. Specifically determine whether hypothalamic AMPK activity is altered by increased ARC glucokinase activity, using a specific and sensitive biochemical assay.
 - d. Determine the effect of altering ARC K_{ATP} channel activation on food intake and glucose appetite, by stereotactically delivering K_{ATP} channel activators and inhibitors to the ARC of rats.
7. Investigate altered neurotransmitter release in animals with increased ARC glucokinase activity.

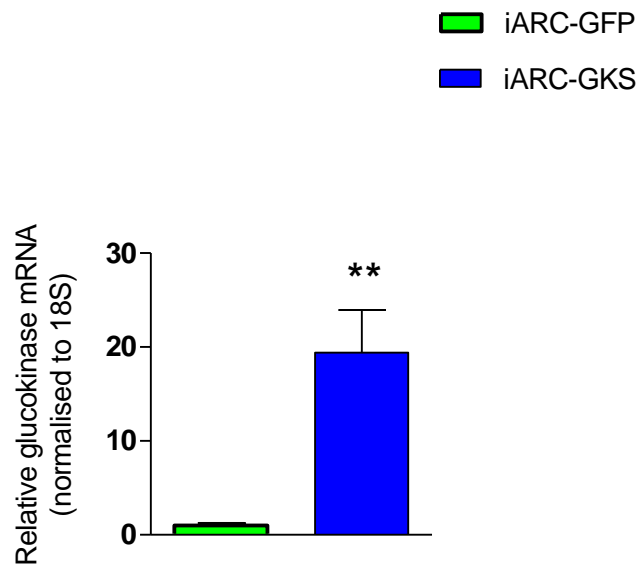
- a. Determine whether hypothalamic NPY, POMC, AgRP and CART neuropeptide expression is altered by increased ARC glucokinase activity using quantitative PCR.
- b. Determine the effect of increased arcuate glucokinase activity on glucose stimulated NPY-release from hypothalamic explants from iARC-GKS and iARC-GFP, incubated in varying concentrations of glucose.

5.3 Results

5.3.1 Effect of increasing arcuate glucokinase activity on enzyme expression in chow-fed animals

There was a significant 19.3 fold increase in relative hypothalamic glucokinase mRNA expression (iARC-GFP 1.00 \pm 0.18 arbitrary units vs. iARC-GKS 19.4 \pm 4.54 arbitrary units, n=9-12, p<0.01) (figure 5.1a). There was a significant 1.5 fold increase in relative hypothalamic FAS expression (iARC-GFP 1.00 \pm 0.125 arbitrary units vs. iARC-GKS 1.50 \pm 0.17 arbitrary units, n=9-12, p<0.01) (figure 5.1c) in the iARC-GKS group, as compared to the iARC-GFP group. Expression of other energy sensing enzymes was not altered between the groups.

a



b

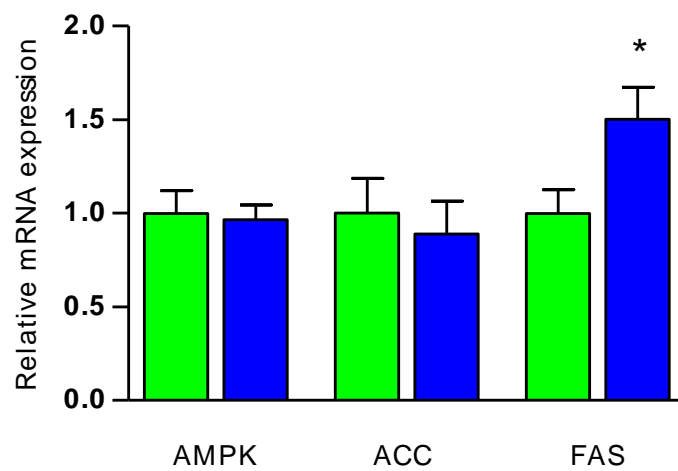


Figure 5.1 Effect of increased arcuate glucokinase activity on energy-sensing enzymes (a) Relative hypothalamic glucokinase mRNA expression in iARC-GFP and iARC-GKS rats. (b) Relative hypothalamic AMPK, ACC and FAS expression in iARC-GFP and iARC-GKS rats on normal chow diet. Data are expressed as mean +/- SEM for all groups, n=9-12. Statistical significance was analysed by student's t test: *=p<0.05.

5.3.2 Effect of increasing arcuate glucokinase activity on hypothalamic AMPK activity

There was no change in hypothalamic AMPK activity between the two groups (iARC-GFP 100 \pm 8.18 % control vs. iARC-GKS 110 \pm 8.18 % control, n=10) (figure 5.2).

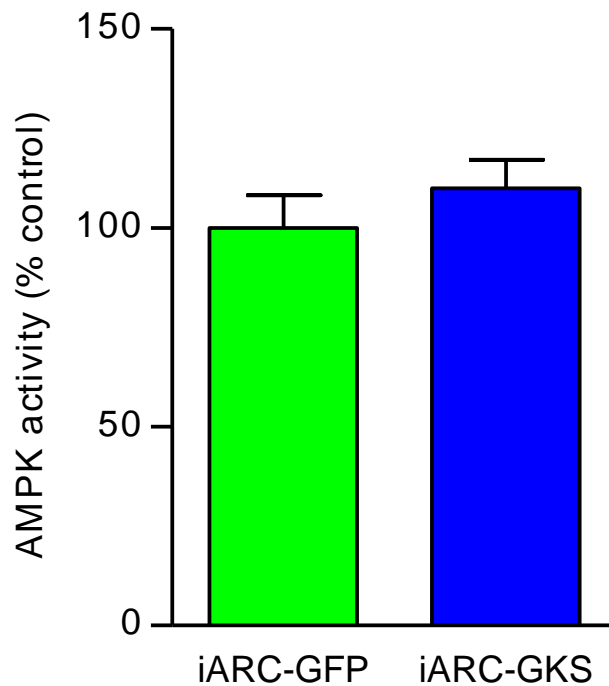


Figure 5.2 Effect of increased arcuate glucokinase activity on hypothalamic AMPK activity. Hypothalamic AMPK activity measured using a SAMS peptide assay on hypothalami from iARC-GFP and iARC-GKS rats on normal chow diet. Data are expressed as mean \pm SEM for all groups, n=10. Statistical significance was analysed by student's t test.

5.3.3 Effect of inhibiting K_{ATP} channels in the arcuate nucleus on food intake, glucose intake and glucose preference

5.3.3.1 *Effect on food intake*

ARC K_{ATP} channels were inhibited acutely using glibenclamide, injected via cannulas stereotactically implanted into the ARC. Acute arcuate K_{ATP} channel inhibition increased food intake at four hours after injection, as compared to vehicle injected controls using a cross-over study protocol, where each animal acted as their own control (Glibenclamide, 2.22±0.77 fold change relative to control; n=12, p<0.05) (figure 5.3 a). This increase in food intake was not significant at later time points (At 24 hours: Glibenclamide, 1.28±0.27 fold change relative to control; n=12) (figure 5.3 b).

5.3.3.2 *Effect on glucose intake*

ARC K_{ATP} channels were inhibited acutely using glibenclamide, injected via cannulas stereotactically implanted into the ARC. Acute K_{ATP} channel inhibition increased glucose intake at four hours after injection, as compared to vehicle injected controls using a cross-over study protocol (Glibenclamide, 2.63±0.99 fold change relative to control; n=11, p<0.05) (figure 5.4 a). There was a significant increase in glucose intake at 8 hours, however this was not significant at 24hours (At 24 hours: Glibenclamide, 1.26±0.28 fold change relative to control; n=11) (figure 5.4 b and c).

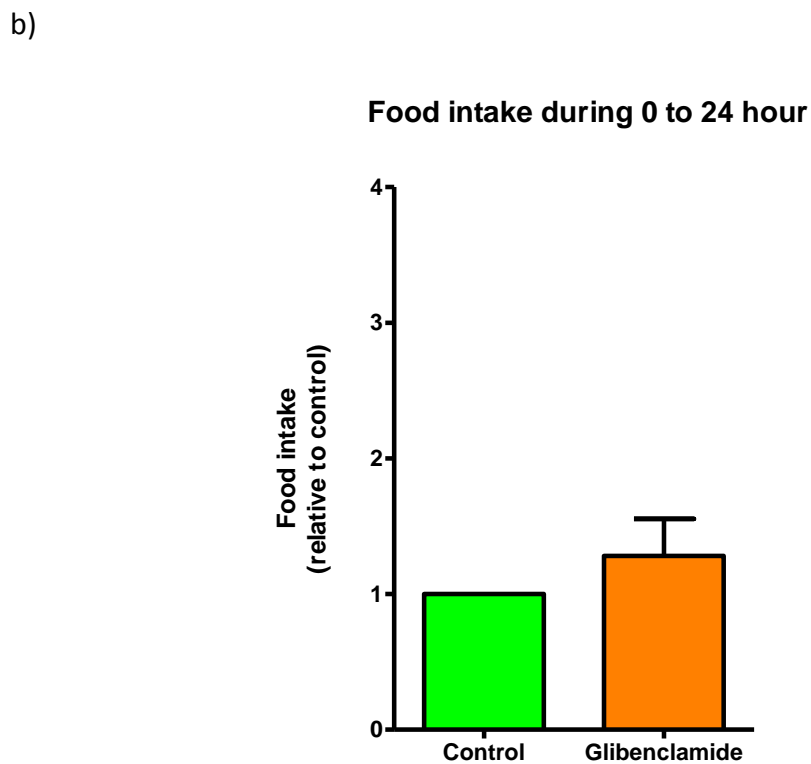
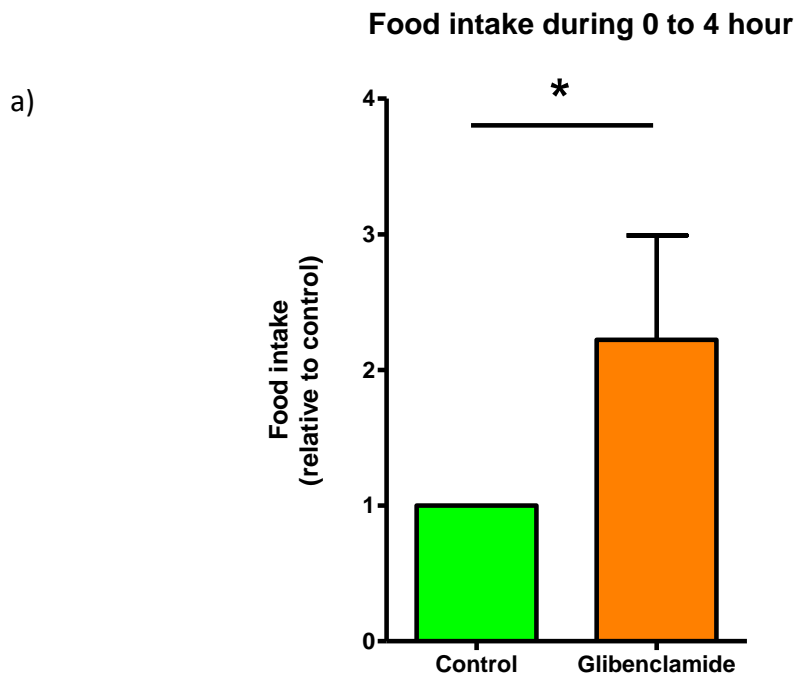
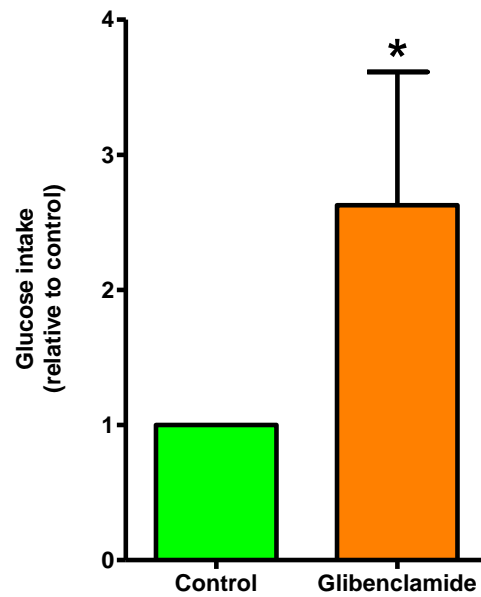


Figure 5.3 Effect of inhibiting arcuate nucleus K_{ATP} channels on food intake. Normal chow intake (a) four hours (b) twenty-four hours after ARC K_{ATP} channel inhibition using stereotactic injection of glibenclamide as compared to vehicle injected controls during a crossover study. Data are expressed as mean \pm SEM fold change relative to controls, $n=12$. Statistical significance was analysed by student's t test: $*=p<0.05$.

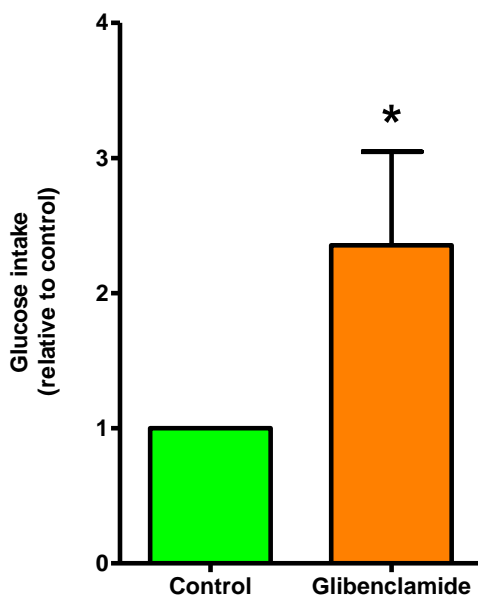
a)

Glucose intake during 0 to 4 hour



b)

Glucose intake during 0 to 8 hour



c)

Glucose intake during 0 to 4 hour

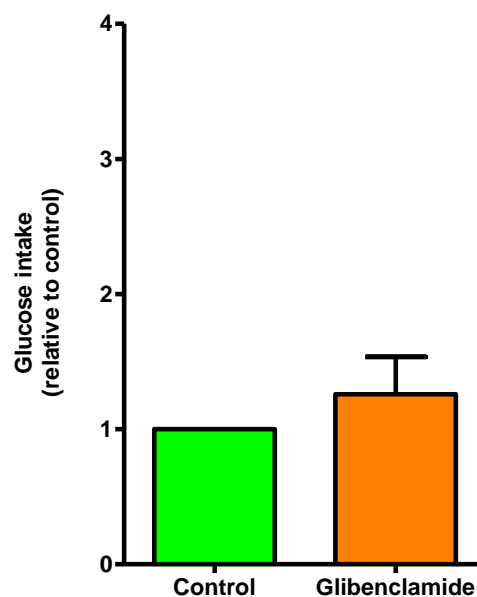


Figure 5.4 Effect of inhibiting arcuate nucleus K_{ATP} channels on glucose intake. (a) 2% w/v glucose intake (a) four hours, (b) eight hours and (c) twenty-four hours after ARC K_{ATP} channel inhibition using stereotactic injection of glibenclamide as compared to vehicle injected controls during a crossover study. Data are expressed as mean \pm SEM fold change relative to control, $n=11$. Statistical significance was analysed by student's t test: $*=p<0.05$.

5.3.3.3 *Effect on food and glucose intake when normal chow and 2% w/v glucose were given ad libitum*

When normal chow food and 2% w/v glucose were given together during a cross-over study, acute arcuate K_{ATP} channel inhibition resulted in similar food intake but increased glucose intake at four hours after injection, as compared to vehicle injected controls (glucose intake: Glibenclamide, 1.93 ± 0.57 fold change relative to control; food intake: Glibenclamide, 0.97 ± 0.19 fold change relative to control, $n=10$, $p < 0.05$ for glucose intake) (figure 5.5 a & b). Glucose intake and food intake were similar at twenty-four hours (figure 5.5 c & d)

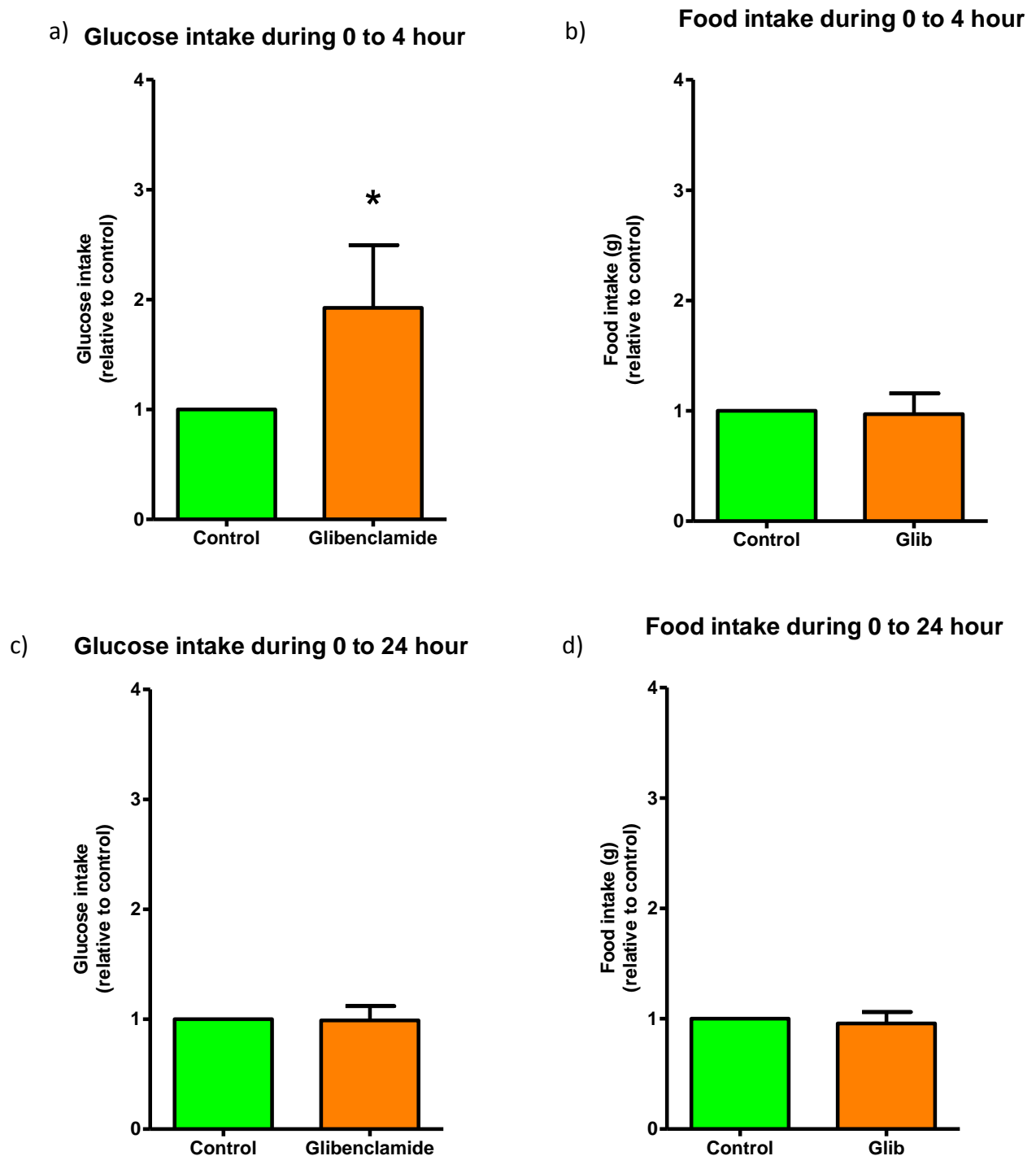


Figure 5.5 Effect of inhibiting arcuate nucleus K_{ATP} channels on glucose appetite. (a) 2% w/v glucose intake and (b) food intake four hours after ARC K_{ATP} channel inhibition using stereotactic injection of glibenclamide as compared to vehicle injected controls during a crossover study. (c) Cumulative 2% w/v glucose intake and (d) food intake twenty-four hours after ARC K_{ATP} channel inhibition using stereotactic injection of glibenclamide as compared to vehicle injected controls during a crossover study. Data are expressed as mean \pm SEM relative to control, $n=11$. Statistical significance was analysed by student's t test: $*=p<0.05$.

5.3.4 Effect of activating ATP sensitive potassium channels in the arcuate nucleus on food intake, glucose intake and glucose preference

5.3.4.1 *Effect on food intake*

ARC K_{ATP} channels were activated acutely using diazoxide, injected via cannulas stereotactically implanted into the ARC during a cross-over study. Acute arcuate K_{ATP} channel activation decreased food intake at thirty minutes after injection, as compared to vehicle injected controls (Diazoxide, 0.79 ± 0.04 fold change relative to control; $n=9$, $p < 0.05$) (figure 5.6 a). There was a no significant decrease in food intake at 24 hours (Diazoxide, 0.99 ± 0.18 fold change relative to control; $n=9$) (figure 5.6 b).

5.3.4.2 *Effect on glucose intake*

Acute arcuate K_{ATP} channel activation decreased glucose intake at two and four hours after injection, as compared to vehicle injected controls (At 2 hours: Diazoxide, 0.74 ± 0.08 fold change relative to control; $n=9$, $p < 0.05$) (figure 5.7 a & b). This effect was not significant at 24 hours (Diazoxide, 0.99 ± 0.14 fold change relative to control; $n=9$) (figure 5.7 c).

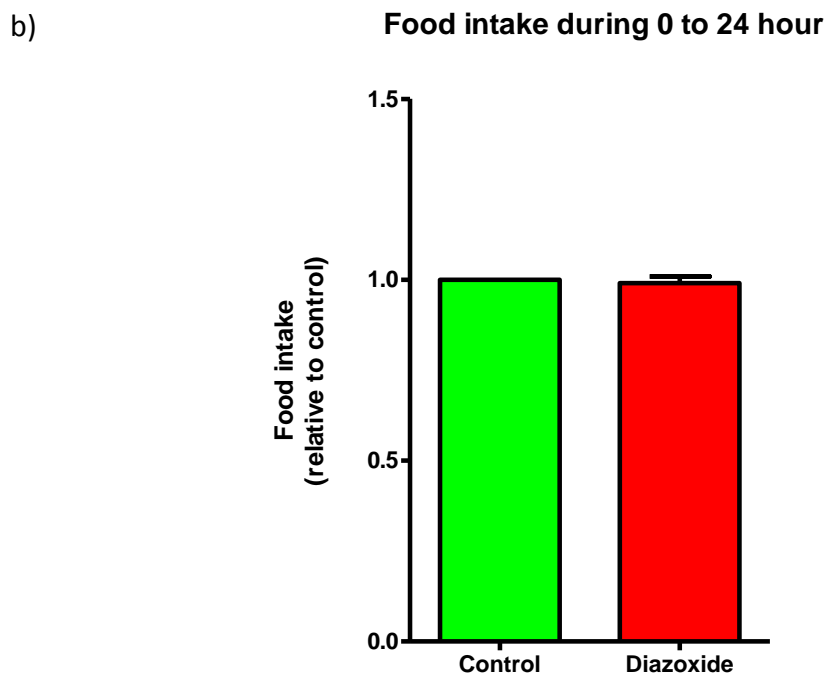
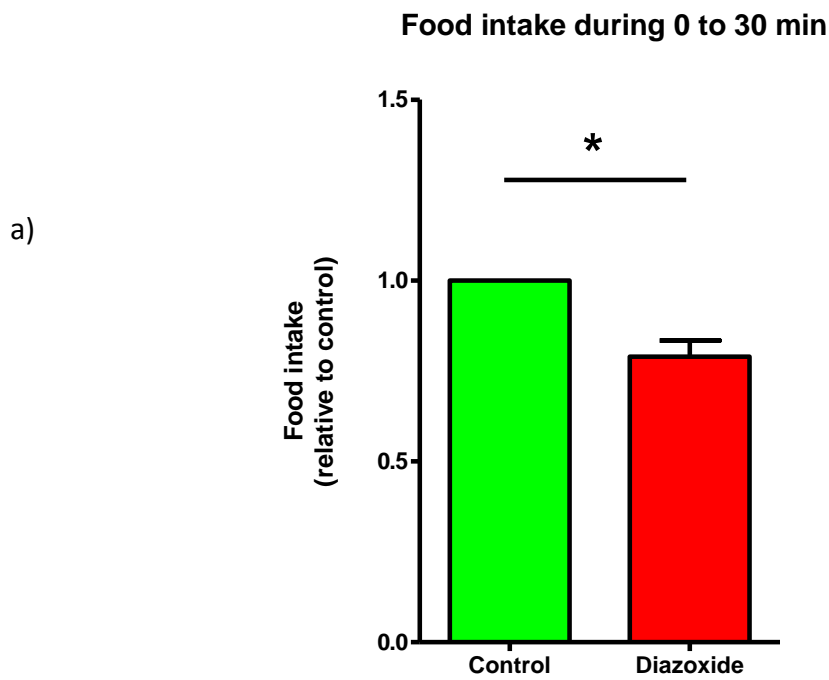
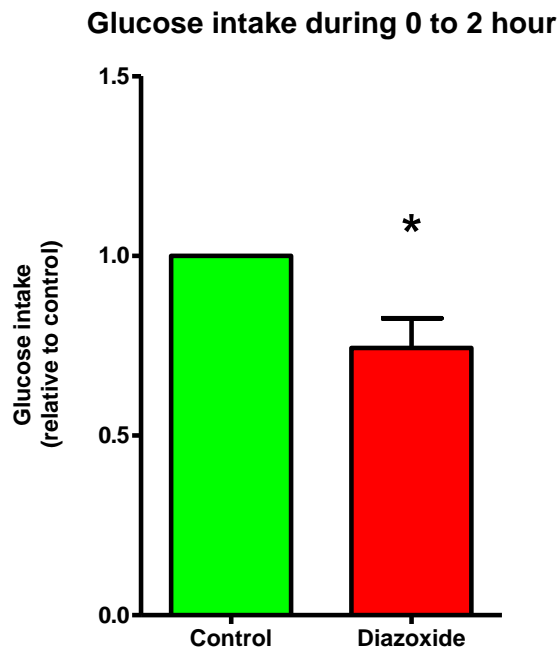


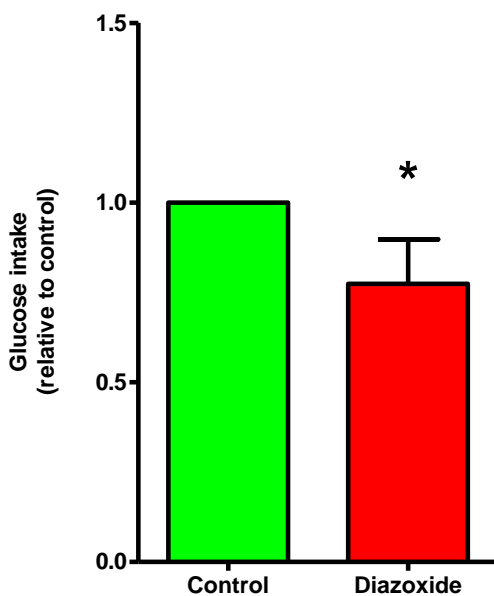
Figure 5.6 Effect of activating arcuate nucleus K_{ATP} channels on food intake. (a) Normal chow intake thirty minutes and (b) twenty-four hours after ARC K_{ATP} channel activation using stereotactic injection of diazoxide as compared to vehicle injected controls during a crossover study. Data are expressed as mean \pm SEM fold change relative to control, $n=10$. Statistical significance was analysed by student's t test: $*=p<0.05$.

a)



b)

Glucose intake during 0 to 4 hour



c)

Glucose intake during 0 to 24 hour

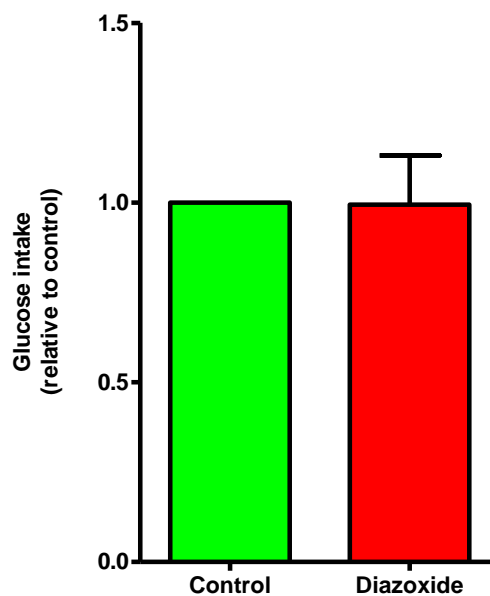


Figure 5.7 Effect of activating arcuate nucleus K_{ATP} channels on glucose intake. 2% w/v glucose intake (a) two hours, (b) eight hours and (c) twenty-four hours after ARC K_{ATP} channel activation using stereotactic injection of diazoxide as compared to vehicle injected controls during a crossover study. Data are expressed as mean \pm SEM fold change relative to control, $n=9$. Statistical significance was analysed by student's t test: $*=p<0.05$.

5.3.4.3 Effect on food and glucose intake when normal chow and 2% w/v glucose were given ad libitum

When normal chow food and 2% w/v glucose were given together, acute arcuate K_{ATP} channel activation resulted in similar food intake but decreased glucose intake at two hours after injection, as compared to vehicle injected controls (glucose intake at two hours: Diazoxide, 0.79 ± 0.11 fold change relative to control; food intake at thirty minutes: Diazoxide, 1.28 ± 0.22 fold change relative to control; food intake at two hours: Diazoxide, 1.09 ± 0.07 fold change relative to control, $n=9$, $p < 0.05$ for glucose intake) (figure 5.8 a, b & c). Glucose intake and food intake were similar at later time points (figure 5.9 a & b)

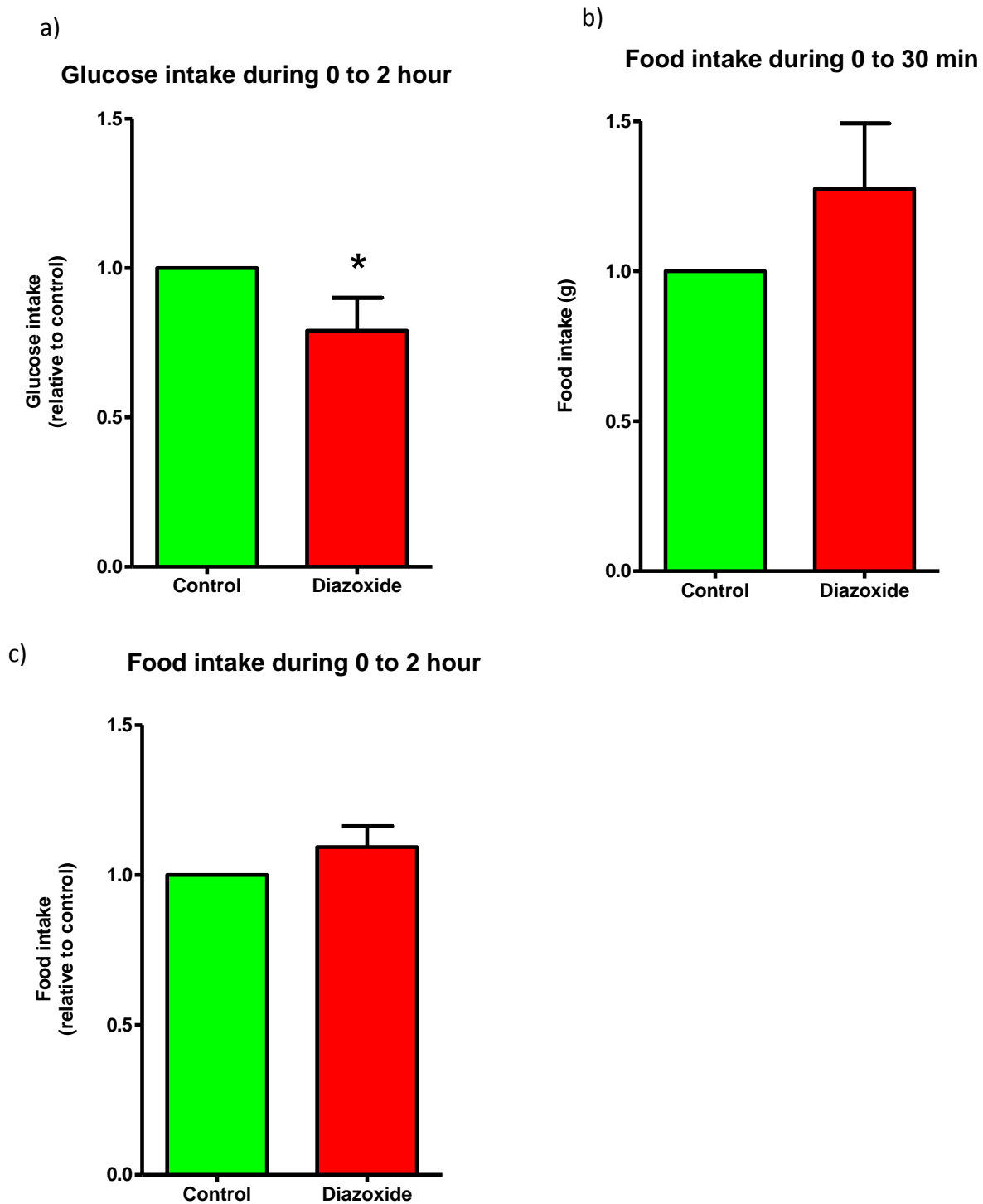
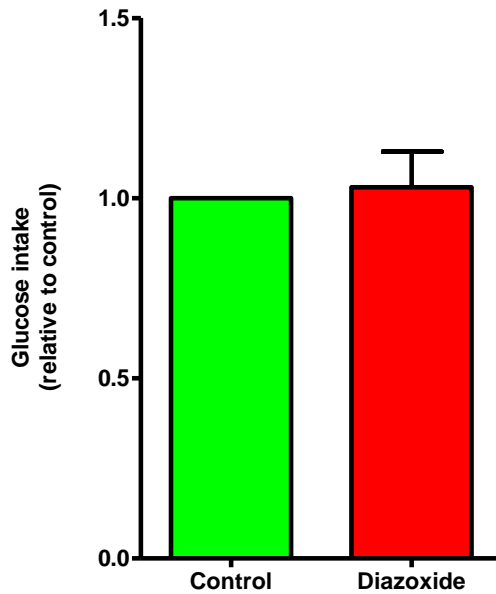


Figure 5.8 Effect of activating arcuate nucleus K_{ATP} channels on glucose appetite. (a) 2% w/v glucose intake two hours after and food intake (b) thirty minutes and (c) two hours after ARC K_{ATP} channel activation using stereotactic injection of diazoxide as compared to vehicle injected controls during a crossover study. Data are expressed as mean \pm SEM fold change relative to control, $n=9$. Statistical significance was analysed by student's t test: $*=p<0.05$.

a) **Glucose intake during 0 to 24 hour**



b) **Food intake during 0 to 24 hour**

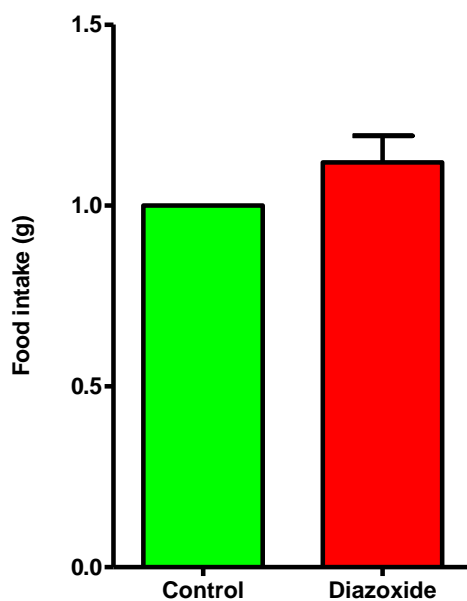


Figure 5.9 Effect of activating arcuate nucleus K_{ATP} channels on glucose appetite. (a) Cumulative glucose intake and (b) cumulative food intake twenty-four hours after ARC K_{ATP} channel activation using stereotactic injection of diazoxide as compared to vehicle injected controls during a crossover study. Data are expressed as mean \pm SEM fold change relative to control, $n=9$. Statistical significance was analysed by student's t test: $*=p<0.05$.

5.3.5 Effect of increasing arcuate glucokinase activity on hypothalamic neuropeptide expression in chow-fed animals

Relative hypothalamic expression of NPY, POMC and CART was similar in both groups (figure 5.10).

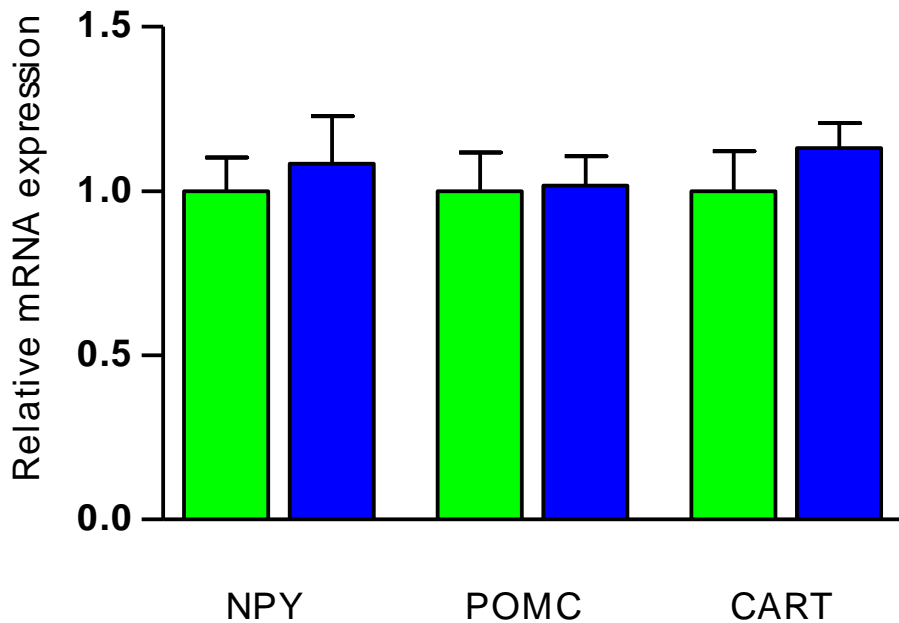


Figure 5.10 Effect of increased arcuate glucokinase activity on energy-sensing enzymes. Relative hypothalamic NPY, POMC and CART expression in iARC-GFP and iARC-GKS rats on normal chow diet. Data are expressed as mean \pm SEM for all groups, $n=9-12$. Statistical significance was analysed by student's t test: $*=p<0.05$.

5.3.6 Effect of increased arcuate glucokinase activity on glucose-stimulated NPY-release from hypothalamic neurons

NPY release from hypothalamic explant slices was similar between the two groups at 3 mM glucose (iARC-GFP: 13.75 ± 2.55 fmol/hypothalamic slice; iARC-GKS: 13.57 ± 2.31 fmol/hypothalamic slice) (figure 5.11). NPY release from hypothalamic explant slices was increased in iARC-GKS rats versus controls at both 8mM and 15mM glucose (For 8mM glucose: iARC-GFP: 6.91 ± 0.53 fmol/hypothalamic slice; iARC-GKS: 13.74 ± 2.88 fmol/hypothalamic slice; for 15mM glucose: iARC-GFP: 6.86 ± 1.07 fmol/hypothalamic slice; iARC-GKS: 12.29 ± 1.95 fmol/hypothalamic slice) (figure 5.11).

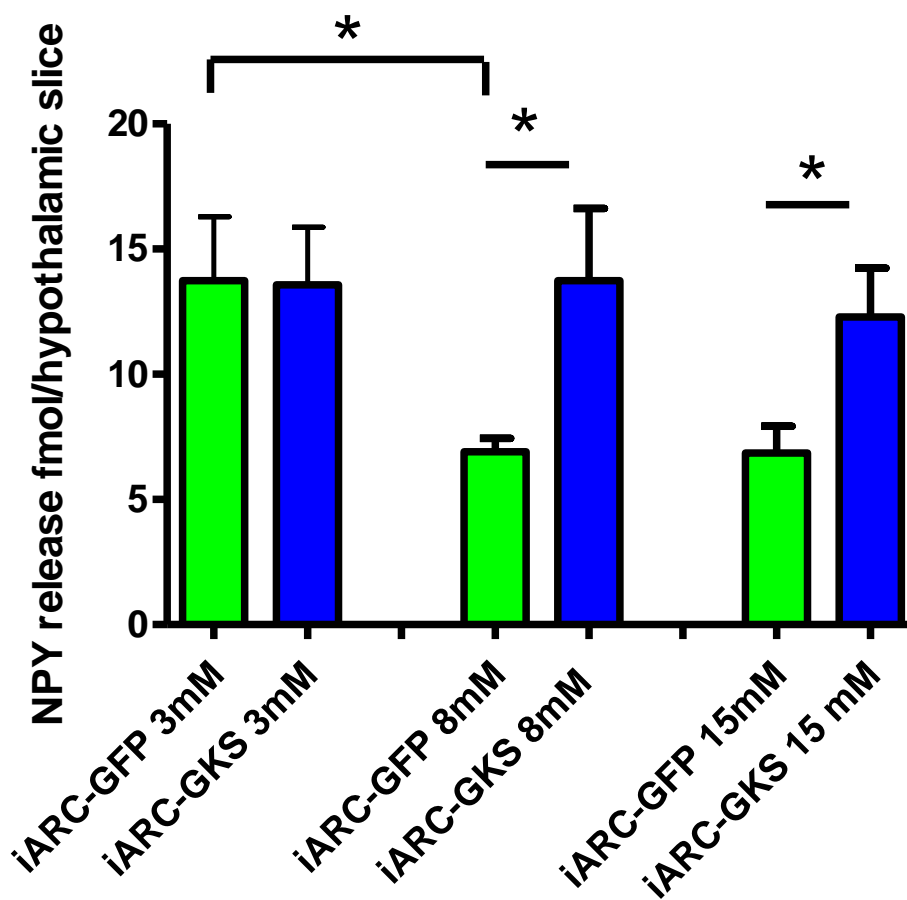


Figure 5.11 Effect of increased arcuate glucokinase activity on glucose-stimulated NPY-release from hypothalamic neurons. NPY release from hypothalamic explant slices in response to changes in artificial CSF glucose levels. Data are expressed as mean \pm SEM for all groups, $n=7-8$. Statistical significance was analysed by one-way ANOVA followed by post-hoc Holms-Sidak test: $*=p<0.05$.

5.3.7 Effect of increased arcuate glucokinase activity on glucose-stimulated α -MSH release from hypothalamic neurons

α -MSH release from hypothalamic explant slices was similar between the two groups at 3 mM, 8mM and 15mM glucose (For 3mM glucose: iARC-GFP: 9.04 ± 1.08 fmol/hypothalamic slice; iARC-GKS: 12.54 ± 3.49 fmol/hypothalamic slice; for 8mM glucose: iARC-GFP: 8.03 ± 1.18 fmol/hypothalamic slice; iARC-GKS: 9.60 ± 2.75 fmol/hypothalamic slice; for 15mM glucose: iARC-GFP: 14.97 ± 3.62 fmol/hypothalamic slice; iARC-GKS: 14.41 ± 2.02 fmol/hypothalamic slice) (figure 5.12).

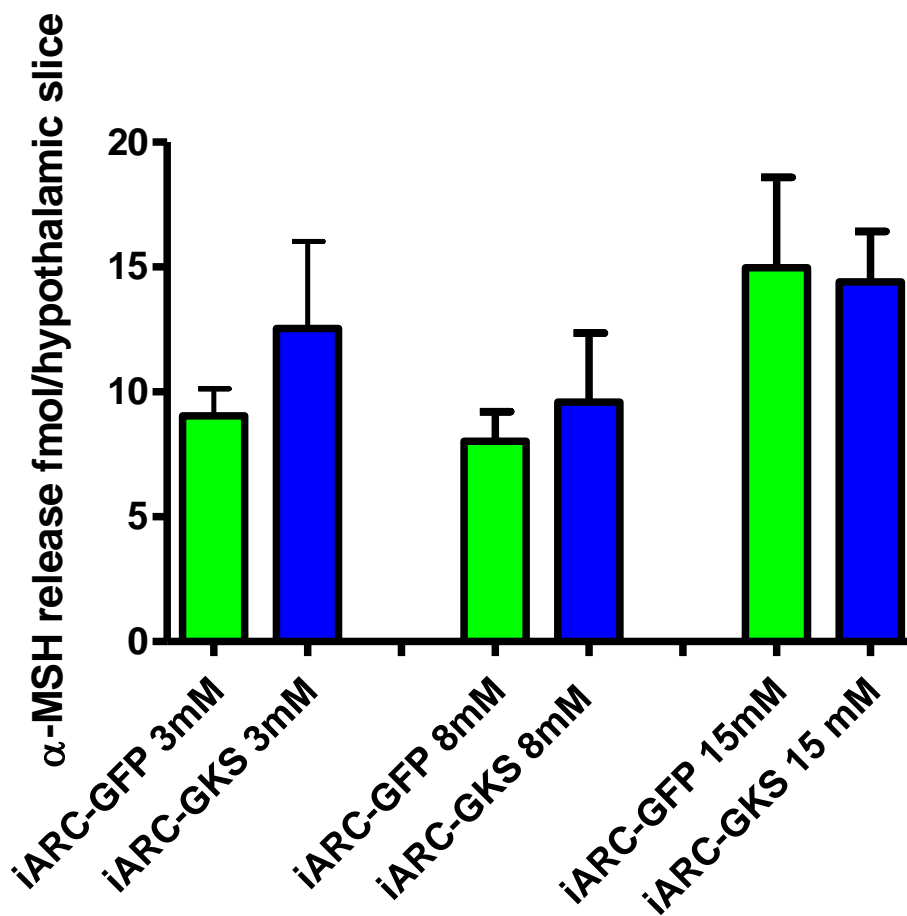


Figure 5.12 Effect of increased arcuate glucokinase activity on glucose-stimulated α -MSH release from hypothalamic neurons. α -MSH release from hypothalamic explant slices in response to changes in artificial CSF glucose levels. Data are expressed as mean \pm SEM for all groups, $n=7-8$. Statistical significance was analysed by student's t test against corresponding control values: $*=p<0.05$.

5.4 Discussion

5.4.1 Changes in hypothalamic energy-sensing enzymes with increased ARC glucokinase activity

In keeping with the results of increased ARC glucokinase activity and in-situ hybridisation in chapter 3, results from quantitative PCR demonstrated significantly increased hypothalamic glucokinase activity. Results from qPCR do not reveal any differences in any of the other energy sensing enzymes, except FAS. Changes in activity of hypothalamic enzymes due to altered biochemistry may not always be reflected by gene expression. Therefore AMPK activity assays were undertaken. No difference in AMPK activity was found between the two groups. This is in contrast to previous observations and theories with respect to AMPK activity and glucose-sensing by glucokinase (Mountjoy and Rutter, 2007, Claret et al., 2007). It is possible that ARC glucokinase does not reduce AMPK activity as previously suggested or that this occurs only in a small proportion of neurons. Therefore, changes in AMPK are unlikely to be of significance in our model of increased ARC glucokinase activity. Our phenotypic findings of increased food intake and glucose intake with increased ARC glucokinase activity are also in keeping with a non-AMPK mediated effect on neuronal activity and energy homeostasis.

The slight increase in FAS expression may provide a possible explanation for altered neuronal depolarization and an orexigenic affect in our rat model. FAS is an enzyme that catalyses the synthesis of LCFA-CoA from acetyl-CoA and malonyl-CoA (Loftus et al., 2000). The accumulation of acetyl-CoA and malonyl-CoA following increase glycolytic flux in iARC-GKS animals may result in upregulation of FAS expression the ARC (figure 1.3). This increase in FAS expression may increase food intake by effecting neuronal nutrient sensing and activity (Loftus et al., 2000). This mechanism also provides a possible explanation for the similar insulin sensitivity, despite alterations in adiposity, between our model and controls. Increased hypothalamic LCFA-CoA reduces hepatic gluconeogenesis, improving insulin sensitivity (Lam et al., 2005b). One caveat with this mechanism is that an up-regulation in FAS and increase glycolytic flux should increase fatty acid production and lipid accumulation in the cytoplasm of hypothalamic neurons. Lipid administration in the VMH reduces feeding and therefore increased lipid accumulation in the hypothalamus should have an anorexigenic effect (Lam et al., 2005c). Therefore, it is unlikely that increased FAS

expression is the dominant mechanism of altered ARC neuronal activity and energy homeostasis in our model given the slight increase and variable consequences that may generate from this.

5.4.2 K_{ATP} channels play a part in transducing the effects of ARC glucokinase

The involvement of K_{ATP} channels in mediating effect of ARC glucokinase on neuronal activity and energy homeostasis was investigated by injecting a pharmacological inhibitor (glibenclamide) or activator (diazoxide) into the ARC. Food intake and glucose intake were significantly increased four hours after injection with glibenclamide. Furthermore, when chow diet and 2% w/v the glucose were provided, only glucose intake was increased in glibenclamide injected rats, suggesting a specific intake on increase in glucose appetite. Conversely, injection of diazoxide into the ARC inhibited food intake and glucose intake when each was available separately. However, only glucose intake was inhibited when both were available. Hence, both alterations in glucokinase activity and K_{ATP} channels have an effect on glucose appetite in a manner that is consistent with previous suggestions. Although this work does not provide direct neurophysiological evidence, these results and those from previous studies support the possibility that K_{ATP} channels play a part in transducing the effects of glucokinase in the ARC (Routh, 2010).

Previous investigations on the effects of K_{ATP} channel inhibition on food intake have been conducted in rats cannulated in the lateral hypothalamus (Plum et al., 2006). The results suggested that there was no alteration in feeding behaviour in rats treated with tolbutamide K_{ATP} channel inhibitor. These rats were anaesthetised daily prior to injection of the medication. This is likely to severely affect appetite. Hence the results suggested in the study are confounded by limitations of the technique.

5.4.3 Changes in neuropeptide expression and NPY release with increased ARC glucokinase activity

Our phenotype suggests that increasing ARC glucokinase in rats has an orexigenic effect resulting in increased food intake and body weight. Subsets of orexigenic NPY/ AgRP and anorexigenic POMC/ CART neurons in the ARC are glucose-sensing neurons and express glucokinase. Therefore, changes in NPY and POMC/ α -MSH expression may play a role in the altered feeding behaviour of rat model. However, qPCR on hypothalami from animals killed

after overnight feeding, reveals similar NPY, POMC and CART expression to controls. There may be several reasons why a change in expression was not noted in this study.

Firstly, the mRNA extracted is from whole hypothalamus, as opposed to the ARC. Although POMC is only expressed in the ARC and NPY is predominantly expressed in the ARC, gene expression quantified by qPCR is expressed as a ratio to a control gene in the whole hypothalamus. It is possible that a subtle difference could be masked by inaccuracies caused due to this. Micro-punches of the ARC may allow more precise dissection of the individual nuclei but also carry the risk of introducing inaccuracies from punching incorrect areas and contamination from other nuclei. Laser capture microdissection can improve quality of dissection but requires significant technical expertise and specialised equipment. Single cell qPCR may allow detection of gene expression in specific neuronal subtypes, e.g. NPY/CART or POMC/ α -MSH, but the neurons of interest need to be tagged and considerable expertise is needed to select and extract RNA from the individual neuron. Secondly, the feeding status and time at which the animals are killed is likely to influence differences in anorexic or orexigenic neuropeptide signalling. NPY or POMC/ α -MSH signalling may be different in response to changes in glucose or other metabolites, such as leptin. Changes in expression of neuropeptides in the hypothalamus may mirror these transient alterations in neuropeptide release in response to small and brief fluctuations in glucose. The stimulus from glucose change may only lead to transient alterations in neuropeptide expression.

As discussed previously, electrophysiological studies on ARC neurons and hypothalamic explant incubation studies may provide further insight into neuropeptide release. Results from ex-vivo hypothalamic explant suggest that NPY release is increased in iARC-GKS rats as compared to controls, especially at higher aCSF glucose levels. α -MSH release is similar between iARC-GKS rats and controls. This may explain the increased orexigenic drive in these animals and could also explain increased drive to consume glucose. One potential caveat with this work is that glucose level used in our study was 2, 8 and 15 mmol per litre. These levels are the same as in previous published work using the same technique (Parton et al., 2007b). CSF glucose is normally half of that of plasma (Routh, 2002, de Vries et al., 2003). Therefore the glucose levels used here could be higher than what would be expected in vivo. However, if the neurons in the ARC lack a complete blood-brain barrier, brain glucose levels may reach plasma glucose levels in these neurons. Nevertheless, this ex-vivo

technique illustrates the principle of altered hypothalamic neurotransmitter release in response to glucose in our rat model. These results are in line with the co-localisation of K_{ATP} channels and glucokinase in NPY neurons and augmented NPY release in response to glucose infusions in mice with disrupted K_{ATP} channels (Lynch et al., 2000, Van den Top et al., 2007, Park et al., 2011). Furthermore, increase in NPY release has also been demonstrated to increase carbohydrate craving in preference to other foods in line with our work (Morley et al., 1987). Our phenotypic and explant results are in accord with these links between K_{ATP} channels and glucokinase in NPY neurons and NPY and food selectivity.

5.4.4 Conclusion

Results from this chapter suggest that ARC glucokinase inhibits K_{ATP} channels. This may cause membrane depolarisation and neurotransmitter release in the ARC. Results from our phenotype, suggest that ARC glucokinase may have an effect on increasing orexigenic NPY release in response to glucose. Altered NPY release may account for the increased food intake and glucose appetite in our model. These suggestions linking ARC glucokinase with K_{ATP} channel inhibition, NPY release and increased glucose appetite are in accord with previous studies.

6 Discussion

6.1 Summary of results and mechanisms involved

The ARC of the hypothalamus plays an important role in energy homeostasis. The enzyme glucokinase is expressed in the ARC where it can act as a neuronal glucose sensor. This work addresses the role of ARC glucokinase in energy homeostasis.

In order to confirm the involvement of ARC glucokinase in the control of energy homeostasis, I demonstrated that ARC glucokinase activity is increased after a twenty-four hour fast in rats. In line with this, pharmacological increase of ARC glucokinase activity in rats resulted in an acute increase of food intake. To further investigate this, rAAV encoding rat pancreatic glucokinase mRNA was made (rAAV-GKS). In vitro testing of this confirmed that the construct for rAAV-GKS increased ARC glucokinase activity. rAAV-GKS and rAAV-GFP were injected stereotactically into the ARC of rats. This resulted in a significant increase in ARC glucokinase activity in the ARC, with in situ hybridisation confirming increased ARC glucokinase mRNA expression in rAAV-GKS injected rats (iARC-GKS) as compared to controls (iARC-GFP). On a normal chow diet, chronic increase of ARC glucokinase activity in rats resulted in an increase of food intake, body weight gain and percentage fat, as compared to controls. These results were replicated using a high-energy diet, similar to modern day obesogenic diets, in a second cohort of animals. These results confirmed that manipulating ARC glucokinase alters energy homeostasis with increased glucokinase activity resulting in an obesogenic effect on appetite.

ARC glucokinase increased intake of glucose, but not of fructose, a closely related sugar that is not metabolised by glucokinase and does not cross the blood-brain barrier. Both pharmacological and genetic increase of ARC glucokinase selectively increased glucose consumption in rats given both glucose and normal chow separately during short-term studies. In this setting, normal chow consumption, which was previously increased when given alone to rats with increased ARC glucokinase activity, was similar to that of controls. These effects were replicated and confirmed in a longitudinal 31-day study, where rats were offered 10% w/v glucose with normal chow ad libitum. Glucose intake was significantly increased. Chow intake, body weight and total caloric intake was similar to that of controls. These results confirmed that increased ARC glucokinase alters glucose intake by increasing glucose appetite. When glucose is given separately in addition to the mixed diet, glucose

intake is selectively increased and that of the mixed diet is not altered. When a single mixed diet is given alone, the increase in glucose appetite in iARC-GKS rats results in an increased consumption of the single mixed diet. This leads to an increase in food intake and body weight.

Results from activation and inhibition of K_{ATP} channels in the ARC of rats suggest that glucokinase is mediating its effect on energy homeostasis and glucose appetite in the ARC via K_{ATP} channels. There were no changes in the expression or activity of AMPK suggesting that the effects of glucokinase in our model are not mediated via AMPK. There were no changes in the expression of ARC neuropeptides involved in energy homeostasis. However, NPY release was increased in iARC-GKS rats.

These results suggest that the mechanism by which ARC glucokinase alters appetite in our model involves increased glycolytic flux in the ARC via increased glucokinase activity (lynedjian, 2009). This leads to increased local ATP generation and inhibition of K_{ATP} channel activity with subsequent neuronal depolarisation. This leads to altered neurotransmitter release in the ARC. In keeping with this, NPY release is increased in our model. NPY is implicated in regulating carbohydrate preference, further supporting its potential involvement in phenotype of iARC-GKS rats (Morley et al., 1987). It is therefore possible that ARC glucokinase and K_{ATP} channels mediate glucose preference and have an orexigenic effect via altered NPY signalling. Further mechanisms by which ARC neuronal activity may increase glucose preference are not clear but may involve interaction between homeostatic and non-homeostatic centres. The figure below (figure 6.1) summarises the mechanism by which ARC glucokinase may lead to altered food and glucose intake in rats.

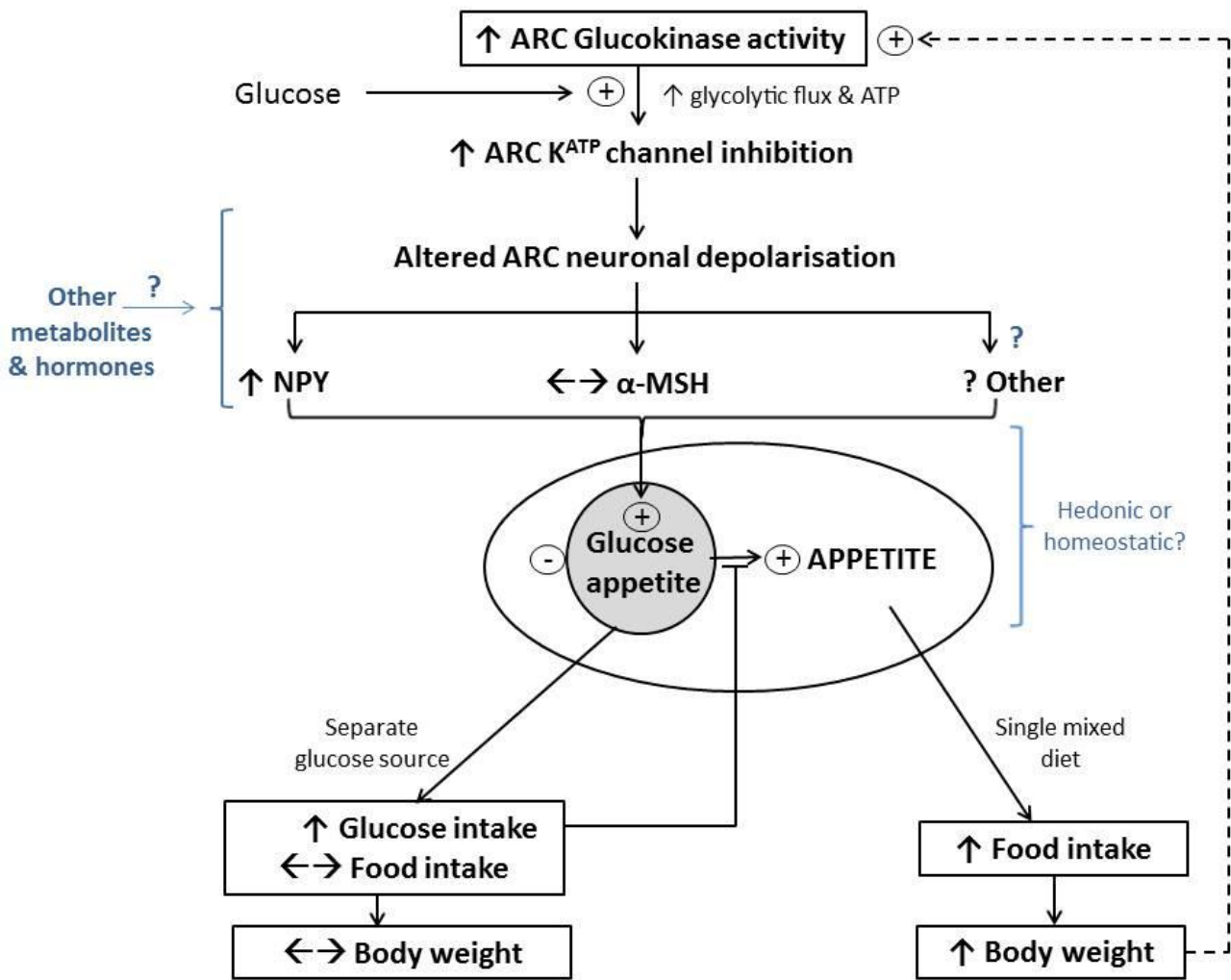


Figure 6.1 Proposed mechanism for the effects of ARC glucokinase on energy homeostasis: Increased ARC glucokinase alters glycolytic flux and ATP generation resulting in K_{ATP} channel inhibition. This leads to altered neuronal activity in response to metabolites, such as glucose. Release of the orexigenic NPY neurotransmitter is enhanced whereas that of α -MSH is not affected. The release of other neurotransmitters, such as GABA, may also be altered. The net effect of these changes is to increase glucose appetite either by a direct homeostatic affect or by interactions between hedonic and homeostatic appetite centres. Glucose appetite partially drives food intake. In the absence of a separate source of glucose, increased glucose appetite results in increased food intake and body weight, as that seen on a mixed diet. When a separate glucose source is present, glucose intake is selectively increased, whereas food intake is not altered.

6.2 Implications for current understanding of energy homeostasis

This work demonstrates that ARC glucokinase is an important regulator of food and glucose intake. This is in line with previous work demonstrating that glucokinase mRNA expression is increased in diet-induced obese and obese-prone rats and that obesity leads to a bias towards calorie dense foods (Dunn-Meynell et al., 2002b, Page et al., 2011b). This is also in keeping with our observations of increased ARC glucokinase activity in the fasting state where drive to consume calorogenic food is enhanced (Goldstone et al., 2009). However, as detailed in chapter 3, this work is different from the results of two previous groups which used non-specific, potentially toxic or immunogenic agents to reduce glucokinase activity in cannulated animals (Dunn-Meynell et al., 2009, Zhou et al., 2011). Furthermore, these studies were not specific to the ARC and did not demonstrate alterations in ARC glucokinase activity. This work improves on their studies by using a strategy that encompasses a non-immunogenic, non-toxic, neuronal specific vector to achieve sustained increase in glucokinase expression specifically in the ARC (Daly, 2004b, Ponnazhagan et al., 1997, Gardiner et al., 2005). This work also confirmed a specific increase in ARC glucokinase activity to levels comparable to those seen in fasting. Hence, it is likely that the previous studies failed to demonstrate similar effects due to severe limitations imposed by their methods.

It has also been postulated that glucose may exert a negative feedback on the hypothalamus to alter appetite via neuronal glucose-sensing. Glucokinase is an important part of the glucose-sensing mechanism in the hypothalamus. Therefore, based on this, an increase in glucokinase activity is likely to increase the sensitivity of neuronal glucose-sensing and enhance negative feedback effect from glucose to diminish appetite. Although this work is not directly assessing glucose-sensing, it suggests that the opposite occurs since increased ARC glucokinase activity has an orexigenic effect. It is possible that a feed forward mechanism in relation to appetite and glucose-sensing is occurring, possibly in conjunction with reward pathways or via a direct hypothalamic effect to promote consumption of nutrient rich foods when they are available. This has the biological advantage of maximising gain in energy stores while energy rich foods are present. Hence in rats with increased ARC glucokinase activity and increased glucose-sensing, this feed forward mechanism results in increased food intake and glucose intake. Therefore this work may relate glucose-sensing to

physiological, day-to-day food intake as well as modern-day obesity in a manner that has not been previously demonstrated.

This work also supports the involvement of K_{ATP} channels in mediating the effect of glucokinase in the hypothalamus (Ashford et al., 1990c). The results on food intake and glucose appetite noted are also in keeping with leptin activating K_{ATP} channels to inhibit food intake (Spanswick et al., 1997, Mirshamsi et al., 2004). However, selective ablation of K_{ATP} channels in POMC neurons have no effect on food intake and body weight (Parton et al., 2007b). It is possible that K_{ATP} channels on NPY neurons have a more prominent role on food intake and body weight. This is in keeping with glucokinase altering NPY release in response to glucose, demonstrated in this work. Increased food intake and increased preference to glucose rich carbohydrates is noted with work augmentation of NPY signalling in the hypothalamus (Morley et al., 1987). These data further support the involvement of K_{ATP} channels and NPY in mediating the effect of ARC glucokinase on appetite. Glucokinase and K_{ATP} channels co-localise in NPY neurons (Lynch et al., 2000, Van den Top et al., 2007).

The brain relies mainly on glucose for energy (Amiel, 1995). Taste-independent mechanisms that enable the brain to obtain a steady intake of glucose have been postulated but not conclusively demonstrated in mammals. In invertebrates such mechanisms have been recently found (Dus et al., 2011). In mammals, modulation of hedonic centres increases the reward value and consumption of nutrient by taste independent pathways (Domingos et al., 2011, Ren et al., 2010). Work in this thesis highlights that ARC glucokinase activity can regulate glucose appetite. In animals with increased ARC glucokinase activity, if glucose is available as an independent source it restores appetite and food intake. Otherwise it leads to an increased drive to consume food leading to increased weight gain (fig 6.1). Its relevance to human obesity is further strengthened by increased food intake and body weight gain in iARC-GKS rats on a high energy diet, similar to current Western obesogenic diets. It suggests that maintenance of a glucose source in the diet of obese individuals is important to satiate glucose appetite given that hypothalamic glucokinase expression is likely to be elevated in obese individuals. It is possible that the recent rise in fructose consumption may not satiate the glucose appetite, resulting in increased consumption of further foods (Bray, 2008). In other words, suggestions that all calories are not equal are further strengthened by this work.

The findings of this work also have important implications for the use of sulphonylureas and potential use of glucokinase activators in the treatment of type II diabetes (Matschinsky and Porte, 2010). These agents may enhance glucose appetite and food intake which may have detrimental effects on body weight in patients with type II diabetes. This also may, in part, explain the increase in body weight in patients treated with sulphonylureas (UKPDS, 1998).

6.3 Limitations, unresolved questions and future work

Possible limitations of the current work include that iARC-GKS rats may be influenced by a gain of function in ARC glucokinase expression in neurones that do not normally express glucokinase. AAV expresses in neurons indiscriminately and a constitutively active promoter was used in our construct. Nevertheless, the use of pharmacological agents to increase ARC glucokinase activity produced similar effects on food intake and glucose appetite as that seen in iARC-GKS rats. Pharmacological activators of glucokinase will only influence glucokinase activity in neurons that normally express glucokinase. Furthermore, neuronal glucokinase require the presence of certain other cellular components to regulate its activity or subcellular localisation in response to glucose, as seen in hepatocytes (Stubbs et al., 2000, de la Iglesia et al., 2000, Farrelly et al., 1999). If this is true, increasing the glucokinase expression in cells that do not normally express glucokinase may not have a significant effect on their function. Nevertheless, similar results with both pharmacological and genetic activation of glucokinase suggest a physiologically relevant effect on food intake and glucose appetite. To further confirm the physiological relevance of findings in this study, anti-sense for glucokinase mRNA could be injected stereotactically into the ARC. Knock-down of glucokinase expression will only occur in neurons that normally express glucokinase and will have no biological effect in neurons that do not express glucokinase.

Another limitation includes the use of glibenclamide and diazoxide to alter the activity of K_{ATP} channels. These agents were injected stereotactically and are likely to influence K_{ATP} channels in non-glucokinase expressing neurons as well. Although this may lead to unwanted effects, this strategy supported our hypothesis that K_{ATP} channels are involved in mediating the effects of glucokinase. Similar food intake and glucose appetite effects are seen with both glucokinase and K_{ATP} channel modulation. This reinforces the suggestion that glucokinase is mediating its effects on energy homeostasis via K_{ATP} channels and is in line

with previous work. More specific strategies to alter K_{ATP} channel activity can be considered by using Cre-Lox or specific promoters to drive gene expression on AAV.

This work investigated the release of NPY and α -MSH from hypothalamic explants in response to glucose. The significant alterations noted in NPY are in keeping with our phenotype. However it is possible that the picture could be complicated by the effect of other neurotransmitters such as GABA. The influence of other metabolites, such as leptin and fatty acids, have not been investigated either due to practical limitations. The net effect of these neurotransmitters and metabolites leads to the phenotype of increased glucose appetite in our model of increased ARC glucokinase activity. The mechanism presented above may be over simplistic and other factors may be involved in regulating glucose appetite. The influence of leptin and fatty acids can be tested in animals with increased ARC glucokinase by stereotactically delivering leptin or fatty acids into the ARC and studying the effect on appetite. More selective models of altered glucokinase activity may allow precise determination of neuronal subtypes involved in mediating the phenotype in this work. Mice with loxp-sites inserted into the glucokinase mRNA are commercially available. Crossing such mice with POMC-Cre and NPY-Cre mice would be useful to understand the precise role of neuronal subtypes.

Energy expenditure has not been directly measured in this work. Given our results it is very likely that the increased body weight is due to increased appetite. In line with this, BAT weight and BAT UCP-1 mRNA expression was similar in iARC-GKS and controls. Nevertheless more extensive investigations on this can be performed using a Comprehensive Laboratory Animal Monitoring System and pair-fed animals.

This work demonstrated that insulin sensitivity is not significantly altered despite increased adiposity in iARC-GKS rats versus controls. Increased ARC glucokinase activity may prevent deteriorations in insulin resistance noted in obesity. In this regard, it has been demonstrated that increased hypothalamic LCFA-CoA concentrations results in reduced hepatic glucose output (Lam et al., 2005b). This work indicated an increase in FAS expression in iARC-GKS rats. As discussed in chapter 5, this may indicate increased conversion of malonyl-CoA and acetyl-CoA to long-chain fatty acids. Increased presence of long-chain fatty acids in iARC-GKS rats may lead to reduced hepatic glucose output and

improved insulin sensitivity despite increased adiposity. It is also possible that altered ARC neurotransmitter release may influence glucose homeostasis (Parton et al., 2007b, Thorens, 2011). Further work on confirming similar insulin sensitivity can be done using an insulin tolerance test. Techniques such as glycaemic clamps with tracer glucose may help define this better, however due to practical limitations this technique is not currently feasible. Nevertheless, glucose homeostasis assessments warrant more extensive assessment and glucose tolerance tests and insulin tolerance tests should be considered to assess this.

The increase in drive to consume glucose in iARC-GKS rats may be occurring via augmenting a post-ingestive, taste independent reward pathway or form a separate homeostatic regulatory mechanism, similar to those seen in lower order animals (Dus et al., 2011). Further work is needed to elucidate the precise mechanism. Work on reward pathways is technically difficult. Possible ways of studying reward pathways in our model could be via measuring dopamine levels, dopamine mRNA expression or neuronal activity via c-fos in the ventral tegmental area of the brain in response to glucose. This timing of sample collection with respect to glucose stimulus will be difficult to predict. Delivering dopamine inhibitors to the VTA of iARC-GKS rats to determine if this diminishes the increased glucose appetite provides an alternative approach. Functional MRI also provides a strategy to assess activity of neuronal pathways in reward centres. Unfortunately current setups are mainly applicable to mice rather than rats. A number of other strategies are possible in mice including methods encompassing optogenetics to develop reference assays for reward mediated preference in mice (Domingos et al., 2011). Such strategies could be applied to different mouse models but are outside the scope of this particular study.

The relevance of this to modern obesity needs to be investigated further especially in relation to increased fructose consumption and obesity, discussed above. This can be tested by giving both iARC-GKS and control animals fructose in addition to normal chow. Given our postulated mechanism, we would expect similar fructose consumption between the groups but increased chow consumption in iARC-GKS rats. It is also unclear if the effect of increased ARC glucokinase on glucose appetite extends to other hexose based carbohydrates that can be rapidly metabolised. Further work on this can be done using different carbohydrate solutions, such as maltodextrin. This will be important as it may demonstrate that ARC glucokinase regulates carbohydrate craving and not just glucose appetite.

Conclusion

The primary aim of this work was to investigate the physiological role of ARC glucokinase in energy homeostasis. This work reveals that increasing ARC glucokinase activity has an orexigenic effect that leads to increased glucose appetite and can drive food intake resulting in increased adiposity. Inhibition of K_{ATP} channels and altered NPY release may play a role in mediating this effect of ARC glucokinase on energy homeostasis. This work further clarifies the role of ARC glucokinase and K_{ATP} channels in energy homeostasis and has implications for the use of glucokinase activators and sulphonylureas in the management of type II diabetes. However it raises a number of questions. Further work will increase our understanding of energy homeostasis and macronutrient preference and hopefully improve our currently futile efforts at curbing the obesity epidemic.

7 References

- ABBOTT, C. R., KENNEDY, A. R., WREN, A. M., ROSSI, M., MURPHY, K. G., SEAL, L. J., TODD, J. F., GHATEI, M. A., SMALL, C. J. & BLOOM, S. R. 2003. Identification of hypothalamic nuclei involved in the orexigenic effect of melanin-concentrating hormone. *Endocrinology*, 144, 3943-9.
- ABRAHAM, S., LOWENSTEIN, F. W., O'CONNELL, D. E., NATIONAL CENTER FOR HEALTH STATISTICS (U.S.) & NATIONAL HEALTH AND NUTRITION EXAMINATION SURVEY (U.S.) 1975. *Preliminary findings of the first Health and Nutrition Examination Survey, 1971-72 : anthropometric and clinical findings*, U.S. Dept. of Health, Education, and Welfare, Public Health Service, Health Resources Administration.
- ADRIAN, T. E., FERRI, G. L., BACARESE-HAMILTON, A. J., FUESSL, H. S., POLAK, J. M. & BLOOM, S. R. 1985. Human distribution and release of a putative new gut hormone, peptide YY. *Gastroenterology*, 89, 1070-7.
- AFIONE, S. A., WANG, J., WALSH, S., GUGGINO, W. B. & FLOTTE, T. R. 1999. Delayed expression of adeno-associated virus vector DNA. *Intervirology*, 42, 213-20.
- AKABAYASHI, A., ZAIA, C. T., SILVA, I., CHAE, H. J. & LEIBOWITZ, S. F. 1993. Neuropeptide Y in the arcuate nucleus is modulated by alterations in glucose utilization. *Brain Res*, 621, 343-8.
- ALLEN, J. M., YEATS, J. C., ADRIAN, T. E. & BLOOM, S. R. 1984. Radioimmunoassay of neuropeptide Y. *Regul Pept*, 8, 61-70.
- AMIEL, S. A. 1995. Organ fuel selection: brain. *Proc Nutr Soc*, 54, 151-5.
- ANAND, B. K. & BROBECK, J. R. 1951. Localization of a "feeding center" in the hypothalamus of the rat. *Proc Soc Exp Biol Med*, 77, 323-4.
- ANAND, B. K. & PILLAI, R. V. 1967. Activity of single neurones in the hypothalamic feeding centres: effect of gastric distension. *J Physiol*, 192, 63-77.
- ANDERSSON, U., FILIPSSON, K., ABBOTT, C. R., WOODS, A., SMITH, K., BLOOM, S. R., CARLING, D. & SMALL, C. J. 2004. AMP-activated protein kinase plays a role in the control of food intake. *J Biol Chem*, 279, 12005-8.
- ASHCROFT, F. M. 1988. Adenosine 5'-triphosphate-sensitive potassium channels. *Annu Rev Neurosci*, 11, 97-118.
- ASHFORD, M. L., BODEN, P. R. & TREHERNE, J. M. 1990a. Glucose-induced excitation of hypothalamic neurones is mediated by ATP-sensitive K⁺ channels. *Pflugers Arch*, 415, 479-83.
- ASHFORD, M. L., BODEN, P. R. & TREHERNE, J. M. 1990b. Tolbutamide excites rat glucoreceptive ventromedial hypothalamic neurones by indirect inhibition of ATP-K⁺ channels. *Br J Pharmacol*, 101, 531-40.
- ASHFORD, M. L. J., BODEN, P. R. & TREHERNE, J. M. 1990c. Glucose-Induced Excitation of Hypothalamic Neurons Is Mediated by Atp-Sensitive K⁺ Channels. *Pflugers Archiv-European Journal of Physiology*, 415, 479-483.
- ATCHISON, R. W., CASTO, B. C. & HAMMON, W. M. 1965. Adenovirus-Associated Defective Virus Particles. *Science*, 149, 754-6.
- BADY, I., MARTY, N., DALLAPORTA, M., EMERY, M., GYGER, J., TARUSSIO, D., FORETZ, M. & THORENS, B. 2006. Evidence from glut2-null mice that glucose is a critical physiological regulator of feeding. *Diabetes*, 55, 988-95.

- BARTLETT, J. S., SAMULSKI, R. J. & MCCOWN, T. J. 1998. Selective and rapid uptake of adeno-associated virus type 2 in brain. *Hum Gene Ther*, 9, 1181-6.
- BEAK, S. A., HEATH, M. M., SMALL, C. J., MORGAN, D. G., GHATEI, M. A., TAYLOR, A. D., BUCKINGHAM, J. C., BLOOM, S. R. & SMITH, D. M. 1998. Glucagon-like peptide-1 stimulates luteinizing hormone-releasing hormone secretion in a rodent hypothalamic neuronal cell line. *J Clin Invest*, 101, 1334-41.
- BELGARDT, B. F., OKAMURA, T. & BRUNING, J. C. 2009. Hormone and glucose signalling in POMC and AgRP neurons. *Journal of Physiology-London*, 587, 5305-5314.
- BENOIT, S. C., CLEGG, D. J., SEELEY, R. J. & WOODS, S. C. 2004. Insulin and leptin as adiposity signals. *Recent Prog Horm Res*, 59, 267-85.
- BERGMEYER, H. U. & GAWEHN, K. 1974. *Methods of enzymatic analysis*, Weinheim, Verlag Chemie ; New York ; London : Academic Press.
- BERNS, K. I. & ADLER, S. 1972. Separation of two types of adeno-associated virus particles containing complementary polynucleotide chains. *J Virol*, 9, 394-6.
- BERNSTEIN, L. M. & GROSSMAN, M. I. 1956. An experimental test of the glucostatic theory of regulation of food intake. *J Clin Invest*, 35, 627-33.
- BERRIDGE, K. C. 1996. Food reward: brain substrates of wanting and liking. *Neurosci Biobehav Rev*, 20, 1-25.
- BERRIDGE, K. C., ROBINSON, T. E. & ALDRIDGE, J. W. 2009. Dissecting components of reward: 'liking', 'wanting', and learning. *Curr Opin Pharmacol*, 9, 65-73.
- BERTHOUD, H. R. 2006. Homeostatic and non-homeostatic pathways involved in the control of food intake and energy balance. *Obesity*, 14, 197-200.
- BERTHOUD, H. R. 2011. Metabolic and hedonic drives in the neural control of appetite: who is the boss? *Curr Opin Neurobiol*, 21, 888-96.
- BERTHOUD, H. R. & MORRISON, C. 2008. The brain, appetite, and obesity. *Annu Rev Psychol*, 59, 55-92.
- BERTHOUD, H. R., MUNZBERG, H., RICHARDS, B. K. & MORRISON, C. D. 2012. Neural and metabolic regulation of macronutrient intake and selection. *Proc Nutr Soc*, 71, 390-400.
- BERTONI, J. M. 1981. Competitive-Inhibition of Rat-Brain Hexokinase by 2-Deoxyglucose, Glucosamine, and Metrizamide. *Journal of Neurochemistry*, 37, 1523-1528.
- BEWICK, G. A., GARDINER, J. V., DHILLO, W. S., KENT, A. S., WHITE, N. E., WEBSTER, Z., GHATEI, M. A. & BLOOM, S. R. 2005. Post-embryonic ablation of AgRP neurons in mice leads to a lean, hypophagic phenotype. *FASEB J*, 19, 1680-2.
- BIGGERS, D. W., MYERS, S. R., NEAL, D., STINSON, R., COOPER, N. B., JASPAN, J. B., WILLIAMS, P. E., CHERRINGTON, A. D. & FRIZZELL, R. T. 1989. Role of brain in counterregulation of insulin-induced hypoglycemia in dogs. *Diabetes*, 38, 7-16.
- BLACKLOW, N. R., HOGGAN, M. D., KAPIKIAN, A. Z., AUSTIN, J. B. & ROWE, W. P. 1968. Epidemiology of adenovirus-associated virus infection in a nursery population. *Am J Epidemiol*, 88, 368-78.
- BLEVINS, J. E. & BASKIN, D. G. 2010. Hypothalamic-Brainstem Circuits Controlling Eating. *Frontiers in Eating and Weight Regulation*, 63, 133-140.
- BOHENZKY, R. A., LEFEBVRE, R. B. & BERNS, K. I. 1988. Sequence and symmetry requirements within the internal palindromic sequences of the adeno-associated virus terminal repeat. *Virology*, 166, 316-27.

- BORG, M. A., SHERWIN, R. S., BORG, W. P., TAMBORLANE, W. V. & SHULMAN, G. I. 1997. Local ventromedial hypothalamus glucose perfusion blocks counterregulation during systemic hypoglycemia in awake rats. *J Clin Invest*, 99, 361-5.
- BORG, W. P., SHERWIN, R. S., DURING, M. J., BORG, M. A. & SHULMAN, G. I. 1995. Local ventromedial hypothalamus glucopenia triggers counterregulatory hormone release. *Diabetes*, 44, 180-4.
- BORGLAND, S. L., TAHA, S. A., SARTI, F., FIELDS, H. L. & BONCI, A. 2006. Orexin A in the VTA is critical for the induction of synaptic plasticity and behavioral sensitization to cocaine. *Neuron*, 49, 589-601.
- BOURET, S. G., DRAPER, S. J. & SIMERLY, R. B. 2004. Formation of projection pathways from the arcuate nucleus of the hypothalamus to hypothalamic regions implicated in the neural control of feeding behavior in mice. *Journal of Neuroscience*, 24, 2797-2805.
- BOUTREL, B., KENNY, P. J., SPECIO, S. E., MARTIN-FARDON, R., MARKOU, A., KOOB, G. F. & DE LECEA, L. 2005. Role for hypocretin in mediating stress-induced reinstatement of cocaine-seeking behavior. *Proc Natl Acad Sci U S A*, 102, 19168-73.
- BRAY, G. A. 2004. Medical consequences of obesity. *Journal of Clinical Endocrinology & Metabolism*, 89, 2583-2589.
- BRAY, G. A. 2008. Fructose: should we worry? *Int J Obes (Lond)*, 32 Suppl 7, S127-31.
- BROADWELL, R. D., BALIN, B. J., SALCMAN, M. & KAPLAN, R. S. 1983. Brain-blood barrier? Yes and no. *Proc Natl Acad Sci U S A*, 80, 7352-6.
- BROBERGER, C., DE LECEA, L., SUTCLIFFE, J. G. & HOKFELT, T. 1998. Hypocretin/orexin- and melanin-concentrating hormone-expressing cells form distinct populations in the rodent lateral hypothalamus: relationship to the neuropeptide Y and agouti gene-related protein systems. *J Comp Neurol*, 402, 460-74.
- BURDAKOV, D., GERASIMENKO, O. & VERKHRATSKY, A. 2005a. Physiological changes in glucose differentially modulate the excitability of hypothalamic melanin-concentrating hormone and orexin neurons in situ. *J Neurosci*, 25, 2429-33.
- BURDAKOV, D., LUCKMAN, S. M. & VERKHRATSKY, A. 2005b. Glucose-sensing neurons of the hypothalamus. *Philos Trans R Soc Lond B Biol Sci*, 360, 2227-35.
- CAMPFIELD, L. A., BRANDON, P. & SMITH, F. J. 1985. On-line continuous measurement of blood glucose and meal pattern in free-feeding rats: the role of glucose in meal initiation. *Brain Res Bull*, 14, 605-16.
- CANABAL, D. D., SONG, Z., POTIAN, J. G., BEUVE, A., MCARDLE, J. J. & ROUTH, V. H. 2007. Glucose, insulin, and leptin signaling pathways modulate nitric oxide synthesis in glucose-inhibited neurons in the ventromedial hypothalamus. *Am J Physiol Regul Integr Comp Physiol*, 292, R1418-28.
- CARLING, D. 2004. The AMP-activated protein kinase cascade--a unifying system for energy control. *Trends Biochem Sci*, 29, 18-24.
- CHAN, O., LAWSON, M., ZHU, W., BEVERLY, J. L. & SHERWIN, R. S. 2007. ATP-sensitive K(+) channels regulate the release of GABA in the ventromedial hypothalamus during hypoglycemia. *Diabetes*, 56, 1120-6.
- CHENG, K., SIMPSON, S. J. & RAUBENHEIMER, D. 2008. A geometry of regulatory scaling. *Am Nat*, 172, 681-93.
- CLARET, M., SMITH, M. A., BATTERHAM, R. L., SELMAN, C., CHOUDHURY, A. I., FRYER, L. G. D., CLEMENTS, M., AL-QASSAB, H., HEFFRON, H., XU, A. W., SPEAKMAN, J. R., BARSH, G. S., VIOLLET, B., VAULONT, S., ASHFORD, M. L. J., CARLING, D. & WITHERS, D. J.

2007. AMPK is essential for energy homeostasis regulation and glucose sensing by POMC and AgRP neurons. *Journal of Clinical Investigation*, 117, 2325-2336.
- CLEARY, J., WELDON, D. T., O'HARE, E., BILLINGTON, C. & LEVINE, A. S. 1996. Naloxone effects on sucrose-motivated behavior. *Psychopharmacology (Berl)*, 126, 110-4.
- CONE, R. D., COWLEY, M. A., BUTLER, A. A., FAN, W., MARKS, D. L. & LOW, M. J. 2001. The arcuate nucleus as a conduit for diverse signals relevant to energy homeostasis. *Int J Obes Relat Metab Disord*, 25 Suppl 5, S63-7.
- DALY, T. M. 2004a. AAV-mediated gene transfer to the liver. *Methods Mol Biol*, 246, 195-9.
- DALY, T. M. 2004b. Overview of adeno-associated viral vectors. *Methods Mol Biol*, 246, 157-65.
- DAVIES, S. P., CARLING, D. & HARDIE, D. G. 1989. Tissue distribution of the AMP-activated protein kinase, and lack of activation by cyclic-AMP-dependent protein kinase, studied using a specific and sensitive peptide assay. *Eur J Biochem*, 186, 123-8.
- DAVIS, J. D., WIRTSHAFTER, D., ASIN, K. E. & BRIEF, D. 1981. Sustained intracerebroventricular infusion of brain fuels reduces body weight and food intake in rats. *Science*, 212, 81-3.
- DAYA, S. & BERNS, K. I. 2008. Gene therapy using adeno-associated virus vectors. *Clin Microbiol Rev*, 21, 583-93.
- DE LA IGLESIA, N., MUKHTAR, M., SEOANE, J., GUINOVART, J. J. & AGIUS, L. 2000. The role of the regulatory protein of glucokinase in the glucose sensory mechanism of the hepatocyte. *J Biol Chem*, 275, 10597-603.
- DE LECEA, L., KILDUFF, T. S., PEYRON, C., GAO, X., FOYE, P. E., DANIELSON, P. E., FUKUHARA, C., BATTENBERG, E. L., GAUTVIK, V. T., BARTLETT, F. S., 2ND, FRANKEL, W. N., VAN DEN POL, A. N., BLOOM, F. E., GAUTVIK, K. M. & SUTCLIFFE, J. G. 1998. The hypocretins: hypothalamus-specific peptides with neuroexcitatory activity. *Proc Natl Acad Sci U S A*, 95, 322-7.
- DE SILVA, A., SALEM, V., LONG, C. J., MAKWANA, A., NEWBOULD, R. D., RABINER, E. A., GHATEI, M. A., BLOOM, S. R., MATTHEWS, P. M., BEAVER, J. D. & DHILLO, W. S. 2011. The Gut Hormones PYY3-36 and GLP-1(7-36) amide Reduce Food Intake and Modulate Brain Activity in Appetite Centers in Humans. *Cell Metabolism*, 14, 700-706.
- DE VRIES, M. G., ARSENEAU, L. M., LAWSON, M. E. & BEVERLY, J. L. 2003. Extracellular glucose in rat ventromedial hypothalamus during acute and recurrent hypoglycemia. *Diabetes*, 52, 2767-73.
- DE VRIES, M. G., LAWSON, M. A. & BEVERLY, J. L. 2005. Hypoglycemia-induced noradrenergic activation in the VMH is a result of decreased ambient glucose. *Am J Physiol Regul Integr Comp Physiol*, 289, R977-81.
- DEFALCO, J., TOMISHIMA, M., LIU, H., ZHAO, C., CAI, X., MARTH, J. D., ENQUIST, L. & FRIEDMAN, J. M. 2001. Virus-assisted mapping of neural inputs to a feeding center in the hypothalamus. *Science*, 291, 2608-13.
- DHILLON, H., ZIGMAN, J. M., YE, C. P., LEE, C. E., MCGOVERN, R. A., TANG, V. S., KENNY, C. D., CHRISTIANSEN, L. M., WHITE, R. D., EDELSTEIN, E. A., COPPARI, R., BALTHASAR, N., COWLEY, M. A., CHUA, S., ELMQUIST, J. K. & LOWELL, B. B. 2006. Leptin directly activates SF1 neurons in the VMH, and this action by leptin is required for normal body-weight homeostasis. *Neuron*, 49, 191-203.
- DIGGS-ANDREWS, K. A., SILVERSTEIN, J. M. & FISHER, S. J. 2009. Glucose Sensing in the Central Nervous System

- DOMINGOS, A. I., VAYNSHTEYN, J., VOSS, H. U., REN, X., GRADINARU, V., ZANG, F., DEISSEROTH, K., DE ARAUJO, I. E. & FRIEDMAN, J. 2011. Leptin regulates the reward value of nutrient. *Nat Neurosci*, 14, 1562-8.
- DUALE, H., KASPAROV, S., PATON, J. F. & TESCHEMACHER, A. G. 2005. Differences in transductional tropism of adenoviral and lentiviral vectors in the rat brainstem. *Exp Physiol*, 90, 71-8.
- DUAN, D., SHARMA, P., YANG, J., YUE, Y., DUDUS, L., ZHANG, Y., FISHER, K. J. & ENGELHARDT, J. F. 1998. Circular intermediates of recombinant adeno-associated virus have defined structural characteristics responsible for long-term episomal persistence in muscle tissue. *J Virol*, 72, 8568-77.
- DUNN-MEYNELL, A. A., ROUTH, V. H., KANG, L., GASPERS, L. & LEVIN, B. E. 2002a. Glucokinase is the likely mediator of glucosensing in both glucose-excited and glucose-inhibited central neurons. *Diabetes*, 51, 2056-2065.
- DUNN-MEYNELL, A. A., ROUTH, V. H., KANG, L., GASPERS, L. & LEVIN, B. E. 2002b. Glucokinase is the likely mediator of glucosensing in both glucose-excited and glucose-inhibited central neurons. *Diabetes*, 51, 2056-65.
- DUNN-MEYNELL, A. A., SANDERS, N. M., COMPTON, D., BECKER, T. C., EIKI, J., ZHANG, B. B. & LEVIN, B. E. 2009. Relationship among brain and blood glucose levels and spontaneous and glucoprivic feeding. *J Neurosci*, 29, 7015-22.
- DUS, M., MIN, S., KEENE, A. C., LEE, G. Y. & SUH, G. S. 2011. Taste-independent detection of the caloric content of sugar in *Drosophila*. *Proc Natl Acad Sci U S A*, 108, 11644-9.
- EGECIOGLU, E., SKIBICKA, K. P., HANSSON, C., ALVAREZ-CRESPO, M., FRIBERG, P. A., JERLHAG, E., ENGEL, J. A. & DICKSON, S. L. 2011. Hedonic and incentive signals for body weight control. *Rev Endocr Metab Disord*, 12, 141-51.
- EMMANS, G. C. 1991. Diet selection by animals: theory and experimental design. *Proc Nutr Soc*, 50, 59-64.
- EVANS, S. B., WILKINSON, C. W., GRONBECK, P., BENNETT, J. L., TABORSKY, G. J., JR. & FIGLEWICZ, D. P. 2003. Inactivation of the PVN during hypoglycemia partially simulates hypoglycemia-associated autonomic failure. *Am J Physiol Regul Integr Comp Physiol*, 284, R57-65.
- EVANS, S. B., WILKINSON, C. W., GRONBECK, P., BENNETT, J. L., ZAVOSH, A., TABORSKY, G. J., JR. & FIGLEWICZ, D. P. 2004. Inactivation of the DMH selectively inhibits the ACTH and corticosterone responses to hypoglycemia. *Am J Physiol Regul Integr Comp Physiol*, 286, R123-8.
- FAROOQI, I. S., BULLMORE, E., KEOGH, J., GILLARD, J., O'RAHILLY, S. & FLETCHER, P. C. 2007. Leptin regulates striatal regions and human eating behavior. *Science*, 317, 1355.
- FARRELLY, D., BROWN, K. S., TIEMAN, A., REN, J., LIRA, S. A., HAGAN, D., GREGG, R., MOOKHTIAR, K. A. & HARIHARAN, N. 1999. Mice mutant for glucokinase regulatory protein exhibit decreased liver glucokinase: a sequestration mechanism in metabolic regulation. *Proc Natl Acad Sci U S A*, 96, 14511-6.
- FENNER, D., ODILI, S., HONG, H. K., KOBAYASHI, Y., KOHSAKA, A., SIEPKA, S. M., VITATERNA, M. H., CHEN, P., ZELENT, B., GRIMSBY, J., TAKAHASHI, J. S., MATSCHINSKY, F. M. & BASS, J. 2011. Generation of N-ethyl-N-nitrosourea (ENU) diabetes models in mice demonstrates genotype-specific action of glucokinase activators. *J Biol Chem*, 286, 39560-72.

- FERRARI, F. K., SAMULSKI, T., SHENK, T. & SAMULSKI, R. J. 1996. Second-strand synthesis is a rate-limiting step for efficient transduction by recombinant adeno-associated virus vectors. *J Virol*, 70, 3227-34.
- FIORAMONTI, X., MARSOLLIER, N., SONG, Z., FAKIRA, K. A., PATEL, R. M., BROWN, S., DUPARC, T., PICA-MENDEZ, A., SANDERS, N. M., KNAUF, C., VALET, P., MCCRIMMON, R. J., BEUVE, A., MAGNAN, C. & ROUTH, V. H. 2010. Ventromedial hypothalamic nitric oxide production is necessary for hypoglycemia detection and counterregulation. *Diabetes*, 59, 519-28.
- FRIEDMAN, J. M. 2003. A war on obesity, not the obese. *Science*, 299, 856-8.
- GARDINER, J. V., KONG, W. M., WARD, H., MURPHY, K. G., DHILLO, W. S. & BLOOM, S. R. 2005. AAV mediated expression of anti-sense neuropeptide Y cRNA in the arcuate nucleus of rats results in decreased weight gain and food intake. *Biochem Biophys Res Commun*, 327, 1088-93.
- GARDLIK, R., PALFFY, R., HODOSY, J., LUKACS, J., TURNA, J. & CELEC, P. 2005. Vectors and delivery systems in gene therapy. *Med Sci Monit*, 11, RA110-21.
- GLASS, M. J., BILLINGTON, C. J. & LEVINE, A. S. 2000. Naltrexone administered to central nucleus of amygdala or PVN: neural dissociation of diet and energy. *Am J Physiol Regul Integr Comp Physiol*, 279, R86-92.
- GOLDSTONE, A. P., PRECHTL DE HERNANDEZ, C. G., BEAVER, J. D., MUHAMMED, K., CROESE, C., BELL, G., DURIGHEL, G., HUGHES, E., WALDMAN, A. D., FROST, G. & BELL, J. D. 2009. Fasting biases brain reward systems towards high-calorie foods. *Eur J Neurosci*, 30, 1625-35.
- GORDON, J. W., SCANGOS, G. A., PLOTKIN, D. J., BARBOSA, J. A. & RUDDLE, F. H. 1980. Genetic-Transformation of Mouse Embryos by Micro-Injection of Purified DNA. *Proceedings of the National Academy of Sciences of the United States of America-Biological Sciences*, 77, 7380-7384.
- GOWARD, C. R., HARTWELL, R., ATKINSON, T. & SCAWEN, M. D. 1986. The purification and characterization of glucokinase from the thermophile *Bacillus stearothermophilus*. *Biochem J*, 237, 415-20.
- GRIJALVA, C. V. & NOVIN, D. 1990. The Role of the Hypothalamus and Dorsal Vagal Complex in Gastrointestinal Function and Pathophysiology. *Neurobiology of Stress Ulcers*, 597, 207-222.
- GRILL, H. J. & KAPLAN, J. M. 2002. The neuroanatomical axis for control of energy balance. *Frontiers in Neuroendocrinology*, 23, 2-40.
- GRILL, H. J., SCHWARTZ, M. W., KAPLAN, J. M., FOXHALL, J. S., BREININGER, J. & BASKIN, D. G. 2002. Evidence that the caudal brainstem is a target for the inhibitory effect of leptin on food intake. *Endocrinology*, 143, 239-246.
- GRILL, H. J., SKIBICKA, K. P. & HAYES, M. R. 2007. Imaging obesity: fMRI, food reward, and feeding. *Cell Metabolism*, 6, 423-425.
- GRIMM, D., KERN, A., RITTNER, K. & KLEINSCHMIDT, J. A. 1998. Novel tools for production and purification of recombinant adenoassociated virus vectors. *Hum Gene Ther*, 9, 2745-60.
- HAJNAL, A., SMITH, G. P. & NORNGREN, R. 2004. Oral sucrose stimulation increases accumbens dopamine in the rat. *Am J Physiol Regul Integr Comp Physiol*, 286, R31-7.
- HARRIS, G. C., WIMMER, M. & ASTON-JONES, G. 2005. A role for lateral hypothalamic orexin neurons in reward seeking. *Nature*, 437, 556-9.

- HE, B., WHITE, B. D., EDWARDS, G. L. & MARTIN, R. J. 1998. Neuropeptide Y antibody attenuates 2-deoxy-D-glucose induced feeding in rats. *Brain Res*, 781, 348-50.
- HOESS, R. H. & ABREMSKI, K. 1985. Mechanism of Strand Cleavage and Exchange in the Cre-Lox Site-Specific Recombination System. *Journal of Molecular Biology*, 181, 351-362.
- HORVATH, T. L., DIANO, S. & VAN DEN POL, A. N. 1999. Synaptic interaction between hypocretin (orexin) and neuropeptide Y cells in the rodent and primate hypothalamus: a novel circuit implicated in metabolic and endocrine regulations. *J Neurosci*, 19, 1072-87.
- HUSSAIN, S. S. & BLOOM, S. R. 2011a. The pharmacological treatment and management of obesity. *Postgrad Med*. 2011 Feb (accepted for publication).
- HUSSAIN, S. S. & BLOOM, S. R. 2011b. The pharmacological treatment and management of obesity. *Postgrad Med*, 123, 34-44.
- HUSSAIN, S. S. & BLOOM, S. R. 2012. The regulation of food intake by the gut-brain axis: implications for obesity. *Int J Obes (Lond)*.
- IBRAHIM, N., BOSCH, M. A., SMART, J. L., QIU, J., RUBINSTEIN, M., RONNEKLEIV, O. K., LOW, M. J. & KELLY, M. J. 2003. Hypothalamic proopiomelanocortin neurons are glucose responsive and express K(ATP) channels. *Endocrinology*, 144, 1331-40.
- IINO, T., HASHIMOTO, N., SASAKI, K., OHYAMA, S., YOSHIMOTO, R., HOSAKA, H., HASEGAWA, T., CHIBA, M., NAGATA, Y., EIKI, J. & NISHIMURA, T. 2009. Structure-activity relationships of 3,5-disubstituted benzamides as glucokinase activators with potent in vivo efficacy. *Bioorg Med Chem*, 17, 3800-9.
- IM, D. S. & MUZYCZKA, N. 1990. The AAV origin binding protein Rep68 is an ATP-dependent site-specific endonuclease with DNA helicase activity. *Cell*, 61, 447-57.
- ISHIHARA, H., MAECHLER, P., GJINOVCI, A., HERRERA, P. L. & WOLLHEIM, C. B. 2003. Islet beta-cell secretion determines glucagon release from neighbouring alpha-cells. *Nat Cell Biol*, 5, 330-5.
- IYNEDJIAN, P. B. 2009. Molecular physiology of mammalian glucokinase. *Cell Mol Life Sci*, 66, 27-42.
- IYNEDJIAN, P. B., PILOT, P. R., NOUSPIKEL, T., MILBURN, J. L., QUADE, C., HUGHES, S., UCLA, C. & NEWGARD, C. B. 1989. Differential expression and regulation of the glucokinase gene in liver and islets of Langerhans. *Proc Natl Acad Sci U S A*, 86, 7838-42.
- JAMES, W. P. 2008. The fundamental drivers of the obesity epidemic. *Obes Rev*, 9 Suppl 1, 6-13.
- JAY, F. T., LAUGHLIN, C. A. & CARTER, B. J. 1981. Eukaryotic translational control: adeno-associated virus protein synthesis is affected by a mutation in the adenovirus DNA-binding protein. *Proc Natl Acad Sci U S A*, 78, 2927-31.
- JORDAN, S. D., KONNER, A. C. & BRUNING, J. C. 2010. Sensing the fuels: glucose and lipid signaling in the CNS controlling energy homeostasis. *Cell Mol Life Sci*, 67, 3255-73.
- KALRA, S. P., DUBE, M. G., PU, S. Y., XU, B., HORVATH, T. L. & KALRA, P. S. 1999. Interacting appetite-regulating pathways in the hypothalamic regulation of body weight. *Endocrine Reviews*, 20, 68-100.
- KAMATA, K., MITSUYA, M., NISHIMURA, T., EIKI, J. & NAGATA, Y. 2004. Structural basis for allosteric regulation of the monomeric allosteric enzyme human glucokinase. *Structure*, 12, 429-38.
- KANAREK, R. B., MATHES, W. F. & PRZYPEK, J. 1996. Intake of dietary sucrose or fat reduces amphetamine drinking in rats. *Pharmacol Biochem Behav*, 54, 719-23.

- KANG, L., DUNN-MEYNELL, A. A., ROUTH, V. H., GASPERS, L. D., NAGATA, Y., NISHIMURA, T., EIKI, J., ZHANG, B. B. & LEVIN, B. E. 2006. Glucokinase is a critical regulator of ventromedial hypothalamic neuronal glucosensing. *Diabetes*, 55, 412-20.
- KANG, L., ROUTH, V. H., KUZHIKANDATHIL, E. V., GASPERS, L. D. & LEVIN, B. E. 2004. Physiological and molecular characteristics of rat hypothalamic ventromedial nucleus glucosensing neurons. *Diabetes*, 53, 549-59.
- KANG, L., SANDERS, N. M., DUNN-MEYNELL, A. A., GASPERS, L. D., ROUTH, V. H., THOMAS, A. P. & LEVIN, B. E. 2008. Prior hypoglycemia enhances glucose responsiveness in some ventromedial hypothalamic glucosensing neurons. *Am J Physiol Regul Integr Comp Physiol*, 294, R784-92.
- KAPLAN, J. M., ARMENTANO, D., SPARER, T. E., WYNN, S. G., PETERSON, P. A., WADSWORTH, S. C., COUTURE, K. K., PENNINGTON, S. E., ST GEORGE, J. A., GOODING, L. R. & SMITH, A. E. 1997. Characterization of factors involved in modulating persistence of transgene expression from recombinant adenovirus in the mouse lung. *Hum Gene Ther*, 8, 45-56.
- KELLEY, A. E. & BERRIDGE, K. C. 2002. The neuroscience of natural rewards: relevance to addictive drugs. *J Neurosci*, 22, 3306-11.
- KIM, M. S., SMALL, C. J., STANLEY, S. A., MORGAN, D. G., SEAL, L. J., KONG, W. M., EDWARDS, C. M., ABUSNANA, S., SUNTER, D., GHATEI, M. A. & BLOOM, S. R. 2000. The central melanocortin system affects the hypothalamo-pituitary thyroid axis and may mediate the effect of leptin. *J Clin Invest*, 105, 1005-11.
- KLEIN, R. L., HAMBY, M. E., GONG, Y., HIRKO, A. C., WANG, S., HUGHES, J. A., KING, M. A. & MEYER, E. M. 2002. Dose and promoter effects of adeno-associated viral vector for green fluorescent protein expression in the rat brain. *Exp Neurol*, 176, 66-74.
- KOKATNUR, M. G., OALMANN, M. C., JOHNSON, W. D., MALCOM, G. T. & STRONG, J. P. 1979. Fatty acid composition of human adipose tissue from two anatomical sites in a biracial community. *Am J Clin Nutr*, 32, 2198-205.
- KONG, D., VONG, L., PARTON, L. E., YE, C. P., TONG, Q. C., HU, X. X., CHOI, B., BRUNING, J. C. & LOWELL, B. B. 2010. Glucose Stimulation of Hypothalamic MCH Neurons Involves K-ATP Channels, Is Modulated by UCP2, and Regulates Peripheral Glucose Homeostasis. *Cell Metabolism*, 12, 545-552.
- KONNER, A. C., KLOCKENER, T. & BRUNING, J. C. 2009. Control of energy homeostasis by insulin and leptin: targeting the arcuate nucleus and beyond. *Physiol Behav*, 97, 632-8.
- KURATA, K., FUJIMOTO, K., SAKATA, T., ETOU, H. & FUKAGAWA, K. 1986. D-glucose suppression of eating after intra-third ventricle infusion in rat. *Physiol Behav*, 37, 615-20.
- KYOSTIO, S. R., OWENS, R. A., WEITZMAN, M. D., ANTONI, B. A., CHEJANOVSKY, N. & CARTER, B. J. 1994. Analysis of adeno-associated virus (AAV) wild-type and mutant Rep proteins for their abilities to negatively regulate AAV p5 and p19 mRNA levels. *J Virol*, 68, 2947-57.
- LAM, C. K., CHARI, M. & LAM, T. K. 2009. CNS regulation of glucose homeostasis. *Physiology (Bethesda)*, 24, 159-70.
- LAM, C. K., CHARI, M., WANG, P. Y. & LAM, T. K. 2008. Central lactate metabolism regulates food intake. *Am J Physiol Endocrinol Metab*, 295, E491-6.
- LAM, T. K., GUTIERREZ-JUAREZ, R., POCAI, A. & ROSSETTI, L. 2005a. Regulation of blood glucose by hypothalamic pyruvate metabolism. *Science*, 309, 943-7.

- LAM, T. K., POCAI, A., GUTIERREZ-JUAREZ, R., OBICI, S., BRYAN, J., AGUILAR-BRYAN, L., SCHWARTZ, G. J. & ROSSETTI, L. 2005b. Hypothalamic sensing of circulating fatty acids is required for glucose homeostasis. *Nat Med*, 11, 320-7.
- LAM, T. K., SCHWARTZ, G. J. & ROSSETTI, L. 2005c. Hypothalamic sensing of fatty acids. *Nat Neurosci*, 8, 579-84.
- LAUTERIO, T. J., BOND, J. P. & ULMAN, E. A. 1994. Development and characterization of a purified diet to identify obesity-susceptible and resistant rat populations. *J Nutr*, 124, 2172-8.
- LEBRUN, B., BARIOHAY, B., MOYSE, E. & JEAN, A. 2006. Brain-derived neurotrophic factor (BDNF) and food intake regulation: A minireview. *Autonomic Neuroscience-Basic & Clinical*, 126, 30-38.
- LENIN KAMATCHI, G., VEERARAGAVAN, K., CHANDRA, D. & BAPNA, J. S. 1986. Antagonism of acute feeding response to 2-deoxyglucose and 5-thioglucoose by GABA antagonists: the relative role of ventromedial and lateral hypothalamus. *Pharmacol Biochem Behav*, 25, 59-62.
- LENOIR, M., SERRE, F., CANTIN, L. & AHMED, S. H. 2007. Intense sweetness surpasses cocaine reward. *PLoS One*, 2, e698.
- LEVIN, B. E. 2006. Metabolic sensing neurons and the control of energy homeostasis. *Physiol Behav*, 89, 486-9.
- LEVIN, B. E., BECKER, T. C., EIKI, J., ZHANG, B. B. & DUNN-MEYNELL, A. A. 2008a. Ventromedial hypothalamic glucokinase is an important mediator of the counterregulatory response to insulin-induced hypoglycemia. *Diabetes*, 57, 1371-9.
- LEVIN, B. E., BECKER, T. C., EIKI, J., ZHANG, B. B. & DUNN-MEYNELL, A. A. 2008b. Ventromedial hypothalamic glucokinase is an important mediator of the counterregulatory response to insulin-induced hypoglycemia. *Diabetes*, 57, 1371-1379.
- LEVIN, B. E., MAGNAN, C., DUNN-MEYNELL, A. & LE FOLL, C. 2011. Metabolic sensing and the brain: who, what, where, and how? *Endocrinology*, 152, 2552-7.
- LEVIN, B. E., ROUTH, V. H., KANG, L., SANDERS, N. M. & DUNN-MEYNELL, A. A. 2004. Neuronal glucosensing: what do we know after 50 years? *Diabetes*, 53, 2521-8.
- LEVIN, B. E., TRISCARI, J. & SULLIVAN, A. C. 1983. Relationship between sympathetic activity and diet-induced obesity in two rat strains. *Am J Physiol*, 245, R364-71.
- LEVINE, A. S., KOTZ, C. M. & GOSNELL, B. A. 2003. Sugars and fats: the neurobiology of preference. *J Nutr*, 133, 831S-834S.
- LIEDTKE, W. B., MCKINLEY, M. J., WALKER, L. L., ZHANG, H., PFENNING, A. R., DRAGO, J., HOCHENDONER, S. J., HILTON, D. L., LAWRENCE, A. J. & DENTON, D. A. 2011. Relation of addiction genes to hypothalamic gene changes subserving genesis and gratification of a classic instinct, sodium appetite. *Proc Natl Acad Sci U S A*, 108, 12509-14.
- LIVAK, K. J. & SCHMITTGEN, T. D. 2001. Analysis of relative gene expression data using real-time quantitative PCR and the 2(-Delta Delta C) method. *Methods*, 25, 402-408.
- LOFTUS, T. M., JAWORSKY, D. E., FREHYWOT, G. L., TOWNSEND, C. A., RONNETT, G. V., LANE, M. D. & KUHAJDA, F. P. 2000. Reduced food intake and body weight in mice treated with fatty acid synthase inhibitors. *Science*, 288, 2379-81.
- LUCAS, L. R., POMPEI, P. & MCEWEN, B. S. 1999. Correlates of deoxycorticosterone-induced salt appetite behavior and basal ganglia neurochemistry. *Ann N Y Acad Sci*, 897, 423-8.

- LUSBY, E., FIFE, K. H. & BERNS, K. I. 1980. Nucleotide sequence of the inverted terminal repetition in adeno-associated virus DNA. *J Virol*, 34, 402-9.
- LUTTER, M. & NESTLER, E. J. 2009. Homeostatic and hedonic signals interact in the regulation of food intake. *J Nutr*, 139, 629-32.
- LYNCH, R. M., TOMPKINS, L. S., BROOKS, H. L., DUNN-MEYNELL, A. A. & LEVIN, B. E. 2000. Localization of glucokinase gene expression in the rat brain. *Diabetes*, 49, 693-700.
- MA, X., ZUBCEVIC, L. & ASHCROFT, F. M. 2008a. Glucose regulates the effects of leptin on hypothalamic POMC neurons. *Proc Natl Acad Sci U S A*, 105, 9811-6.
- MA, X., ZUBCEVIC, L. & ASHCROFT, F. M. 2008b. Glucose regulates the effects of leptin on hypothalamic POMC neurons (Retracted article. See vol. 106, pg 7263, 2009). *Proceedings of the National Academy of Sciences of the United States of America*, 105, 9811-9816.
- MARKS-KAUFMAN, R. & KANAREK, R. B. 1981. Modifications of nutrient selection induced by naloxone in rats. *Psychopharmacology (Berl)*, 74, 321-4.
- MARKS-KAUFMAN, R. & KANAREK, R. B. 1990. Diet selection following a chronic morphine and naloxone regimen. *Pharmacol Biochem Behav*, 35, 665-9.
- MASSA, M. L., GAGLIARDINO, J. J. & FRANCINI, F. 2011. Liver glucokinase: An overview on the regulatory mechanisms of its activity. *IUBMB Life*, 63, 1-6.
- MATSCHINSKY, F. M., MAGNUSON, M. A., ZELENT, D., JETTON, T. L., DOLIBA, N., HAN, Y., TAUB, R. & GRIMSBY, J. 2006. The network of glucokinase-expressing cells in glucose homeostasis and the potential of glucokinase activators for diabetes therapy. *Diabetes*, 55, 1-12.
- MATSCHINSKY, F. M. & PORTE, D. 2010. Glucokinase activators (GKAs) promise a new pharmacotherapy for diabetics. *F1000 Med Rep*, 2.
- MAYER, J. 1952. The glucostatic theory of regulation of food intake and the problem of obesity. *Bull New Engl Med Cent*, 14, 43-9.
- MAYER, J. 1953. Glucostatic mechanism of regulation of food intake. *N Engl J Med*, 249, 13-6.
- MAYER, J. & THOMAS, D. W. 1967. Regulation of food intake and obesity. *Science*, 156, 328-37.
- MCCRIMMON, R. 2008. The mechanisms that underlie glucose sensing during hypoglycaemia in diabetes. *Diabet Med*, 25, 513-22.
- MELANSON, K. J., WESTERTERP-PLANTENGA, M. S., SARIS, W. H., SMITH, F. J. & CAMPFIELD, L. A. 1999. Blood glucose patterns and appetite in time-blinded humans: carbohydrate versus fat. *Am J Physiol*, 277, R337-45.
- MILLER, D. G., ADAM, M. A. & MILLER, A. D. 1990. Gene transfer by retrovirus vectors occurs only in cells that are actively replicating at the time of infection. *Mol Cell Biol*, 10, 4239-42.
- MIRSHAMSI, S., LAIDLAW, H. A., NING, K., ANDERSON, E., BURGESS, L. A., GRAY, A., SUTHERLAND, C. & ASHFORD, M. L. 2004. Leptin and insulin stimulation of signalling pathways in arcuate nucleus neurones: PI3K dependent actin reorganization and KATP channel activation. *BMC Neurosci*, 5, 54.
- MISELIS, R. R. & EPSTEIN, A. N. 1975. Feeding induced by intracerebroventricular 2-deoxy-D-glucose in the rat. *Am J Physiol*, 229, 1438-47.
- MIWA, I., MITA, Y., MURATA, T., OKUDA, J., SUGIURA, M., HAMADA, Y. & CHIBA, T. 1994. Utility of 3-O-methyl-N-acetyl-D-glucosamine, an N-acetylglucosamine kinase

- inhibitor, for accurate assay of glucokinase in pancreatic islets and liver. *Enzyme Protein*, 48, 135-42.
- MIYOSHI, H., TAKAHASHI, M., GAGE, F. H. & VERMA, I. M. 1997. Stable and efficient gene transfer into the retina using an HIV-based lentiviral vector. *Proc Natl Acad Sci U S A*, 94, 10319-23.
- MORLEY, J. E., LEVINE, A. S., GOSNELL, B. A., KNEIP, J. & GRACE, M. 1987. Effect of neuropeptide Y on ingestive behaviors in the rat. *Am J Physiol*, 252, R599-609.
- MOUNIEN, L., MARTY, N., TARUSSIO, D., METREF, S., GENOUX, D., PREITNER, F., FORETZ, M. & THORENS, B. 2010. Glut2-dependent glucose-sensing controls thermoregulation by enhancing the leptin sensitivity of NPY and POMC neurons. *FASEB J*, 24, 1747-58.
- MOUNTJOY, P. D. & RUTTER, G. A. 2007. Glucose sensing by hypothalamic neurones and pancreatic islet cells: AMPle evidence for common mechanisms? *Exp Physiol*, 92, 311-9.
- MUKHTAR, M., STUBBS, M. & AGIUS, L. 1999. Evidence for glucose and sorbitol-induced nuclear export of glucokinase regulatory protein in hepatocytes. *FEBS Lett*, 462, 453-8.
- MUROYA, S., YADA, T., SHIODA, S. & TAKIGAWA, M. 1999. Glucose-sensitive neurons in the rat arcuate nucleus contain neuropeptide Y. *Neurosci Lett*, 264, 113-6.
- NALDINI, L., BLOMER, U., GALLAY, P., ORY, D., MULLIGAN, R., GAGE, F. H., VERMA, I. M. & TRONO, D. 1996. In vivo gene delivery and stable transduction of nondividing cells by a lentiviral vector. *Science*, 272, 263-7.
- OLDENDORF, W. H. 1971. Brain uptake of radiolabeled amino acids, amines, and hexoses after arterial injection. *Am J Physiol*, 221, 1629-39.
- OLNEY, J. W. 1969. Brain lesions, obesity, and other disturbances in mice treated with monosodium glutamate. *Science*, 164, 719-21.
- OOMURA, Y., KIMURA, K., OOHAMA, H., MAENO, T., IKI, M. & KUNIYOSHI, M. 1964. Reciprocal Activities of the Ventromedial and Lateral Hypothalamic Areas of Cats. *Science*, 143, 484-5.
- ORBAN, P. C., CHUI, D. & MARTH, J. D. 1992. Tissue-Specific and Site-Specific DNA Recombination in Transgenic Mice. *Proceedings of the National Academy of Sciences of the United States of America*, 89, 6861-6865.
- OSUNDIJI, M. A., LAM, D. D., SHAW, J., YUEH, C. Y., MARKKULA, S. P., HURST, P., COLLIVA, C., RODA, A., HEISLER, L. K. & EVANS, M. L. 2012. Brain Glucose Sensors Play a Significant Role in the Regulation of Pancreatic Glucose-Stimulated Insulin Secretion. *Diabetes*, 61, 321-328.
- OSUNDIJI, M. A., ZHOU, L., SHAW, J., MOORE, S. P., YUEH, C. Y., SHERWIN, R., HEISLER, L. K. & EVANS, M. L. 2010. Brain glucosamine boosts protective glucoprivic feeding. *Endocrinology*, 151, 1499-508.
- PAGE, K. A., SEO, D., BELFORT-DEAGUIAR, R., LACADIE, C., DZUIRA, J., NAIK, S., AMARNATH, S., CONSTABLE, R. T., SHERWIN, R. S. & SINHA, R. 2011a. Circulating glucose levels modulate neural control of desire for high-calorie foods in humans. *J Clin Invest*.
- PAGE, K. A., SEO, D., BELFORT-DEAGUIAR, R., LACADIE, C., DZUIRA, J., NAIK, S., AMARNATH, S., CONSTABLE, R. T., SHERWIN, R. S. & SINHA, R. 2011b. Circulating glucose levels modulate neural control of desire for high-calorie foods in humans. *Journal of Clinical Investigation*, 121, 4161-4169.
- PALKOVITS, M. 1983. Punch sampling biopsy technique. *Methods Enzymol*, 103, 368-76.

- PALOMEQUE, J., CHEMALY, E. R., COLOSI, P., WELLMAN, J. A., ZHOU, S., DEL MONTE, F. & HAJJAR, R. J. 2007. Efficiency of eight different AAV serotypes in transducing rat myocardium in vivo. *Gene Ther*, 14, 989-97.
- PANKSEPP, J. & ROSSI, J., 3RD 1981. D-glucose infusions into the basal ventromedial hypothalamus and feeding. *Behav Brain Res*, 3, 381-92.
- PARK, Y. B., CHOI, Y. J., PARK, S. Y., KIM, J. Y., KIM, S. H., SONG, D. K., WON, K. C. & KIM, Y. W. 2011. ATP-Sensitive Potassium Channel-Deficient Mice Show Hyperphagia but Are Resistant to Obesity. *Diabetes Metab J*, 35, 219-25.
- PARTON, L. E., YE, C. P., COPPARI, R., ENRIORI, P. J., CHOI, B., ZHANG, C. Y., XU, C., VIANNA, C. R., BALTHASAR, N., LEE, C. E., ELMQUIST, J. K., COWLEY, M. A. & LOWELL, B. B. 2007a. Glucose sensing by POMC neurons regulates glucose homeostasis and is impaired in obesity. *Nature*, 449, 228-U7.
- PARTON, L. E., YE, C. P., COPPARI, R., ENRIORI, P. J., CHOI, B., ZHANG, C. Y., XU, C., VIANNA, C. R., BALTHASAR, N., LEE, C. E., ELMQUIST, J. K., COWLEY, M. A. & LOWELL, B. B. 2007b. Glucose sensing by POMC neurons regulates glucose homeostasis and is impaired in obesity. *Nature*, 449, 228-32.
- PATTERSON, M., MURPHY, K. G., LE ROUX, C. W., GHATEI, M. A. & BLOOM, S. R. 2005. Characterization of ghrelin-like immunoreactivity in human plasma. *J Clin Endocrinol Metab*, 90, 2205-11.
- PATTERSON, M., MURPHY, K. G., PATEL, S. R., PATEL, N. A., GREENWOOD, H. C., COOKE, J. H., CAMPBELL, D., BEWICK, G. A., GHATEI, M. A. & BLOOM, S. R. 2009. Hypothalamic injection of oxyntomodulin suppresses circulating ghrelin-like immunoreactivity. *Endocrinology*, 150, 3513-20.
- PAXINOS, G. & WATSON, C. 2009. *The rat brain in stereotaxic coordinates*, London, Academic.
- PELLERIN, L., PELLEGRINI, G., BITTAR, P. G., CHARNAY, Y., BOURAS, C., MARTIN, J. L., STELLA, N. & MAGISTRETTI, P. J. 1998. Evidence supporting the existence of an activity-dependent astrocyte-neuron lactate shuttle. *Dev Neurosci*, 20, 291-9.
- PENICAUD, L., LELOUP, C., FIORAMONTI, X., LORSIGNOL, A. & BENANI, A. 2006. Brain glucose sensing: a subtle mechanism. *Curr Opin Clin Nutr Metab Care*, 9, 458-62.
- PLUM, L., MA, X., HAMPEL, B., BALTHASAR, N., COPPARI, R., MUNZBERG, H., SHANABROUGH, M., BURDAKOV, D., ROTHER, E., JANOSCHEK, R., ALBER, J., BELGARDT, B. F., KOCH, L., SEIBLER, J., SCHWENK, F., FEKETE, C., SUZUKI, A., MAK, T. W., KRONE, W., HORVATH, T. L., ASHCROFT, F. M. & BRUNING, J. C. 2006. Enhanced PIP3 signaling in POMC neurons causes KATP channel activation and leads to diet-sensitive obesity. *J Clin Invest*, 116, 1886-901.
- PONNAZHAGAN, S., MUKHERJEE, P., YODER, M. C., WANG, X. S., ZHOU, S. Z., KAPLAN, J., WADSWORTH, S. & SRIVASTAVA, A. 1997. Adeno-associated virus 2-mediated gene transfer in vivo: organ-tropism and expression of transduced sequences in mice. *Gene*, 190, 203-10.
- POSTIC, C., SHIOTA, M. & MAGNUSON, M. A. 2001. Cell-specific roles of glucokinase in glucose homeostasis. *Recent Prog Horm Res*, 56, 195-217.
- PRICE, C. J., HOYDA, T. D. & FERGUSON, A. V. 2008. The area postrema: A brain monitor and integrator of systemic autonomic state. *Neuroscientist*, 14, 182-194.
- PRINTZ, R. L., MAGNUSON, M. A. & GRANNER, D. K. 1993. Mammalian glucokinase. *Annu Rev Nutr*, 13, 463-96.

- QIAN, S., CHEN, H., WEINGARTH, D., TRUMBAUER, M. E., NOVI, D. E., GUAN, X. M., YU, H., SHEN, Z., FENG, Y., FRAZIER, E., CHEN, A. R., CAMACHO, R. E., SHEARMAN, L. P., GOPAL-TRUTER, S., MACNEIL, D. J., VAN DER PLOEG, L. H. T. & MARSH, D. J. 2002. Neither agouti-related protein nor neuropeptide Y is critically required for the regulation of energy homeostasis in mice. *Molecular and Cellular Biology*, 22, 5027-5035.
- QU, D. Q., LUDWIG, D. S., GAMMELTOFT, S., PIPER, M., PELLEYMOUNTER, M. A., CULLEN, M. J., MATHES, W. F., PRZYPEK, J., KANAREK, R. & MARATOSFLIER, E. 1996. A role for melanin-concentrating hormone in the central regulation of feeding behaviour. *Nature*, 380, 243-247.
- RAUBENHEIMER, D. & SIMPSON, S. J. 1997. Integrative models of nutrient balancing: application to insects and vertebrates. *Nutr Res Rev*, 10, 151-79.
- REN, X. Y., FERREIRA, J. G., ZHOU, L. G., SHAMMAH-LAGNADO, S. J., YECKEL, C. W. & DE ARAUJO, I. E. 2010. Nutrient Selection in the Absence of Taste Receptor Signaling. *Journal of Neuroscience*, 30, 8012-8023.
- RONCERO, I., ALVAREZ, E., VAZQUEZ, P. & BLAZQUEZ, E. 2000. Functional glucokinase isoforms are expressed in rat brain. *J Neurochem*, 74, 1848-57.
- ROSE, J. A., MAIZEL, J. V., JR., INMAN, J. K. & SHATKIN, A. J. 1971. Structural proteins of adenovirus-associated viruses. *J Virol*, 8, 766-70.
- ROSICKA, M., KRSEK, M., MATOULEK, M., JARKOVSKA, Z., MAREK, J., JUSTOVA, V. & LACINOVA, Z. 2003. Serum ghrelin levels in obese patients: The relationship to serum leptin levels and soluble leptin receptors levels. *Physiological Research*, 52, 61-66.
- ROSSI, J., BALTHASAR, N., OLSON, D., SCOTT, M., BERGLUND, E., LEE, C. E., CHOI, M. J., LAUZON, D., LOWELL, B. B. & ELMQUIST, J. K. 2011. Melanocortin-4 Receptors Expressed by Cholinergic Neurons Regulate Energy Balance and Glucose Homeostasis. *Cell Metabolism*, 13, 195-204.
- ROSSI, M., CHOI, S. J., OSHEA, D., MIYOSHI, T., GHATEI, M. A. & BLOOM, S. R. 1997. Melanin-Concentrating hormone acutely stimulates feeding, but chronic administration has no effect on body weight. *Endocrinology*, 138, 351-355.
- ROUTH, V. H. 2002. Glucose-sensing neurons: are they physiologically relevant? *Physiol Behav*, 76, 403-13.
- ROUTH, V. H. 2010. Glucose sensing neurons in the ventromedial hypothalamus. *Sensors (Basel)*, 10, 9002-25.
- SACHDEVA, G., D'COSTA, J., CHO, J. E., KACHAPATI, K., CHOUDHRY, V. & ARYA, S. K. 2007. Chimeric HIV-1 and HIV-2 lentiviral vectors with added safety insurance. *Journal of Medical Virology*, 79, 118-126.
- SAKURAI, T., AMEMIYA, A., ISHII, M., MATSUZAKI, I., CHEMELLI, R. M., TANAKA, H., WILLIAMS, S. C., RICHARDSON, J. A., KOZLOWSKI, G. P., WILSON, S., ARCH, J. R. S., BUCKINGHAM, R. E., HAYNES, A. C., CARR, S. A., ANNAN, R. S., MCNULTY, D. E., LIU, W. S., TERRETT, J. A., ELSHOURBAGY, N. A., BERGSMA, D. J. & YANAGISAWA, M. 1998. Orexins and orexin receptors: A family of hypothalamic neuropeptides and G protein-coupled receptors that regulate feeding behavior (vol 92, pg 573, 1998). *Cell*, 92, U29-U29.
- SALKOVIC-PETRISIC, M. & LACKOVIC, Z. 2003. Intracerebroventricular administration of betacytotoxics alters expression of brain monoamine transporter genes. *J Neural Transm*, 110, 15-29.

- SAMBROOK, J., FRITSCH, E. F. & MANIATIS, T. 1989. *Molecular cloning : a laboratory manual*, Cold Spring Harbor, N.Y., Cold Spring Harbor Laboratory.
- SAMULSKI, R. J., CHANG, L. S. & SHENK, T. 1989. Helper-free stocks of recombinant adeno-associated viruses: normal integration does not require viral gene expression. *J Virol*, 63, 3822-8.
- SCHWARTZ, G. J. 2000. The role of gastrointestinal vagal afferents in the control of food intake: current prospects. *Nutrition*, 16, 866-73.
- SCHWARTZ, M. W., WOODS, S. C., PORTE, D., JR., SEELEY, R. J. & BASKIN, D. G. 2000. Central nervous system control of food intake. *Nature*, 404, 661-71.
- SCLAFANI, A., TOUZANI, K. & BODNAR, R. J. 2011. Dopamine and learned food preferences. *Physiol Behav*, 104, 64-8.
- SERGEYEV, V., BROBERGER, C., GORBATYUK, O. & HOKFELT, T. 2000. Effect of 2-mercaptoacetate and 2-deoxy-D-glucose administration on the expression of NPY, AGRP, POMC, MCH and hypocretin/orexin in the rat hypothalamus. *Neuroreport*, 11, 117-21.
- SILVER, I. A. & ERECINSKA, M. 1994. Extracellular glucose concentration in mammalian brain: continuous monitoring of changes during increased neuronal activity and upon limitation in oxygen supply in normo-, hypo-, and hyperglycemic animals. *J Neurosci*, 14, 5068-76.
- SIMPSON, S. J. & RAUBENHEIMER, D. 1997. Geometric analysis of macronutrient selection in the rat. *Appetite*, 28, 201-213.
- SIMPSON, S. J. & RAUBENHEIMER, D. 2005. Obesity: the protein leverage hypothesis. *Obes Rev*, 6, 133-42.
- SINDELAR, D. K., STE MARIE, L., MIURA, G. I., PALMITER, R. D., MCMINN, J. E., MORTON, G. J. & SCHWARTZ, M. W. 2004. Neuropeptide Y is required for hyperphagic feeding in response to neuroglucopenia. *Endocrinology*, 145, 3363-8.
- SMITH, G. P. & EPSTEIN, A. N. 1969. Increased feeding in response to decreased glucose utilization in the rat and monkey. *Am J Physiol*, 217, 1083-7.
- SORENSEN, A., MAYNTZ, D., RAUBENHEIMER, D. & SIMPSON, S. J. 2008. Protein-leverage in mice: the geometry of macronutrient balancing and consequences for fat deposition. *Obesity (Silver Spring)*, 16, 566-71.
- SPANSWICK, D., SMITH, M. A., GROPPI, V. E., LOGAN, S. D. & ASHFORD, M. L. 1997. Leptin inhibits hypothalamic neurons by activation of ATP-sensitive potassium channels. *Nature*, 390, 521-5.
- SRIVASTAVA, A., LUSBY, E. W. & BERNS, K. I. 1983. Nucleotide sequence and organization of the adeno-associated virus 2 genome. *J Virol*, 45, 555-64.
- STUBBS, M., AISTON, S. & AGIUS, L. 2000. Subcellular localization, mobility, and kinetic activity of glucokinase in glucose-responsive insulin-secreting cells. *Diabetes*, 49, 2048-55.
- SUMMERFORD, C. & SAMULSKI, R. J. 1998. Membrane-associated heparan sulfate proteoglycan is a receptor for adeno-associated virus type 2 virions. *J Virol*, 72, 1438-45.
- SWANSON, L. W. 1999. The neuroanatomy revolution of the 1970s and the hypothalamus. *Brain Res Bull*, 50, 397.
- TEMIN, H. M. & BALTIMORE, D. 1972. RNA-directed DNA synthesis and RNA tumor viruses. *Adv Virus Res*, 17, 129-86.

- TER HORST, G. J., LUITEN, P. G. & KUIPERS, F. 1984. Descending pathways from hypothalamus to dorsal motor vagus and ambiguous nuclei in the rat. *J Auton Nerv Syst*, 11, 59-75.
- THOMPSON, D. A. & CAMPBELL, R. G. 1977. Hunger in humans induced by 2-deoxy-D-glucose: glucoprivic control of taste preference and food intake. *Science*, 198, 1065-8.
- THORENS, B. 2011. Brain glucose sensing and neural regulation of insulin and glucagon secretion. *Diabetes Obes Metab*, 13 Suppl 1, 82-8.
- TIESJEMA, B., LA FLEUR, S. E., LUIJENDIJK, M. C. & ADAN, R. A. 2009. Sustained NPY overexpression in the PVN results in obesity via temporarily increasing food intake. *Obesity (Silver Spring)*, 17, 1448-50.
- TKACS, N. C., DUNN-MEYNELL, A. A. & LEVIN, B. E. 2000. Presumed apoptosis and reduced arcuate nucleus neuropeptide Y and pro-opiomelanocortin mRNA in non-coma hypoglycemia. *Diabetes*, 49, 820-6.
- TORDOFF, M. G., TLUCZEK, J. P. & FRIEDMAN, M. I. 1989. Effect of hepatic portal glucose concentration on food intake and metabolism. *Am J Physiol*, 257, R1474-80.
- TREMPE, J. P. & CARTER, B. J. 1988. Regulation of adeno-associated virus gene expression in 293 cells: control of mRNA abundance and translation. *J Virol*, 62, 68-74.
- TSUJII, S. & BRAY, G. A. 1990. Effects of glucose, 2-deoxyglucose, phlorizin, and insulin on food intake of lean and fatty rats. *Am J Physiol*, 258, E476-81.
- UKPDS 1998. Intensive blood-glucose control with sulphonylureas or insulin compared with conventional treatment and risk of complications in patients with type 2 diabetes (UKPDS 33). *Lancet*, 352, 837-53.
- UNITED STATES. DEPARTMENT OF HEALTH, E., WELFARE. HEALTH, S. & MENTAL HEALTH ADMINISTRATION. CENTER FOR DISEASE, C. 1972. *Ten-state nutrition survey : 1968-1970*, Atlanta, [Ga], DHEW.
- VAN DEN TOP, M., LYONS, D. J., LEE, K., CODERRE, E., RENAUD, L. P. & SPANSWICK, D. 2007. Pharmacological and molecular characterization of ATP-sensitive K⁺ conductances in cart and NPY/AgRP expressing neurons of the hypothalamic arcuate nucleus. *Neuroscience*, 144, 815-824.
- WANG, R., CRUCIANI-GUGLIELMACCI, C., MIGRENNE, S., MAGNAN, C., COTERO, V. E. & ROUTH, V. H. 2006. Effects of oleic acid on distinct populations of neurons in the hypothalamic arcuate nucleus are dependent on extracellular glucose levels. *J Neurophysiol*, 95, 1491-8.
- WELCH, C. C., GRACE, M. K., BILLINGTON, C. J. & LEVINE, A. S. 1994. Preference and diet type affect macronutrient selection after morphine, NPY, norepinephrine, and deprivation. *Am J Physiol*, 266, R426-33.
- WELDON, D. T., O'HARE, E., CLEARY, J., BILLINGTON, C. J. & LEVINE, A. S. 1996. Effect of naloxone on intake of cornstarch, sucrose, and polycose diets in restricted and nonrestricted rats. *Am J Physiol*, 270, R1183-8.
- WHO. 2006. *Obesity and overweight factsheet* [Online]. Available: <http://www.who.int/mediacentre/factsheets/fs311/en/index.html> [Accessed 2nd January 2011].
- WOOD, S. M., WOOD, J. R., GHATEI, M. A., LEE, Y. C., O'SHAUGHNESSY, D. & BLOOM, S. R. 1981. Bombesin, somatostatin and neurotensin-like immunoreactivity in bronchial carcinoma. *J Clin Endocrinol Metab*, 53, 1310-2.

- WURTMAN, J. J. 1985. Neurotransmitter control of carbohydrate consumption. *Ann N Y Acad Sci*, 443, 145-51.
- WURTMAN, J. J. & WURTMAN, R. J. 1979. Drugs that enhance central serotonergic transmission diminish elective carbohydrate consumption by rats. *Life Sci*, 24, 895-903.
- XU, B. J., GOULDING, E. H., ZANG, K. L., CEPOI, D., CONE, R. D., JONES, K. R., TECOTT, L. H. & REICHARDT, L. F. 2003. Brain-derived neurotrophic factor regulates energy balance downstream of melanocortin-4 receptor. *Nature Neuroscience*, 6, 736-742.
- YANG, X. J., MASTAITIS, J., MIZUNO, T. & MOBBS, C. V. 2007. Glucokinase regulates reproductive function, glucocorticoid secretion, food intake, and hypothalamic gene expression. *Endocrinology*, 148, 1928-32.
- ZARJEVSKI, N., CUSIN, I., VETTOR, R., ROHNERJEANRENAUD, F. & JEANRENAUD, B. 1993. Chronic Intracerebroventricular Neuropeptide-Y Administration to Normal Rats Mimics Hormonal and Metabolic Changes of Obesity. *Endocrinology*, 133, 1753-1758.
- ZHANG, Y., ZHOU, J., CORLL, C., PORTER, J. R., MARTIN, R. J. & ROANE, D. S. 2004. Evidence for hypothalamic K⁺(ATP) channels in the modulation of glucose homeostasis. *Eur J Pharmacol*, 492, 71-9.
- ZHOU, L., PODOLSKY, N., SANG, Z., DING, Y., FAN, X., TONG, Q., LEVIN, B. E. & MCCRIMMON, R. J. 2010. The medial amygdalar nucleus: a novel glucose-sensing region that modulates the counterregulatory response to hypoglycemia. *Diabetes*, 59, 2646-52.
- ZHOU, L. G., YUEH, C. Y., LAM, D. D., SHAW, J., OSUNDIJI, M., GARFIELD, A. S., EVANS, M. & HEISLER, L. K. 2011. Glucokinase inhibitor glucosamine stimulates feeding and activates hypothalamic neuropeptide Y and orexin neurons. *Behavioural Brain Research*, 222, 274-278.

8 APPENDIX

8.1 Appendix I – Solutions

3M Alcoholic KOH solution:

Add 39g KOH pastels to 200 ml 65% ethanol

5M ammonium acetate

Dissolve 385g $\text{CH}_3\text{COONH}_4$ in 600ml autoclaved distilled water, then make up to 1l.

Buffer R

40mM Pipes buffer pH 7.6, 1.5mM DCHBS, 17.5mM magnesium-ions.

2M Calcium chloride:

10.8g $\text{CaCl}_2 \cdot 6\text{H}_2\text{O}$ was dissolved in 20ml GDW and sterilise by filtration through 0.22 μm filter and store in 1ml aliquots at -20°C

Caesium chloride-saturated propan-2-ol:

Mix 100g CsCl_2 , 100ml GDW and 100ml propan-2-ol and leave to settle.

0.5M ethylenediaminetetra-acetic acid (EDTA):

In 800ml autoclaved water dissolve 186.1g $C_{10}H_{14}H_2O_8Na_{2.2}H_2O$ and adjust to pH 8.0 with 1M NaOH. Make up to 1L with water

Gel loading buffer:

Mix 3.125ml 80% glycerol, 50 μ l 0.5M EDTA, and 10mg orange G in 6.075ml of autoclaved distilled water.

Glucokinase extraction buffer:

Dissolve 0.508g $MgCl_2$, 0.913g Sodium ethylenediamine tetraacetate, 5.591g KCl and 0.35ml 2-mercaptoethanol in 500ml GDW. Use 1M KOH to alter the pH of the solution to 7.3.

Gly- Gly:

Dissolve 6.6g Gly –gly in 500ml. Use 5M KOH to alter pH to 8.

GTE

Mix 2.5ml 1M Tris-HCl, pH 8.0, 2ml 0.5M $C_{10}H_{14}H_2O_8Na_{2.2}H_2O$ and 5ml 18% glucose and top up to 100ml. Sterilise by passing through a 0.2 μ m filter.

HEPES-buffered saline (HBS)

280mM NaCl, 10mM KCl, 1.5mM Na₂HPO₄, 12mM dextrose, 50mM HEPES (Sigma) pH7.07. Sterilise by filtration through 0.22µm filter and store in 5ml aliquots at -20°C

Hybridisation buffer

Dissolve 0.5g dried milk powder in 48ml GDW and 0.5ml 500mM EDTA. Add 25ml 1M Na phosphate, 25 ml 20 % SDS, 2.5mM ATA.

LB culture media

Dissolve 5g sodium chloride, 10g tryptone and 5g yeast extract to 1l of distilled water. Adjust to pH 7.5 with 10M sodium hydroxide and sterilise by autoclaving.

Lysis buffer

Add 8.765g NaCl, 6.055g Tris, make up to 1l with GDW and adjust to pH8.5.

1M magnesium chloride

Dissolve 203.3g MgCl₂ in 1L GDW.

0.06M Phosphate buffer

Dissolve 48g Na₂HPO₄·2H₂O, 4.13g KHPO₄, 18.61g C₁₀H₁₄H₂ONa₂·2H₂O and 2.5g NaN₃ in 5l. GDW that has been boiled and allowed to cool. Adjust pH to 7.4 and store at 4°C.

3M potassium acetate

Dissolve 294.4g CH₃COOK in 500ml water, add 115ml glacial acetic acid and water up to 1L.

Reagent R

0.4mM aminophenazonel, 1mM ATP, glycerol-kinase > 0.4 U/ml, glycerol-3-phosphate oxidase > 1.5 U/ml, peroxidase > 0.5 U/ml. ascorbic acid oxidase > 7.0 KU/l.

2M sodium acetate

pH 5.2: Dissolve 164.1g CH₃COONa in 800ml a/c water, adjust to pH 5.2 with glacial acetic acid and make up to 1L with water

5M sodium chloride

Dissolve 292.2 g NaCl in 1L GDW.

20% sodium dodecyl sulphate (SDS)

Add 200g SDS to 800ml a/c water, heat to 60°C while stirring. Allow to cool and make up to 1L with water.

0.2% sodium hydroxide 1% SDS

Add 3ml 10M NaOH to 140ml GDW, mix and add 7.5ml 20% SDS.

20xSSC

Dissolve 1.753g NaCl, 14.2g Na₂HPO₄ and 7.4g C₁₀H₁₄H₂O₈Na₂·2H₂O in 700ml GDW, adjust to pH 7.7 with 10M NaOH and make up to 1L with GDW.

50 x TAE

Dissolve 242g Trizma base in 843ml water and mix in 57ml glacial acetic acid and 100ml 0.5M C₁₀H₁₄H₂O₈Na₂·2H₂O.

0.1 x TE

1mM Tris-HCl, pH 0.8 and 0.1mM EDTA, pH 0.8

2M Tris-HCl, pH 8.0:

dissolve 121.1g Trizma base in 450ml GDW and adjust to pH 8.0 with HCl. Make up to 500ml.

Versene

2.7mM KCl, 0.14M NaCl 1.5mM KH₂PO₄, 8mM Na₂HPO₄·2H₂O, 3mM EDTA, 0.1% phenol red. 230

8.2 Appendix II – Coronal section of rat brain

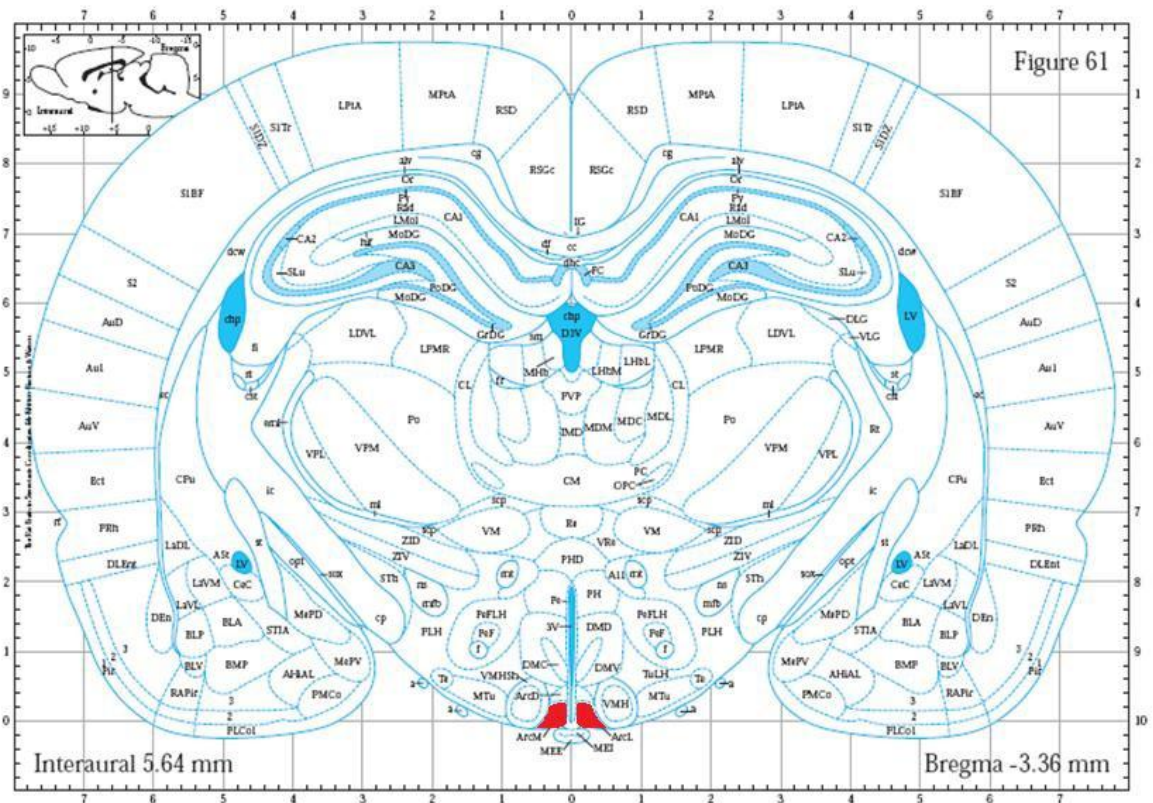


Figure Appendix 1: Coronal section of the rat brain

Schematic showing 3.36mm posterior to bregma of the rat brain, which approximately corresponds to the co-ordinates used to target the arcuate nucleus in this work (-3.4 from bregma). The arcuate nucleus is highlighted in red. Reproduced from “The Rat Brain in Stereotaxic Co-ordinates” (Paxinos & Watson C, 2007).

8.3 Appendix III – Nutritional information for RM1 normal chow diet


| NUTRIENTS | | Total | Supp (9) | NUTRIENTS | | Total | Supp (9) |
|--|-------|-------|----------|--|-------|---------|----------|
| Proximate Analysis | | | | Macro Minerals | | | |
| Moisture (1) | % | 10.00 | | Calcium | % | 0.73 | 0.63 |
| Crude Oil | % | 2.71 | | Total Phosphorus | % | 0.52 | 0.04 |
| Crude Protein | % | 14.38 | | Phytate Phosphorus | % | 0.24 | |
| Crude Fibre | % | 4.65 | | Available Phosphorus | % | 0.28 | 0.04 |
| Ash | % | 6.00 | | Sodium | % | 0.25 | 0.19 |
| Nitrogen Free Extract | % | 61.73 | | Chloride | % | 0.38 | 0.32 |
| Digestibility Co-Efficients (7) | | | | Potassium | % | 0.67 | |
| Digestible Crude Oil | % | 2.47 | | Magnesium | % | 0.23 | |
| Digestible Crude Protein | % | 12.92 | | Micro Minerals | | | |
| Carbohydrates, Fibre and Non Starch Polysaccharides (NSP) | | | | Iron | mg/kg | 159.30 | 82.50 |
| Total Dietary Fibre | % | 17.05 | | Copper | mg/kg | 11.50 | 1.94 |
| Pectin | % | 1.52 | | Manganese | mg/kg | 72.44 | 19.22 |
| Hemicellulose | % | 10.17 | | Zinc | mg/kg | 35.75 | |
| Cellulose | % | 4.32 | | Cobalt | µg/kg | 634.10 | 550.00 |
| Lignin | % | 1.68 | | Iodine | µg/kg | 1202.69 | 1085.00 |
| Starch | % | 44.97 | | Selenium | µg/kg | 298.99 | 100.00 |
| Sugar | % | 4.05 | | Fluorine | mg/kg | 10.49 | |
| Energy (5) | | | | Vitamins | | | |
| Gross Energy | MJ/kg | 14.74 | | β-Carotene (2) | mg/kg | 0.16 | |
| Digestible Energy (15) | MJ/kg | 11.90 | | Retinol (2) | µg/kg | 2566.38 | 2400.00 |
| Metabolisable Energy (15) | MJ/kg | 10.74 | | Vitamin A (2) | iu/kg | 8554.27 | 8000.00 |
| Atwater Fuel Energy (AFE)(8) | MJ/kg | 13.75 | | Cholecalciferol (3) | µg/kg | 15.54 | 15.00 |
| AFE from Oil | % | 7.42 | | Vitamin D (3) | iu/kg | 621.70 | 600.00 |
| AFE from Protein | % | 17.49 | | α-Tocopherol (4) | mg/kg | 76.45 | 56.82 |
| AFE from Carbohydrate | % | 75.09 | | Vitamin E (4) | iu/kg | 84.10 | 62.50 |
| Fatty Acids | | | | Vitamin B ₁ (Thiamine) | mg/kg | 8.58 | 1.96 |
| Saturated Fatty Acids | | | | Vitamin B ₂ (Riboflavin) | mg/kg | 4.33 | 2.94 |
| C12:0 Lauric | % | 0.02 | | Vitamin B ₃ (Pyridoxine) | mg/kg | 4.81 | 0.98 |
| C14:0 Myristic | % | 0.14 | | Vitamin B ₁₂ (Cyanocobalamin) | µg/kg | 7.49 | 6.00 |
| C16:0 Palmitic | % | 0.31 | | Vitamin C (Ascorbic Acid) | mg/kg | 2.59 | |
| C18:0 Stearic | % | 0.04 | | Vitamin K (Menadione) | mg/kg | 10.17 | 9.36 |
| Monounsaturated Fatty Acids | | | | Folic Acid (Vitamin B ₉) | mg/kg | 0.79 | |
| C14:1 Myristoleic | % | 0.02 | | Nicotinic Acid (Vitamin PP) (6) | mg/kg | 61.32 | 2.45 |
| C16:1 Palmitoleic | % | 0.09 | | Pantothenic Acid (Vitamin B ₅) | mg/kg | 20.17 | 5.80 |
| C18:1 Oleic | % | 0.77 | | Choline (Vitamin B ₄) | mg/kg | 1080.14 | 366.60 |
| Polyunsaturated Fatty Acids | | | | Inositol | mg/kg | 2369.59 | |
| C18:2(ω6) Linoleic | % | 0.69 | | Biotin (Vitamin H) (6) | µg/kg | 277.13 | |
| C18:3(ω3) Linolenic | % | 0.06 | | Notes | | | |
| C20:4(ω6) Arachidonic | % | 0.13 | | 1. All values are calculated using a moisture basis of 100%. | | | |
| C22:5(ω3) Clupanodonic | % | | | Typical moisture levels will range between 95 - 11.5%. | | | |
| Amino Acids | | | | 2. a. Vitamin A includes Retinol and the Retinol equivalents of β-carotene | | | |
| Arginine | % | 0.91 | | b. Retinol includes the Retinol equivalents of β-Carotene. | | | |
| Lysine (6) | % | 0.66 | 0.07 | c. 0.48 µg Retinol = 1 µg β-carotene = 1.6 iu Vitamin A activity | | | |
| Methionine | % | 0.22 | 0.04 | d. 1 µg Retinol = 3.33* iu Vitamin A activity | | | |
| Cystine | % | 0.24 | | e. 1 iu Vitamin A = 0.3 µg Retinol = 0.6 µg β-carotene | | | |
| Tryptophan | % | 0.18 | | f. The standard analysis for Vitamin A does not detect β-carotene | | | |
| Histidine | % | 0.35 | | 3. 1 µg Cholecalciferol (D ₃) = 400 iu Vitamin D | | | |
| Threonine | % | 0.49 | | 4. 1 mg all- <i>cis</i> -α-tocopherol = 1.1 iu Vitamin E activity | | | |
| Isoleucine | % | 0.54 | | 1 mg all- <i>cis</i> -α-tocopherol acetate = 1.0 iu Vitamin E activity | | | |
| Leucine | % | 0.98 | | 5. 1 MJ = 239.23 Kcalories = 239.23 Calories = 239,230 calories | | | |
| Phenylalanine | % | 0.66 | | 6. These nutrients coming from natural raw materials such as cereals may have low availabilities due to the interactions with other compounds. | | | |
| Valine | % | 0.69 | | 7. Based on in-vitro digestibility analysis. | | | |
| Tyrosine | % | 0.49 | | 8. AF Energy = Atwater Fuel Energy = ((CO% / 100) * 9000) + ((CP% / 100) * 4000) + ((NFE% / 100) * 4000) / 2.39.23 | | | |
| Taurine | % | | | 9. Supplemented nutrients from manufactured and mined sources. | | | |
| Glycine | % | 1.11 | | 15. Calculated. | | | |
| Aspartic Acid | % | 0.67 | | | | | |

Figure Appendix 2: Nutritional information for RM1 normal chow diet

8.4 Appendix IV – Nutritional information for high energy diet (Research Diets Inc, USA)

Product Data

D12266B



Description
Condensed milk diet. Purified match to C11024.

Used in Research
Obesity
Diabetes
Hypertension

Packaging
Product is packed in 12.5 kg box. Each box is identified with the product name, description, lot number and expiration date.

Lead Time
IN-STOCK. Ready for next day shipment.

Gamma-Irradiation
Yes. Add 10 days to delivery time.

Form
Pellet, Powder, Liquid

Shelf Life
Most diets require storage in a cool dry environment. Stored correctly they should last 3-6 months.

Control Diets
D12489B
D10001

Formula

| Product # | D12266B | |
|--------------|--------------|--------------|
| | gm% | kcal% |
| Protein | 18.5 | 16.8 |
| Carbohydrate | 56.7 | 51.4 |
| Fat | 15.6 | 31.8 |
| | Total | 100.0 |
| | kcal/gm | |
| | 4.41 | |

| Ingredient | gm | kcal |
|--------------------------|--------|--------|
| Casein, 80 Mesh | 190 | 760 |
| DL-Methionine | 3 | 12 |
| Corn Starch | 215 | 860 |
| Maltodextrin 10 | 75 | 300 |
| Sucrose | 290 | 1160 |
| Cellulose, BW200 | 30 | 0 |
| Butter Fat | 44.2 | 397.8 |
| Corn Oil | 118 | 1062 |
| Mineral Mix S10001 | 40 | 0 |
| Calcium Carbonate | 5.5 | 0 |
| Sodium Chloride | 5.5 | 0 |
| Potassium Citrate, 1 H2O | 13.5 | 0 |
| Vitamin Mix V10001 | 11 | 44 |
| Choline Bitartrate | 2 | 0 |
| FD&C Yellow Dye #5 | 0 | 0 |
| FD&C Red Dye #40 | 0.1 | 0 |
| Total | 1042.8 | 4595.8 |

Figure Appendix 3: Nutritional information for high-energy diet (D12266B, Research Diets Inc, USA)

8.5 Appendix V – List of suppliers

Advanced Biotechnology Centre, Imperial College, London, UK

Animalcare Limited, Dunnington, York, UK

Applied Biosystems, Warrington, UK

ATCC, Middlesex, UK

Bayer UK Ltd, Bury St Edmunds, UK

Beckman Coulter (U.K.), Buckinghamshire, UK

Bright Instrument Company, Huntingdon, Cambridgeshire, UK

Boehringer Ingelheim, Berkshire, UK

Charles River, Bicester, UK

Clintech, Dublin, Ireland

CrystalChem, Illinois, USA

David Kopf Instruments, Tujunga, CA, USA

Du Pont, Bristol, UK

Eli Lilly & Co.Ltd, Basingstoke, UK

Eppendorf, Hamburg, Germany

Fine Science Tools, Linton, UK

Fisher Scientific UK, Loughborough, Leicestershire, UK

GE Healthcare, Buckinghamshire, UK

Genomics Core Laboratory, Imperial College London, UK

Graphpad Prism, Graphpad Software, San Diego, CA, USA

Helena biosciences, Sunderland, UK

Invitrogen Life Technologies, Paisley, UK

Kodak, Hemel Hempstead, Hertfordshire, UK

LEO Pharma, Buckinghamshire, UK

L.E West, Barking, UK

Life Sciences Technology, Eggenstein, Germany

Linco Research, Missouri, USA

Merck4Biosciences, UK

Microvette, Sarstedt, Numbrecht, Germany

Millipore, Watford, Hertfordshire, UK

Millpledge Veterinary, Nottinghamshire, UK

New England Biolabs (UK) Ltd, Hitchin, Hertfordshire, UK

Novagen, Nottingham, UK

Oswell DNA Services, Southampton, UK 236

Parke-Davis, Pontypool, UK

Plastics-One, Roanoke, Virginia, USA

Pierce, Rockford, IL, USA

Promega, Madison, WI, USA

Radox Laboratories Ltd, County Antrim, UK

Research Diets Inc, New Brunswick, NJ, USA

Shandon Southern Products Ltd, Runcorn, UK

Sigma Ltd, Poole, Dorset, UK

Special Diet Services, Witham, Essex, UK

ThermoFisher Leicestershire, UK

Tyco Healthcare, Hampshire, UK

Vet Tech Solutions Ltd, Cheshire, UK

VWR International Ltd, Poole, UK

Wallac, Waltham, MA, USA

WPA, Cambridgeshire, UK